Solutions Manual to Accompany

Inorganic Chemistry

International Edition

Alen Hadzovic
University of Toronto

OXFORD
University Press

Solutions Manual to Accompany Inorganic Chemistry, International Edition

Oxford University Press
Great Clarendon Street Oxford, OX2 6DP United Kingdom

www.oup.com

TABLE OF CONTENTS

PREFACE

This *Solutions Manual* accompanies *Inorganic Chemistr*y, International Edition by Mark Weller, Tina Overton, Jonathan Rourke, and Fraser Armstrong. Here, you will find the detailed solutions for all self-tests and end of chapter exercises. Many solutions include figures specifically prepared for the solution, and not found in the main text. As you master each chapter in *Inorganic Chemistry*, this manual will help you not only to confirm your answers and understanding but also to expand the material covered in the textbook.

The Solutions Manual is a learning aid—its primary goal is to provide you with means to ensure that your own understanding and your own answers are correct. If you see that your solution differs from the one offered in the Solutions Manual, do not simply read over the provided answer. Go back to the main text, reexamine and reread the important concepts required to solve that problem, and then, with this fresh insight, try solving the same problem again. The self-tests are closely related to the examples that precede them. Thus, if you had a problem with a self-test, read the preceding text and analyze the worked example. The solutions to the end of chapter exercises direct you to the relevant sections of the textbook, which you should reexamine if the exercise proves challenging to you.

Inorganic chemistry is a beautiful, rich, and exciting discipline, but it also has its challenges. The self-tests, exercises, and tutorial problems have been designed to help you test your knowledge and meet the challenges of inorganic chemistry. The Solutions Manual is here to help you on your way, provide guidance through the world of chemical elements and their compounds and, together with the text it accompanies, take you to the very frontiers of this world.

With a hope you will find this manual useful,
Alen Hadzovic

ACKNOWLEDGMENTS

I would like to thank the authors Mark Weller, Tina Overton, Jonathan Rourke, and Fraser Armstrong for their insightful comments, discussions, and valuable assistance during the preparation of this Solutions Manual. I would also like to express my gratitude to Roseanne Levermore, Editor for Oxford University Press, for all of her efforts and dedication to the project.

Chapter 1 Atomic Structure

Self-Tests

S1.1 **a)** For the Paschen series $n_1 = 3$ and $n_2 = 4, 5, 6, \ldots$ The second line in the Paschen series is observed when $n_2 = 5$. Hence, starting from equation 1.1, we have

$$\frac{1}{\lambda} = R\left(\frac{1}{n_1^2} - \frac{1}{n_2^2}\right) = 1.097\times10^7\,\mathrm{m}^{-1}\left(\frac{1}{3^2} - \frac{1}{5^2}\right) = 1.097\times10^7\,\mathrm{m}^{-1}\times 0.071 = 779967\mathrm{m}^{-1}.$$

The wavelength is the reciprocal value of the above-calculated wavenumber: $\frac{1}{779967\mathrm{m}^{-1}} = 1.28\times10^{-6}\mathrm{m}$ or 1280 nm.

b) For the Lyman series $n_1 = 1$ is set while n_2 has to be calculated. We can re-write equation 1.1 as

$$\frac{1}{\lambda} = R\left(\frac{1}{n_1^2} - \frac{1}{n_2^2}\right) = \frac{R}{n_1^2} - \frac{R}{n_2^2}.$$

From here:

$$\frac{R}{n_2^2} = \frac{R}{n_1^2} - \frac{1}{\lambda} = \frac{1.097\times10^7\,\mathrm{m}^{-1}}{1^2} - \frac{1}{103\mathrm{nm}\times10^{-9}\,\frac{\mathrm{m}}{\mathrm{nm}}} = 1.097\times10^7\,\mathrm{m}^{-1} - 9.71\times10^6\,\mathrm{m}^{-1} = 1.26\times10^6\,\mathrm{m}^{-1}.$$

And

$$n_2^2 = \frac{R}{1.26\times10^6\,m^{-1}} = \frac{1.097\times10^7\,m^{-1}}{1.26\times10^6\,m^{-1}} = 8.71.$$

Finally

$$n_2 = \sqrt{8.71} = 2.95.$$

Since n values are integer, our n_2 equals 3.

S1.2 **a)** The third shell is given by $n = 3$, and the subshell for $l = 2$ consists of the d orbitals. Therefore, the quantum numbers $n = 3$, $l = 2$ define a 3d set of orbitals. For $l = 2$, there are $2l + 1 = 5$ m_l values: +2, +1, 0, –1, –2. Thus, there are five orbitals in this set.

b) The value of quantum number $n = 5$ is given. The value of quantum number l can be determined from the letter designation f as $l = 3$. The number of orbitals in this set is given by the number of possible m_l values: $2l + 1 = 2\times3 + 1 = 7$. The allowed m_l values in this case are +3, +2, +1, 0, –1, –2 and –3.

S1.3 **a)** The number of radial nodes is given by the expression: $n–l–1$. For the 5s orbital, $n = 5$ and $l = 0$. Therefore: 5–0–1 = 4. Thus, there are four radial nodes in a 5s orbital. Remember, the first occurrence of a radial node for an s orbital is the 2s orbital, which has one radial node, the 3s has two, the 4s has three, and finally the 5s has four. If you forget the expression for determining radial nodes, just count by a unit of one from the first occurrence of a radial node for that particular "shape" of orbital. Figure 1.9 shows the radial wavefuntions of 1s, 2s, and 3s hydrogenic orbitals. The radial nodes are found where the radial wavefunction has a value of zero (i.e., it intersects the x-axis).

b) In this case we have to determine the value of quantum number n for which a p orbital ($l = 1$) would have two radial nodes. Thus:

$$n - l - 1 = 2$$
$$n - 1 - 1 = 2$$
$$n = 4.$$

All three 4p orbitals have two radial nodes.

S1.4 There is no figure showing the radial distribution functions for 3p and 3d orbitals, so you must reason by analogy. In the example, you saw that an electron in a p orbital has a smaller probability of close approach to the nucleus than in an s orbital, because an electron in a p orbital has a greater angular momentum than in an s orbital. Visually, Figure 1.12 shows this. The area under the graph represents where the electron has the highest probability of being found. The origin of the graph is the nucleus, so one can see that the 2s orbital, on average, spends more time closer to the nucleus than a 2p orbital. Similarly, an electron in a d orbital has a greater angular momentum than in a p orbital: $l(\mathrm{d}) > l(\mathrm{p}) > l(\mathrm{s})$. Therefore, an electron in a p orbital has a greater probability than in a d orbital of close approach to the nucleus.

S1.5 **a)** To start with, we write down the ground state electronic configuration of Si atom:

$$1s^2 2s^2 2p^6 3s^2 3p^2.$$

From this electronic configuration we see that silicon's outermost electron resides in one of three 3p orbitals. Now we group the orbitals as described in the text and in Example 1.5:

$$(1s^2)(2s^2 2p^6)(3s^2 3p^2).$$

Next, we analyse the groups as follows:

- There are three additional electrons in the same group as our outmost electron (two in 3s and one more in 3p orbital). Each of them contributes 0.35 to the screening constant.
- There are eight electrons in $n - 1$ group (two in 2s and six in 2p orbitals). Each contributes 0.85 to the screening constant.
- Finally, there are just two electrons (1s electrons) in one lower shell/group contributing 1.00 to the screening constant.

Adding all this together we have:

$$\sigma = (3 \times 0.35) + (8 \times 0.85) + (2 \times 1.00) = \mathbf{8.95}.$$

b) Recall that effective nuclear charge is given by:

$$Z_{eff} = Z - \sigma.$$

The full nuclear charge, Z, is also the atomic number, and for chlorine it is 17. Now we have to determine s following previous examples.

For Cl atom:

$$(1s^2)(2s^2 2p^6)(3s^2 3p^5)$$

$$\sigma = (6 \times 0.35) + (8 \times 0.85) + (2 \times 1.00) = \mathbf{10.9}.$$

We can now calculate Z_{eff}:

$$Z_{eff} = Z - \sigma = 17 - 10.9 = \mathbf{6.1}.$$

S1.6 **a)** The configuration of the valence electrons, called the valence configuration, is as follows for the four atoms in question:

Li: $2s^1$	B: $2s^2 2p^1$
Be: $2s^2$	C: $2s^2 2p^2$.

We can use the effective nuclear charge values from Table 1.2 in the textbook to analyse the trends. Thus, when an electron is added to the 2s orbital on going from Li to Be, Z_{eff} increases by 0.63. When an electron is added to an empty p orbital on going from B to C, Z_{eff} increases by 0.72. The s electron already present in Li repels the incoming electron more strongly than the p electron already present in B repels the incoming p electron, because the incoming p electron goes into a new orbital. Therefore, Z_{eff} increases by a smaller amount on going from Li to Be than from B to C. However, extreme caution must be exercised with arguments like this because the effects of electron–electron repulsions are very subtle. This is illustrated in period 3, where the effect is opposite to that just described for period 2.

b) Al is below B in the same group of the periodic table. In this case Z significantly increases (from $Z = 5$ for B to $Z = 13$ for Al) because of the added protons as we move through the elements. However, the increase in Z_{eff} is smaller (from $Z_{eff} = 2.42$ for B to $Z_{eff} = 4.07$ for Al) because the Al atoms contain one extra filled electronic shell of eight electrons ($2s^2 2p^6$) that shield the outermost electrons from the full nuclear charge.

S1.7 **a)** Following the example, for an atom of Ni with $Z = 28$ the electron configuration is:

$$\text{Ni: } 1s^2 2s^2 2p^6 3s^2 3p^6 3d^8 4s^2 \text{ or } [Ar]3d^8 4s^2.$$

Once again, the 4s electrons are listed last because the energy of the 4s orbital is higher than the energy of the 3d orbitals. Despite this ordering of the individual 3d and 4s energy levels for elements past Ca (see Figure 1.19), interelectronic repulsions prevent the configuration of an Ni atom from being $[Ar]3d^{10}$. For an Ni^{2+} ion, with two fewer electrons than an Ni atom but with the same Z as an Ni atom, interelectronic repulsions are less important. Because of the higher energy 4s electrons as well as smaller Z_{eff} than the 3d electrons, the 4s electrons are removed from Ni to form Ni^{2+}, and the electron configuration of the ion is:

$$Ni^{2+}: 1s^2 2s^2 2p^6 3s^2 3p^6 3d^8 \text{ or } [Ar]3d^8.$$

b) The ground state electronic configuration of Cu atom is:

$$1s^2 2s^2 2p^6 3s^2 3p^6 3d^{10} 4s^1 \text{ or } [Ar]3d^{10} 4s^1.$$

Recall form the textbook Section 1.5(b) that copper atom is one exception to the expected electronic configuration: it is not $3d^9 4s^2$ (as would be anticipated following nickel's $3d^8 4s^2$) but rather $3d^{10} 4s^1$. Note that this leaves 4s orbital half-filled and 3d orbitals filled.
Taking this electronic configuration of the neutral Cu, we can easily obtain the electronic configurations for ions by removing the outermost electrons:

$$Cu^+ : 1s^2 2s^2 2p^6 3s^2 3p^6 3d^{10} \text{ or } [Ar]3d^{10}$$

and

$$Cu^{2+} : 1s^2 2s^2 2p^6 3s^2 3p^6 3d^9 \text{ or } [Ar]3d^9.$$

S1.8 **a)** The valence electrons are in the $n = 4$ shell. Therefore, the element is in period 4 of the periodic table. It has two valence electrons that are in a 4s orbital, indicating that it is in Group 2. Therefore, the element is calcium, Ca.

b) In this case the highest value for the quantum number n is 5 placing the element in period 5. Note that there is an incomplete d subshell in shell 4: $4d^4$. This means that our element belongs in d block and has six valence electrons in total (four in 4d and two in 5s). The element is in group 6. This place in the periodic table belongs to molybdenum (Mo).

S1.9 **a)** When considering questions like these, it is always best to begin by writing down the electron configurations of the atoms or ions in question. If you do this routinely, a confusing comparison may become more understandable. In this case the relevant configurations are:

$$\text{F: } 1s^2 2s^2 2p^5 \text{ or } [He]2s^2 2p^5$$

$$\text{Cl: } 1s^2 2s^2 2p^6 3s^2 3p^5 \text{ or } [Ne]3s^2 3p^5.$$

The electron removed during the ionization process is a 2p electron for F and a 3p electron for Cl. The principal quantum number, n, is lower for the electron removed from F ($n = 2$ for a 2p electron), so this electron is bound more strongly by the F nucleus than a 3p electron in Cl is bound by its nucleus.

A general trend: within a group, the first ionization energy decreases down the group because in the same direction the atomic radii and principal quantum number n increase. There are only a few exceptions to this trend, and they are found in Groups 13 and 14.

b) It is important to recall that s orbitals are somewhat lower in energy than the p orbitals with the same quantum number n. Looking at the relevant electronic configurations

$$\text{Mg: } 1s^2 2s^2 2p^6 3s^2$$
$$\text{Al: } 1s^2 2s^2 2p^6 3s^2 3p^1$$

we see that ionization removes a 3s electron from Mg atom and the 3p electron from Al atom. Greater stability of s electrons requires greater ionization energy, and magnesium's I_1 is greater than aluminium's.

S1.10 When considering questions like these, look for the highest jump in energies. This occurs for the fifth ionization energy of this element: $I_4 = 6229$ kJ mol^{-1}, while $I_5 = 37838$ kJ mol^{-1}, indicating breaking into a complete subshell after the removal of the fourth electron. Therefore, the element is in the Group 14 (C, Si, Ge, etc.).

S1.11 **a)** The electron configurations of these two atoms are:

C: [He]$2s^2 2p^2$ and N: [He]$2s^2 2p^3$

An additional electron can be added to the empty 2p orbital of C, and this is a favourable process (A_e = 122 kJ mol^{-1}). However, all 2p orbitals of N are already half occupied, so an additional electron added to N would experience sufficiently strong interelectronic repulsions. Therefore, the electron-gain process for N is unfavourable (A_e = –8 kJ mol^{-1}). This is despite the fact that the 2p Z_{eff} for N is larger than the 2p Z_{eff} for C (see Table 1.2). This tells you that attraction to the nucleus is not the only force that determines electron affinities (or, for that matter, ionization energies). Interelectronic repulsions are also important.

b) Recall from section 1.7(c) "Electron affinity" that negative values of E_a indicate lower stability of $A^-(g)$ than A(g). The fact that all Group 18 elements have negative E_a values indicates that their anions are less stable than neutral atoms in the gas phase. A new electron would occupy completely new electronic shell for the Group 18 elements (for example He(g) would accept an electron in 2s orbital to become $He^-(g)$). These are well shielded from the nucleus by completely filled shells of neutral atoms and are consequently very weakly bound making an electron gain for all these elements endothermic.

S1.12 **a)** According to Fajan's rules, small, highly charged cations have polarizing ability. Cs^+ has a larger ionic radius than Na^+. Both cations have the same charge, but because Na^+ is smaller than Cs^+, Na^+ is more polarizing.

b) The important difference between NaF and NaI s the size of the anion: I^- is significantly larger than F^-. Recall from Fajan's rules that larger anions are easier to polarize, and (following Example 1.12 as well), I^- is easier to polarize. Consequently, Na^+ can distort the electron distribution of I^- more than that of F^- pulling electron cloud closer and making NaI bond more covalent in character.

Exercises

E1.1 The energy of a hydrogenic ion, like He^+ or Be^{3+}, is defined by equation 1.3:

$$E_n = -\frac{Z^2 Rhc}{n^2}.$$

Both He^+ and Be^{3+} have ground state electronic configuration $1s^1$; thus, for both, the principal quantum number n in the above equation equals 1. For the ratio $E(He^+)/E(Be^{3+})$, after cancelling all constants, we obtain:

$$E(He^+)/E(Be^{3+}) = Z^2(He^+)/Z^2(Be^{3+}) = 2^2/4^2 = 0.25.$$

E1.2 The expression for E given in Equations 1.3 and 1.4 can be used for a hydrogen atom as well as for hydrogenic ions. For the ratio $E(H, n = 1)/E(H, n = 6)$, after canceling all constants, we obtain:

$$E(H, n = 1)/E(H, n = 6) = (1/1^2)/(1/6^2) = 36.$$

The value for $E(H, n = 1)$ has been given in the problem (13.6 eV). From this value and above ratio we can find $E(H, n = 6)$ as: $E(H, n = 6) = (E(H, n = 1))/36$ = 13.6eV/36 = 0.378 eV, and the difference is:

$$E(H, n = 1) – E(H, n = 6) = 13.6 \text{ eV} – 0.378 \text{ eV} = 13.2 \text{ eV}.$$

E1.3 When a photon emitted from the helium lamp collides with an electron in an atom, one part of its energy is used to ionize the atom while the rest is converted to the kinetic energy of the electron ejected in the ionization process. Thus, the total energy of a photon ($h\nu$) is equal to the sum of the first ionization energy (I_1) and the kinetic energy of an electron ($m_e v_e^2/2$):

$$h\nu = I_1 + \frac{m_e v_e^2}{2}.$$

From here the ionization energy is:

$$I_1 = h\nu - \frac{m_e v_e^2}{2}.$$

Since both krypton and rubidium atoms are ionized with the same radiation, we can calculate the energy of one photon emitted from the helium discharge lamp:

$$h\nu = h \times \frac{c}{\lambda} = 6.626 \times 10^{-34}\,\text{Js} \times \frac{2.998 \times 10^{8}\,\text{ms}^{-1}}{58.4 \times 10^{-9}\,\text{m}} = 3.40 \times 10^{-18}\,\text{J}\,.$$

Now we can calculate the first ionization energies using given velocities of respective electrons:

$$I_1^{Kr} = h\nu - \frac{m_e v_{e,Kr}^2}{2} = 3.40 \times 10^{-18}\,J - \frac{9.109 \times 10^{-31}\,\text{kg} \times \left(1.59 \times 10^{6}\,\text{ms}^{-1}\right)^2}{2} = 2.25 \times 10^{-18}\,\text{J}$$

$$I_1^{Rb} = h\nu - \frac{m_e v_{e,Rb}^2}{2} = 3.40 \times 10^{-18}\,J - \frac{9.109 \times 10^{-31}\,\text{kg} \times \left(2.45 \times 10^{6}\,\text{ms}^{-1}\right)^2}{2} = 6.68 \times 10^{-18}\,\text{J}\,.$$

Note that calculated energies are the first ionization energies per one atom because we used only one photon. To calculate the first ionization energies in eV as asked in the exercise, the above energies must be multiplied by the Avogadro's constant (to obtain the energies in J mol^{-1}) and then divided by the conversion factor 96485 J mol^{-1} eV^{-1} to obtain the values in eV:

$$I_{1,eV}^{Kr} = 2.25 \times 10^{-18}\,\text{J} \times \frac{6.022 \times 10^{23}\,\text{mol}^{-1}}{96485\,\text{Jmol}^{-1}\,\text{eV}^{-1}} = 14.0\,\text{eV}$$

$$I_{1,eV}^{Rb} = 6.68 \times 10^{-18}\,\text{J} \times \frac{6.022 \times 10^{23}\,\text{mol}^{-1}}{96485\,\text{Jmol}^{-1}\,\text{eV}^{-1}} = 4.16\ \text{eV}\,.$$

E1.4 The visible region starts when $n_1 = 2$. The next transition is for $n_2 = 3$. This can be determined using the Rydberg equation (Equation 1.1).

$$\frac{1}{\lambda} = R\left(\frac{1}{2^2} - \frac{1}{3^2}\right) = 1.524 \times 10^{-3}\,\text{nm}^{-1}\,.$$

And from the above result, $\lambda = 656.3$ nm.

E1.5 The principal quantum number n labels one of the shells of an atom. For a hydrogen atom or a hydrogenic ion, n alone determines the energy of all orbitals contained in a given shell (since there are n^2 orbitals in a shell, these would be n^2-fold degenerate). For a given value of n, the angular momentum quantum number l can assume all integer values from 0 to $n - 1$.

E1.6 Completed the table:

n	l	m_l	Orbital designation	Number of orbitals
2	**1**	**+1, 0, –1**	2p	**3**
3	2	**+2, +1, …, –2**	**3d**	**5**
4	**0**	**0**	4s	**1**
4	**3**	+3, +2, …, –3	**4f**	**7**

(Note: the table entries in bold are the sought solutions.)

E1.7 The plots of R (the radial part of the wavefunction ψ) vs. r shown in Figures 1.8 and 1.9 are plots of the radial parts of the total wavefunctions for the indicated orbitals. Notice that the function $R(2s)$ can take both positive and negative values (Figure 1.8), requiring that for some value of r the wavefunction $R(2s) = 0$ (i.e., the wavefunction has a node at this value of r; for a hydrogen atom or a hydrogenic ion, $R(2s) = 0$ when $r = 2a_0/Z$). Notice also that the plot of $R(2p)$ vs. r is positive for all values of r (Figure 1.9). Although a 2p orbital does have a node, it is not due to the radial part of the total wavefunction but rather due to the angular part, Y.

The radial distribution function is $P(r) = r^2R^2$ (for the s orbitals this expression is the same as $4\pi r^2\psi^2$). The plot of r^2R^2 vs. r for a 1s orbital in Figure 1.10 is a radial distribution function. Figure 1.12 provides plots of the radial distribution functions for the hydrogenic 2s and 2p orbitals.

Comparing the plots for 1s (Figure 1.10) and 2s (Figure 1.12) orbitals we should note that the radial distribution function for a 1s orbital has a single maximum, and that for a 2s orbital has two maxima and a minimum (at $r = 2a_0/Z$ for hydrogenic 2s orbitals). The presence of the node at $r = 2a_0/Z$ for $R(2s)$ requires the presence of the two maxima and the minimum in the 2s radial distribution function. Using the same reasoning, the absence of a radial node for $R(2p)$ requires that the 2p radial distribution function has only a single maximum, as shown in Figure 1.12.

E1.8 An orbital defined with the quantum number l has l nodal planes (or angular nodes). For a 4p set of atomic orbitals $l = 1$, and each 4p orbital has one nodal plane. The number of radial nodes is given by $n - l - 1$; and 4p orbitals have $4 - 1 - 1 = 2$ radial nodes. The total number of nodes is thus 3. (Note that the total number of nodes, angular and radial, is given by $n - 1$.)

E1.9 In an atom with more than one electron, as beryllium, the outer electrons (the 2s electrons in this case) are simultaneously attracted to the positive nucleus (the protons in the nucleus) and repelled by the negatively charged electrons occupying the same orbital. The two electrons in the 1s orbital on average are statically closer to the nucleus than the 2s electrons, thus the 1s electrons "feel" more positive charge than the 2s electrons. The 1s electrons also shield that positive charge from the 2s electrons, which are further out from the nucleus than the 1s electrons. Consequently, the 2s electrons "feel" less positive charge than the 1s electrons for beryllium.

E1.10 The second ionization energies of the elements calcium through manganese increase from left to right in the periodic table with the exception that $I_2(\text{Cr}) > I_2(\text{Mn})$. The electron configurations of the elements are:

Ca	Sc	Ti	V	Cr	Mn
$[Ar]4s^2$	$[Ar]3d^14s^2$	$[Ar]3d^24s^2$	$[Ar]3d^34s^2$	$[Ar]3d^54s^1$	$[Âr]3d^54s^2$

Both the first and the second ionization processes remove electrons from the 4s orbital of these atoms, except for Cr. In general, the 4s electrons are poorly shielded by the 3d electrons, so $Z_{\text{eff}}(4s)$ increases from left to right and I_2 also increases from left to right. While the I_1 process removes the sole 4s electron for Cr, the I_2 process must remove a 3d electron. The higher value of I_2 for Cr relative to Mn is a consequence of the special stability of half-filled subshell configurations and the higher Z_{eff} of a 3d electron vs. a 4s electron.

E1.11 The first ionization energies of strontium, barium, and radium are 5.69, 5.21, and 5.28 eV. Normally, atomic radius increases and ionization energy decreases down a group in the periodic table. However, in this case $I(\text{Ba}) < I(\text{Ra})$. Study the periodic table, especially the elements of Group 2 (the alkaline earth elements). Notice that Ba is 18 elements past Sr, but Ra is 32 elements past Ba. The difference between the two corresponds to the fourteen 4f elements (the lanthanoids) between Ba and Lu. Therefore, radium has a higher first ionization energy because it has such a large Z_{eff} due to the insertion of the lanthanides.

E1.12 See Example and Self-Test 1.7 in your textbook (if necessary review Section 1.5(a) of your textbook).

(a) C? Carbon is the sixth element in the periodic table and we have to sort six electrons in atomic orbitals obeying the build-up principle and the Hund's rule. Starting from the bottom we place two electrons in 1s, two in 2s (this fills both 1s and 2s) and finally two remaining electrons are placed in two different 2p orbitals with parallel spins. This gives us the configuration $1s^22s^22p^2$. Recognizing that $1s^2$ is in fact the electronic configuration of preceding noble gas helium, the short-hand configuration is $[He]2s^22p^2$. Follow the same principle for questions (b)–(f).

(b) F? Atomic number (Z) is 9, and nine electrons have to be sorted: $1s^22s^22p^2$ or $[He]2s^22p^5$.

(c) Ca? Z = 20, and 20 electrons: $1s^2 2s^2 2p^6 3s^2 3p^6 4s^2$ or $[Ar]4s^2$. Note that we have placed 19th and 20th electron in 4s and not 3d orbitals. Review section 1.4 of your textbook and pay attention to Figure 1.20 if you need further explanation for this apparent reversal in expected filling order.

(d) Ga^{3+}? Z = 31, Ga has 31 electrons, but we have to sort 28 because we are looking at a 3+ cation: $1s^2 2s^2 2p^6 3s^2 3p^6 3d^{10}$ or $[Ar]3d^{10}$. Note that Ga is just past the first row of the d-block so the 3d orbitals are filled.

(e) Bi? Z = 83 and 83 electrons. We have to be a bit careful here: before Bi in, the periodic table, we find d-block elements (La to Hg) of the sixth row, as well as elements Ce to Lu from the f-block. So Bi would have filled 5d and 4f atomic orbitals. Starting from the bottom we would have: $1s^2 2s^2 2p^6 3s^2 3p^6 3d^{10} 4s^2 4p^6 4d^{10} 4f^{14} 5s^2 5p^6 5d^{10} 6s^2 6p^3$ and $[Xe]4f^{14} 5d^{10} 6s^2 6p^3$. Note that Xe ends period 5 of the periodc table and has 5d and 4f subshells empty.

(f) Pb^{2+}? Z = 82, but 80 electrons (because it is a 2+ cation): $1s^2 2s^2 2p^6 3s^2 3p^6 3d^{10} 4s^2 4p^6 4d^{10} 4f^{14} 5s^2 5p^6 5d^{10} 6s^2$ or $[Xe]4f^{14} 5d^{10} 6s^2$.

E1.13 Following instructions for Question 1.12:

(a) W? Z = 74. If you assumed that the configuration would resemble that of chromium, you would write $[Xe]4f^{14} 5d^5 6s^1$. It turns out that the actual configuration is $[Xe]4f^{14} 5d^4 6s^2$. The configurations of the heavier d- and f-block elements show some exceptions to the trends for the lighter d-block elements.

(b) Rh^{3+}? Z = 45 but 3+ charge leaves us with 42 electrons to sort: $1s^2 2s^2 2p^6 3s^2 3p^6 3d^{10} 4s^2 4p^6 4d^6$ or $[Kr]4d^6$.

(c) Eu^{3+}? Z = 63 but 3+ charge leaves us with 61 electrons to sort (similar to Gd^{3+} in the previous Exercise) $1s^2 2s^2 2p^6 3s^2 3p^6 3d^{10} 4s^2 4p^6 4d^{10} 4f^7 5s^2 5p^6$ or $[Xe]4f^6$.

(d) Eu^{2+}? This will have one more electron than Eu^{3+}. Therefore, the ground-state electron configuration of Eu^{2+} is $[Xe]4f^7$.

(e) V^{5+}? Z = 23 but with its 5+ charge it has the *same* number of electrons (18) and electron configuration as Ar: $1s^2 2s^2 2p^6 3s^2 3p^6$ or $[Ar]3d^0$. See the note for Exercise 1.24(f) above.

(f) Mo^{4+}? Z = 42 but 4+ charge leaves us with 38 electrons to sort: $1s^2 2s^2 2p^6 3s^2 3p^6 3d^{10} 4s^2 4p^6 4d^2$ or $[Kr]4d^2$.

E1.14 See Figure 1.22 and the front of this book. You should start learning the names and positions of elements that you do not know. Start with the alkali metals and the alkaline earths. Then learn the elements in the p block. A blank periodic table can be found on the inside back cover of this book. You should make several photocopies of it and should test yourself from time to time, especially after studying each chapter. This will equip you with a very important skill for mastering inorganic chemistry: being able to navigate through the periodic table is essential for many topics covered in this book.

E1.15 To follow the answer for this question you should have a copy of the periodic table of elements in front of you. If you look at Table 1.3 in your textbook, you will see that this is a general trend. Normally, the period 6 elements would be expected to have larger metallic radii than their period 5 vertical neighbours; only Cs and Ba follow this trend; Cs is larger than Rb and Ba is larger than Sr. Lutetium, Lu, is significantly smaller than yttrium, Y, and Hf is almost the same size as Zr. The same similarity in radii between the period 5 and period 6 vertical neighbours can be observed for the rest of the d-block. This phenomenon can be explained as follows. There are no intervening elements between Sr and Y, but there are 14 intervening elements, the lanthanides, between Ba and Lu. A contraction of the radii of the elements starting with Lu is due to incomplete shielding by the 4f electrons. By the time we pass the lanthanides and reach Hf and Ta, the atomic radii have been contracted so much that the d-block period 6 elements have almost identical radii to their vertical neighbours in the period 5.

E1.16 Mulliken defined electronegativity as an average value of the ionization energy (I) and electron affinity (E_a) of the element, that is, $\chi_M = ½ (I + E_a)$, thus making electronegativity an atomic property (just like atomic radius or ionization energy). Since both I and E_a should have units eV for Mulliken electronegativity scale, the data in Tables 1.6 and 1.7 have to be converted from J/mol to eV (these can also be found in the Resource Section 2 of your textbook). The graph below plots variation of $I_1 + E_a$ (vertical axis) across the second row of the

periodic table. The numbers next to the data points are the values of Mulliken electronegativity for the element shown on the x-axis. As we can see, the trend is almost linear, supporting Mulliken's proposition that electronegativity values are proportional to $I + E_a$. There are, however, two points on the plot, namely for B and O, that significantly deviate from linearity. Boron (B) should have significatly higher electronegativity than lithium (Li) because: (1) its I_1 is higher than that for Li and (2) B's E_a is more negative than Li's. This discrepancy is due to the fact that Mulliken's electronegativity scale does not use I and E_a values for the atomic ground-states (which are the values of I_1 and E_a used to construct the above graph). It rather uses the values for valence states; for boron this state is $2s^1 2p^1\ 2p^1$ (an elctronic state that allows B atom to have its normal valency 3). It is easier to remove the electron from B's valence configuration and the I_1 drops resulting in lower-than-expected electronegativity for B. Similarly, the graph uses E_{a1} for oxygen (which is positive). Oxygen's normal valency, however, is 2, and its E_{a2} (which should also be taken in consideration) has negative value.

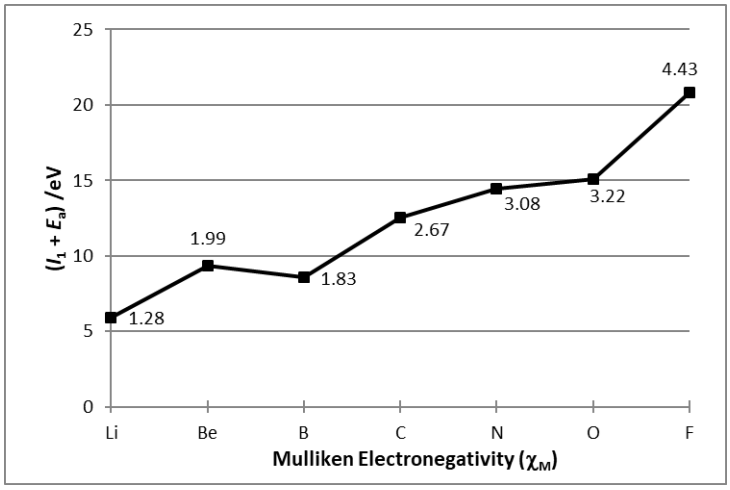

Chapter 2 Molecular Structure and Bonding

Self-Tests

S2.1 **a)** One phosphorus and three chlorine atoms supply 5 + (3 × 7) = 26 valence electrons. Since P is less electronegative than Cl, it is likely to be the central atom, so the 13 pairs of electrons are distributed as shown below. In this case, each atom obeys the octet rule. Whenever it is possible to follow the octet rule without violating other electron counting rules, you should do so.

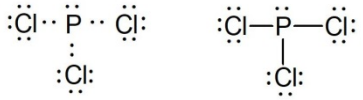

b) BF_3 has in total 3 + 3×7 = 24 valence electrons or 12 electron pairs. B atom is less electronegative and it is a likely central atom. The 12 electron pairs can be distributed as follows:

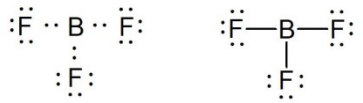

S2.2 The Lewis structures and the shapes of H_2S, XeO_4, and SOF_4 are shown below. According to the VSEPR model, electrons in bonds and in lone pairs can be thought of as charge clouds that repel one another and stay as far apart as possible. First, write a Lewis structure for the molecule, and then arrange the lone pairs and atoms around the central atom, such that the lone pairs are as far away from each other as possible.

Lewis Structures		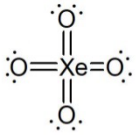	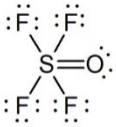
Molecular geometry (shape of the molecule)	 bent	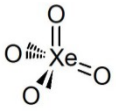 tetrahedral	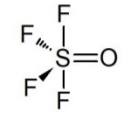 trigonal bipyramidal

All atoms in both structures have formal charges of zero. The actual structure of XeO_4 is tetrahedral; it is a highly unstable colourless gas. Note that the oxygen atom in SOF_4 molecules lies in one plane with two fluorine atoms. This is because the double bonds contain higher density of negative charge and cause higher repulsion in comparison to single bonds. Placing O atom and four electrons forming S=O bond in equatorial plane reduces repulsion.

S2.3 The Lewis structures and molecular shapes for XeF_2 and ICl_2^+ are shown below. The XeF_2 Lewis structure has an octet for the 4 F atoms and an expanded valence shell of 10 electrons for the Xe atom, with the 8 + (2 × 7) = 22 valence electrons provided by the three atoms. The five electron pairs around the central Xe atom will arrange themselves at the corners of a trigonal bipyramid (as in PF_5). The three lone pairs will be in the equatorial plane, to minimize lone pair–lone pair repulsions. The resulting shape of the molecule, shown at the right, is linear (i.e., the F–Xe–F bond angle is 180°).

Two chlorine atoms and one iodine atom in total have 21 electrons. However, we have a cationic species at hand, so we have to remove one electron and start with a total of 20 valence electrons for ICl_2^+. That gives a Lewis structure in which iodine is a central atom (being the more electropositive of the two) and is bonded to two chlorines with a single bond to each. All atoms have a precise octet. Looking at iodine, there are two bonding

electron pairs and two lone electron pairs making overall tetrahedral electron pair geometry. The lone pair–bonding pair repulsion is going to distort the ideal tetrahedral geometry lowering the Cl – I – Cl angle to less than 109.5°, resulting in bent molecular geometry.

Lewis structure	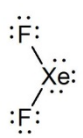	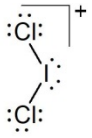
Molecular geometry (shape of the molecule)	F—Xe—F linear	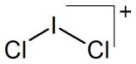 bent

S2.4 **(a)** Figure 2.17 gives the distribution of electrons in molecular orbitals of O_2 molecule. We see that $1\pi_g$ level is a set of two degenerate (of same energy) molecular orbitals. Thus, following the Hund's rule, we obtain the $1\pi_g^2$ electronic configuration of O_2 molecule by placing one electron in each $1\pi_g$ orbital with spins parallel. This gives two unpaired electrons in O_2 molecule.

If we add one electron to O_2 we obtain the next species, the anion O_2^-. This extra electron continues to fill $1\pi_g$ level but it has to have an antiparallel spin with respect to already present electron. Thus, after O_2 molecule receives an electron, one electron pair is formed and only one unpaired electron is left.

Addition of second electron fills $1\pi_g$ set, and O_2^{2-} anion has no unpaired electrons.

(b) The first of these two anions, S_2^{2-}, has the same Lewis structure as peroxide, O_2^{2-}. It also has a similar electron configuration to that of peroxide, except for the use of sulfur atom valence 3s and 3p atomic orbitals instead of oxygen atom 2s and 2p orbitals. There is no need to use sulfur atom 3d atomic orbitals, which are higher in energy than the 3s and 3p orbitals, because the 2(6) + 2 = 14 valence electrons of S_2^{2-} will not completely fill the stack of molecular orbitals constructed from sulfur atom 3s and 3p atomic orbitals. Thus, the electron configuration of S_2^{2-} is $1\sigma_g^2 2\sigma_u^2 3\sigma_g^2 1\pi_u^4 2\pi_g^4$. The Cl_2^- anion contains one more electron than S_2^{2-}, so its electron configuration is $1\sigma_g^2 2\sigma_u^2 3\sigma_g^2 1\pi_u^4 2\pi_g^4 4\sigma_u^1$.

S2.5 ClO^- anion is isoelectronic (has the same number of electrons) with ICl. The orbitals to be used are chlorine's 3s and 3p valence shell orbitals and the oxygen's 2s and 2p valence shell orbitals. The bonding orbitals will be predominantly O in character being that O is more electronegative but the MO diagram of ClO^- will be similar to ICl. We have seven valence electrons from Cl, six from O and one for negative charge giving us a total of 14 electrons. Therefore, the ground-state electron configuration is $1\sigma^2 2\sigma^2 3\sigma^2 1\pi^4 2\pi^4$, same as ICl.

S2.6 **a)** The number of valence electrons for C_2^{2-} is equal to 10 (4 + 4 + 2 (for charge)). Thus C_2^{2-} is isoelectronic with N_2 (which has 10 valence electrons as well). The configuration of C_2^{2-} would be $1\sigma_g^2 1\sigma_u^2 1\pi_u^4 2\sigma_u^2$. The bond order would be ½[2–2+4+2] = 3. C_2^{2-} has a triple bond.

b) The number of valence electrons for Ne_2 is 16. The electronic configuration is $1\sigma_g^2 1\sigma_u^2 2\sigma_g^2 1\pi_u^4 1\pi_g^4 2\sigma_u^2$. The bond order is ½ [2–2+2+4–4–2] = 0. In this case the bond order is 0 because the bonding and antibonding MOs are equally populated. Consequently the molecule Ne_2 does not exist.

S2.7 In general, the more bonds you have between two atoms, the shorter the bond length and the stronger the bond. Therefore, the ordering for bond length going from shortest to longest is C≡N, C=N, and C–N. For bond strength, going from strongest to weakest, the order is C≡N > C=N > C–N.

S2.8 **a)** The synthesis reaction is:

$$H_2 + F_2 \rightarrow 2HF$$

Looking at the reaction we see that 1 mol of H–H and 1 mol of F–F bonds must be broken. Therfore, we must use 436 kJ mol^{-1} for H_2 and 155 kJ mol^{-1} for F_2 to break the bonds. On the right side of the reaction we form 2 mols of HF, indicating that 2×565 kJ mol^{-1} has been released. Accounting the use and release of energies with plus and minus signs respectively, we have:

$$\Delta_f H = +436 \text{ kJ mol}^{-1} + 155 \text{ kJ mol}^{-1} - (2\times565 \text{ kJ mol}^{-1}) = -539 \text{ kJ mol}^{-1}$$

b) You can prepare H_2S from H_2 and S_8 in the following reaction:

$$^1/_8S_8 \; + \; H_2 \rightarrow \; H_2S$$

On the left side, you must break one H–H bond and produce one sulfur atom from cyclic S_8. Since there are eight S–S bonds holding eight S atoms together, you must supply the mean S–S bond enthalpy *per S atom*. On the right side, you form two H–S bonds. From the values given in Table 2.8, you can estimate:

$$\Delta_f H = +436 \text{ kJ mol}^{-1} + \; 264 \text{ kJ mol}^{-1} \; - \; (2\times338 \text{ kJ mol}^{-1}) \; = 24 \text{ kJ mol}^{-1}$$

This estimate indicates a slightly endothermic enthalpy of formation, but the experimental value, –21 kJ mol^{-1}, is slightly exothermic.

S2.9 **(a)** The Pauling electronegativity values from Table 1.7 for Be and F are 1.57 and 3.98 respectively. The difference in electronegativities is:

$$\Delta\chi = 3.98 - 1.57 = 2.41$$

The average electronegativity is:

$$\chi_{mean} = (3.98 + 1.57)/2 = 2.77$$

These values place BeF_2 within the ionic bonding region.

(b) Following the same procedure and taking the electronegativity values χ(N) = 3.04 and χ(O) = 3.44 we get:

$$\Delta\chi = 3.44 - 3.04 = 0.40 \text{ and } \chi_{mean} = (3.44 + 3.04)/2 = 3.24$$

These two values place NO within the covalent bonding region.

Exercises

E2.1 **a)** NO^+ has in total 10 valence electrons (5 from N + 6 from O and –1 for a positive charge). The most feasible Lewis structure is the one shown below with a triple bond between the atoms and an octet of electrons on each atom.

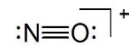

b) ClO^- has in total 16 valence electrons (7 from Cl + 6 from O + 1 for a negative charge). The most feasible Lewis structure is the one shown below with a single Cl–O bond and an octet of electrons on both atoms.

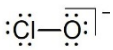

c) H_2O_2 has 14 valence electrons and the most feasible Lewis structure is shown below. Note that the structure requires O–O bond.

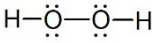

d) The most feasible Lewis structure for CCl_4 is shown below. Each element has a precise octet.

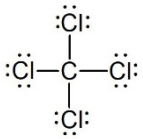

e) The most feasible Lewis structure for HSO_3^- is shown below. Being the most electropositive of the three elements, sulfur is the central atom.

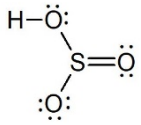

E2.2 **a)** The Lewis structure for hydrogen selenide, H_2Se, is shown below. The shape would be expected to be bent with the H–Se–H angle less than 109°. However, the angle is actually close to 90°, indicative of considerable p character in the bonding between S and H.
b) The BF_4^- structure is shown below (for the Lewis structure see Example 2.1 of your textbook). The shape is tetrahedral with all angles 109.5°.
c) The NH_4^+ structure of the ammonium ion is shown below. Again, the shape is tetrahedral with all angles 109.5°.

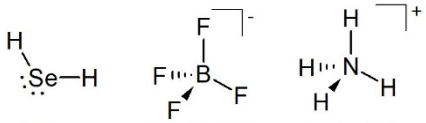

E2.3 **a)** The central iodine atom in IF_6^+ is bonded to the six fluorine atoms through sigma bonds and has no lone electron pairs. Thus, the six bonding electron pairs repel each other equally and the cation has octahedral geometry.

b) In this case the central iodine atom forms three sigma bonds with three fluorine atoms and has two lone electron pairs. These lone electron pairs and one fluorine atom would form a trigonal plane with two more fluorine atoms residing above and below that plane. Overall electron group geometry would then be trigonal bipyramidal but molecular geometry would be T-shaped.

c) The central xenon atom forms single bonds with four fluorine atoms and a double bond with one oxygen atom. It also has a lone electron pair. Thus, the electron group geometry would be octahedral, but the molecular geometry is square pyramidal.

The Lewis structures and molecular shapes for each species a) – c) are summarized in the table below:

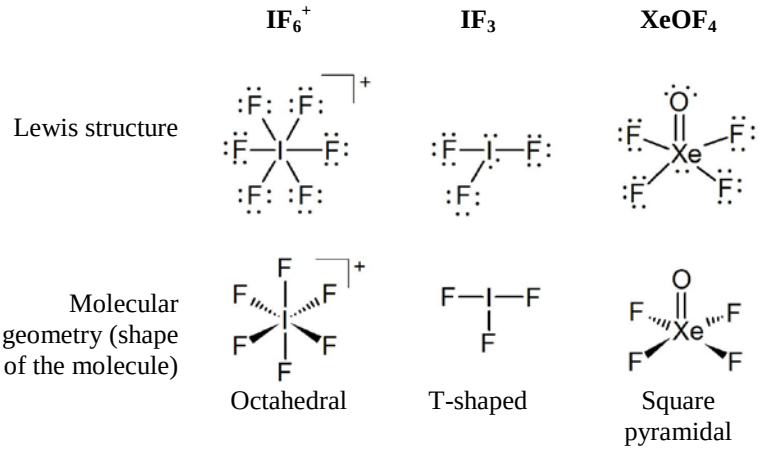

E2.4 The Lewis structure of ICl_6^- and its geometry based on VSEPR theory is shown below. The central iodine atom is surrounded by six bonding and one lone pair. However, this lone pair in the case of ICl_6^- is a *stereochemically inert* lone electron pair. This is because of the size of iodine atom—large size of this atom spread around all seven

electron pairs resulting in a minimum repulsion between electron pairs. Therefore, all bond angles are expected to be equal to 90° with overall octahedral geometry.

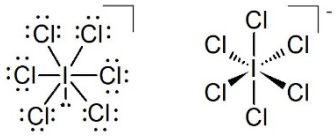

The VSEPR model and actual structure of SF_4 are shown below. Remember, lone pairs repel bonding regions, read Section 2.3 (b). The VSEPR theory predicts a see-saw structure with a bond angle of 120° between the S and equatorial F's and a bond angle of 180° between the S and the axial F's. The bond angle is actually 102° for the S and equatorial F's and 173° for the S and the axial F's. This is due to the equatorial lone pair repelling the bonding S-F atoms.

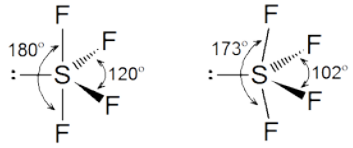

VSEPR model Actual structure

E2.5 **a)** From the covalent radii values given in Table 2.7, 77 pm for single-bonded C and 99 pm for Cl, the C–Cl bond length in CCl_4 is predicted to be 77 pm + 99 pm = 176 pm. The agreement with the experimentally observed value of 177p m is excellent.

b) The covalent radius for Si is 118 pm. Therefore, the Si–Cl bond length in $SiCl_4$ is predicted to be 118 pm + 99 pm = 217 pm. This is 8% longer than the observed bond length, so the agreement is not as good as in the case of C – Cl.

c) The covalent radius for Ge is 122 pm. Therefore, the Ge–Cl bond length in $GeCl_4$ is predicted to be 221 pm. This is 5% longer than the observed bond length.

E2.6 You need to consider the enthalpy difference between one mole of Si=O double bonds and two moles of Si–O single bonds. The difference is:

$$2(\text{Si–O}) - (\text{Si=O}) = 2\times(466\ \text{kJ mol}^{-1}) - (640\ \text{kJ mol}^{-1}) = 292\ \text{kJ mol}^{-1}.$$

Therefore, the two single bonds will always be better enthalpically than one double bond. If silicon atoms only have single bonds to oxygen atoms in silicon-oxygen compounds, the structure around each silicon atom will be tetrahedral: each silicon will have four single bonds to four different oxygen atoms.

E2.7 Consider the reaction:

$$2H_2(g) + O_2(g) \rightarrow 2H_2O(g).$$

Since you must break two moles of H–H bonds and one mole of O=O bonds on the left-hand side of the equation and form four moles of O–H bonds on the right-hand side, the enthalpy change for the reaction can be estimated as:

$$\Delta H = 2\times(436\ \text{kJ mol}^{-1}) + 497\ \text{kJ mol}^{-1} - 4\times(463\ \text{kJ mol}^{-1}) = -483\ \text{kJ mol}^{-1}.$$

The experimental value is –484 kJ, which is in closer agreement with the estimated value than ordinarily expected. Since Table 2.8 contains average bond enthalpies, there is frequently a small error when comparing estimates to a specific reaction.

E2.8 Consider the first reaction:

$$S_2^{2-}(g) + {}^1/_4S_8(g) \rightarrow S_4^{2-}(g).$$

Hypothetically, two S–S single bonds (of S_8) are broken to produce two S atoms, which combine with S_2^{2-} to form two new S–S single bonds in the product S_4^{2-}. Since two S–S single bonds are broken and two are made, the net enthalpy change is zero.

Now consider the second reaction:

$$O_2^{2-}(g) + O_2(g) \rightarrow O_4^{2-}(g).$$

Here there is a difference. A mole of O=O double bond of O_2 is broken, and two moles of O–O single bonds are made. The overall enthalpy change, based on the mean bond enthalpies in Table 2.8, is:

$$O{=}O - 2{\times}(O{-}O) = 497 \text{ kJ mol}^{-1} - 2{\times}(146 \text{ kJ mol}^{-1}) = 205 \text{ kJ mol}^{-1}.$$

The large positive value indicates that this is not a favourable process.

E2.9 The differences in electronegativities are AB 0.5, AD 2.5, BD 2.0, and AC 1.0. The increasing covalent character is AD < BD < AC < AB.

E2.10 **a)** BCl_3 has a trigonal planar geometry, according to Table 2.4, the most likely hybridization would be sp^2.

b) NH_4^+ has a tetrahedral geometry, so the most likely hybridization would be sp^3.

c) SF_4 has distorted see-saw geometry, with the lone pair occupying one of the equatorial sites, see Exercise 2.4 above. Therefore, it would be sp^3d or spd^3.

d) XeF_4 has a square planar molecular geometry with two lone pairs on the central Xe atom, so its hybridization is sp^3d^2.

E2.11 **a) Be_2^+?** Two Be atoms have in total four valence electrons. We have to remove one to account for a positive charge of this diatomic cation. This gives the electron configuration $1\sigma_g^2 1\sigma_u^1$. The HOMO (highest occupied molecular orbital) for Be_2 is a σ ungerade antibonding orbital formed from two 2s atomic orbitals, shown below. (The black spheres are atomic nuclei; different shading represents two opposite phases of the orbital wavefunctions. The same applies for the solutions b) – d).)

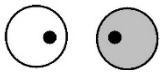

b) B_2^-? Two boron atoms have six valence electrons in total. We have to add one more to account for the negative charge. The electron configuration is $1\sigma_g^2 1\sigma_u^2 1\pi_u^3$. The HOMO for B_2 is a π ungerade bonding MO, shown below.

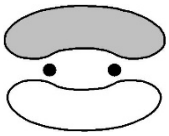

c) C_2^-? The total number of valence electrons is eight, but we again have to add one electron to account for the negative charge. The electron configuration is $1\sigma_g^2 1\sigma_u^2 1\pi_u^4 2\sigma_g^1$. The HOMO for C_2^- is a σ bonding MO formed from mixing two 2p atomic orbitals, shown below.

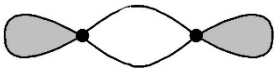

(d) F_2^+? The total number of valence electrons is 14 (seven from each F atom) but we must subtract one to account for the plus one charge. The electron configuration is $1\sigma_g^2 1\sigma_u^2 2\sigma_g^2 1\pi_u^4 1\pi_g^3$. The HOMO for F_2^+ is a π gerade antibonding MO, shown below.

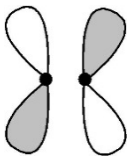

E2.12 The configuration of C_2^{2-} would be $1\sigma_g^2 1\sigma_u^2 1\pi_u^4 2\sigma_g^2$. The bond order would be ½[2–2+4+2] = 3. So C_2^{2-} has a triple bond, as discussed in the self test S2.6, above. The HOMO is in a sigma bonding orbital.

The configuration for the neutral C_2 would be $1\sigma_g^2 1\sigma_u^2 1\pi_u^4$ (see Figure 2.17). The bond order would be ½[2–2+4] = 2.

E2.13 Your molecular orbital diagram should look like Figure 2.22 showing the MO diagram for CO molecule. There are several important differences between this diagram and that for C_2 from Exercise 2.12. First, the energies of B and N atomic orbitals are different. The atomic orbitals on N atom are lower in energy than corresponding atomic orbitals on B atom. Recall from Chapter 1 that N should have lower atomic radius and higher Z_{eff} than B. These differences result in higher stability (lower energy) of N atomic orbitals. Also, nitrogen is more electronegative than boron. Thus, B atom should be on the left-hand side, and N should be on the right-hand side of your diagram. Second, because of this difference in the atomic orbital energies, the MO are localized differently. For example, while all MO orbitals in C_2 molecule were equally localized over both nuclei (because the molecule is homonuclear), in the case of BN, 1σ is more localized on N while 2σ is more localized on B. BN molecule has a total of eight valence electrons (three from B atom and five from N atom). Thus, after we fill the MOs with electrons we should get the following electronic configuration $1\sigma^2 2\sigma^2 1\pi^4$. This means that a degenerate set of two 1π molecular orbitals is HOMO of BN while empty 3σ are LUMO of this molecule.

E2.14 **a)** The electron configuration of S_2 molecule is $1\sigma_g^2 1\sigma_u^2 2\sigma_g^2 1\pi_u^4 1\pi_g^2$. The bonding molecular orbitals are $1\sigma_g$, $1\pi_u$, and $2\sigma_g$, while the antibonding molecular orbitals are $1\sigma_u$, and $1\pi_g$. Therefore, the bond order is ½ ((2 + 4 + 2) – (2 + 2)) = 2, which is consistent with the double bond between the S atoms as predicted by Lewis theory.

b) The electron configuration of Cl_2 is $1\sigma_g^2 2\sigma_u^2 3\sigma_g^2 1\pi_u^4 2\pi_g^4$. The bonding and antibonding orbitals are the same as for S_2, above. Therefore, the bond order is (1/2)((2 + 4 + 2) – (2 + 4)) = 1 again as predicted by Lewis theory.

c) The electron configuration of NO^+ is $1\sigma^2 1\sigma^2 2\sigma^2 1\pi^4$. The bond order for NO^+ is ½ ((2 + 2 +4) – 2) = 3, as predicted by the Lewis theory.

E2.15 Recall from Section 2.8(b) that molecular frontier orbitals are lowest unoccupied molecular orbital (LUMO) and highest occupied molecular orbital (HOMO). It is also good to have Figures 2.12, 2.17 and 2.18 in front while analysing this exercise.

For C_2^{2-}: In Exercise 2.23 we have seen that the electronic configuration of C_2^{2-} is $1\sigma_g^2 1\sigma_u^2 1\pi_u^4 2\sigma_g^2$. From this configuration we see that the HOMO of this anion is $2\sigma_g$. This MO is bonding and formed from overlap of two p_z atomic orbitals. (If you do not know this already, refer to Figure 2.18 and keep in mind that σ orbitals must have cylindrical symmetry. Note that this orbital also has some contribution form 2s atomic orbitals; but for this type of analysis, this contribution can be neglected because $2\sigma_g$ is close in energy to atomic 2p orbitlas.). The HOMO can be sketched as

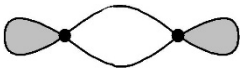

Now refer to Figure 2.17. The next orbital, one step higher in energy, is $1\pi_g$. It is a set of two degenerate, unoccupied MOs forming a LUMO frontier orbital. These are formed in π-overlap from p_x and p_y atomic orbitals. One of the $1\pi_g$ is sketched below.

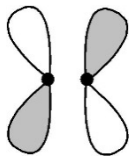

LUMO is the last bonding MO for C_2^{2-}; higher in energy are empty antibonding orbitals. Adding electrons to HOMO would decrease the bond order and weaken the C–C bond in the anion.

For N_2: Note that N_2 and C_2^{2-} are isolelectronic (they have the same number of electrons). Thus, the same discussion applies for N_2 and the frontier orbitals would look the same. The major difference between the MOs of these two chemical species is in relative energies of molecular orbitals. The atomic orbitals on N atom are lower in energy than corresponding orbitals on C atom. Consequently, the MOs of N_2 molecule are lower in energy than C_2^{2-}. The same sketches as above as well as chemical consequences.

For CO: Refer to the Figure 2.23 of your textbook. From the diagram, we can see that the frontier orbitals are 3σ (HOMO) and doubly degenerate set of 2π MOs. The figure also shows simple sketches of these orbitals. Note that the smaller orbital lobes are located on O atom because oxygen atomic orbitals are lower in energy than carbon's. Because of this difference and electron configuration, CO molecule is polar with negative side of the dipol oriented towards C atom. Adding an electron to CO molecule would decrease CO bond order, elongate the bond and weaken it.

For O_2: Referring to figure 2.17 again we see that HOMO of O_2 is doubly degenerate set of $1\pi_g$ while LUMO is $2\sigma_u$. LUMO orbitals are formed from p_x and p_y atomic orbitals and their sketch looks like the one for C_2^{2-} above. The HOMO is antibonding σ_u MO formed from p_z atomic orbitals and can be sketched as:

Both HOMO and LUMO are antibonding MOs and adding electrons would significantly weaken O–O bond. At the same time the paramagnetic character of this molecule would decrease as well (see Example 2.4).

E2.16 Four atomic orbitals can yield four independent linear combinations, each giving one molecular orbital. The four relevant ones for a hypothetical linear H_4 molecule are shown on the left, and for a hypothetical square H_4 on the right. The orbital energies are increasing from bottom to top. The most stable orbital has the fewest nodes, the next orbital in energy has only one node, and so on to the fourth and highest energy orbital. Note that for the square geometry two linear combinations have one node only and, consequently, have the same energy – they form a doubly degenerate set.

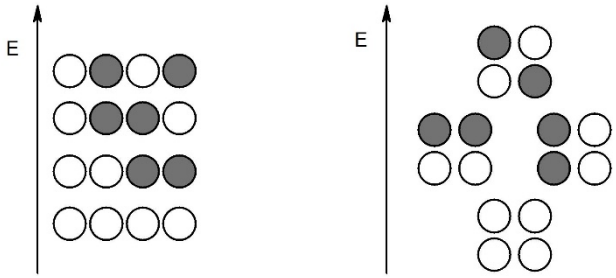

Both linear and square geometry produce the same number of MOs and must accommodate the same number of electrons – four (one from each H atom). Looking at the linear molecule (left hand diagram) we can place two electrons in the lowest MO and two electrons in the next MO. Thus, all electrons are paired and the linear H_4 molecule is diamagnetic. The square geometry also accepts two electrons in the lowest MO, but the degenerate set of two orbitals that come next accept one electron each (recall Hund's rule). SO, square H_4 has two unpaired electrons and is paramagnetic.

Molecular orbitals of linear $[HHeH]^{2+}$? The three atoms of $[HHeH]^{2+}$ will form a set of three molecular orbitals; one bonding, one nonbonding, and one antibonding. They are shown below. You should note that

helium's 1s atomic orbital is lower in energy than 1s in hydrogen atom. Therefore, He 1s orbital contributes more to the bonding MO than hydrogen's 1s. Since $[HHeH]^{2+}$ has two electrons, only the bonding orbital is filled.

Helium, being a noble gas and unreactive, holds tight to its electrons and is not keen on losing them or sharing them; thus it is unlikely that $[HHeH]^{2+}$ would last long and would decompose to $2H^+$ and He. In isolation the cation should be only moderately stable. There are two reasons for this low stability: (1) Although only the bonding MO is filled, it spans over three nuclei, making the average H–He bond order about 0.5 (note that bond order 1 requires two electrons shared between two nuclei; here we have two electrons shared between three nuclei–situation referred to as 3 centre-2 electron bonding); (2) H and (particularly) He are small atoms. Bonding them together brings three nuclei in proximity: +/2+/+ repulsion between H–He–H nuclei is going to be strong particularly because it is "diluted" by only two electrons.

In solution it would be unstable particularly with respect to proton transfer to another chemical species that can act as a base, such as the solvent or counterion. Removal of one proton would produce HeH^+, a species with lower positive charge and H–He bond order of 1. Any substance is more basic than helium.

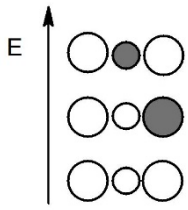

E2.17 **(a) Square H_4^{2+}?** The drawing below shows a square array of four hydrogen atoms. Clearly, each line connecting any two of the atoms is not a typical bond in which two electrons are shared between two nuclei because this molecular ion has only two electrons and is electron deficient. It is a hypothetical example of (4c,2e) bonding. We cannot write a Lewis structure for this species. It is not likely to exist; it should be unstable with respect to two separate H_2^+ diatomic species.

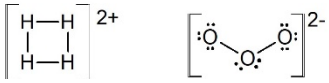

(b) Angular O_3^{2-}? A proper Lewis structure for this 20-electron ion is shown above. Therefore, it is electron precise. It could very well exist.

Chapter 3 The Structures of Simple Solids

Self-Tests

S3.1 By examining Figures 3.7 and 3.32, we note that the caesium cations sit on a primitive cubic unit cell (lattice type P) with chloride anion occupying the cubic hole in the body centre. Alternatively, one can view the structure as P-type lattice of chloride anions with caesium cation in cubic hole. Keep in mind that caesium chloride does not have a body centred cubic lattice although it might appear so at a first glance. The body centred lattice has all points identical, whereas in CsCl lattice the ion at the body centre is different from those at the corners.

S3.2 The 3D structure of SiS_2 is shown below:

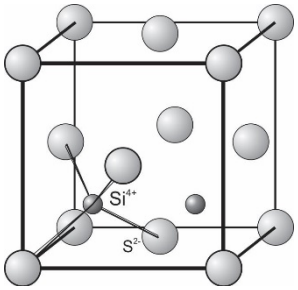

S3.3 **a)** Figures 3.3 and 3.23 show the primitive cubic unit cell. Each unit cell contains one sphere (equivalent to 8 × 1/8 spheres on the vertices of the cell in contact along the edges). The volume of a sphere with radius r is $4/3\times\pi\times r^3$, whereas the volume of the cubic unit cell is $a^3 = (2r)^3$ (where a is a length of the edge of the unit cell). Thus, the fraction filled is $\frac{3/4\,\pi r^3}{(2r^3)} = 0.52$: 52% of the volume in the primitive cubic unit cell is filled.

b) Figures 3.8 and 3.29(a, the structure of iron) show the body-centred unit cell. Each unit cell contains two spheres (one in the middle of the cell and an equivalent of one sphere at eight corners of a cube, see part (i) above). The volume of a sphere is $4/3\ \pi r^3$ (where r is the sphere radius), thus the total volume is $2\times 4/3\ \pi\ r^3 = 8/3\ \pi\ r^3$. Now, we have to find a way to represent the length of the unit cell, a, in terms of r. In a body-centred cubic unit cell the spheres are in contact along the space diagonal of the cube (labelled D on the figure below). Thus

$$D = r + 2r + r = 4r \qquad (1)$$

based on the same arguments as in Example 3.3.

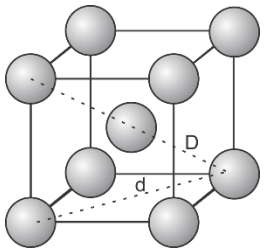

If we apply Pythagoras' theorem to this case, we obtain

$$D^2 = d^2 + a^2, \qquad (2)$$

where d is the length of a face diagonal of the cube and a the length of cube's edge. As we have also seen in the Example 3.3, the face diagonal of the cube can be calculated from $d^2 = 2a^2$. Substituting this result in equation (1) above, we have:

$$D = 2a^2 + a^2 = 3a^2. \qquad (3)$$

Finally, we can square the result in (1) and equate this to (3) to obtain the relationship between r and a in a body-centred unit cell as:

$$16r^2 = 3a^2, \text{ and } a = \frac{4r}{\sqrt{3}}.$$

From here the volume of the cell is $a^3 = \frac{64r^3}{(\sqrt{3})^3}$. Thus the fraction of space occupied by identical spheres in this unit cell is:

$$\frac{\frac{8}{3}\pi r^3}{\frac{64r^3}{(\sqrt{3})^3}} = \frac{8\pi(\sqrt{3})^3}{3\times 64} = 0.68 \text{ or } 68\%.$$

From these results and Example 3.3, it becomes clear that closed-packed cubic lattice has the best space economy (best packing, least empty space), followed by the body-centred lattice, whereas the simple cubic packing has the lowest space economy with the highest fraction of unoccupied space.

S3.4 See Figure 3.19b for important distances and geometrical relations. Note that the distance S–T = $r + r_{hole}$, by definition. Therefore, you must express S–T in terms of r. Note also that S–T is the hypotenuse of the right triangle STX, with sides SX, XT, and TS. Point X is at the midpoint of line SS, and because SS = 2r, so SX = r. The angle θ is 54.74°, one-half of the tetrahedral angle S–T–S (109.48°). Therefore, sin 54.74° = $r/(r + r_{hole})$, and r_{hole} = 0.225r. This is the same as $r_{hole} = ((3/2)^{1/2} - 1)r$.

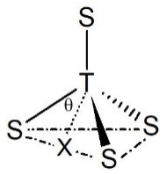

S3.5 The position of tetrahedral holes in a ccp unit cell is shown in Figure 3.20(b). From the figure, we see that each unit cell contains eight tetrahedral holes, each inside the unit cell. As outlined in Example 3.5, the ccp unit cell has four identical spheres. Thus, the spheres-to-tetrahedral holes ratio in this cell is 4 : 8 or 1 : 2.

S3.6 The ccp unit cell contains four silver atoms that weigh together (4 mol Ag × 107.87 g/mol)/(6.022 × 10^{23} Ag/mol) g or 7.165 × 10^{-22} g. The volume of the unit cell is a^3, where a is the length of the edge of the unit cell. The density equals mass divided by volume or:

$$10.5 \text{ g cm}^{-3} = 7.165 \times 10^{-22} \text{ g} / a^3 \text{ with } a \text{ in cm}$$

$$a = 4.09 \times 10^{-8} \text{ cm or } 409 \text{ pm}$$

S3.7 For the bcc structure, $a = 4r/\sqrt{3}$. This relation can be derived simply by considering the right triangle formed from the body diagonal, face diagonal, and edge of the bcc unit cell (see also self-test 3.3(a) above). Using the Pythagorean theorem, we have $(4r)^2 = a^2 + (a\sqrt{2})^2$. Solving for a in terms of r, we have $a = 4r/\sqrt{3}$. From Example 3.7, we know that the metallic radius of Po is 174 pm. Therefore, using the derived relation we can calculate a = 401 pm.

S3.8 The lattice type of this Fe/Cr alloy is that of body-centred packing which can be deduced by comparing the unit cells shown in Figure 3.29(a) and (c). The stoichiometry is 1.5 Cr [4×(1/8) corners + 1×(1) body] atoms and 0.5 Fe [4(1/8) corners] atoms per unit cell. This would give Cr-to-Fe ratio of 1.5 : 0.5 which when multiplied by 2 provides whole numbers required for the formula 3 : 1. The formula for the alloy is therefore $FeCr_3$.

S3.9 For close-packed structures, N close-packed ions lead to N octahedral sites. Therefore, if we assume three close-packed anions (A), then there should also be three octahedral holes. Since only two thirds are filled with cations, there are two cations (X) in two octahedral sites and the stoichiometry for the solid is X_2A_3.

S3.10 Following the lead from Example 3.10, we'll first use Table 3.4 to find possible structures for each compound, and then consult Resource Section 1 to compare ionic sizes and suggest a possible structure.

a) PrO_2 is an AX_2 compound. Looking at Table 3.4 we see that it can have one of the two commonly adopted AX_2 structures: either fluorite (CaF_2) or rutile (TiO_2). To decide which one, we have to compare the ionic radii. A glance at the periodic table of elements can provide a shortcut: Pr is in the f block just like U (UO_2 is in the list of compounds with fluorite-type structure) so it is a good idea to first compare ionic radii of Pr^{4+} and U^{4+}. From Resource Section 1 we find $r(Pr^{4+})$ = 96 pm and $r(U^{4+})$ = 100 pm. The two values are very close bringing us to the conclusion that PrO_2 very likely has the same structure as UO_2, i.e. fluorite type. Note that we compared the radii for coordination number 8. This is because the cation's coordination number in fluorite type structure is eight (see Figure 3.38 in your textbook and accompanying description in the text).

b) CrO_2 can have again either fluorite or rutile structure type. Cr is in the d block like most metallic elements under "Rutile" line in Table 3.4. Thus, it is reasonable to compare Cr^{4+} radius with the radii of these cations. The coordination of cation in TiO_2 is close to octahedral with coordination number 6 (more strictly, the coordination is 4+2, see Figure 3.39 and he explanation in the text). For Cr^{4+} r = 55 pm and for Mn^{4+} r = 53 pm; the two values are very close so it is reasonable to suggest that CrO_2 likely has rutile type structure.

c) The $CrTaO_4$ analysis follows the same reasoning as for $LiNiO_2$ found in the discussion of rock salt type of structure and in Example 3.10(d). The general formula can be written as $(AX_2)_2$, with A = $Cr_{½}Ta_{½}$ and X=O, so the compound again can have either fluorite or rutile structure. We have already seen that Cr^{4+} is very similar in size to Mn^{4+}, now we can confirm that Ta^{4+} is similar in size to W^{4+}; 68 pm vs. 66 pm, respectively. Thus, $CrTaO_4$ likely has rutile type structure as well.

d) AcOF can be viewed as and AB_2 compound and hence have either fluorite or rutile type of structure. The ionic radius of Ac^{3+} (81 pm) is close to that of U^{4+} (86 pm) and we can expect fluorite structure for AcOF.

e) The case of Li_2TiF_6 is similar to the one in Example 3.10(c). This compound is composed of Li^+ cations and $[TiF_6]^{2-}$ anions and can be rewritten as having the general formula A_2X. Looking at the Table 3.4, we see that only antifluorite structure has this formula. Thus, the likely structure is antifluorite.

S3.11 The perovskite, $CaTiO_3$, structure is shown in Figure 3.42. The large calcium cations occupy site A whereas smaller Ti^{4+} cations site B. The O^{2-} anions are located at site X. Thus, we can see two different coordination environments of O^{2-}: one with respect to Ca^{2+} (A site) and the other with respect to Ti^{4+} (B site). Ti^{4+} is located on the corners of the cube whereas O^{2-} anions are located on the middle of every edge. Thus, there are two Ti^{4+} surrounding each O^{2-}, which are oxygen's nearest neighbours. To see how many Ca^{2+} surround each O^{2-}, we have to add three unit cells horizontally, each sharing a common edge. Then we can see that there are four Ca^{2+} cations as next nearest neighbours. Thus, the coordination of O^{2-} is two Ti^{4+} and four Ca^{2+} and longer distances, this is sometimes written as CN 2+4.

S3.12 La^{3+} would have to go on the larger A site, and to maintain charge balance it would be paired with the smaller In^{3+} and thus the composition would be $LaInO_3$.

S3.13 Follow the procedure outlined in the example. From the Resource Section 1 we find the following radii for coordination number 6: $r(Ca^{2+})$ = 100pm, $r(Bk^{4+})$ = 63pm and $r(O^{2-})$ = 140pm. From here we can calculate the ratios:

- For CaO: 100pm/140pm = 0.714, within the 0.414–0.732 range for the AB structure type, and the most plausible structure is NaCl structure.
- For BkO_2: 63pm/140pm = 0.450, is also within the 0.414–0.732 range but this time we have to look under AB_2 structure-type column; thus, we can predict TiO_2 structure type. For this oxide, however, this is only a predicted structure—BkO_2 actually has a fluorite-type structure. Thus, this example shows a limitation of this method. Even if we were to use ionic radii for correct coordination numbers (8 for Bk^{4+} and 4 for O^{2-} in CaF_2 structure type), the γ value would still fall within the TiO_2 structure range.

S3.14 You should proceed as in the example, calculating the total enthalpy change for the Born-Haber cycle and setting it equal to $\Delta_L H$. In this case, it is important to recognize that two Br^- ions are required, so the enthalpy changes for (i) vaporization of $Br_2(l)$ and (ii) breaking the Br–Br bond in $Br_2(g)$ are used without dividing by 2, as was done for Cl_2 in the case of KCl described in Example 3.14. The Born-Haber cycle for $MgBr_2$ is shown below, with all of

the enthalpy changes given in kJ mol^{-1}. These enthalpy changes are not to scale. The lattice enthalpy is equal to 2421 kJ mol^{-1}. Note that $MgBr_2$ is a stable compound despite the enormous enthalpy of ionization of magnesium. This is because the very large lattice enthalpy more than compensates for this positive enthalpy term. Note the standard convention used; lattice enthalpies are positive enthalpy changes.

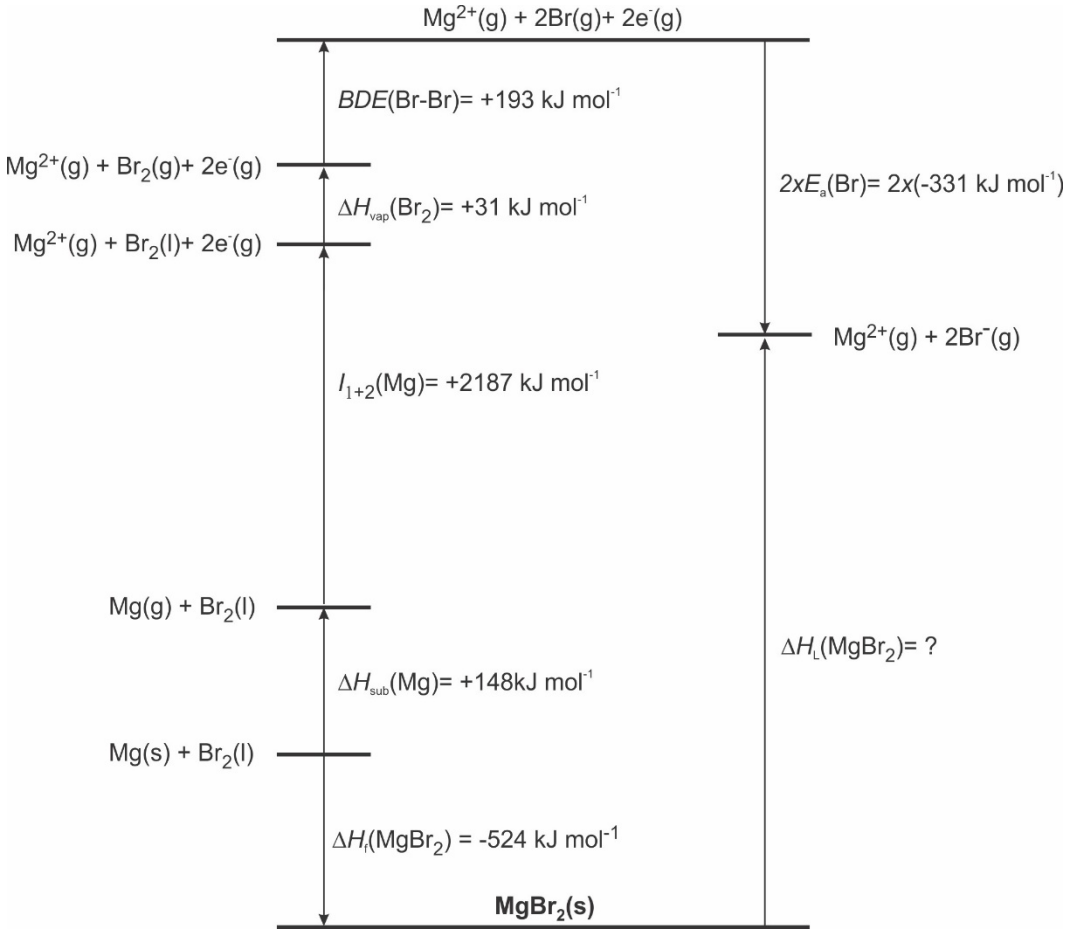

The Born-Haber cycle for $MgBr_2$

S3.15 This compound is unlikely to exist owing to a large positive value for the heat of formation for $CsCl_2$ that is mainly due to the large second ionization energy for Cs (I_1 = 375 kJ mol^{-1} vs. I_2 = 2420 kJ mol^{-1}; the I_2 alone for Cs is higher than the sum of I_1 and I_2 for Mg; see Self-Test 3.14.). The compound is predicted to be unstable with respect to its elements mainly because the large ionization enthalpy to form Cs^{2+} is not compensated by the lattice enthalpy.

S3.16 Closely following Example 3.16, using $r(Li^+)$ = 76 pm and provided thermochemical radius for N_2^{2-}:

$$\Delta_L H = \frac{3\times|(+1)(-2)|}{(76+173)\text{pm}}\times(1.08\times10^5)\text{kJ mol}^{-1} = 2602\,\text{kJ mol}^{-1}$$

S3.17 The enthalpy change for the reaction

$$MSO_4(s) \rightarrow MO(s) + SO_3(g)$$

includes several terms, including the lattice enthalpy for MSO_4, the lattice enthalpy for MO, and the enthalpy change for removing O^{2-} from SO_4^{2-}. The last of these remains constant as you change M^{2+} from Mg^{2+} to Ba^{2+}, but the lattice enthalpies change considerably. The lattice enthalpies for $MgSO_4$ and MgO are both larger than those for $BaSO_4$ and BaO, simply because Mg^{2+} is a smaller cation than Ba^{2+}. However, the *difference* between the lattice enthalpies for $MgSO_4$ and $BaSO_4$ is a smaller number than the difference between the lattice enthalpies for MgO and BaO (the larger the anion, the less changing the size of the cation affects ΔH_L). Thus going from $MgSO_4$ to MgO is thermodynamically more favourable than going from $BaSO_4$ to BaO because the *change* in ΔH_L is greater for the former than for the latter. Therefore, magnesium sulfate will have the lowest decomposition temperature and barium sulfate the highest, and the order will be $MgSO_4 < CaSO_4 < SrSO_4 < BaSO_4$.

S3.18 The most important concept for this question from Section 3.15(c) *Solubility* is the general rule that compounds that contain ions with widely different radii are more soluble in water than compounds containing ions with similar radii. The six-coordinate radii of Na^+ and K^+ are 1.02 and 1.38 Å, respectively (see Table 1.4), whereas the thermochemical radius of the perchlorate ion is 2.36 Å (see Table 3.10). Therefore, because the radii of Na^+ and ClO_4^- differ more than the radii of K^+ and ClO_4^-, the salt $NaClO_4$ should be more soluble in water than $KClO_4$.

S3.19 **a)** HgS has the sphalerite type structure and a high degree of covalency in the bonding, thus it would favour Frenkel defects.

b) CsF has the rock-salt structure and ionic bonding. This type of compound generally forms Schottky defects.

Note that you can determine possible structures for both compounds using radius ratio γ and radii given in Resource Section 1. You can make a judgement on bonding type using the Ketelaar triangle. All of these have been covered in this chapter.

S3.20 We need to identify ions of similar charge (+4) and size (r = 40 pm) to silicon. Ionic radii are listed in Resource Section 1. Two obvious choices are phosphorus (r = 31 pm, charge +3) and aluminium (r = 53, charge +3).

S3.21 The d_{x2-y2} and d_{z2} have lobes pointing along the cell edges to the nearest neighbour metals. See Figure 1.15 for review of the shape of 3d orbitals.

S3.22 **(a) V_2O_5:** *n*-type is expected when a metal is in a high oxidation state, such as vanadium(V), and is likely to undergo reduction.

(b) CoO: *p*-type is expected when a metal is in a lower oxidation state and is likely to undergo oxidation. Recall that upon oxidation, holes are created in the conduction band of the metal and the charge carriers are now positive, leading the classification.

Exercises

E3.1 Consulting Table 3.1, for the monoclinic crystal system we have the following unit cell parameters: $a \neq b \neq c$ and $\alpha = 90°$, $\beta \neq 90°$, $\gamma = 90°$. See Figure 3.2 for a three-dimensional structure of this type of unit cell. Note that angle b is between *a* and *c* edges. The projection along *b* direction means that the *b* length is perpendicular to the paper. Hence the projection is a rhombus (Figure E3.1-A). The origin of the unit cell is marked with 0, while the dark circles at the corners represent lattice points. The angle β is also shown. In Figure E3.1-B we have replaced the lattice points with atoms (grey spheres). To show that the space is indeed filled, we translate the projection along *a* and *c* (Figure E3.1-C).

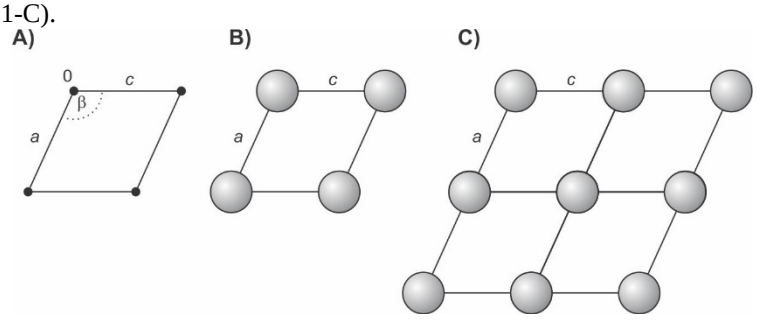

Figure E3.1

E3.2 **a)** First start with an outline of a cubic unit cell with defined edges and origin (Figure E3.3a-A). Then add the three points along the edges: (½, 0, 0), (0, ½, 0) and (0, 0, ½) (Figure E3.3a-B, three dark circles). Since the cell is cubic, the three directions must be the same, thus there must be a point in the middle of each edge. These are shown now on Figure E3.3a-C. Finally, the point (½, ½, ½) is added in Figure E3.3a-D. If you had trouble with this part, have a look at Figures 3.3 and 3.4 of your textbook. To make the lattice type more obvious we can translate this unit cell to get two of them sharing one face, Figure E3.3a-E. It is easy to see now that we have a face-centred unit cell and cubic closed-packing (Figure E3.3a-F). Note that in final figure our original two unit cells have been indicated with dashed lines while the new, face-centred unit cell with solid lines. Figure E3.3a-E also shows that the new unit cell has the same parameters as the original one.

The number of lattice points in face-centred unit cell is four (see Section 3.1(a) of your textbook if necessary).

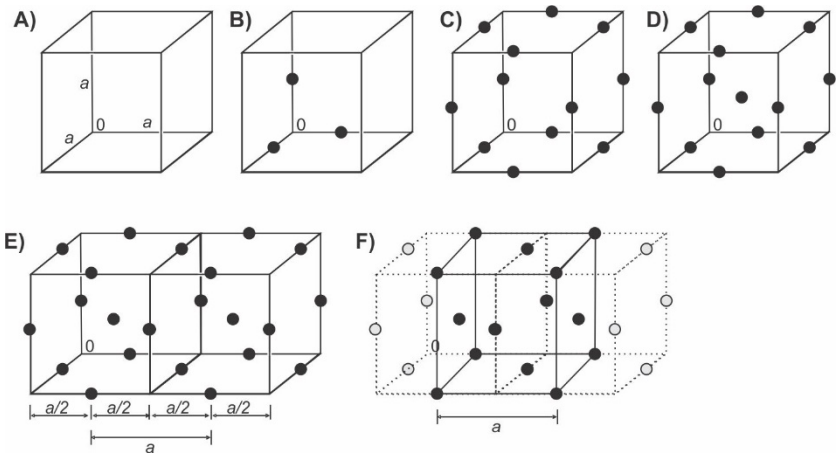

Figure E3.3a

b) The approach is similar to that in part a). The general parameters of an orthorhombic unit cell can be found in Table 3.1 and the outline in Figure 3.2. The starting point is a simple outline of an orthorhombic unit cell. Figure E3.3b-A shows such an outline with indicated cell origin and cell dimensions. Figure E3.3b-B shows lattice points that correspond to assigned point (0, 0, 0). Note that this point is translated from the origin to each corner. The (½, ½, 0) point is added in Figure E4.4b-C. At this point we can assign this lattice to the C type (or base-centred) orthorhombic lattice. This packing has two lattice points in the unit cell: 8 × 1/8 for each corner plus 2 × ½ for two faces.

We can go one step further, however, and place two of these unit cells next to each other (Figure E3.3b-D). Analysing this set-up we see that new, simpler, unit cell can be defined (Figure E3.3b-E). Note that the *c* axis is the same but two new directions, *a*' and *b*', are not identical to the original *a* and *b*Also, angle γ is not 90°. This unit cell has only one lattice point: 8 × 1/8 roe each corner.

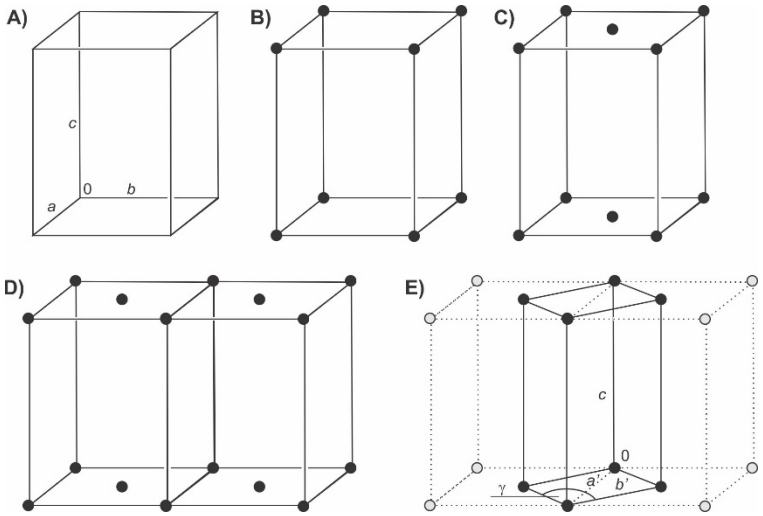

Figure E3.3b

E3.3 **a) CBACBA…:** Any ordering scheme of planes is close-packed if no two adjacent planes have the same position (i.e., if no two planes are *in register*). When two planes are in register, the packing looks like the figure below and to the right (the spheres in the upper layer lie exactly on top of the spheres in a layer below), whereas the packing in a close-packed structure allows the atoms of one layer to fit more efficiently into the spaces *between* the atoms in an adjacent layer, like the figure below and to the left. Notice that the empty spaces between the atoms in the figure to the left are much smaller than in the figure to the right. The efficient packing exhibited by close-packed structures is why, for a given type of atom, close-packed structures are denser than any other possible structure. In the case of a CBACBA … structure, no two adjacent planes are in register, so the ordering scheme is close-packed.

Close-packed structure
(not in register, corresponding to AB layers)

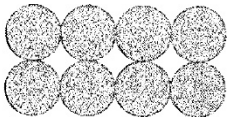

Non–close-packed structure
(in register, corresponding to AA layers)

b) ABAC…: Once again, no two adjacent planes are in register, so the ordering scheme is close-packed.

c) ABBA…: The packing of planes using this sequence will put two B planes next to each other as well as two A planes next to each other, so the ordering scheme is not close-packed.

d) ABCBC…: No two adjacent planes are in register, so the ordering scheme is close-packed.

e) ABABC…: No two adjacent planes are in register, so the ordering scheme is close-packed.

f) ABCBCA…: No two adjacent planes are in register, so the ordering scheme is close-packed.

E3.4 The sketch of the unit cell should look like the one on Figure 3.5 in your textbook. The shortest copper atom to copper atom is along face diagonal, as shown on the figure below. The distance between two closest copper neighbours is denoted 2*r* to indicate that it equals two Cu atom radii. It is easy to construct a 45-45-90 isosceles triangle formed by two 2*r* sides with the third being *a* unit cell parameter. Thus, we determine first *a* from given density and number of Cu atoms per unit cell, then use the Pythagoras's theorem to determine 2*r* and then *r*.

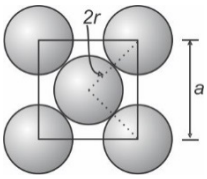

Since Cu has fcc structure, there are four Cu atoms per unit cell (see Section 3.1(a) of your textbook if necessary). The density is a mass-to-volume ratio; fcc unit cell is a cube so the volume is a^3:

$$d = \frac{m}{V} = \frac{m}{a^3}.$$

We have to calculate the mass of four copper atoms that we find in one unit cell volume. The atomic mass of copper is 63.55 g mol^{-1} telling us that one mole of copper, or Avogadro's number of copper atoms, weighs 63.55 g. Thus, our four Cu atoms weigh:

$$m = 4 \times \frac{63.55\,\text{g mol}^{-1}}{6.022 \times 10^{23}\,\text{mol}^{-1}} = 4.22 \times 10^{-22}\,\text{g} = 4.22 \times 10^{-25}\,\text{kg}.$$

Now we can calculate a:

$$a^3 = \frac{m}{d} = \frac{4.22 \times 10^{-25}\,\text{kg}}{8960\,\text{kg m}^{-3}} = 4.71 \times 10^{-29}\,\text{m}^3 \Rightarrow a = \sqrt[3]{4.71 \times 10^{-29}\,\text{m}^3} = 3.61 \times 10^{-10}\,\text{m} = 361\,\text{pm}.$$

Based on the above sketch and applying the Pythagoras's theorem, we have:

$$(2r)^2 + (2r)^2 = a^2$$
$$8r^2 = a^2$$
$$r = \sqrt{\frac{a^2}{8}} = \sqrt{\frac{(361\,\text{pm})^2}{8}} = 128\,\text{pm}.$$

E3.5 The AAA… layering has hexagonal layers that in the structure lie exactly on top of each other. Inspection of two such layers AA (see Figure E3.9 below) easily reveals the trigonal prismatic holes. A top and side view of the hole is given at the far right of Figure E3.9. Since each S atom in this packing contributes only one-sixth to the hole, and the trigonal prism has six corners, we have N trigonal prismatic holes per N sulfur atoms. Since the formula is MoS_2, every second hole in the structure contains Mo atom.

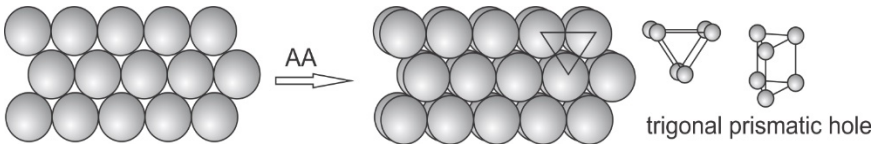

Figure E3.9

E3.6 The bcc unit cell contains two atoms that weigh together (2 mol Li × 6.941 g/mol)/(6.022 × 10^{23} Li/mol) g or 2.305 × 10^{-26} kg. The volume of the unit cell is a^3, where a is the length of the edge of the unit cell. The density equals mass divided by volume or:

$$535\ \text{kg m}^{-3} = 2.305 \times 10^{-26}\,\text{kg} / a^3 \text{ with } a \text{ in m}$$

$$a = 3.506 \times 10^{-10}\ \text{m or } 351\ \text{pm}$$

E3.7 The electronegativity difference is 0.86 for Sr and Ga and the mean is 1.38. Using Ketelaar's triangle (see Figure 2.28 and particularly Figure 3.27) and calculated values for the *y* and *x* axes, respectively, we find that the compound is an alloy because it falls in the metallic bond region of Figure 2.28 and alloy region of Figure 3.27.

.

E3.8 **(a) Coordination numbers.** The rock-salt polymorph of RbCl is based on a ccp array of Cl^- ions in which the Rb^+ ions occupy all the octahedral holes. An octahedron has six vertices, so the Rb^+ ions are six-coordinate. Since RbCl is a 1:1 salt, the Cl^- ions must be six-coordinate as well. The caesium-chloride polymorph is based on a cubic array of Cl^- ions with Rb^+ ions at the unit cell centres. A cube has eight vertices, so the Rb^+ ions are eight-coordinate, and therefore the Cl^- ions are also eight-coordinate.

(b) Larger Rb^+ radius. If more anions are packed around a given cation, the hole that the cation sits in will be larger. You saw an example of this when the radii of tetrahedral (0.225*r*) and octahedral holes (0.414*r*) were compared (*r* is the radius of the anion). Therefore, the cubic hole in the caesium-chloride structure is larger than the octahedral hole in the rock-salt structure. A larger hole means a longer distance between the cation and anion, and hence a larger apparent radius of the cation. Therefore, the apparent radius of rubidium is larger when RbCl has the caesium-chloride structure and smaller when RbCl has the rock-salt structure.

E3.9 The ReO_3 unit cell is shown in Figure E3.17a). We can easily see that the coordination number of O atoms is two: each O atom located on the edges is surrounded by two Re atoms. The coordination number of Re atoms is six: we can see that if we extend environment around one Re atom into the neighbouring unit cells (Figure E3.17b). Finally, if we insert one cation in the middle of ReO_3 unit cell (white circle on Figure E3.17c), we generate a perovskite- type structure.

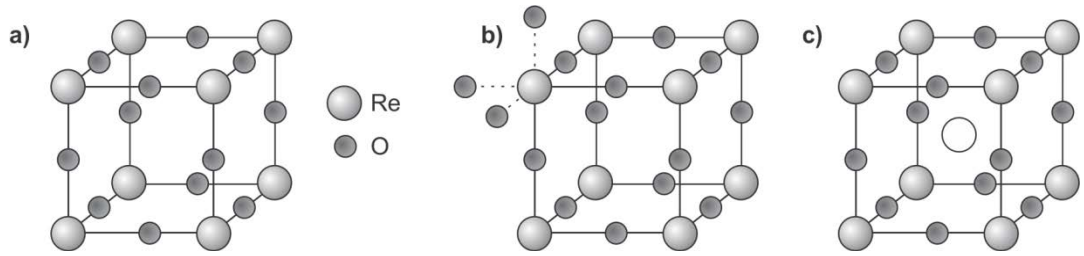

Figure E3.17

E3.10 In the perovskite structure, cations in site A have coordination number 12, whereas those in site B have coordination number six. See Figure 3.42 for more information on the perovskite structure.

E3.11 The closed packed array of A and X in the perovskite structure has $N = 4$ and so there would be 4(=*N*) octahedral holes per AX_3 unit. Therefore, to preserve the stoichiometry, one quarter of the octahedral holes have to be filled with B cations (these are the quarter that have just X anion at the octahedron vertices).

E3.12 The unit cell of rock-salt structure is shown on Figure 3.30. We have to remember that the cations fill the holes in closed-packed structure of Se^{2-} anion. The geometrical approach to calculating the cationic radii is shown in Figure E3.20 below. Both sketches show only one face of a rock-salt unit cell. The one on the left is for MgSe, showing Se^{2-} anions in contact and smaller Mg^{2+} filling the holes. The sketch on the right shows the other three cases. It is clear that we need Se^{2-} radius first to calculate radii of cations. From MgSe structure:

$$d^2 = (4r)^2 = a^2 + a^2 \quad \text{and} \quad 16r^2 = 2a^2 \Rightarrow r = \frac{a}{2\sqrt{2}} = \frac{545\text{pm}}{2\sqrt{2}} = 192.7\text{pm}.$$

where *a* is the length of unit cell, *r* is radius of Se^{2-}, anion and *d* is the length of face diagonal of the unit cell. From shown measurements we see that in each case the length of the unit cell, *a*, is given by:

$$a = 2r + 2r^+$$

where r^+ is the cation radius and r is Se^{2-} radius. From here, we have: $r^+ = \frac{a-2r}{2}$.

Thus, after substitutions we obtain: $r(Mg^{2+})$ = 79.8 pm, $r(Ca^{2+})$ = 102.8 pm, $r(Sr^{2+})$ = 118.8 pm, and $r(Ba^{2+})$ = 138.3 pm.

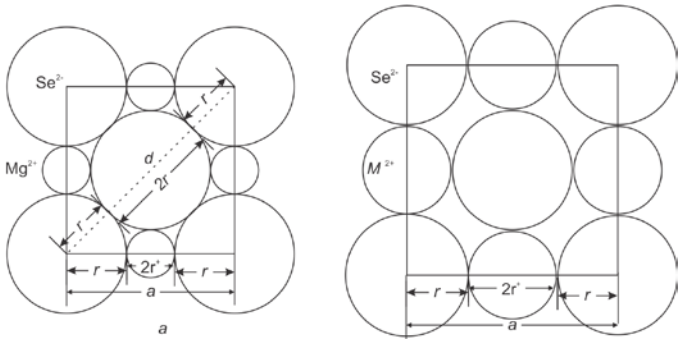

Figure E3.23

E3.13 Each of the complex ions in this exercise ($[PtCl_6]^{2-}$, $[Ni(H_2O)_6]^{2+}$, $[SiF_6]^{2-}$, PF_6^-) is highly symmetric and their shape can be approximated with a sphere (each of these structures is octahedral, thus around each a sphere can be constructed a radius equal to that of half height of octahedron or approximately element–element bond). Thus, for (a) we could predict that K_2PtCl_6 has an antifluorite structure with large anions $[PtCl_6]^{2-}$ forming a ccp array and small K^+ cations occupying each tetrahedral hole. For (b) we have a large cation $[Ni(H_2O)_6]^{2+}$ and a large anion $[SiF_6]^{2-}$ in the stoichiometric ratio 1:1 so could predict a CsCl structure type. (c) CN^- is a similar sized anion (the CN^- ionic radius has been estimated as 192 pm) compared to Cs^+ cationic radius of ~180 pm and with a 1:1 stoichiometry would predict 8:8 coordination and CsCN does indeed adopt a CsCl structure type with CN^- replacing Cl^-. In (d) with the much larger $[PF_6]^-$ anions (thermochemical radius 242 pm) the ion size mismatch leads to 6:6 coordination and adoption of a NaCl structure type with alternating Cs^+ and $[PF_6]^-$ anion.

E3.14 The structure on Figure 3.77 is actually the structure of wurtzite (ZnS, see Figure 3.35 in your textbook). The stoichiometry is therefore AB (p = 1, q = 1). The number of formula units in the unit cell is: 8 Bs on the corners each contributing an eight to the composition of the cell plus one full B inside the unit cell totals two Bs; 4 As on the unit cell edges each contributing a fourth to the composition of the unit cell plus one full A inside the unit cell totals two As; hence the composition is $(AB)_2$. The coordination number and geometry can be extrapolated from wurtzite structure to be four and tetrahedral (for both A and B). It can be deduced from the unit cell projection as well: consider the A cation inside the unit cell at 1/8 position. It has four neighbours–one B anion at ½ and three B anions at position 1 forming a triangle around A. This gives a tetrahedral geometry. Similarly, we can analyse B anion inside the cell at ½ as being surrounded by four A cations: one at 1/8 and three at 5/8 again forming a triangle. The structure that corresponds to the formula A_pB_{2q} can be derived by removing every second A from the structure of AB.

E3.15 The terms in the Born-Haber cycle to consider are (X stands for F or Cl):

$Ag(s) \rightarrow Ag(g)$, $\Delta_{sub}H(Ag)$

$Ag(g) \rightarrow Ag^{2+}(g)$, $I_1 + I_2$

$X_2(g) \rightarrow 2X(g)$, $BDE(X_2)$

$2X(g) + 2e^- \rightarrow 2X^-(g)$, $2\times EA(X)$

$Ag^{2+}(g) + 2X^-(g) \rightarrow AgX_2(s)$, $\Delta_{latt}H(AgX_2)$

Looking at the steps involved, we can expect significant energy demand for the Ag(g) ionization step ($I_1 + I_2$) for both compounds. The bond dissociation energy (*BDE*) for Cl_2 is higher than that for F_2 adding in energy requirement for $AgCl_2$. The electron affinity, a process that releases energy, is more negative for F(g) than for

Cl(g). Also, it is expected that AgF_2 lattice enthalpy will be much higher than that of $AgCl_2$ on the account of smaller F^- size as $\Delta H°_L$ is proportional to $1/d$. This combined suggests that $AgCl_2$ is less stable (higher energy demand in gas phase ion formation, but lower energy gain in lattice formation from the gas phase ions) than AgF_2.

E3.16 The lattice enthalpy for MgO will be approximately equal to *four* times the NaCl value or 3144 $kJmol^{-1}$ because the charges on both the anion and the cation are doubled in the Born-Mayer equation. For AlN the charges are tripled and the lattice enthalpy will be close to *nine* times the NaCl value or 7074 kJ mol^{-1}.

E3.17 To use the Born-Mayer equation, we first must estimate the radius of Ca^+ and choose the appropriate Madelung constant for the equation.

Looking at the trends in atomic properties, we can see that K atom is bigger than Ca and consequently that Ca^+ is smaller than K^+ but bigger than Ca^{2+}. Thus, the ionic radius for Ca^+ can be approximated as in between that of K^+ and Ca^{2+}. Since KCl has an NaCl-type structure, we can safely assume that CaCl would have the same, so we are using cationic radii for coordination six: (138 + 100)pm/2 = 119 pm. We have:

$$\Delta H_L^0 = \frac{N_A|z_A z_B|e^2}{4\pi\varepsilon_0 d}\left(1-\frac{d^*}{d}\right)A =$$

$$= \frac{6.022\times10^{23}\,\text{mol}\times|1\times(-1)|\times\left(1.602\times10^{-19}\,\text{C}\right)^2}{4\times3.14\times(8.854\times10^{-12}\,\text{C}^2\text{J}^{-1}\text{m}^{-1})\times(119+181)\times10^{-12}\,\text{m}}\left(1-\frac{34.5\text{pm}}{119\text{pm}+181\text{pm}}\right)\times1.748 =$$

$$= 7.17\times10^5\,\text{J mol}^{-1} = 717\,\text{kJ mol}^{-1}.$$

The values for ionic radii (Ca^{2+}, K^+ and Cl^-) have been taken from Table 1.4 and the value for the Madelung constant from Table 3.8.

We can now use this lattice energy to construct the Born-Haber cycle for CaCl and show that it is indeed an exothermic compound. The cycle is shown below with all values taken from Table 1.5 in your textbook except the Ca sublimation energy given in the exercise text:

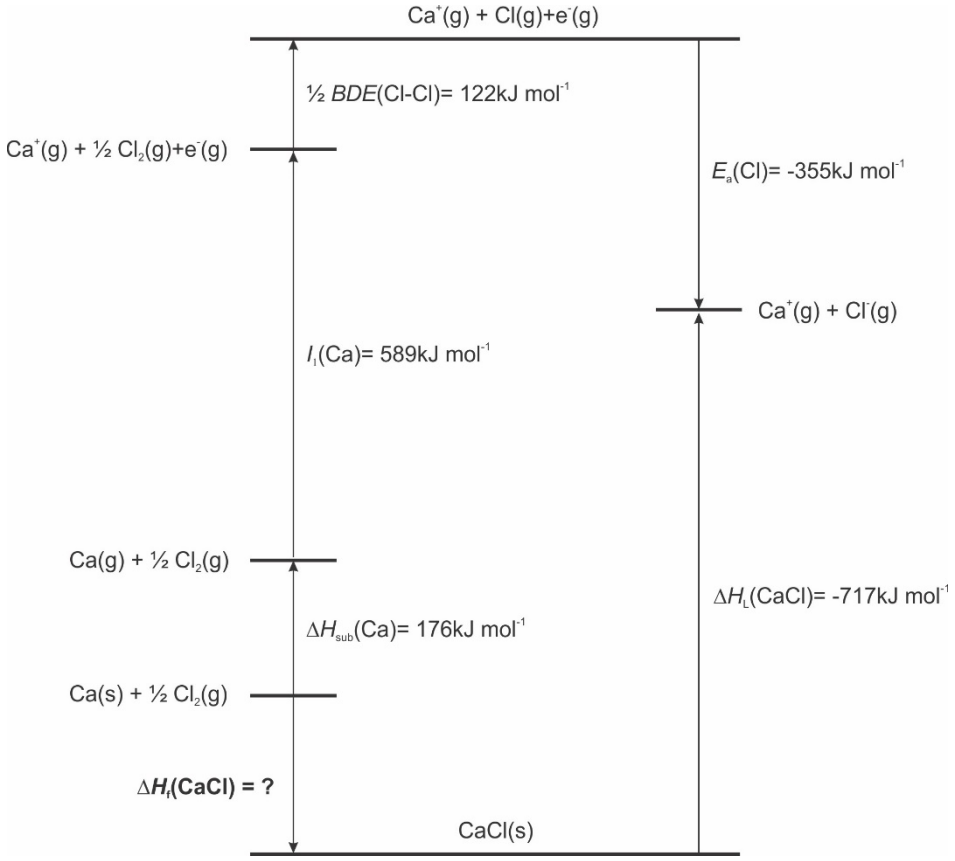

From the cycle, $\Delta_f H$(CaCl) = +176 kJ mol^{-1} + 589 kJ mol^{-1} + 122 kJ mol^{-1} – 355 kJ mol^{-1} – 717 kJ mol^{-1} = –185 kJ mol^{-1}, showing that CaCl is an exothermic salt.

Although CaCl has a favourable (negative) $\Delta_f H$, this compound does not exist and would convert to metallic Ca and $CaCl_2$ ($2CaCl \rightarrow Ca + CaCl_2$). This reaction is very favourable because $CaCl_2$ has a higher lattice enthalpy (higher cation charge). The higher lattice enthalpy combined with gain of I_1 for Ca ($Ca^+(g) + e^- \rightarrow Ca(g)$) are sufficient to compensate for I_2 ($Ca^+(g) \rightarrow Ca^{2+}(g) + e^-$) required to form $CaCl_2$.

E3.18 **a)** The Born-Mayer equation is based on electrostatic interaction between cations and anions in the lattice. Thus, it works very well for the ionic structures like LiCl. However, it does not provide good estimates for the salts that have significant covalent character in the bonding. One such case is AgCl.

b) A good example of M^{2+} pair is Ca^{2+} and Hg^{2+} (one main group metal and one late transition metal, just like in the case of M^+ cations in (a) part).

E3.19 **a) $BaSeO_4$ or $CaSeO_4$?** In general, difference in size of the ions favours solubility in water. The thermochemical radius of selenate ion is 240 pm (see Table 3.10), whereas the six-coordinate radii of Ba^{2+} and Ca^{2+} are 135 pm and 100 pm, respectively. Since the difference in size between Ca^{2+} and SeO_4^{2-} is greater than the difference in size between Sr^{2+} and SeO_4^{2-}, $CaSeO_4$ is predicted to be more soluble in water than $BaSeO_4$.

(b) NaF or $NaBF_4$? This exercise can be answered without referring to tables in the text. The ions Na^+ and F^- are isoelectronic, so clearly Na^+ is smaller than F^-. It should also be obvious that the radius of BF_4^- is larger than the radius of F^-. Therefore, the difference in size between Na^+ and BF_4^- is greater than the difference in size between Na^+ and F^-; $NaBF_4$ is more soluble in water than NaF.

E3.20 To quantitatively precipitate SeO_4^{2-} ion from an aqueous solution, we must find a cation that is of approximately the same size as SeO_4^{2-}. Table 3.10 lists the thermodynamic radius for this anon as 240 pm. From Resource Section 1, Ba^{2+} emerges as a good candidate. The 2+ charge can help to increase the lattice enthalpy, whereas the relatively large size of this cation reduces the cost of hydration enthalpy. Both factors decrease the solubility of $BaSeO_4$.

The thermochemical radius of phosphate ion is 238 pm. Thus, smaller cations like Na^+ and K^+ would give soluble phosphates, whereas larger cations of heavier Group 2 elements (i.e., Ba^{2+}) would likely produce insoluble phosphates.

E3.21 Of the three anions listed, $[ICl_4]^-$ is the largest. Thus, it can be preferentially stabilized in the presence of a large, 1+ cation such as Cs^+. Also, a good choice would be tetraalkylammonium cations, for example tetraethylammonium.

E3.22 In sapphire, the blue colour is due to the electron transfer between Fe^{2+} and Ti^{4+} substituting for Al^{3+} in adjacent octahedral sites in Al_2O_3 structure. Considering that beryl also contains Al^{3+} in octahedral sites, it is plausible that the blue colour of aquamarine is due to the same two dopants replacing Al^{3+} (see Table B3.1).

E3.23 The formation of defects is normally endothermic because as the lattice is disrupted the enthalpy of the solid rises. However, the term $-T\Delta S$ becomes more negative as defects are formed because they introduce more disorder into the lattice and the entropy rises. If we are not at absolute zero, the Gibbs energy will have a minimum at a nonzero concentration of defects and their formation will be spontaneous. As temperature is raised, this minimum in G shifts to higher defect concentrations as shown in Figure 3.52b in your textbook, so solids have a greater number of defects as temperatures approach their melting points. Increase in pressure would result in fewer defects in the solid. This is because at higher pressures, higher coordination numbers (tighter packing) are preferred and vacancies (present with both Schottky and Frenkel defects) become less energetically favourable. Increase in the pressure also reduces the spacing between the ions in the structure increasing the energy associated with ion removal and displacement within the structure, thereby increasing the free energy of defect formation.

E3.24 **a)** Ga is in Group 13 whereas Ge is in Group 14 of the periodic table of elements. Since Ga has one less valence electron than Ge, this would be a p-type semiconductor.

b) As is in Group 15 whereas Si is in Group 14 of the periodic table. Since As has one more valence electron than Si, this would be an n-type semiconductor.

c) $In_{0.49}As_{0.51}$ shows nonstoichiometry: it has more of (formally) As^{3-} than In^{3+} and should be also an n-type semiconductor.

E3.25 A semiconductor is a substance with an electrical conductivity that decreases with increasing temperature. It has a small, measurable band gap. A semimetal is a solid whose band structure has a zero density of states and no measurable band gap as shown in Figure 3.70. Graphite is a classic example of a semimetal with conduction in the plane parallel to the sheets of carbon atoms.

E3.26 In KC_8 potassium donates the electrons to the upper band which was originally empty in the graphite structure. In C_8Br bromine removes some electrons from the filled lower band in the graphite structure. In either case the net result is a partially filled band (formed either by addition of electrons to the originally empty band or by removal of electrons from the initially filled band) and both KC_8 and C_8Br should have metallic properties.

Chapter 4 Molecular Symmetry

Self-Tests

S4.1 See Figure 4.7 for the sketch of S_4 in a structurally similar CH_4 molecule. The S_4 axis is best shown by separating it into its two components: rotation by 90^o (or ¼ of a turn around the axis and reflection (see the figure below). This ion has three S_4 axes.

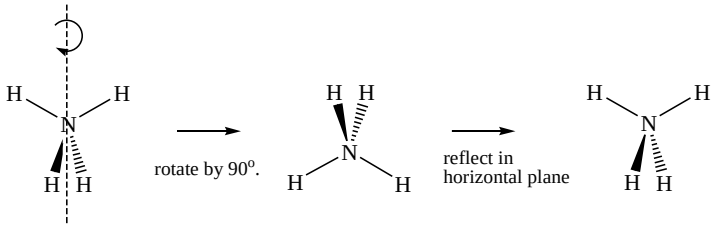

S4.2 Using the decision tree in Figure 4.9 is generally the easiest way to determine the point group of a molecule or ion. You might find it helpful to make a model of molecule or ion if you have a molecular modelling kit. This can help you visualize the structure. If the molecular geometry is not given in the problem (i.e., you have been provided with a molecular formula only), you can use VSEPR theory to determine the geometry of the molecule/ion in question.

a) BF_3 point group: According to the decision tree on Figure 4.9, the first step is answering the question "Is the molecule/ion linear?" Since BF_3 is a planar molecule, the answer is NO. Following the "N" line from "Linear?" we find the next question we have to answer: "Are there two or more C_n with n > 2?" The answer is again NO: BF_3 possesses only one three-fold rotation axis (C_3) which passes through B atom and is perpendicular to the plane of the molecule. Keep in mind that the highest order axis, in this case C_3, is the principal axis. The molecule should be repositioned in such a way that the principal axis (i.e., C_3 here) is vertical (thus, it coincides with the *z* coordinate axis). We have to follow "N" line again to the next step: "Are there any rotational axes (C_n)?" The answer is YES: BF_3 has one C_3 (already mentioned above) and three C_2 symmetry axes. We follow the "Y" path and look if the three C_2 axes are perpendicular to the principal axis C_3. Since C_2 axes coincide with three B – F bonds, they are perpendicular to the principal axis—so the answer is YES. Again, we follow the "Y" path and then ask "Are there any horizontal mirror planes (σ_h)?" The answer is YES: there is a mirror plane perpendicular to C_3, the principal axis. This mirror plane coincides with the plane of BF_3 molecule. Finally, the "Y" path leads us to the D_{nh} point group where *n* in the subscript stands for the order of the principal axis. Since the order of the principal axis in our case is 3, the point group to which BF_3 belongs is D_{3h}.

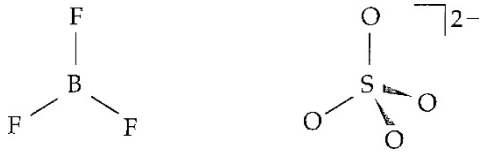

b) SO_4^{2-} point group: The sulfate anion belongs to the group T_d. The sulfate ion (i) is nonlinear; (ii) possesses four three-fold axes (C_3), like NH_4^+ (see the answer to S6.1), and (iii) does not have a centre of symmetry. The sequence of "no, yes, no" on the decision tree leads to the conclusion that SO_4^{2-} belongs to the T_d point group.

S4.3 H_2S molecule is in the same point group as H_2O, C_{2v}. For the location of symmetry elements of H_2S we can refer to Figure 4.10, and for the C_{2v} character table to Table 4.4 in your textbook. The convention we always follow is to place the z-axis along the highest order axis, in this case C_2 symmetry axis, and the mutually perpendicular mirror planes σ_v and $\sigma_{v'}$ in planes of *xz* and *yz* axes respectively. Now check how all d orbitals behave under symmetry operations of C_{2v} group. (To successfully work through this problem, you should know the shapes, orientation, and signs of d orbital lobes with respect to the coordinate axes (x, y, and z)—refer to Figure 1.13 to refresh your memory if necessary.) Keep in mind that all d orbitals will remain unchanged by *E* (as a matter of fact, everything remains unchanged by *E*, hence 1 under its column) so we can concentrate on remaining symmetry elements. The

d_{z^2} atomic orbital remains unchanged by C_2, hence it has character 1 for this symmetry element. It also remains unchanged by σ_v and σ_v', thus for both the character would be 1. Thus, the characters of this orbital are (1, 1, 1, 1) for E, C_{2v}, σ_v and σ_v'. The only row in Table 4.4 that has these four characters is A_1—therefore the d_{z^2} orbital has symmetry species A_1 (i.e., this orbital is totally symmetric under C_{2v}). The $d_{x^2-y^2}$ orbital remains unchanged by all symmetry operations as well; it also has characters (1, 1, 1, 1) and symmetry species A_1. The d_{xy} orbital, with its lobes between x and y axes remains unchanged by C_2 (hence character 1) but it would change the sign by both σ_v and $\sigma_{v'}$. For σ_v and σ_v', d_{xy} has characters –1 and –1. Overall, this orbital has (1, 1, –1, –1) as its characters, which corresponds to the symmetry species A_2. The d_{yz} orbital, once rotated around C_2 (i.e., around z axis for 180°) would change its sign, thus the C_2 character for this orbital is –1. It would also change its sign after reflection through σ_v (which we have placed in the xz plane)—the character is again –1. And finally, the reflection through $\sigma_{v'}$ would leave this orbital unchanged for character 1. Therefore, d_{yz} orbital has characters (1, –1, –1, 1) and has symmetry species B_2. Following similar analysis, we can find that d_{zx} orbital has symmetry species B_1.

S4.4 The SF_6 molecule has octahedral geometry and belongs to the O_h space group. If you refer to the character table for this group, which is given in Resource Section 4, you find that there are characters of 1, 2, *and* 3 in the column headed by the identity element, E. Therefore, the *maximum* possible degree of degeneracy of the orbitals in SF_6 is 3 (although nondegenerate and twofold degenerate orbitals are also allowed as revealed by 1 and 2 characters).

S4.5 Like the pentagonal prismatic (or eclipsed) configuration, the pentagonal antiprismatic (or staggered) conformation of ruthenocene has a C_5 axis passing through the centroids of the C_5H_5 rings and the central Ru atom. It also has five C_2 axes that pass through the Ru atom but are perpendicular to the principal C_5 axis, so it belongs to one of the D point groups. The staggered conformation, however, lacks the σ_h plane of symmetry that the pentagonal prismatic structure has. Thus, it cannot be in the D_{5h} space group. It does have five dihedral mirror planes, located between C_2 symmetry axes. Thus, the pentagonal antiprismatic conformation of ruthenocene belongs to the D_{5d} point group. Since this point group has a C_5 axis *and* perpendicular C_2 axes, it is not polar (see Section 4.3). You may find it difficult to find the n C_2 axes for a D_{nd} structure. However, if you draw the mirror planes, the C_2 axes lie between them. In this case, one C_2 axis interchanges the front vertex of the top ring with one of the two front vertices of the bottom ring, while a second C_2 axis, rotated exactly 36° from the first one, interchanges the same vertex on top with the other front bottom one.

S4.6 Except for the identity, E, the only element of symmetry that this conformation of hydrogen peroxide possesses is a C_2 axis that passes through the midpoint of the O–O bond and bisects the two O–O–H planes (these are *not* mirror planes of symmetry). Hence this form of H_2O_2 belongs to the C_2 point group, and it is chiral because this group does not contain any S_n axes. In general, any structure that belongs to a C_n or D_n point group is chiral, as are molecules that are asymmetric (C_1 symmetry). However, considering the free rotation around O – O bond we would not be able to observe optically active H_2O_2 under ordinary conditions. Optically active H_2O_2 might be observable, even transiently, if bound in a chiral host such as the active site of an enzyme. Or if the rotation is prevented in any other way (e.g., very low temperature in solid state).

S4.7 The Lewis structure of linear nitrous oxide molecule is shown below. However, unlike similarly linear CO_2 with which it is isoelectronic, N_2O does not have a centre of symmetry. Therefore, the exclusion rule does not apply, and a band that is IR active *can* be Raman active as well.

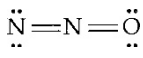

S4.8 All of the operations of the D_{2h} point group leave the displacement vectors unchanged during the symmetric stretching of Pd–Cl bonds in the *trans* isomer. Therefore, all the operations have a character of 1. This corresponds to the first row in the D_{2h} character table, which is the A_g symmetry type.

S4.9 The reducible representation is obtained as follows:

D_{4h}	E	$2C_4$	C_2	$2C_2'$	$2C_2''$	i	$2S_4$	σ_h	$2\sigma_v$	$2\sigma_d$
Γ_{3N}	4	0	0	2	0	0	0	4	2	0

This reduces to $A_{1g} + B_{1g} + E_u$.

A_{1g} and B_{1g} transform as $x^2 + y^2$, z^2 and $x^2 - y^2$ respectively and are thus Raman active but not IR active. E_u is IR active but not Raman active as it transforms as (x, y).

S4.10 The molecule CH_4 has T_d symmetry, and the given symmetry-adapted linear combination (SALC) of H atom's 1s orbitals must also have T_d symmetry. This is true because each time the set of four H atom orbitals is subjected to an operation in the T_d point group, the set changes into itself. The sketch below shows the 1s orbitals around carbon atom and location of one of the three C_3 axes. You can make a similar sketch and confirm that all symmetry elements leave the set unchanged and thus have a character 1. This places SALC in A_1 symmetry species.

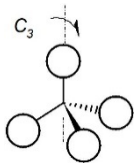

S4.11 You must adopt some conventions to answer this question. First, you assume that the combination of H atom 1s orbitals given looks like the figure below showing four H atoms arranged with D_{4h} symmetry. Note that shaded circles correspond to the H atoms whose 1s orbital did not change the sign (A1s and C1s) while open circles represent the H atoms whose 1s orbital did change the sign (B1s and D1s)—the change of sign is indicated by a minus sign in front of the wavefunction Ψ. Inspection of the character table for this group, which is given in Resource Section 4, reveals that there are three different types of C_2 rotation axes, that is, there are three columns labelled C_2, C_2', and C_2''. The first of these is the C_2 axis that is coincident with the C_4 axis; the second type, C_2', represents two axes in the H_4 plane that pass through pairs of opposite H atoms; the third type, C_2'', represents two axes in the H_4 plane that do not pass through H atoms but rather between them (see Figure 4.3 in the textbook). Now, instead of applying operations from all ten columns to this array, to see if it changes into itself (i.e., the +/– signs of the lobes stay the same) or if it changes sign, you can make use of a shortcut. Notice that the array changes into itself under the inversion operation through the centre of symmetry. Thus, the character for this operation, *i*, is 1. This means that the symmetry label for this array is one of the first four in the character table, A_{1g}, A_{2g}, B_{1g}, or B_{2g}. Notice also that for these four, the symmetry type is uniquely determined by the characters for the first five columns of operations, which are:

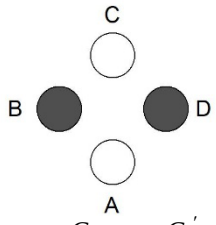

E	C_4	C_2	C_2'	C_2''
1	–1	1	1	-1

These match the characters of the B_{1g} symmetry label.

Note that this SALC also looks like $d_{x^2-y^2}$, thus the above SALC and $d_{x^2-y^2}$ have to have the same symmetry—look at the last column of D_{4h} character table for the B_{1g}.

S4.12 By consulting Resource Section 5 and the D_{4h} character table, we note that Pt's 5s and $4d_{z2}$ have A_{1g} symmetry so they would combine with A_{1g} SALCs; the d_{x2-y2} has B_{1g} symmetry and can combine with B_{1g} SACLs. Finally, $5p_x$ and $5p_y$ with E_u symmetry can combine with E_u SALCs. Therefore, these Pt orbitals with matching symmetries can be used to generate SALCs.

S4.13 Recall that symmetry types with the same symmetry as the function $x^2 + y^2 + z^2$ are Raman active, not IR active. On the other hand, symmetry types with the same symmetry as the functions *x*, *y*, or *z* are IR active, not Raman active.

SF_6 has O_h symmetry. Analysis of the stretching vibrations leads to (see Example 4.13):

$$A_{1g} \text{ (Raman, polarized)} + E_g \text{ (Raman)} + T_{1u} \text{ (IR)}.$$

Trans-SF_4Cl_2 belongs to the D_{4h} point group. (Note: *trans* means that the two Cl atoms are located on the opposite sides of the molecule, see the structure below). Analysis of the stretching vibrations leads to:

$$A_{2u} \text{ (IR)} + 2E_u \text{ (IR)} + A_{1g} \text{ (Raman, polarized)} + B_{1g} \text{ (Raman)} + B_{2g} \text{ (Raman)}.$$

Thus, for *trans*-SF_4Cl_2 we will observe two IR and three Raman stretching absorptions, whereas for SF_6 only one IR and two Raman absorptions.

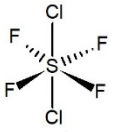

The structure of *trans*-SF_4Cl_2

S4.14 For the molecule or ion with D_{4h} symmetry,

D_{4h}	E	$2C_4$	C_2	$2C_2'$	$2C_2''$	i	$2S_4$	σ_h	$2\sigma_v$	$2\sigma_d$
Γ_{3N}	15	1	−1	−3	−1	−3	−1	5	3	1

This reduces to $A_{1g} + A_{2g} + B_{1g} + B_{2g} + E_g + 2A_{2u} + B_{2u} + 3E_u$.

The translations span A_{2u} and E_u and the rotations span A_{2g} and E_g. Subtracting these terms gives:

$$A_{1g} + B_{1g} + B_{2g} + A_{2u} + B_{2u} + 2E_u$$

as the symmetries for the vibration modes.

S4.15 $A_{1g} + E_g + T_{1u}$, see Resource Section 5.

Exercises

E4.1 The analysis here is going to focus on the topic of this chapter, i.e. molecular symmetry. The VSEPR model has been covered in quite a detail in the previous chapter and only the basic overview is going to be given here. If you have trouble determining the geometries of molecules and ions in this exercise, you should revisit the relevant parts of Chapter 2.

To predict the structure of $\mathbf{BrF_4^-}$ using VSEPR model, we have to take care of 36 valence electrons. The correct Lewis structure places four bonding and two lone electron pairs on the central Br atom resulting in an octahedral electron geometry but square planar molecular geometry. The principal rotation axis in this case is C_4 perpendicular to the square plane. The ion also has one horizontal mirror plane and two vertical mirror planes (only one shown below) as well as the centre of inversion located at Br atom (plus two diagonal mirror planes). For illustration showing all symmetry elements of a square planar molecule/ion, please refer to Figure 4.3 in your textbook.

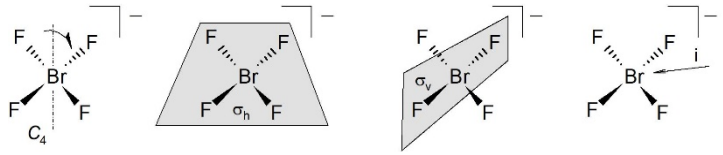

The molecular geometry of $\mathbf{TeCl_4}$ is see-saw. If you had trouble deducing this geometry, review Example 2.3. This problem looked at the geometry of SF_4, more specifically the effect of lone electron pair on central S atom on the overall geometry. Note that Te and Cl are in the same group of periodic table as S and F respectively. That means the total number of valence electrons in $TeCl_4$ matches the one for SF_4. Since both Te and Cl have larger atomic radii than S and F respectively, the effect of lone electron pair on geometry is going to be diminished and overall $TeCl_4$ is going to be very close to ideal see-saw geometry. $TeCl_4$ molecule has a C_2 axis as a principal axis and two

vertical mirror planes. It does not have *i*. Note that ideally the molecule should be rotated so that C_2 axis, as a principal axis in this case, is vertical.

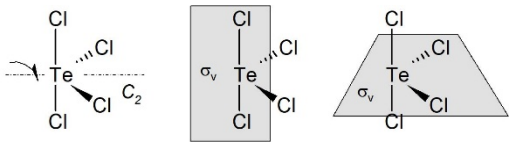

The $\mathbf{I_2Cl_6}$ molecule is planar. It is a dimer consisting of two ICl_3 monomers bridged by two Cl atoms. There is one principal C_2 axis (there are two more C_2 axes), one horizontal mirror plane and two vertical mirror planes (only one shown). The centre of inversion lies in the middle of I–Cl–I–Cl rhombohedron.

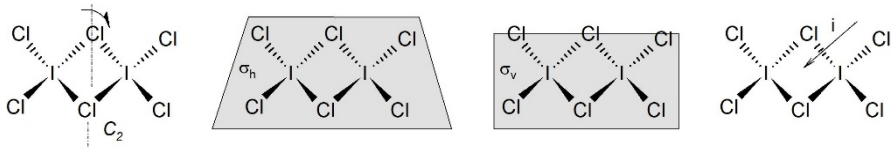

The anion $\mathbf{ClO_3^-}$ has 26 valence electrons with trigonal pyramidal molecular geometry. The principal axis is C_3, there are no horizontal mirror planes but there are three vertical ones. The anion does not possess a centre of inversion.

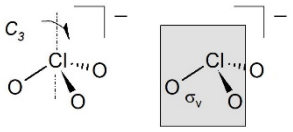

E4.2 **a) $\mathbf{CO_2}$:** This linear molecule has both a centre of inversion, *i*, and S_4

b) $\mathbf{C_2H_2}$: This linear molecule also has both *i* and S_4

c) $\mathbf{BF_3}$: This molecule possesses neither *i* nor S_4

d) $\mathbf{SO_4^{2-}}$: This ion has three different S_4 axes, which are coincident with three C_2 axes, but there is no *i*

E4.3 Overall, benzene molecule has seven mirror planes: $3\sigma_v$, $3\sigma_d$, and $1\sigma_h$. It has a C_6 axis perpendicular to six C_2 axes and a horizontal mirror plane that contains all the atoms in the ring. Hence, the point group symmetry of the benzene molecule is D_{6h}. The chloro-substituted, $C_6H_3Cl_3$, with chlorines on alternating carbons around the ring (1,3,5-trichlorobenzene), has a D_{3h} symmetry and four mirror planes: $3\sigma_v$ and $1\sigma_h$.

E4.4 **a)** Using the decision tree shown in Figure 4.9, you will find the point group of SO_3^{2-} anion (trigonal pyramidal geometry) to be C_{3v} (it is nonlinear; it only has one proper rotation axis, a C_3 axis; and it has three σ_v mirror planes of symmetry).

b) Inspection of the C_{3v} character table (Resource Section 4) shows that the characters under the column headed by the identity element, *E*, are 1 and 2. Therefore, the maximum degeneracy possible for molecular orbitals of SO_3^{2-} anion is 2.

c) According to the character table in Resource Section 5, the S atom 3s and $3p_z$ orbitals are each singly degenerate (and belong to the A_1 symmetry type), but the $3p_x$ and $3p_y$ orbitals are doubly degenerate (and belong to the *E* symmetry type). Thus, the $3p_x$ and $3p_y$ atomic orbitals on sulfur can contribute to molecular orbitals that are two-fold degenerate.

E4.5 PF_5 is a non-linear molecule, thus the number of expected number of vibrational modes is $3N - 6 = 3\times6 - 6 = 12$. To determine the symmetries of vibrations, we have to consider the reducible representation of D_{3h}. Since we have six atoms with three displacement directions each, there are a total of $6\times3 = 18$ displacements in this molecule. These displacements remain unchanged after identity operation; hence the character for *E* is 18. You can follow

this procedure for all symmetry elements in D_{3h} (as well as consult Example 4.14) to construct the following reducible representation:

D_{3h}	E	$2C_3$	$3C_2$	σ_h	$2S_3$	$3\sigma_v$
Γ_{3N}	18	0	−2	4	−2	4

Γ_{3N} reduces to: $2A_1' + A_2' + 4E' + 3A_2'' + 2E''$; subtracting Γ_{trans} ($E' + A_2''$) and Γ_{rot} ($A_2' + E''$), we obtain Γ_{vib} : $2A_1' + 3E' + 2A_2'' + E''$. Thus, we expect six Raman bands: $2A_1' + 3E' + E''$ (note that A_2'' is inactive in Raman because symmetry type does not contain the same symmetry as the function $x^2 + y^2 + z^2$).

E4.6 **a) SF_6:** Since sulfur hexafluoride has a centre of symmetry, the exclusion rule applies. Therefore, none of the vibrations of this molecule can be *both* IR and Raman active. A quick glance at the O_h character table in Resource Section 4 confirms that the functions *x*, *y*, and *z* (required for IR activity) have the T_{1u} symmetry type and that all the binary product functions such as x^2, *xy*, etc. (required for Raman activity) have different symmetry types.

O_h	E	$8C_3$	$6C_2$	$6C_4$	$6C_2$	i	$6S_4$	$8S_6$	$3\sigma_h$	$6\sigma_d$
Γ_{3N}	21	0	−1	3	−3	−3	−1	0	5	3

Γ_{3N} reduces to: $A_{1g} + E_g + T_{1g} + T_{2g} + 3T_{1u} + T_{2u}$.

Then subtracting Γ_{trans} (T_{1u}) and Γ_{rot} (T_{1g}), we obtain Γ_{vib} : $A_{1g} + E_g + T_{2g} + 2T_{1u} + T_{2u}$.

None of these modes are both IR and Raman active as there is a centre of inversion.

b) BF_3: Boron trifluoride does not have a centre of symmetry. Therefore, it is possible that some vibrations are both IR and Raman active. You should consult the D_{3h} character table in Resource Section 4. Notice that the pairs of functions (*x*, *y*) and ($x^2 - y^2$, *xy*) have the *E´* symmetry type. Therefore, any *E´* symmetry vibration will be observed as a band in both IR and Raman spectra.

D_{3h}	E	$2C_3$	$3C_2$	σ_h	$2S_3$	$3\sigma_v$
Γ_{3N}	12	0	−2	4	−2	2

Γ_{3N} reduces to: $A_1' + A_2' + 3E' + 2A_2'' + E''$.

Subtracting Γ_{trans} ($E' + A_2''$) and Γ_{rot} ($A_2' + E''$), we obtain Γ_{vib} : A_1' (Raman) + $2E'$ (IR and Raman) + A_2'' (IR).

The *E*′ modes are active in both IR and Raman.

E4.7 **a) BF_3:**

$(1/\sqrt{3})(\varphi_1 + \varphi_2 + \varphi_3)$ $(= A_1')$

$(1/\sqrt{6})(2\varphi_1 - \varphi_2 - \varphi_3)$ and $(1/\sqrt{2})(\varphi_2 - \varphi_3)$ $(= E')$

Note that $(1/\sqrt{2})(\varphi_2 - \varphi_3)$ is obtained by combining the other two E'-type SALCs, that is, $(2\varphi_2 - \varphi_3 - \varphi_1) - (2\varphi_3 - \varphi_1 - \varphi_2)$.

b) PF_5: (axial F atoms are $\varphi_4 + \varphi_5$)

$(1/\sqrt{2})(\varphi_4 + \varphi_5)$ $(= A_1')$

$(1/\sqrt{2})(\varphi_4 - \varphi_5)$ $(= A_2'')$

$(1/\sqrt{3})(\varphi_1 + \varphi_2 + \varphi_3)$ $(= A_1')$

$(1/\sqrt{6})(2\varphi_1 - \varphi_2 - \varphi_3)$ and $(1/\sqrt{2})(\varphi_2 - \varphi_3)$ $(= E')$

E4.8 The molecular orbital energy diagram for sulfur hexafluoride is shown in Figure 4.32. The HOMO of SF_6 is the nonbonding *e* set of MOs. These are pure F atom symmetry-adapted orbitals, and they do not have any S atom character whatsoever. On the other hand, the antibonding $2t_1$ orbitals, a set of LUMO orbitals, have both a sulfur

and a fluorine character. Since sulfur is less electronegative than fluorine, its valence orbitals lie at higher energy than the valence orbitals of fluorine (from which the *t* symmetry-adapted combinations were formed). Thus, the $2t_1$ orbitals lie closer in energy to the S atomic orbitals and hence they contain more S character.

Chapter 5 Acids and Bases

Self-Tests

S5.1 **a) $HNO_3 + H_2O \rightarrow H_3O^+ + NO_3^-$.** The compound HNO_3 transfers a proton *to* water, so it is an acid. The nitrate ion is its conjugate base. In this reaction, H_2O accepts a proton, so it is a base. The hydronium ion, H_3O^+, is its conjugate acid.

b) $CO_3^{2-} + H_2O \rightarrow HCO_3^- + OH^-$. A carbonate ion accepts a proton from water, so it is a base. The hydrogen carbonate, or bicarbonate, ion is its conjugate acid. In this reaction, H_2O donates a proton, so it is an acid. A hydroxide ion is its conjugate base.

c) $NH_3 + H_2S \rightarrow NH_4^+ + HS^-$. Ammonia accepts a proton from hydrogen sulfide, so it is a base. The ammonium ion, NH_4^+, is its conjugate acid. Since hydrogen sulfide donated a proton, it is an acid, while HS^- is its conjugate base.

S5.2 With $K_a < 1$, HF is a weak acid only partially dissociated in water. The dissociation equation is:

$$HF + H_2O \rightleftharpoons H_3O^+ + F^-$$

Applying what you have learned in general chemistry, this type of problem can best be solved using the initial concentration, change in concentration, and final concentrations according to the table below.

	$HF + H_2O \rightleftharpoons$	H_3O^+	F^-
Initial (M)	0.10	0.0	0.0
Change (M)	–x	+x	+x
Equilibrium (M)	0.10–x	x	x

Insert these values into the acidity constant expression for HF.

$$K_a = \frac{[H_3O^+][F^-]}{[HF]} = 3.5\times10^{-4} = \frac{x^2}{0.10 - x}.$$

From here we obtain the following quadratic equation:

$$x^2 + 3.4 \times 10^{-4}x - 3.5 \times 10^{-4} = 0.$$

With roots (solutions):

$$x = \frac{3.5\times10^{-4} \pm \sqrt{\left(3.5\times10^{-4}\right)^2 - 4\times1\times(3.5\times10^{-5})}}{2\times1}.$$

The two roots are $x = 5.7 \times 10^{-3}$ M and -6.1×10^{-3} M. Obviously, the negative root is physically impossible, so our final result is $[H_3O^+] = 5.7 \times 10^{-3}$ M. Taking the negative log gives the pH of the solution.

$$pH = -\log[H_3O^+] = 2.24.$$

S5.3 Tartaric acid is a diprotic weak acid and must be solved in two equilibrium steps, similar to **S5.2**. The first equilibrium, and ICE table is shown below:

	$H_2C_4O_6 + H_2O \rightleftharpoons$	H_3O^+	$HC_4O_6^-$
Initial (M)	0.20	0.0	0.0
Change (M)	–x	+x	+x
Equilibrium (M)	0.20–x	x	x

The equilibrium values are substituted in the acidity constant for the first deprotonation step:

$$K_{a1} = 1.0\times10^{-3} = \frac{[H_3O^+][HC_4O_6^-]}{[H_2C_4O_6]} = \frac{x^2}{0.2 - x}.$$

Now we must solve the following quadratic equation:

$$x^2 + 1.0 \times 10^{-3}x - 2.0 \times 10^{-4} = 0$$

$$x = \frac{1.0\times10^{-3} \pm \sqrt{\left(1.0\times10^{-3}\right)^2 - 4\times1\times(-2.0\times10^{-4})}}{2\times1}$$

$$x = 0.014 \text{ M or } -0.015 \text{ M.}$$

So, our $[H_3O^+]$ = 0.014 M which is also equal to $[HC_4O_6^-]$. Now we have to consider the second deprotonation step using the same approach as above and calculate $[C_4O_6^{2-}]$.

	$HC_4O_6^-$ + H_2O ⇌	H_3O^+ +	$C_4O_6^{2-}$
Initial (M)	0.014	0.014	0.0
Change (M)	–x	+x	+x
Equilibrium (M)	0.014–x	0.014+x	x

Insert these values into the equilibrium expression:

$$K_{a2} = 4.6\times10^{-5} = \frac{[H_3O^+][C_4O_6^{2-}]}{[HC_4O_6^-]} = \frac{(0.014+x)x}{(0.014-x)}.$$

Now we can assume that 0.014 ± x ≈ 0.014, so x is simply equal to 4.6×10^{-5}.

This means our total $[H_3O^+]$ = 0.014 M + 4.6×10^{-5}, which is essentially 0.014 M meaning the second deprotonation does not affect the pH in this solution. Our pH is:

$$pH = -\log[H_3O^+] = 1.85.$$

S5.4 Since the acid strength of aqua acids increases as the charge density of the central metal cation increases, the strongest acid will have the highest charge and the smallest radius. Thus $[Na(H_2O)_6]^+$, with the lowest charge, will be the weakest of the four aqua acids, and $[Sc(H_2O)_6]^{3+}$, with the highest charge, will be the strongest. The remaining two aqua acids have the same charge, and so the one with the smaller ionic radius, *r*, will have the higher charge density and hence the greater acidity. Since Ni^{2+} is on the right from Mn^{2+} in the periodic table of the elements, it has a smaller radius, and so $[Ni(H_2O)_6]^{2+}$ is more acidic than $[Mn(H_2O_6]^{2+}$. The order of increasing acidity is $[Na(H_2O)_6]^+ < [Mn(H_2O)_6]^{2+} < [Ni(H_2O)_6]^{2+} < [Sc(H_2O)_6]^{3+}$.

S5.5 **a) H_3PO_4?** Pauling's first rule for predicting the pK_{a1} of an oxoacid is $pK_a \approx 8 - 5p$ (where *p* is the number of oxo groups attached to the central element).
Since *p* = 1 (see the structure of H_3PO_4 below), the predicted value of pK_{a1} for H_3PO_4 is 8 – (5 × 1) = 3. The actual value, given in Table 5.3, is 2.1.

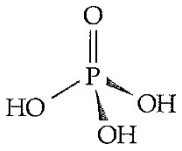

b) $H_2PO_4^-$? Pauling's second rule for predicting the pK_a values of a polyprotic oxoacid is that successive pK_a values for polyprotic acids increase by five units for each successive proton transfer. Since pK_{a1} for H_3PO_4 was predicted to be 3 (see above), the predicted value of pK_a for $H_2PO_4^-$, which is pK_{a2} for H_3PO_4, is 3 + 5 = 8. The actual value, given in Table 5.3, is 7.4.

c) HPO_4^{2-}? The pK_a for HPO_4^{2-} is the same as pK_{a3} for H_3PO_4, so the predicted value is 3 + (2 × 5) = 13. The actual value, given in Table 5.3, is 12.7.

S5.6 According to Figure 5.6, Ti(IV) is amphoteric. Treatment of an aqueous solution containing Ti(IV) ions with ammonia causes the precipitation of TiO_2, but further treatment with NaOH causes the TiO_2 to redissolve. H_2O_2 would not react with Ti(IV) since Ti(IV) cannot be further oxidized.

S5.7 **a) $FeCl_3 + Cl^- \rightarrow [FeCl_4]^-$?** The acid $FeCl_3$ forms a complex, $[FeCl_4]^-$, with the base Cl^-.

b) $I^- + I_2 \rightarrow I_3^-$? The acid I_2 forms a complex, I_3^-, with the base I^-.

S5.8 If the N atom lone pair of $(H_3Si)_3N$ is delocalized onto the three Si atoms, it cannot exert its normal repulsion influence as predicted by VSEPR rules. The N atom of $(H_3Si)_3N$ is trigonal planar, whereas the N atom of $(H_3C)_3N$ is trigonal pyramidal. The structures of $(H_3Si)_3N$ and $(H_3C)_3N$, excluding the hydrogen atoms are:

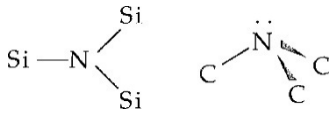

S5.9 The two solvents in Figure 5.12 for which the window covers the range 25 to 27 are dimethylsulfoxide (DMSO) and ammonia.

S5.10 We need to identify the autoionization products of the solvent, BrF_3, and then decide whether the solute increases the concentration of the cation (an acid) or the anion (a base). The autoionization products of BrF_3 are:

$$2BrF_3(l) \rightleftharpoons BrF_2^+(sol.) + BrF_4^-(sol.)$$

The solute would ionize to give K^+ and BrF_4^-. Since BrF_4^- will increase the amount of the anion, $KBrF_4$ is a base when dissolved in BrF_3.

S5.11 The ether oxygen atom will behave as a Lewis base and donate one of its lone electron pairs forming a dative bond with the boron atom of BF_3. The geometry at the boron atom will go from trigonal planar in BF_3 to tetrahedral in $F_3B{-}OEt_2$. The structure of the complex is shown below.

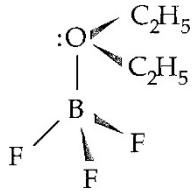

Exercises

E5.1 See the diagram below for the outline of the acid-base properties of main group oxides. The elements that form basic oxides have symbols printed in bold, those forming acidic oxides are underlined, and those forming amphoteric oxides are in italics. Note the diagonal region from upper left to lower right that includes the elements forming amphoteric oxides. The elements As, Sb, and Bi are shown both underlined and in italics. This is because their oxides in highest oxidation state (+5) are acidic, but the oxides in lower oxidation state (+3) are amphoteric. There are no oxides for fluorine. Fluorine forms two compounds with oxygen, O_2F_2 and OF_2; but because F is more electronegative than O these compounds have oxygen in a positive oxidation state (+1 and +2 respectively) and thus are not oxides (oxides have O in a negative oxidation state). For elements 113-117 there is no data.

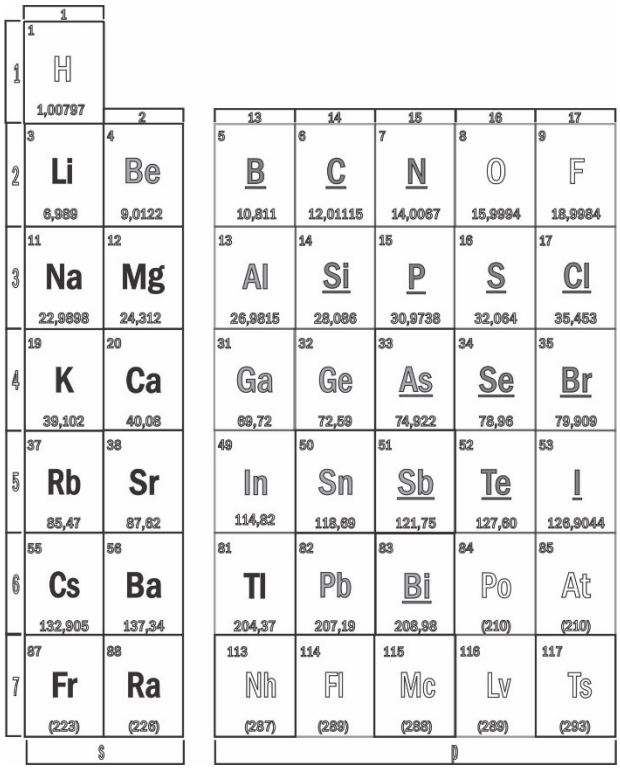

E5.2 Remember that a conjugate acid is a species with one more proton than the parent base.

(a) C_5H_5N (pyridine): The conjugate acid in this case is the pyridinium ion, $C_5H_6N^+$, shown below.

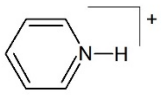

b) HPO_4^{2-}: The conjugate acid is $H_2PO_4^-$.

c) O^{2-}: The conjugate acid is OH^-.

d) CH_3COOH: The conjugate acid is $CH_3C(OH)_2^+$, shown below.

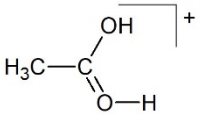

e) $[Co(CO)_4]^-$: The conjugate acid is $HCo(CO)_4$, shown below.

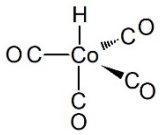

f) CN^-: The conjugate acid is HCN.

E5.3 To find the K_b, use Equation 5.4:

$$K_a \times K_b = K_w$$

$$K_b = K_w/K_a = (1.0 \times 10^{-14})/(1.8 \times 10^{-5}) = 5.6 \times 10^{-10}$$

E5.4 From Table 5.2, the proton affinities (A_p') of $H_2O(l)$ and $OH^-(aq)$ are 1130 kJ mol^{-1} and 1188 kJ mol^{-1} respectively. Thus, although transfer of H^+ from H_3O^+ to F^- is exothermic by –20 kJ mol^{-1}, the transfer of H^+ from H_2O to F^- is endothermic by 38 kJ mol^{-1}. Therefore, in neutral water, F^- will behave as a base.

E5.5 **a) CO_3^{2-} O^{2-}, ClO_4^-, and NO_3^- in water?** You can interpret the term "studied experimentally" to mean that the base in question exists in water (i.e., it is not completely protonated to its conjugate acid) *and* that the base in question can be partially protonated (i.e., it is not so weak that the strongest acid possible in water, H_3O^+, will fail to produce a measurable amount of the conjugate acid). Using these criteria, the base CO_3^{2-} is predicted to be of directly measurable base strength because the equilibrium $CO_3^{2-} + H_2O \rightarrow HCO_3^- + OH^-$ produces measurable amounts of reactants and products. The base O^{2-}, on the other hand, is completely protonated in water to produce OH^-, so the oxide ion is too strong to be studied experimentally in water. The bases ClO_4^- and NO_3^- are conjugate bases of very strong acids, which are completely deprotonated in water. Therefore, since it is not possible to protonate either perchlorate or nitrate ion in water, they are too weak to be studied experimentally.

b) HSO_4^-, NO_3^-, and ClO_4^-, in H_2SO_4? The hydrogen sulfate ion, HSO_4^-, is the strongest base possible in liquid sulfuric acid. However, since acids can protonate it, it is not too strong to be studied experimentally. Nitrate ion is a weaker base than HSO_4^-, a consequence of the fact that its conjugate acid, HNO_3, is a stronger acid than H_2SO_4. However, nitrate is not so weak that it cannot be protonated in sulfuric acid, so NO_3^- is of directly measurable base strength in liquid H_2SO_4. On the other hand, ClO_4^-, the conjugate base of one of the strongest known acids, is so weak that it cannot be protonated in sulfuric acid, and hence cannot be studied in sulfuric acid.

E5.6 The difference in pK_a values can be explained if we look at the structures of the acids in question. (Note: flip through Chapters 15 and 17 to find the structures!)

Structures of H_3PO_4, H_3PO_3, and H_3PO_2

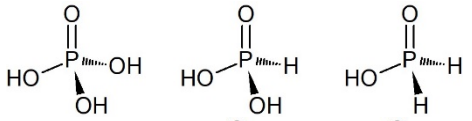

Structures of HOCl, $HClO_2$, and $HClO_3$

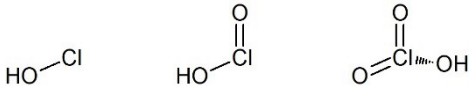

According to the first Pauling rule, p$K_a \approx 8 - 5p$, where p is the number of oxo groups attached to the central element. Looking at the structures of phosphorus containing acids, we can see that all of them actually have only one oxo group attached to the central P atom ($p = 1$). This means that they will all have p$K_a \approx 8 - 5 \times 1 = 3$. On the other hand, the number of oxo groups for chlorine-containing acids is increasing from zero in HOCl to two in $HClO_3$. Thus, the three will have the following approximate pK_a values:

HOCl ($p = 0$): p$K_a \approx 8 - 5 \times 0 = 8$

$HClO_2$ ($p = 1$): p$K_a \approx 8 - 5 \times 1 = 3$

$HClO_3$ ($p = 2$): p$K_a \approx 8 - 5 \times 2 = -2$

E5.7 According to Pauling's first rule for predicting the pK_a of a mononuclear oxoacid, p$K_a \approx 8 - 5p$ (where p is the number of oxo groups attached to the central element).

pK_a for $HNO_2 \approx 8 - (5 \times 1) = 3$

pK_a for $H_2SO_4 \approx 8 - (5 \times 2) = -2$

pK_a for $HBrO_3 \approx 8 - (5 \times 2) = -2$

pK_a for $HClO_4 \approx 8 - (5 \times 3) = -7$

The lowest pK_a is for $HClO_4$, so this is the strongest acid. Next, we have H_2SO_4 and $HBrO_3$, which have the same pK_a of –2 according to Pauling's rules. (Note that the same conclusion can be reached just by comparing the number of oxo groups in each acid without performing the actual calculations.) Bromine is more electronegative than sulfur; inductively, $HBrO_3$ should be a stronger acid than H_2SO_4. HNO_2 has the highest pK_a and is the weakest acid. Therefore, the order is $HClO_4 > HBrO_3 > H_2SO_4 > HNO_2$.

E5.8 First you pick out the intrinsically acidic oxides among those given (Al_2O_3, B_2O_3, BaO, CO_2, Cl_2O_7, and SO_3), because these will be the *least* basic. The compounds B_2O_3, CO_2, Cl_2O_7, and SO_3 are acidic because the central element for each of them is found in the acidic region of the periodic table (see the s- and p-block diagram in the answer to Exercise 5.1; generally the oxides of non-metallic elements are acidic). The most acidic compound, Cl_2O_7, has the highest central-atom oxidation state, +7, whereas the least acidic, B_2O_3, has the lowest, +3. Of the remaining compounds, Al_2O_3 is amphoteric, which puts it on the borderline between acidic and basic oxides, and BaO is basic. Therefore, a list of these compounds in order of increasing basicity is $Cl_2O_7 < SO_3 < CO_2 < B_2O_3 < Al_2O_3 < BaO$.

E5.9 Although Na^+ and Ag^+ ions have about the same ionic radius, Ag^+–OH_2 bonds are much more covalent than Na^+–OH_2 bonds, a common feature of the chemistry of d-block vs. s-block metal ions. The greater covalence of the Ag^+–OH_2 bonds has the effect of delocalizing the positive charge of the cation over the whole aqua complex. Therefore, the departing proton is repelled more by the positive charge of $Ag^+(aq)$ than by the positive charge of $Na^+(aq)$, and the Ag^+ ion is the stronger acid.

E5.10 **a) H_3PO_4 and Na_2HPO_4:** H_3PO_4 is a polyprotic acid and Na_2HPO_4 is its acidic salt. Considering that for a polyprotic acid, the K_{a1} is the highest, H_3PO_4 will be more acidic and HPO_4^{2-} is going to behave like a base:

$$H_3PO_4(aq) + HPO_4^{2-}(aq) \rightleftharpoons 2H_2PO_4^-(aq)$$

b) CO_2 and $CaCO_3$: Keep in mind that CO_2 in aqueous medium partially reacts with H_2O to produce acid H_2CO_3. The overall equation can be written as follows:

$$CO_2(aq) + CaCO_3(s) + H_2O(l) \rightleftharpoons Ca^{2+}(aq) + 2HCO_3^-$$

E5.11 As you go down a family in the periodic chart, the acidity of the homologous hydrogen compounds increases. This is due primarily to the fact that the bond dissociation energy is smaller as you go down a family, due to poorer orbital overlap. Since the H-X bond is weaker for H_2Se, it will release protons more readily than H_2S in each solvent.

E5.12 **a) $SO_3 + H_2O \rightarrow HSO_4^- + H^+$:** The acids in this reaction are the Lewis acids SO_3 and H^+ and the base is the Lewis base OH^-. The complex (or adduct) HSO_4^- is formed by the displacement of the proton from the hydroxide ion by the stronger Lewis acid SO_3. In this way, the water molecule is thought of as a Lewis adduct formed from H^+ and OH^-. Even though this is not explicitly shown in the reaction, the water molecule exhibits Brønsted acidity (not only Lewis basicity). Note that it is easy to tell that this is a displacement reaction instead of just a complex formation reaction because, while there is only one base in the reaction, there are *two* acids. A complex formation reaction only occurs with a single acid and a single base. A double displacement, or metathesis, reaction only occurs with two acids and two bases.

b) $Me[B_{12}]^- + Hg^{2+} \rightarrow [B_{12}] + MeHg^+$: This is a displacement reaction. The Lewis acid Hg^{2+} displaces the Lewis acid $[B_{12}]$ from the Lewis base CH_3^-.

c) $KCl + SnCl_2 \rightarrow K^+ + [SnCl_3]^-$: This is also a displacement reaction. The Lewis acid $SnCl_2$ displaces the Lewis acid K^+ from the Lewis base Cl^-.

d) $AsF_3(g) + SbF_5(g) \rightarrow [AsF_2][SbF_6]$: Even though this reaction produces an ionic substance, it is *not* simply a complex formation reaction. It is a displacement reaction. The very strong Lewis acid SbF_5 (one of the strongest known) displaces the Lewis acid $[AsF_2]^+$ from the Lewis base F^-.

e) EtOH readily dissolves in pyridine: A Lewis acid–base complex formation reaction between EtOH (the acid) and py (the base) produces the adduct EtOH–py, which is held together by a hydrogen bond.

E5.13 **a) $R_3P–BBr_3 + R_3N–BF_3 \rightleftharpoons R_3P–BF_3 + R_3N–BBr_3$:** You know that phosphines are softer bases than amines (see Table 5.4). To determine the position of this equilibrium, you must decide which Lewis acid is softer because the softer acid will preferentially form a complex with a soft base. Boron tribromide is a softer Lewis acid than BF_3, a consequence of the relative hardness and softness of the respective halogen substituents. Therefore, the equilibrium position for this reaction will lie to the left, the side with the soft–soft and hard–hard complexes and the equilibrium constant is less than 1. In general, it is found that soft substituents (or ligands) lead to a softer Lewis acid than for the same central element with harder substituents.

b) $SO_2 + Ph_3P–HOCMe_3 \rightleftharpoons Ph_3P–SO_2 + HOCMe_3$: In this reaction, the soft Lewis acid sulfur dioxide displaces the hard acid *t*-butyl alcohol from the soft base triphenylphosphine. The soft–soft complex is favoured, so the equilibrium constant is greater than 1.

c) $CH_3HgI + HCl \rightleftharpoons CH_3HgCl + HI$: Iodide is a softer base than chloride, an example of the general trend that elements later in a group are softer. The soft acid CH_3Hg^+ will form a stronger complex with iodide than with chloride, whereas the hard acid H^+ will prefer chloride, the harder base. Thus, the equilibrium constant is less than 1.

d) $[AgCl_2]^-(aq) + 2\ CN^-(aq) \rightleftharpoons [Ag\ (CN)_2]^-(aq) + 2Cl^-(aq)$: Cyanide is a softer and generally stronger base than chloride. Therefore, cyanide will displace the relatively harder base from the soft Lewis acid Ag^+. The equilibrium constant is greater than 1.

E5.14 As you add methyl groups to the nitrogen, the nitrogen becomes more basic due to the inductive effect (electron donating ability) of the methyl groups. So the trend $NH_3<NH_2(CH_3)<NH(CH_3)_2$ makes sense, but when you put three methyl groups around nitrogen, sterics come into play. Trimethylamine is sterically large enough to fall out of line with the given enthalpies of reaction.

E5.15 The metathesis of two hard acids with two hard bases occurs as equilibrium is established between solid, insoluble SiO_2, and soluble H_2SiF_6:

$$SiO_2 + 6HF \rightleftharpoons 2H_2O + H_2SiF_6$$

or

$$SiO_2 + 4HF \rightleftharpoons 2H_2O + SiF_4$$

This is both a Brønsted acid–base reaction and a Lewis acid–base reaction. The Brønsted reaction involves the transfer of protons from HF molecules to O^{2-} ions, whereas the Lewis reaction involves complex formation between Si(IV) centre and F^- ions.

E5.16 **a) Favour displacement of Cl^- by I^- from an acid centre:** Since in this case you have no control over the hardness or softness of the acid centre, you must do something else that will favour the acid–iodide complex over the acid-chloride complex. If you choose a solvent that decreases the activity of chloride relative to iodide, you can shift the following equilibrium to the right:

$$\text{acid-}Cl^- + I^- \rightleftharpoons \text{acid-}I^- + Cl^-$$

Such a solvent should interact more strongly with chloride (i.e., form an adduct with chloride) than with iodide. Thus, the ideal solvent properties in this case would be *weak*, *hard*, and *acidic*. It is important that the solvent be a

weak acid because otherwise the activity of both halides would be rendered negligible. An example of a suitable solvent is anhydrous HF. Another suitable solvent is H_2O.

b) Favour basicity of R_3As over R_3N: In this case you wish to enhance the basicity of the soft base trialkylarsine relative to the hard base trialkylamine. You can decrease the activity of the amine if the solvent is a hard acid because the solvent–amine complex would then be less prone to dissociate than the solvent–arsine complex. Alcohols such as methanol or ethanol would be suitable.

c) Favour acidity of Ag^+ over Al^{3+}: If you review the answers to parts (a) and (b) of this exercise, a pattern will emerge. In both cases, a hard acid solvent was required to favour the reactivity of a soft base. In this part of the exercise, you want to favour the acidity of a soft acid, so logically a solvent that is a hard base is suitable. Such a solvent will "tie up" (i.e., decrease the activity of) the hard acid Al^{3+} relative to the soft acid Ag^+. An example of a suitable solvent is diethyl ether. Another suitable solvent is H_2O.

d) Promote the reaction $2FeCl_3 + ZnCl_2 \rightarrow Zn^{2+} + 2[FeCl_4]^-$: Since Zn^{2+} is a softer acid than Fe^{3+}, a solvent that promotes this reaction will be a softer base than Cl^-. The solvent will then displace Cl^- from the Lewis acid Zn^{2+}, forming $[Zn(solv)_x]^{2+}$. The solvent must also have an appreciable dielectric constant because ionic species are formed in this reaction. A suitable solvent is acetonitrile, MeCN.

E5.17 Mercury(II), Hg^{2+}, is a soft Lewis acid, and so is found in nature only combined with soft Lewis bases, the most common of which is S^{2-}. Sulfide can readily and permanently abstract Hg^{2+} from its complexes with harder bases in ore-forming geological reaction mixtures. Zinc(II), which exhibits borderline behaviour, is harder and forms stable compounds (i.e., complexes) with hard bases such as O^{2-}, CO_3^{2-}, and silicates, as well as with S^{2-}. The ore that is formed with Zn^{2+} depends on factors including the relative concentrations of the competing bases.

E5.18 The dissolution of silicates in HF is both a Brønsted acid–base reaction and a Lewis acid–base reaction. The reaction involves proton transfers from HF to the silicate oxygen atoms (a Brønsted reaction), and the formation of complexes such as SiF_6^{2-} from the Lewis acid Si^{4+} and the Lewis base F^- (a Lewis reaction).

E5.19 From Table 5.5 we find $E = 2.05$ and $C = 2.05$ for I_2 and $E = 8.86$ and $C = 0.09$ for phenol. The Drago-Wayland equation gives:

$$\Delta_f H^\circ = -\left[E_A E_B + C_A C_B\right]$$

$$\Delta_f H^\circ = -20.0\text{kJ/mol}$$

Indicating an exothermic reaction for the formation of an I_2–phenol adduct.

E5.20 Since $Si(OH)_4$ is a weaker acid than H_2CO_3, H_2CO_3 can replace $Si(OH)_4$ from its salts; that is, it can protonate the conjugate base of $Si(OH)_4$. The following two equilibria in the system $CO_2(g)/CO_2(aq)$ are important for this exercise:

$$CO_2(g) \rightleftharpoons CO_2(aq) \quad (1)$$

$$CO_2(aq) + H_2O(l) \rightleftharpoons H_2CO_3(aq) \quad (2)$$

The $H_2CO_3(aq)$ that is formed reacts with solid silicate M_2SiO_4 causing the silicate to dissolve according to equation (3) (one of several possible reactions):

$$M_2SiO_4(s) + 4H_2CO_3(aq) \rightleftharpoons 2M^{2+} + Si(OH)_4(aq) + 4HCO_3^-(aq) \quad (3)$$

Equilibrium (3) is going to consume $H_2CO_3(aq)$ present in the aqueous solution. This decrease in $H_2CO_3(aq)$ concentration will perturb the equilibrium given by (2). According to Le Chatelier's principle, reaction (2) has to shift to the right—more $CO_2(aq)$ has to react with water to produce H_2CO_3 in order to re-establish the equilibrium conditions. Since reaction (2) has been shifted to the right, so must reaction (1) be shifted to the right as well—the consumption of $CO_2(aq)$ in (2) disturbs the equilibrium (1) and more $CO_2(g)$ has to dissolve in water to produce $CO_2(aq)$. Overall, the more silicate M_2SiO_4 reacts with $H_2CO_3(aq)$, the less $CO_2(g)$ will be present.

E5.21 The trend in symmetrical M–O stretching vibration frequencies relates very well with the acidities of these aqua acids. The frequencies increase in the order $Ca^{2+} < Mn^{2+} < Zn^{2+}$, the same order that the M–O bond strength increases. This is a reasonable observation because in the same order the radii of M^{2+} cations are decreasing and charge density is increasing. With increasing charge density, the attraction between M^{2+} cation and partially negative O atom in H_2O is increasing. For the same reason, the acidity of these aqua acids is increasing showing that two trends correlate closely.

E5.22 Equation (b) is better in explaining the observations described in the exercise. Most notably it contains the Lewis acid-base adduct $[FeCl_2(OPCl_3)_4]^+$ in which $OPCl_3$ is a Lewis base and coordinates via its O atom, consistent with vibrational data. It also has the $Fe_2Cl_6/[FeCl_4]^-$ (i.e., red/yellow) equilibrium. The titration would have to start in either case from a concentrated (red) solution, and the equivalence point at 1 : 1 mole ratio $FeCl_3/Et_4NCl$ can be explained based on the reaction:

$$Fe_2Cl_6 + 2Et_4NCl \rightleftharpoons 2[FeCl_4]^- + 2Et_4N^+$$

E4.23 The first step in the reaction catalysed by Cl^- ions is formation of $*SO_2Cl^-$ (where *S is the radioactively labelled sulfur atom):

$$*SO_2 + Cl^- \rightleftharpoons *SO_2Cl^-$$

In this reaction SO_2 is a Lewis acid (see Section 5.7(e) *Group 16 Lewis acids*), whereas the catalyst, Cl^-, is a Lewis base. The next step involves reaction between $*SO_2Cl^-$ and $SOCl_2$ in which oxygen and chlorine atoms are exchanged:

$$*SO_2Cl^- + SOCl_2 \rightleftharpoons *SOCl_2 + SO_2Cl^-$$

Finally, newly formed, unlabelled SO_2Cl^- dissociates to release the catalyst and SO_2:

$$SO_2Cl^- \rightleftharpoons SO_2 + Cl^-$$

The first step in the reaction catalysed by $SbCl_5$ is formation of $*SOCl_2{\cdot}SbCl_5$ adduct:

$$*SOCl_2 + SbCl_5 \rightleftharpoons *SOCl_2{\cdot}SbCl_5$$

In this reaction $SbCl_5$ behaves as a Lewis acid (see Section 5.7(d) *Group 15 Lewis acids*), whereas $*SOCl_2$ is a Lewis base. The adduct reacts with SO_2 and the chlorides and oxygen atoms are exchanged:

$$*SOCl_2{\cdot}SbCl_5 \rightleftharpoons SOCl_2{\cdot}SbCl_5 + *SO_2$$

Finally, $SOCl_2{\cdot}SbCl_5$ dissociates to liberate the catalyst:

$$SOCl_2{\cdot}SbCl_5 \rightleftharpoons SOCl_2 + SbCl_5$$

E5.24 **a)** The equilibrium constant for this reaction should be less than 1. This is because the reactants are more stable than the products according to the HSAB theory. According to this theory, hard acids like to bind to hard bases and soft acids like to bind soft bases (see Section 5.9(a) and Table 5.4). Cd^{2+} is a soft Lewis acid, whereas Ca^{2+} is a hard Lewis acid. That means Cd^{2+} is going to prefer the soft base I^- over the hard base, F^-. The opposite holds for Ca^{2+}—it is going to preferably bind to F^- over I^-. Thus, the reactants are more stable than the products, and the equilibrium constant is lower than 1.

b) This problem is also solved by looking at the HSAB theory. The reaction involves Cu^+ and Cu^{2+} Lewis acids and I^- and Cl^- Lewis bases. Cu^+ as a soft Lewis acid is going to prefer soft base I^- over harder base Cl^-, thus it will be more stable as $[CuI_4]^{3-}$ (product) than as $[CuCl_4]^{3-}$ (reactant). Similarly, Cu^{2+} of intermediate hardness is going to bond preferably to Cl^- making the $[CuCl_4]^{2-}$ (product) more stable than the $[CuI_4]^{2-}$ (reactant). Overall, in this case, the products are expected to be more stable than reactants, and the equilibrium constant should be greater than 1.

c) This reaction is analysed as a Brønsted acid–base reaction because it involves proton transfer from H_2O to NH_2^-. In this case the equilibrium constant is also greater than 1 because we have a very strong base, NH_2^- a conjugate base of NH_3 as acid, in water.

E5.25 In general, cations such as I_2^+ and Se_8^{2+} should behave like good Lewis acids. Therefore, these cations should react (even) with a weakly basic solvent and will be lost. Hence, they can survive and be studied *only* in strongly acidic solvents that do not react with them. The same reasoning applies to anions such as S_4^{2-} and Pb_9^{4-}, which are good Lewis bases and can be stabilised by strongly basic solvents because they would react with acidic ones.

E5.26 **a)** Both reactions have the same Lewis base, NMe_3, and the difference in thermodynamic properties between two reactions must lie with the Lewis acids. Note that the steric properties of $B(OMe)_3$ and BEt_3 are about the same. However, oxygen atom has two lone electron pairs. These pairs can donate electrons to the empty p orbital on central B atom reducing the Lewis acidity of this compound through p-p π interaction (similar effect is observed with halogens, see Additional Exercise 5.11). This interaction lowers the Lewis acidity of $B(OMe)_3$ which is reflected in the thermodynamic values.

b) Situation is now inversed on comparison to part a). $N(SiH_3)_3$ is weaker Lewis base than NMe_3 because the lone pair on N atom can be delocalized on Si atoms. This delocalization makes lone electron pair less available for the reaction with Lewis acids (see also Self-Test 5.8).

Chapter 6 An Introduction to Coordination Compounds

Self-Tests

S6.1 **a) Diaquadichloridoplatinum(II).** The formula is $[PtCl_2(OH_2)_2]$. Note the order used in naming complexes of the d-block metals (the metal ion is listed, then ligands are listed in alphabetical order).

b) Diammine*tetra*(thiocyanato-κ*N*)chromate(III). The *-ate* suffix added to the name of the metal indicates an overall negative charge of the complex species. Two NH_3 molecules and four NCS^- anions are bonded to the Cr(III) ion. The NCS^- ligands use their N atoms to bond to Cr(III) as indicated by κ*N* after the ligand name. The formula is $[Cr(\underline{N}CS)_4(NH_3)_2]^-$.

c) *Tris*(1,2-diaminoethane)rhodium(III). The metal ion is Rh(III), there are three bidentate (chelating) ligands (see Table 6.1), and the complex is not anionic (-rhodium(III), not -rhodate(III)). The formula is $[Rh(\kappa^2N\text{-}H_2NCH_2CH_2NH_2)]^{3+}$ where κ^2N indicates that the ligand is bound to Rh^{3+} through both N atoms. Since the accepted abbreviation for 1,2-diaminoethane is en, the formula may be written abbreviated as $[Rh(en)_3]^{3+}$.

d) Bromido*penta*carbonylmanganese(I). The manganese has five CO bonded to it along with one bromide. The formula is $[MnBr(CO)_5]$.

e) Chlorido*tris*(triphenylphosphine)rhodium(I). The formula is $[RhCl(PPh_3)_3]$.

S6.2 The hydrate isomers $[Cr(NO_2)(H_2O)_5]NO_2{\cdot}H_2O$ and $[Cr(H_2O)_6](NO_2)_2$ are possible, as are linkage isomers of the NO_2 group. One possible linkage isomer is $[Cr(ONO)(H_2O)_5]NO_2 \cdot H_2O$.

S6.3 The two square-planar isomers of $[PtBrCl(PR_3)_2]$ are shown below. The NMR data indicate that isomer A is the *trans* isomer because the two trialkylphosphine ligands occupy opposite corners of the square plane and are in the identical magnetic environment (i.e., they are NMR equivalent). As a consequence, both P nuclei appear as a singlet in the ^{31}P NMR spectrum. Isomer B is the *cis* isomer. Note that the two phosphine ligands in the *trans* isomer are related by symmetry elements that this C_{2v} molecule possesses, namely the C_2 axis (the Cl-Pt-Br axis) and the σ_v mirror plane that is perpendicular to the molecular plane. Therefore, they exhibit the same chemical shift in the ^{31}P NMR spectrum of this compound. The two phosphine ligands in the *cis* isomer are not related by the σ mirror plane that this C_s molecule possesses. Since they are chemically nonequivalent, they give rise to separate groups of ^{31}P resonances.

Complex A **Complex B**

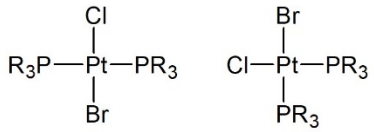

trans-$[PtBrCl(PR_3)]$ *cis*-$[PtBrCl(PR_3)]$

S6.4 The glycinato ligand is an unsymmetrical bidentate ligand (it has a neutral amine nitrogen donor atom and a negatively charged carboxylate oxygen donor atom, see Table 6.1). In the *fac* isomer, the three N atoms (or three O atoms) of glycinato ligand should be adjacent and occupy the corners of one triangular face of the octahedron. In the *mer* isomer, three N atoms should lie in one plane and the O atoms should lie in a perpendicular plane. If you imagine that the complex is a sphere, the three N atoms in the *mer* isomer lie on a *meridian* of the sphere (the largest circle that can be drawn on the surface of the sphere). The two isomers and their non-superimposable mirror images are shown below.

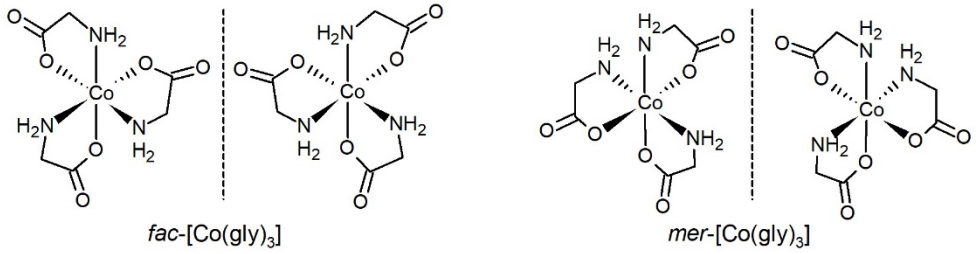

S6.5 **a) *cis*-$[CrCl_2(ox)_2]^{3-}$:** Drawings of two mirror images of this complex are shown below. They are *not* superimposable and neither molecule possesses a mirror plane or a centre of inversion. Therefore, they represent two enantiomers and this complex is chiral.

b) *trans*-$[CrCl_2(ox)_2]^{3-}$: Drawings of two mirror images of this complex are also shown below. They *are* superimposable, and therefore do not represent two enantiomers but only a single isomer. Note that the complex has at least one mirror plane; for example, one that is defined by two Cl and Cr atoms and bisects the ligand backbones.

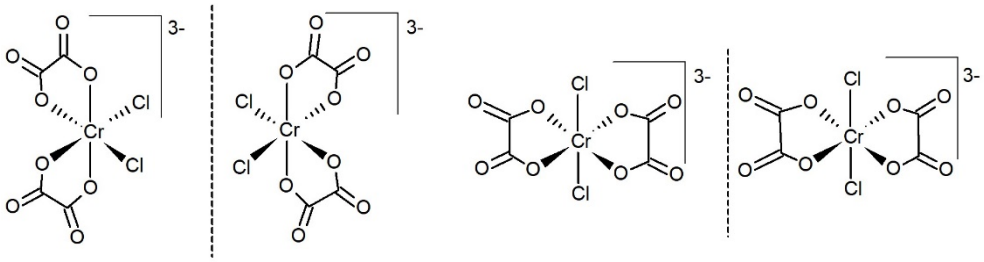

c) *cis*-$[RhH(CO)(PR_3)_2]$: This is a complex of Rh(I), which is a d^8 metal ion. Four-coordinate d^8 complexes of period 5 and period 6 metal ions are almost always square-planar, and $[RhH(CO)(PR_3)_2]$ is no exception. The bulky PR_3 ligands are *cis* to one another. This compound has C_s symmetry, with the mirror plane coincident with the rhodium atom and the four ligand atoms bound to it. A planar complex cannot be chiral, whether it is square-planar, trigonal planar, etc., unless the ligands coordinated to the metal are chiral (see Section 6.11 *Ligand chirality*). In this case none of the ligands are chiral and the complex is achiral.

S6.6 The first substitution step follows the equation:

$$[M(H_2O)_6]^{2+} + L \rightarrow [ML(H_2O)_5]^{2+} + H_2O$$

with $K_{f1} = 1\times10^5$.

The second substitution step is:

$$[ML(H_2O)_5]^{2+} + L \rightarrow [ML_2(H_2O)_4]^{2+} + H_2O.$$

We can see that substitution of any of the five remaining waters leads to the desired product. The replacement of the sixth ligand, L, would result in no net reaction—or substitution of five out of six ligands in the reactant leads to the product. Consequently, we can expect K_{f2} to be 5/6 of the K_{f1}:

$$K_{f2} = K_{f1} \times 5/6 = 1\times10^5 \times 5/6 = 0.83 \times 10^5.$$

The same analysis can be extended to the third step:

$$[ML_2(H_2O)_4]^{2+} + L \rightarrow [ML_3(H_2O)_3]^{2+} + H_2O.$$

In this case substitution of four out of 6 ligands leads to the desired product and

$$K_{f3} = K_{f1} \times 4/6 = 1\times10^5 \times 4/6 = 0.67 \times 10^5.$$

Following the same procedure, we can find other K values:

$$K_{f4} = K_{f1} \times 3/6 = 1\times10^4 \times 3/6 = 0.50 \times 10^5,$$

$$K_{f5} = K_{f1} \times 2/6 = 1\times10^5 \times 2/6 = 0.33 \times 10^5, \text{ and}$$

$$K_{f6} = K_{f1} \times 1/6 = 1\times10^5 \times 1/6 = 1.7 \times 10^5.$$

From here, the overall formation constant (β_6), is the product of these stepwise formation constants:

$$\beta_6 = 1\times10^5 \times 0.83\times10^5 \times 0.67\times 10^5 \times 0.50\times10^5 \times 0.33\times10^5 \times 0.17\times 10^5 = 1.6 \times 10^{28}.$$

Exercises

E6.1 **a) $[Ni(CN)_4]^{2-}$:** Tetracyanidonickelate(II), like most d^8 metal complexes with four ligands, has square-planar geometry, shown below.

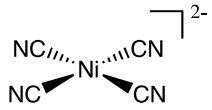

b) $[CoCl_4]^{2-}$: Tetrachloridocobaltate(II) is tetrahedral, like most of the first-row transition metal chlorides.

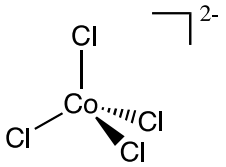

c) $[Mn(NH_3)_6]^{2+}$: Hexaamminemanganese(II) has octahedral geometry, shown below Coordination number 6 in general can have two geometries: octahedral and trigonal prismatic (see Section 6.4(c) *Six-coordination*). The trigonal prismatic geometry is, however, very rare and we can confidently assign octahedral geometry to a vast majority of complexes with this coordination number.

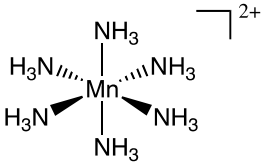

E6.2 **a) *cis*-$[CrCl_2(NH_3)_4]^+$:** *cis*-tetraamminedichloridochromium(III)

b) *trans*-$[Cr(NCS)_4(NH_3)_2]^-$: *trans*-diamminetetra(κ*N*-thiocyanato)chromate(III)

c) $[Co(C_2O_4)(en)_2]^+$: bis(1,2-diaminoethane)ethylenediamineoxalatocobalt(III), which is neither *cis* nor *trans* but does have one optical isomer, shown below.

E7.3(c): $[Co(C_2O_4)(en)_2]^+$

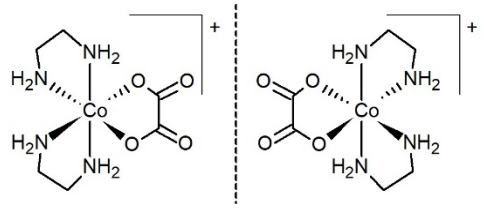

E6.3 With five-coordinate complexes, the two possible geometries are trigonal bipyramidal and square-based pyramidal, as shown below.

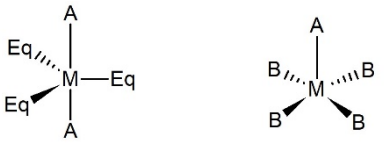

Trigonal bipyramidal:
A = axial ligands
Eq = equatorial ligands

Square pyramidal:
A = axial ligand
B = basal ligands

E6.4 The terms monodentate, bidentate, and tetradentate describe how many Lewis bases you have on your ligand and whether they can physically bind to the metal (i.e., behave as electron pair donors to the metal). A monodentate ligand can bond to a metal atom only at a single atom, also called a donor atom. A bidentate ligand can bond through two atoms, and a tetradentate ligand can bond through four atoms. Examples of monodentate and bidentate ligands are shown below. Tetraazacclotetradecane, from Table 6.1, is an example of a tetradentate ligand—all four nitrogen atoms can donate a lone pair to the metal.

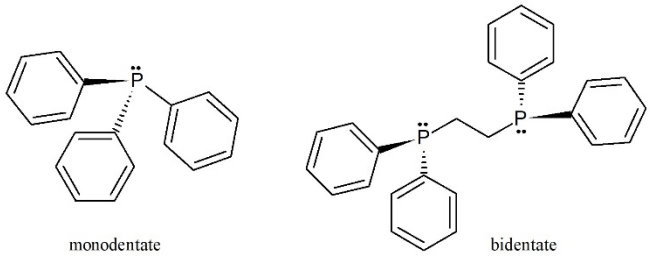

monodentate bidentate

E6.5 **a)** Bisdimethylphosphino ethane (dmpe) bonds to a metal through lone pairs on two phosphorus atoms; thus dmpe is a bidentate, chelating ligand that could also be a bridging ligand due to free rotation around single bonds.

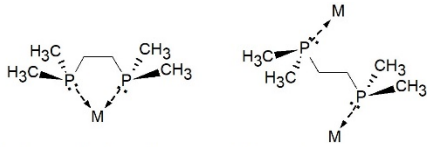

bidentate, chelating dmpe bridging dmpe

b) 2,2′-Bipyridine (bpy) is a bidentate, chelating ligand that is able to bond to a metal through both of its nitrogen atoms.

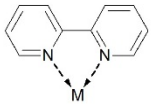

c) Pyrazine is a monodentate ligand even though it has two Lewis basic sites. Because of the location of the nitrogen atoms, the ligand can only bond to one metal; it can, however, bridge two metals, as shown below.

monodentate pyrazine bridging pyrazine

d) Diethylenetriamine (dien) ligand has three Lewis basic nitrogen atoms, thus it could be a tridentate ligand that forms two chelating rings with one metal. It can, however, also act as a bidentate ligand (bonding using only two

N atoms) forming one chelate ring and could be a bridging ligand if the third nitrogen atom is bonded to the second metal (in theory, all three nitrogen atoms could bind to three different metallic centres as well):

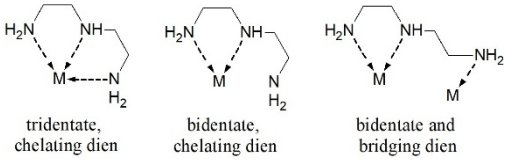

e) Tetraazacyclododecane ligand, with its four Lewis basic nitrogen atoms, could be a tetradentate, macrocyclic ligand. Note that structure **I**, in which M and N atoms are more-or-less in one plane, would be limited to small cations (for example Li^+) because the hole of the macrocycle prevents larger cations from fitting in. For a larger cation, structure **II** in which the ligand's N atoms are above the metal atom, would be expected. This ligand could be bidentate and bridging (e.g., free N atoms in the bidentate structure are free to bind to another metallic centre).

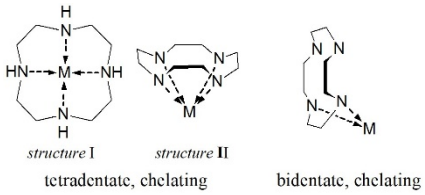

E6.6 $[RuBr(NH_3)_5]Cl$ and $[RuCl(NH_3)_5]Br$ complexes differ as to which halogen is bonded, and as to which one is the counter ion. These types of isomers are known as ionization isomers because they give different ions in the solution. When dissolved $[RuBr(NH_3)_5]Cl$ will dissociate into $[RuBr(NH_3)_5]^+$ and chloride ions, while $[RuCl(NH_3)_5]Br$ will produce $[RuCl(NH_3)_5]^+$ and bromide ions.

E6.7 For square-planar complexes, depending on the ligands, several isomers are possible.

a) $[Pt(ox)(NH_3)_2]$ has no isomers because of the chelating oxalato ligand. The oxalate forces the ammonia molecules to be *cis* only.

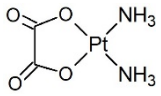

b) $[PdBrCl(PEt_3)_2]$ has two isomers, *cis* and *trans*, as shown below.

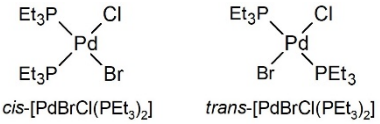

c) $[IrHCO(PR_3)_2]$ has two isomers, *cis* and *trans*, as shown below.

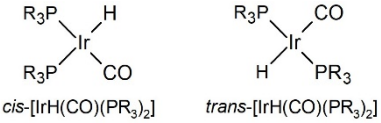

d) $[Pd(gly)_2]$ has two isomers, *cis* and *trans*, as shown below.

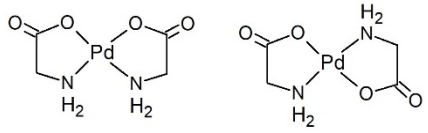

cis-[Pd(gly)$_2$] *trans*-[Pd(gly)$_2$]

E6.8 Ignoring optical isomers, nine isomers are possible. Including optical isomers, 15 isomers are possible! Read Section 6.10(a) *Geometrical isomerism* for a better understanding of all the possible isomers.

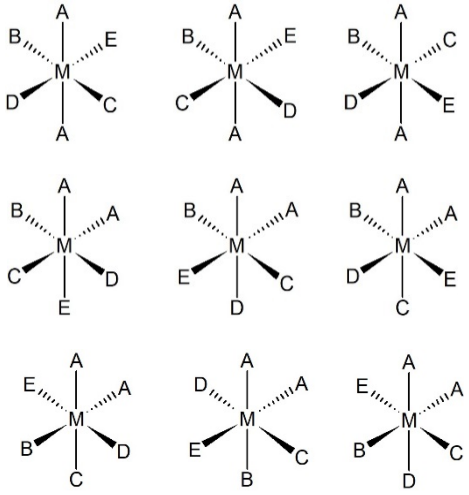

E6.9 Below is a picture of both isomers. The best way to do this problem is to draw both isomers as mirror images of each other, and look along one of the four C_3 symmetry axes found of ideal octahedral structure. If the ligand backbone is rotating clockwise then the structure is the Δ isomer, if it rotates counter clockwise, it is the Λ isomer. When you do this, it is obvious which isomer you have, in the case of this problem, the complex drawn in the exercise is the Λ isomer. For more help with this concept read Section 6.10(b) *Chirality and optical isomerism.*

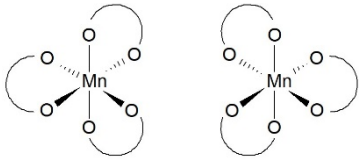

Assigned structure: Δ isomer Mirror image: Λ isomer

E6.10 The values of the stepwise formation constants drop from K_{f1} to K_{f4}, as expected on statistical grounds. However, the fifth stepwise formation constant is substantially lower, suggesting a change in coordination. In fact, what happens is the very stable square planar complex ion $[Cu(NH_3)_4]^{2+}$ is formed, and the addition of the fifth NH_3 ligand is very difficult. The equilibrium for this step is shifted to the left (toward reactants). This results in $K_{f5} < 1$ with a negative log value.

Chapter 7 Oxidation and Reduction

Self-Tests

S7.1 Following the procedure outlined in Example 7.1, we find the following two half-reactions:

$$MnO_4^-(aq) + 8H^+(aq) + 5e^- \rightarrow Mn^{2+}(aq) + 4H_2O(l) \qquad \text{reduction half-reaction}$$

$$Zn(s) \rightarrow Zn^{2+}(aq) + 2e^- \qquad \text{oxidation half-reaction}$$

The reduction half-reaction requires five electrons whereas the oxidation half-reaction requires two electrons; therefore, we must balance electrons so that an equal number of electrons are required in both reactions. The reduction reaction must be multiplied by 2 and the oxidation reaction by 5 to give 10 electrons in each case:

$$2MnO_4^-(aq) + 16H^+(aq) + 10e^- \rightarrow 2Mn^{2+}(aq) + 8H_2O(l) \qquad \text{reduction half-reaction}$$

$$5Zn(s) \rightarrow 5Zn^{2+}(aq) + 10e^- \qquad \text{oxidation half-reaction}$$

Summing two half-reactions and cancelling $10e^-$ found on both the left and right sides of the equation, we obtain the full reaction:

$$2MnO_4^-(aq) + 5Zn(s) + 16H^+(aq) \rightarrow 5Zn^{2+}(aq) + 2Mn^{2+}(aq) + 8H_2O(l).$$

S7.2 No, copper metal is not expected to react with dilute HCl because the $E°$ for the reaction $Cu^{2+}(aq) + 2\ e^- \rightarrow Cu(s)$, $E°(Cu^{2+}, Cu) = +0.34$ V is positive. The oxidation of Cu metal in HCl, $Cu(s) + 2\ H^+(aq) \rightarrow Cu^{2+}(aq) + H_2(g)$, is not favoured thermodynamically because the cell potential for the reaction is negative (–0.34 V), resulting in a positive ΔG.

S7.3 The standard reduction potential for the $Cr_2O_7^{2-}/Cr^{3+}$ couple is +1.38 V, so it can oxidize any couple whose reduction potential is less than +1.38 V. Since the reduction potential for the Fe^{3+}/Fe^{2+} couple (+0.77 V) is less positive than $Cr_2O_7^{2-}/Cr^{3+}$ reduction potential, Fe^{2+} will be oxidized to Fe^{3+} by dichromate. The reduction potential for the Cl_2/Cl^- couple (+1.36 V) is slightly less positive than that of the $Cr_2O_7^{2-}/Cr^{3+}$ couple, so a side reaction with Cl^- should be expected.

S7.4 The potential difference of the cell from Example 7.45 was calculated to be +1.23 V. To calculate the potential difference under non-standard conditions we start with the Nernst equation given by the formula:

$$E_{cell} = E° - \frac{RT}{\nu_e F} \ln Q \text{, where } Q \text{ is the reaction quotient.}$$

For the fuel-cell reaction, $O_2(g) + 2H_2(g) \rightarrow 2\ H_2O(1)$, the reaction quotient is:

$$Q = \frac{1}{p(O_2)\,p(H_2)}.$$

Recalling that ν is the number of electrons exchanged, we have:

$$E_{cell} = E° - [(0.059\text{ V})/4][\log(1/(5.0)^2)]$$

$$= +1.23\text{ V} + 0.02\text{ V} = +1.25\text{ V}.$$

Therefore, the new potential difference for the fuel cell is +1.25 V.

S7.5 The complete coupled reaction for oxidation of $SO_2(aq)$ by atmospheric oxygen is given below:

$$2SO_2(aq) + O_2(g) + 2H_2O(l) \rightarrow 2SO_4^{2-}(aq) + 4H^+(aq)$$

Since the standard reduction potential for the SO_4^{2-}/SO_2 couple is +0.16 V and the standard reduction potential for the O_2/H_2O couple is +1.23 V then the potential difference for the equation above is $E°$ = +1.23 V – 0.16 V = +1.07 V. Since this potential is large and positive, the Gibbs energy of this reaction is negative (reaction is hence spontaneous) and will be driven nearly to completion ($K > 1$). Thus, the expected thermodynamic fate of SO_2 is its conversion to sulfate (or neutral sulfuric acid vapour). This aqueous solution of SO_4^{2-} and H^+ ions precipitates as acid rain, which can have a pH as low as 2 (the pH of rain water that is not contaminated with sulfuric or nitric acid is ~5.6).

S7.6 The disproportionation of Fe^{2+} involves the reduction of one equivalent of Fe^{2+} to Fe^0, a net gain of two equivalents of electrons, and the concomitant oxidation of two equivalents to Fe^{2+} to Fe^{3+}, a net loss of two equivalents of electrons:

$$3\,Fe^{2+}(aq) \rightarrow Fe^{0}(s) + 2Fe^{3+}(aq)$$

The value of E_{cell} for this reaction can be calculated by subtracting $E°$ for the Fe^{2+}/Fe couple (–0.44 V) from $E°$ for the Fe^{3+}/Fe^{2+} couple (+0.77 V),

$$E = –0.44 – 0.77\ V = –1.21\ V$$

This potential is large *and negative*, resulting in a positive $\Delta_r G$ (non-spontaneous reaction), so the disproportionation will *not* occur.

S7.7 Compared to the aqua redox couple of +0.25 V, the given value is higher by +1.01 V and we conclude that bpy binds preferentially to Ru(II).

Using Equation 5.12b from your textbook, we obtain

$$E°(M) – E°(ML) = (0.059V)\times\log(K^{ox}/K^{red})$$

$$E°(Ru^{3+}(aq)) – E°([Ru(bpy)_3]^{3+}) = +0.25V – (+1.26V) = –1.01V$$

$$–1.01V = (0.059V)\times\log(K^{ox}/K^{red})$$

$$-\frac{1.01\text{V}}{0.059\text{V}} = -17.11\log\frac{K^{ox}}{K^{red}} \Rightarrow 17.11\log\frac{K^{red}}{K^{ox}}$$

Thus, the binding of three bpy ligands to Ru(III) is about 17 orders of magnitude decreased relative to binding to Ru(II).

S7.8 We need to consider a theromodynamic cycle that links the solubility product under the experimental condition of Cl^- concentration (here simplified, since $[Cl^-] = 1.0$ mol dm^{-3}). For the thermodynamic cycle $\Delta G = 0$, so we obtain $E_{AgCl/Ag} = RT \ln K_{sp} + E_{Ag+/Ag}$ = –0.577 V + 0.80 V = +0.223 V.

S7.9 **(a)** Pu(IV) disproportionates to Pu(III) and Pu(V) in aqueous solution because Pu(IV) is a stronger oxidant in acidic solution compared to Pu(V).

(b) Pu(V) does not disproportionate into Pu(VI) and Pu(IV).

S7.10 See the figure below. This plot was made using the potentials given, $NE° = 0$ V for Tl^0 ($N = 0$), $NE° = –0.34$ V for Tl^+ ($N = 1$), and $NE° = 2.16$ V for Tl^{3+} ($n = 3$). Note that Tl^+ is stable with respect to disproportionation in aqueous acid. Note also that Tl^{3+} is a strong oxidant (i.e., it is very readily reduced) because the slope of the line connecting it with either lower oxidation state is large and positive.

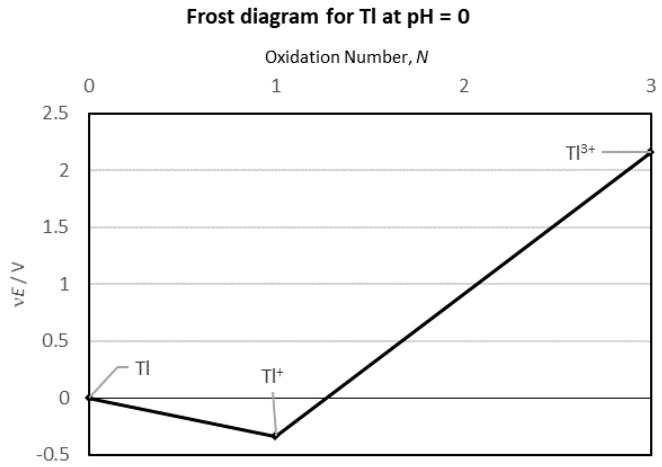

S7.11 When permanganate, MnO_4^-, is used as an oxidant in aqueous solution, the manganese species that will remain is the most stable manganese species under the conditions of the reaction (i.e., acidic or basic). Inspection of the Frost diagram for manganese, shown in Figure 7.10, shows that $Mn^{2+}(aq)$ is the most stable species present because it has the most negative $\Delta_f G$. Therefore, $Mn^{2+}(aq)$ will be the final product of the redox reaction when MnO_4^- is used as an oxidizing agent in aqueous acid.

S7.12 For kinetic reasons, the reduction of nitrate ion usually proceeds to NO, instead of to N_2O or all the way to N_2. That means that our redox couple is NO_3^-/NO and we have to compare the slope of the line connecting the NO_3^- and NO points for both acidic and basic solution. If you compare the Frost diagram for nitrogen in acidic and in basic solutions, you see that the slope for the NO_3^-/NO couple in acidic solution is positive while the slope for basic solution is negative. Therefore, nitrate is a stronger oxidizing agent (i.e., it is more readily reduced) in acidic solution than in basic solution. Even if the reduction of NO_3^- proceeded all the way to N_2, the slope of that line is still less than the slope of the line for the NO_3^-/NO couple in acid solution.

S7.13 According to Figure 7.12, a typical waterlogged soil (rich in organic material but oxygen depleted) has an average pH of about 4 and an average potential of about –0.1 V. If you find this point on the Pourbaix diagram for naturally occurring iron species, shown on Figure 7.11, you see that $Fe(OH)_3$ is not stable and $Fe^{2+}(aq)$ will be the predominant species. In fact, as long as the potential remains at –0.1 V, Fe^{2+} is the predominant species below pH = 8. Above pH = 8, Fe^{2+} is oxidized to Fe_2O_3 at this potential.

S7.14 According to the Ellingham diagram shown in Figure 7.16, at about 2000°C the line (a) for the reducing agent (C/CO) dips below the MgO line, which means that at that temperature the reactions $2Mg(1) + O_2(g) \rightarrow 2MgO(s)$ and $2C(s) + O_2(g) \rightarrow 2CO(g)$ have the same free-energy change. Thus, coupling the two reactions (i.e., subtracting the first from the second) yields the overall reaction $MgO(s) + C(s) \rightarrow Mg(1) + CO(g)$ with $\Delta G = 0$. At 2000°C or above, MgO can be conveniently reduced to Mg by carbon.

Exercises

E7.1 Oxidation numbers for each element in each species are given below the element's symbol:

$2\,NO(g)$	+	$O_2(g)$	→	$2\,NO_2(g)$						
(+2) (–2)		(0)		(+4) (–2)						
$2Mn^{3+}(aq)$	+	$2H_2O$	→	MnO_2	+	Mn^{2+}	+	$4H^+(aq)$		
(+3)		(+1) (–2)		(+4) (–2)		(+2)		(+1)		
$LiCoO_2(s)$	+	$C(s)$	→	$LiC(s)$	+	$CoO_2(s)$				
(+1) (+3) (–2)		(0)		(+1)(–1)		(+4) (–2)				
$Ca(s)$	+	$H_2(g)$	→	$CaH_2(s)$						
(0)		(0)		(+2) (–1)						

E7.2 For all species given in the exercise, you must determine whether they can be oxidized by O_2. The standard potential for the reduction $O_2 + 4H^+ + 4e^- \rightarrow 2H_2O$ is +1.23 V. Therefore, only redox couples with a reduction potential less positive than 1.23 V will be driven to completion to the oxidized member of the couple by the reduction of O_2 to H_2O.

a) Cr^{2+}: Since the Cr^{3+}/Cr^{2+} couple has $E°$ = –0.424 V, Cr^{2+} *will* be oxidized to Cr^{3+} by O_2. The balanced equation is:

$$4Cr^{2+}(aq) + O_2(g) + 4H^+(aq) \rightarrow 4Cr^{3+}(aq) + 2H_2O(l) \qquad E° = +1.65\ V$$

b) Fe^{2+}: Since the Fe^{3+}/Fe^{2+} couple has $E°$ = +0.771 V, Fe^{2+} *will* be oxidized to Fe^{3+} by O_2. The balanced equation is:

$$4Fe^{2+}(aq) + O_2(g) + 4H^+(aq) \rightarrow 4Fe^{3+}(aq) + 2H_2O(l) \qquad E° = +0.46\ V$$

c) Cl^-: Both of the following couples have $E°$ values, shown in parentheses, more positive than +1.23 V, so there will be no reaction when acidic Cl^- solution is aerated: ClO_4^-/Cl^- (+1.387 V); Cl_2/Cl^- (+1.358 V). Therefore, Cl^- is stable under these conditions and there is no reaction.

d) HOCl: Since the $HClO_2$/HClO couple has $E°$ = +1.701 V, the cell potential for oxidation of HOCl by O_2 is –0.47 V (negative, unfavourable). Thus, HClO will not be oxidized to $HClO_2$ by O_2 and there is no reaction.

e) Zn(s): Since the Zn^{2+}/Zn couple has $E°$ = –0.763 V, metallic zinc *will* be oxidized to Zn^{2+} by O_2. The balanced equation is:

$$2\ Zn(s) + O_2(g) + 4H^+(aq) \rightarrow 2\ Zn^{2+}(aq) + 2H_2(l) \qquad E° = +1.99\ V$$

In this case, there is a competing reaction $Zn(s) + 2\ H^+(aq) \rightarrow Zn^{2+}(aq) + H_2(g)$ ($E°$ = +0.763 V).

E7.3 From Section 7.10 *The influence of complexation* we see that the reduction potential of the complex species ML, $E°$(ML), is related to the reduction potential of the corresponding aqua ion M, $E°$(M), through the Equation 7.12a:

$$E°(\mathrm{ML}) = E°(\mathrm{M}) - \frac{RT}{\nu_e F} \ln \frac{K^{ox}}{K^{red}}.$$

The equation shows that $E°$(ML) is influenced by the temperature in two ways: 1) the RT/ν_eF ratio and 2) the values of the equilibrium constants K. The influence of RT/ν_eF is the same for both Ru and Fe complex and $E°$ (ML) values. Thus, the reason must be the equilibrium constant: the change in temperature has the opposite effect on one or both K values for the two complexes. This is reflected in the variation of their respective reduction potentials.

E7.4 The standard reduction potentials are equal to the potential difference measured against SHE:

$$M^{3+}(aq) + 1/2H_2(g) \rightarrow M^{2+}(aq) + H^+(aq) \qquad \Delta_rG = -\nu FE^o.$$

To determine the Δ_rG for the above reaction we have to analyse its thermodynamic cycle. Recall that potential and the Gibbs energy are related through equation 7.2: $\Delta_rG = -\nu FE°$. Recall also that for any process $\Delta_rG = \Delta_rH - T\Delta_rS$. We are going to assume that for each M^{3+}/M^{2+} couple $\Delta_rG \approx \Delta_rH$ because $T\Delta_rS$ is significantly smaller than Δ_rH.

The above redox reaction can be broken into reduction and oxidation reaction:

$$\text{Reduction: } M^{3+}(aq) + e^- \rightarrow M^{2+}(aq) \qquad \Delta_{Red}H$$

$$\text{Oxidation: } ½\ H_2(g) \rightarrow H^+(aq) + e^- \qquad \Delta_{Ox}H.$$

From here we see that $\Delta_rG \approx \Delta_rH = \Delta_{Red}H + \Delta_{Ox}H$. $\Delta_{Ox}H$ equals +445 kJ mol^{-1} (see Section 7.3 *Trends in standard potentials* if you need to recall how this value is obtained) but we have to calculate $\Delta_{Red}H$ which can be done by analyzing the following thermodynamic cycle for reduction reaction:

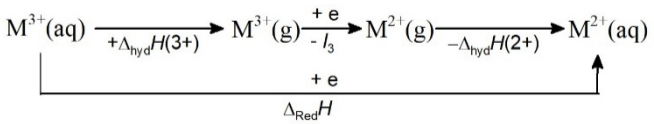

From the cycle, we can see that

$$\Delta_{Red}H = \Delta_{hyd}H(3+) - I_3 - \Delta_{hyd}H(2+).$$

The table below contains the data for all steps of the cycle, estimated ΔrG from the cycle, and final $E°$ values calculated keeping in mind that for these reactions $\nu = 1$:

Redox couple	**Ti^{3+}/Ti^{2+}**	**V^{3+}/V^{2+}**	**Cr^{3+}/Cr^{2+}**	**Mn^{3+}/Mn^{2+}**	**Fe^{3+}/Fe^{2+}**	**Co^{3+}/Co^{2+}**
$\Delta_{hyd}H(3+)$ / kJ mol^{-1}	4154	4375	4560	4544	4430	4651
$-I_3$ / kJ mol^{-1}	-2652	-2828	-2987	-3247	-2957	-3232
$-\Delta_{hyd}H(2+)$ / kJ mol^{-1}	-1882	-1918	-1904	-1841	-1946	-1996
$\Delta_{Red}H$ / kJ mol^{-1}	-380	-371	-331	-544	-473	-577
$\Delta_{Ox}H$ / kJ mol^{-1}	+445	+445	+445	+445	+445	+445
Δ_rH / kJ mol^{-1}	65	74	114	-89	-28	-122
$E°$ ($\approx -\Delta_rH/F$) / V	**+0.67**	**+0.77**	**+1.18**	**+0.92**	**-0.29**	**-1.26**

Although the relative ordering of $E°$ is correct, the quantitative agreement with experimental data is poor, reflecting the fact that we ignored the contributions of entropy.

E7.5 **a)** The Frost diagram for chlorine in basic solution is shown in Figure 7.18. If the points for Cl^- and ClO_4^- are connected by a straight line, Cl_2 lies above it. Therefore, Cl_2 is thermodynamically susceptible to disproportionation to Cl^- and ClO_4^- when it is dissolved in aqueous base. Note that if we would connect Cl^- with other points of the diagram, Cl_2 would always lie above the line. This means that Cl_2 can disproportionate to Cl^- and any other species containing Cl in a positive oxidation state. In practice, however, the disproportionation stops at ClO^- because further oxidation is slow (i.e., a solution of Cl^- and ClO^- is formed when Cl_2 is dissolved in aqueous base).

b) The Frost diagram for chlorine in acidic solution is shown in Figure 7.18. If the points for Cl^- and any positive oxidation state of chlorine are connected by a straight line, the point for Cl_2 lies below it (if only slightly). Therefore, Cl_2 will not disproportionate. However, $E°$ for the Cl_2/Cl^- couple, +1.36 V, is more positive than $E°$ for the O_2/H_2O couple, +1.23 V. Therefore, Cl_2 is (at least thermodynamically) capable of oxidizing water as follows, although the reaction is very slow:

$$Cl_2(aq) + H_2O(l) \rightarrow 2Cl^-(aq) + 2H^+(aq) + \tfrac{1}{2}O_2(g) \qquad E = +0.13\ V$$

c) The point for ClO_3^- in acidic solution on the Frost diagram lies slightly above the single straight line connecting the points for Cl_2 and ClO_4^-. Therefore, since ClO_3^- is thermodynamically unstable with respect to disproportionation in acidic solution (i.e., it *should* disproportionate), the failure of it to exhibit any observable disproportionation must be due to a kinetic barrier.

E7.6 The standard potential for the reduction of Ni^{2+} is +0.25 V. The cell potential, E, is given by the Nernst equation as follows:

$$E = E° - (RT/\nu_eF)\ \ln Q \text{ where } Q = 1/[Ni^{2+}]$$

$[Ni^{2+}]$ can be determined from K_{sp} for $Ni(OH)_2$:

$$K_{sp}[Ni(OH)_2] = [Ni^{2+}][OH^-]^2 \text{ and } [Ni^{2+}] = K_{sp}/[OH^-]^2.$$

Since at pH = 14, $[OH^-] = 1$ M, it follows that $[Ni^{2+}] = K_{sp}$.

Hence:

$$E = +0.25\ \text{V} - \frac{RT}{\nu_e F}\ln\frac{1}{K_{sp}} = +0.025V - \frac{0.059V}{2}\log\frac{1}{1.5\times10^{-16}} = +0.25V - 0.46V = -0.21V$$

The electrode potential is $E = -0.21$ V.

E7.7 The reaction can be broken into two half-reactions as follows:

$$HO_2(aq) \rightarrow O_2(g) + H^+(aq) + \tfrac{1}{2}\,e^- \qquad \text{oxidation half-reaction}$$

$$HO_2 + H^+ + \tfrac{1}{2}\,e \rightarrow H_2O_2 \qquad \text{reduction half-reaction.}$$

The $E°$ for the reaction will be:

$$E° = E_{red} - E_{ox} = +1.150\text{V} - (-0.125\text{V}) = +1.275\text{V}.$$

Looking at the Latimer diagram, we also see that the potential on the right of HO_2 is more positive than the potential on the left of the same species (+1.150 V vs. –0.125 V) informing us immediately that HO_2 has thermodynamic tendency to undergo disproportionation (see Section 7.12(c)).

E7.8 To determine the potential for any couple, you must calculate the *weighted average* of the potentials of intervening couples. In general terms, it is:

$$(n_1E°_1 + n_2E°_2 + \ \ldots\ + n_nE°_n) / (n_1 + n_2 + \ \ldots\ + \ n_n)$$

and in this specific case it is:

$$[(2)(+0.16\ \text{V}) + (2)(+0.40\ \text{V}) + (2)(+0.60\ \text{V})] / (2 + 2 + 2) = +0.387\ \text{V}.$$

E7.9 To calculate an equilibrium constant using thermodynamic data, you can make use of the expressions $\Delta_rG = -RT\ln K$ and $\Delta_rG = -\nu FE$. You can use the given potential data to calculate ΔG for each of the two half-reactions, then you can use Hess's Law to calculate ΔG for the overall process (Δ_rG), and finally calculate K from Δ_rG.
The net reaction $Pd^{2+}(aq) + 4\ Cl^-(aq) \rightarrow [Pd(C1)_4]^{2-}\ (aq)$ is the following sum:

$$Pd^{2+}(aq) + 2e^- \ \rightarrow\ Pd(s)$$

$$Pd(s) + 4C1^-(aq) \ \rightarrow\ [PdC1_4]^{2-}(aq) + 2e^-$$

$$Pd^{2+}(aq) + 4Cl^-(aq) \ \rightarrow\ [PdC1_4]^{2-}(aq)$$

ΔG for the first reaction is $-\nu FE = -(2)(96.5\ \text{kJ mol}^{-1}\ \text{V}^{-1})(+0.915\ \text{V}) = -176.6\ \text{kJ mol}^{-1}$. ΔG for the second reaction is $-(2)(96.5\ \text{kJ mol}^{-1}\ \text{V}^{-1})(-0.6\ \text{V}) = +115.8\ \text{kJ mol}^{-1}$. The net Δ_rG is the sum of these two values, –60.8 kJ mol^{-1}. Therefore, assuming $T = 298$ K:

$$K = \exp[(60.8\ \text{kJ mol}^{-1}) / (\ 8.31\ \text{J K}^{-1}\text{mol}^{-1})(298)] = \exp(24.5) = 4.37 \times 10^{10}.$$

Note that the pH of the solution is 0 because $[H^+] = [HCl] = 1.0$ mol dm^{-3} (HCl is a very strong acid that completely dissociates in water).

E7.10 Since $edta^{4-}$ forms very stable complexes with $M^{2+}(aq)$ ions of 3d-block elements but *not* with the zerovalent metal atoms, the reduction of a $M(edta)^{2-}$ complex will be more difficult than the reduction of the analogous M^{2+} aqua ion. Since the reductions are more difficult, the reduction potentials become less positive (or more negative, as the case may be). The reduction of the $M(edta)^{2-}$complex includes a decomplexation step, with a positive free energy change. The reduction of $M^{2+}(aq)$ does not require this additional expenditure of free energy.

E7.11 **a) Fe?** According to Figure 7.12, the potential range for surface water at pH 6 is between +0.5V and + 0.6 V, so a value of +0.55 V can be used as the approximate potential of an aerated lake at this pH. Inspection of the Pourbaix

diagram for iron (Figure 7.11) shows that at pH 6 and E = +0.55 V, the stable species of iron is $Fe(OH)_3$ precipitate. Therefore, this compound of iron would predominate.

b) Mn? Inspection of the Pourbaix diagram for manganese (Figure 7.13) shows that at pH 6 and E = +0.55 V, the stable species of manganese is solid Mn_2O_3. Therefore, this compound of manganese would predominate.

c) S? At pH 0, the potential for the HSO_4^-/S couple is +0.387 V (this value was calculated using the weighted average of the potentials given in the Latimer diagram for sulfur in Resource Section 3), so the lake will oxidize S_8 all the way to HSO_4^-. At pH 14, the potentials for intervening couples are all negative, so SO_4^{2-} would again predominate. Therefore, HSO_4^- is the predominant sulfur species at pH 6.

E7.12 Any species capable of oxidizing either Fe^{2+} or H_2S at pH 6 cannot survive in this environment. According to the Pourbaix diagram for iron (Figure 7.11), the potential for the $Fe(OH)_3/Fe^{2+}$ couple at pH 6 is approximately 0.3 V. Using the Latimer diagrams for sulfur in acid and base (see Resource Section 2 in the textbook), the S/H_2S potential at pH 6 can be calculated as follows:

$$+0.14\text{ V} - (6/14)[0.14 - (-0.45)] = -0.11\text{ V}.$$

Any potential higher than this will oxidize hydrogen sulfide to elemental sulfur. Therefore, if H_2S is present, the maximum potential possible is approximately –0.1 V.

E7.13 The lines for Al_2O_3 and MgO on the Ellingham diagram (Figure 7.16) represent the change in ΔG^o with temperature for the following reactions:

$$\tfrac{1}{3}Al(l) + O_2(g) \rightarrow \tfrac{2}{3}\,Al_2O_3(s) \quad \text{and} \quad 2Mg(l) + O_2(g) \rightarrow 2MgO(s).$$

At temperatures below about 1600ºC, the Gibbs energy change for the MgO reaction is more negative than for the Al_2O_3 reaction. This means that under these conditions MgO is more stable with respect to its constituent elements than is Al_2O_3, and that Mg will react with Al_2O_3 to form MgO and Al. However, above about 1600ºC the situation reverses, and Al will react with MgO to reduce it to Mg with the concomitant formation of Al_2O_3. This is a rather high temperature, achievable in an electric arc furnace (compare the extraction of silicon from its oxide, discussed in Section 7.16).

E7.14 Since we are not given the oxidation half-reaction (only two reduction half-reactions) we can assume that the $\Delta_r G°$ and K are calculated using SHE for the oxidation half-reaction. For both reactions, we have to work under basic conditions, so we are going to assume "standard basic solution" of pH = 14 (this is the basic medium for which reduction potentials are reported, hence the assumption—see Resource Section 2 in the textbook for examples). The reduction potential of SHE depends on pH (equation 7.9): $E(H^+/H_2) = -0.059\text{ V} \times \text{pH} = -0.059\text{ V} \times 14 = -0.826\text{ V}$.

a) For $CrO_4^{2-}(aq)$ we have:

$$E°_{pH=14} = E_{red} - E_{Ox} = -0.11\text{ V} - (-0.826\text{V}) = 0.716\text{ V}.$$

From here we can use Equations 5.2 and 5.5 to calculate $\Delta_r G°$ and K respectively:

$$\Delta_r G° = -\nu FE° = -3\times 96.48\text{ kC mol}^{-1} \times 0.716\text{ V} = -207.2\text{ kJ mol}^{-1}.$$

$$\ln K = \frac{\nu FE^0}{RT} = \frac{3\times 96.48\text{kC mol}^{-1}\times 0.716\text{V}}{8.314\text{J K}^{-1}\text{mol}^{-1}\times 298\text{K}} = 83.6 \text{ or } K = 2.1\times 10^{36}.$$

b) For $[Cu(NH_3)_2]^+(aq)$ we have

$$E^o_{pH=14} = E_{red} - E_{Ox} = -0.10\text{ V} - (-0.826\text{V}) = 0.726\text{ V}$$

$$\Delta_r G° = -\nu FE° = -1\times 96.48\text{ kC mol}^{-1} \times 0.726\text{ V} = -70.0\text{ kJ mol}^{-1}$$

$$\ln K = \frac{\nu FE^0}{RT} = \frac{1\times 96.48\text{kC mol}^{-1}\times 0.726\text{V}}{8.314\text{J K}^{-1}\text{mol}^{-1}\times 298\text{K}} = 28.3 \text{ or } K = 1.9\times 10^{12}.$$

The values for $\Delta_r G°$ and K in (a) and (b) are noticeably different despite relatively little difference in $E°$ because $E°$ does not depend on the number of exchanged electrons, ν, while $\Delta_r G°$ and K both depend on it.

E7.15 The combined Frost diagram for In and Tl is shown below. From the diagram, we can see that thallium is more stable as Tl^+ in aqueous solutions, and that Tl^{3+} can be expected to behave as a strong oxidizing agent (very steep positive slope of the line connecting Tl^+ and Tl^{3+} points). The reverse is observed for indium: In^{3+} is more stable than In^+ in aqueous solutions. In^+ is actually expected to behave as a reducing agent (a negative slope of the line connecting In^+ and In^{3+} points).

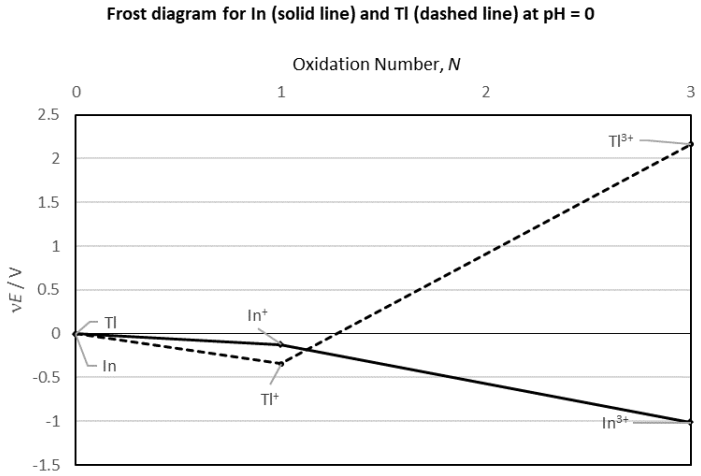

E7.16 i) Following the *weighted average* of the potentials of intervening couples formula:

$$(n_1E°_1 + n_2E°_2 + \ \ldots \ + n_nE°_n) / (n_1 + n_2 + \ \ldots \ + n_n)$$

for the VO^{2+}/V couple we have:

$$[(1)(+0.34V)+(1)(-0.26V)+(2)(-1.13V)] / (1 + 1 + 2) = - 2.18 \text{ V}.$$

Balanced chemical equation is:

$$VO^{2+} + 2H^+ + 4e^- \rightarrow V + H_2O.$$

ii) The Frost diagram is shown below:

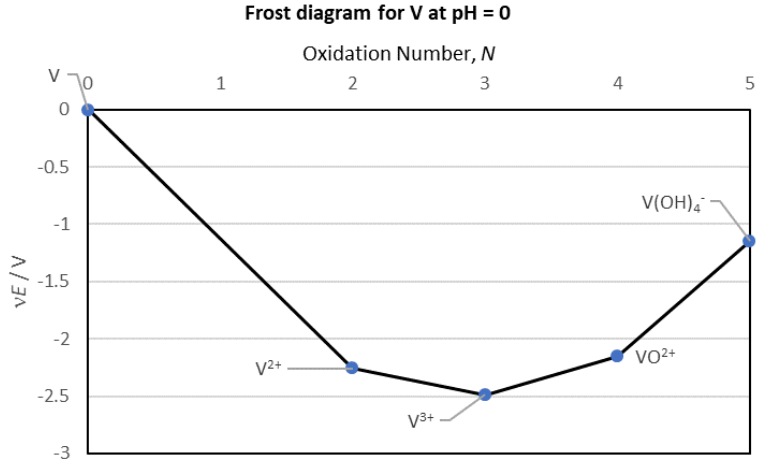

iii) The disproportionation reaction is:

$$2V^{3+}(aq) + H_2O \rightarrow V^{2+}(aq) + VO^{2+}(aq) + 2H^+(aq).$$

The reaction can be broken into two half reactions:

$$V^{3+} + e^- \rightarrow V^{2+} \qquad \text{reduction reaction}$$

$$V^{3+} + H_2O \rightarrow VO^{2+} + 2H^+. \qquad \text{oxidation reaction}$$

Using the data from the Latimer diagram, we can calculate the potential:

$$E° = E°_{red} - E°_{ox} = (-0.26\ V) - (+0.34\ V) = -0.60\ V.$$

Then we calculate the equilibrium constant using Equation 7.5:

$$\ln K = \frac{\nu F E^0}{RT} = \frac{1 \times 96.48 kC\ mol^{-1} \times (-0.60V)}{8.314 J\,K^{-1} mol^{-1} \times 298K} = -23.4 \text{ and}$$

$$K = 4.3 \times 10^{-24}.$$

The value for the equilibrium constant is very small indicating that the disproportionation reaction is actually shifted to the left side (or in other words, the comproprionation reaction is more favourable) telling us that $V^{3+}(aq)$ is stable in acidic solution. The same conclusion can be drawn from the Frost diagram above: $V^{3+}(aq)$ lies below the line connecting V^{2+} and VO^{2+}.

iv) The reduction reaction is:

$$VO^{2+} + 2H^+ + e^- \rightarrow V^{3+} + H_2O.$$

The potential would become more negative with increase in pH. See also Exercise 7.16 and Section 7.6 of your textbook.

E7.17 i) Oxidation states of carbon: CO_2, +4; HCHO, 0; CO_2^-, +3; CO, +2; HCO_2^-, +2; CH_3OH, -2; and CH_4, -4.

ii) To construct the Frost diagram, we need to find relevant reduction potentials. A very clear-cut way to do this is by constructing a Latimer diagram first. To start with we order the carbon species in order of decreasing oxidation number (remember that Latimer diagrams are reduction diagrams, he electrons are added from left to right):

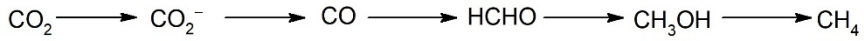

Note that instead of CO you can use HCO_2^- as a species that contains C in +2 oxidation state—the procedure would be the same, just using appropriate potential for HCO_2^- reactivity. Now we start filling the reduction potentials. The second equation given provides us with the reduction potential for the first couple: CO_2/CO_2^-, -1.90 V. The third equation connects CO_2 and nonadjacent CO: CO_2/CO, -0.52 V. We can enter these values into the diagram:

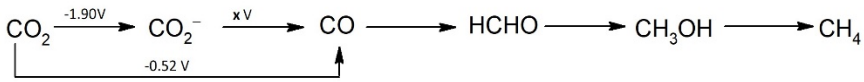

We can use these two values to calculate the CO_2^-/CO potential (marked with 'x V' on the diagram) using the formula for nonadjacent species:

$$(n_1E°_1 + n_2E°_2 + \ \ldots\ + n_nE°_n) / (n_1 + n_2 + \ \ldots\ + n_n)$$

with a difference being that nonadjacent potential is given.

$$E^0_{CO_2/CO} = \frac{n_1 E^0_{CO_2/CO_2^-} + n_2 E^0_{CO_2^-/CO}}{n_1 + n_2}$$

$$-0.52\,\text{V} = \frac{1\times(-1.90\,\text{V}) + 1\times \text{x}}{1+1}$$

$$\text{x} = E^0_{CO_2^-/CO} = +0.86\,\text{V}.$$

We can enter this value in our Latimer diagram:

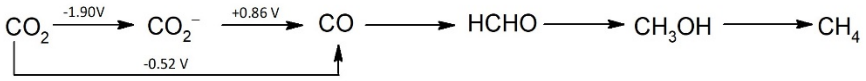

This process is continued until the Latimer diagram is complete:

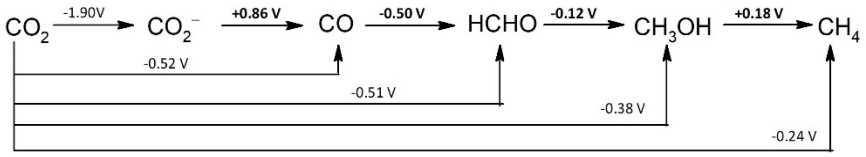

Now the Frost diagram is constructed. Note: if we set HCHO as 0 on the diagram, then moving left from HCHO we have reduction process, but moving right we have oxidation process—important for the signs of potential used for diagram construction.

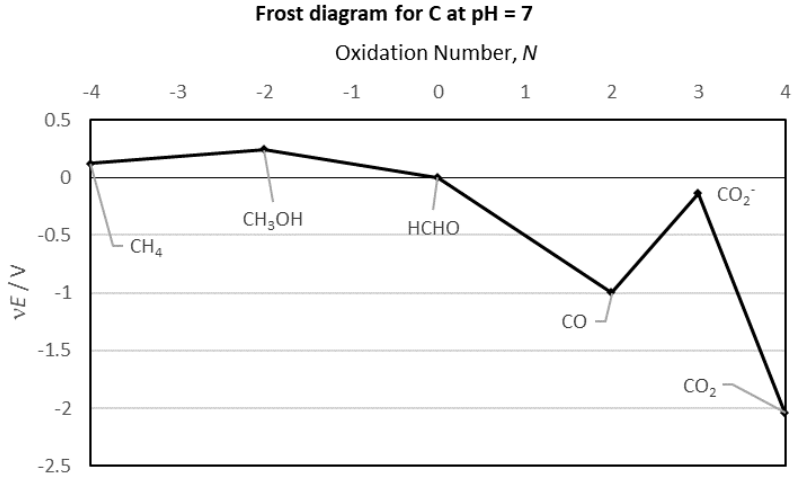

iv) First we have to find a way to make HCO_2^- from CO using given reactions, keeping in mind that the sign of ΔG determines the spontaneity of a reaction. The obvious choice of reaction to cinsider first is the one where HCO_2^- is the product:

$$CO_2(g) + H^+ + 2e^- \rightarrow HCO_2^-(aq),\ E = -0.43\ \text{V}.$$

ΔG for this reaction is (Equation 7.2):

$$\Delta G(CO_2 \rightarrow HCO_2^-) = -\nu F E^0 = -2\times 96480\ \text{C mol}^{-1}\times(-0.43\ \text{V}) = 83\ \text{kJ mol}^{-1}.$$

Now we have to find a way to use CO as a starting material. If we invert the third reaction we get:

$$CO(g) + H_2O \rightarrow CO_2(g) + 2H^+ + 2e^-,\ E = +0.52\ \text{V}.$$

Note that the reduction potential is now oxidation potential and that the sign changed from minus to plus. ΔG for this reaction is:

$$\Delta G(CO \rightarrow CO_2) = -\nu F E^0 = -2\times 96480\ \text{C mol}^{-1}\times(+0.52\ \text{V}) = -100\ \text{kJ mol}^{-1}.$$

Now we can combine the two reactions:

$$CO_2(g) + H^+ + 2e^- \rightarrow HCO_2^-(aq)$$
$$CO(g) + H_2O \rightarrow CO_2(g) + 2H^+ + 2e^-$$
$$CO(g) + H_2O \rightarrow HCO_2^- + H^+$$

ΔG for this reaction is then:

$\Delta G(CO \rightarrow HCO_2^-) = \Delta G(CO_2 \rightarrow HCO_2^-) + \Delta G(CO \rightarrow CO_2) = 83$ kJ mol^{-1} + (-100 kJ mol^{-1}) = **-17 kJ mol^{-1}**.

Since $\Delta G(CO \rightarrow HCO_2^-) < 0$, the hydration of CO to give HCO_2^- is thermodynamically favourable process.

v) Start by inverting hydrogen half reaction:

$$H_2(g) \rightarrow 2H^+(aq) + 2e^-, E = -0.41 \text{ V}.$$

To this reaction we can add the third reaction noting the reduction/oxidation half reactions:

$H_2(g) \rightarrow 2H^+(aq) + 2e^-$ oxidation half-reaction

$CO_2(g) + 2H^+ + 2e^- \rightarrow CO(g) + H_2O$ reduction half-reaction

$$CO_2(g) + H_2(g) \rightarrow CO(g) + H_2O(l)$$

For this reaction:

$$E = -0.52 \text{ V} + (-0.41 \text{ V}) = -0.93 \text{ V}.$$

And the equilibrium constant is:

$$\ln K = \frac{\nu FE}{RT} = \frac{2 \times 96480\, C\, mol^{-1} \times (-0.93 V)}{8.314 JK^1 mol^{-1} \times 298 K} = -72.4$$ and $\boldsymbol{K = 3.5 \times 10^{-32}}$.

Chapter 8 Physical Techniques in Inorganic Chemistry

Self-Tests

S8.1 The ionic radius of Cr(IV), 69 pm, is smaller than that of Ti(IV), 75 pm. The unit cell and *d* spacings will shrink because of the smaller radius of chromium. The XRD pattern for CrO_2 will show identical reflections to those of rutile TiO_2 (see Figure 8.4) but shifted to slightly higher diffraction angles.

S8.2 **a)** The K_2Se_5 crystal with dimensions 5 × 10 × 20 μm would be too small for the single-crystal X-ray diffraction analysis that typically requires a crystal with dimensions of 50 × 50 × 50 μm or above. Smaller crystals, such as the one in this Self-Test require X-ray sources of higher intensity which are obtained using synchrotron radiation. Thus, we would need different source of X-rays (see Section 8.1(b) *Single-crystal X-ray diffraction* and Section 8.1(c) *X-ray diffraction at synchrotron sources*).

b) Recall that X-rays are scattered by the electrons and the neutrons by nuclei. In the case of any element-H bond (specifically in this Self-test, O–H bond), hydrogen's single electron is involved in bonding, and is shared with the other partner in the bond. This means that the X-ray scattering point are electrons in the bond located between the two nuclei, and what we see is short element-H bonds. On the other hand, the neutrons are going to be scattered by a proton in hydrogen's nucleus and the element-H bonds is going to be longer, and more accurate, than that determined with X-ray crystallography.

S8.3 As we can clearly see from Figure 8.13 TiO_2 particles absorb the ultraviolet radiation and prevent this type of radiation from reaching the skin offering protection from the sun's rays that can cause skin cancer.

S8.4 Using the VSEPR theory we find that Xe in XeF_2 has five electron pairs: three lone and two bonding. Thus, the molecular geometry is linear with a $D_{\infty h}$ point group symmetry. As a linear molecule, we expect XeF_2 to have $3N - 5 = 3(3) - 5 = 4$ total vibrational modes. These modes cannot be both IR and Raman active as the molecule has a centre of symmetry (the exclusion rule).

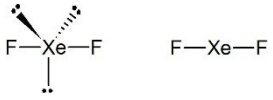

S8.5 **a)** The VSEPR theory would predict a square pyramidal geometry for the BrF_5 molecule. Recall from previous chapters that this geometry would place F atoms in two different environments: axial (F_a) and basal (F_b). Thus, we would expect two different chemical shifts in ^{19}F NMR: one for F_a and one for F_b. The intensity of these signals should have relative ratios 1 : 4 because there is only one F_a whereas there are four F_b atoms. According to the n + 1 rule for the nuclei with $I = ½$, the F_a resonance would be split into five equally spaced lines (i.e., a quintet) by four basal F atoms with line intensities 1 : 4 : 6 : 4 : 1 according to Pascal's triangle. The signal due to F_b atoms will be split into a doublet by one F_a with line intensities 1 : 1.

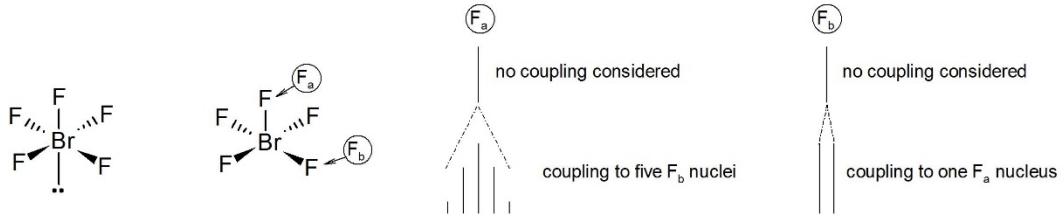

b) The hydride resonance couples to three nuclei (two different ^{31}P nuclei—one *trans* to the hydride and the other one *cis* to the hydride ligand—and the ^{103}Rh nucleus) that are 100% abundant and all of which have $I = ½$ (see Table 8.4). The first doublet is observed due to the coupling between hydride and rhodium. Since the two atoms are directly bonded, the coupling constant is going to be large. Then, through coupling with P atom *trans* to the hydride, each line of the first doublet is going to be split into a doublet creating doublet of doublets. Finally, due to the coupling to the P atom *cis* to the hydride, every line of the doublet of doublets is going to be further split into a doublet giving the observed doublet of doublets of doublets pattern. Since the three coupling constants are

different, the effect is to split the signal into a doublet of doublet of doublets, thus generating eight lines in the NMR of equal intensity.

S8.6 **a)** The assigned compound, $Tm_4(SiO_4)(Si_3O_{10})$, contains two different silicate anions: the orthosilicate, SiO_4^{4-} and chain $Si_3O_{10}^{8-}$. Within $Si_3O_{10}^{8-}$ we have two different Si environments—one Si atom is in the centre of the chain with the remaining two Si atoms on each end. The Si atom in the orthosilicate anion is in its own environment. Thus, we can expect three signals in ^{29}Si-MASNMR of this compound: one for SiO_4^{4-} (with intensity 1) and two for $Si_3O_{10}^{8-}$ (with intensities 1 : 2 for central and terminal Si atoms).

b) The cyclic anion $Si_4O_{12}^{8-}$ would show a single resonance. This anion is very similar to the structure **4**, but has one more $\{SiO_3\}$ ring member.

S8.7 Consulting Table 8.4, we see that 14% of the naturally occurring tungsten is ^{183}W, which has I = ½. Owing to this spin, the EPR signal of a new material should be split into two lines. This doublet would be superimposed on a nonsplit signal that arises from the 86% of tungsten that does not have a spin. The splitting would be a characteristic of a new material containing tungsten.

S8.8 The oxidation state for iron in Sr_2FeO_4 is +4. The outermost electron configuration is $3d^4$. We would expect the isomer shift to be smaller and less positive (below 0.2 mm s^{-1}) due to a slight increase of s-electron density at the nucleus.

S8.9 Generally as the oxidation state of an atom is increasing, the radius is decreasing and the K-shell electrons are moving closer to the nucleus resulting in an increased stability of these electrons. Thus, the energy of XAS K-edge is expected to gradually increase with an increase in oxidation state of sulfur from S(-II) in S^{2-} to S(VI) in SO_4^{2-}.

S8.10 Both chlorine (^{35}Cl 76% and ^{37}Cl 24%) and bromine (^{79}Br 51% and ^{81}Br 49%) exist as two isotopes. Consider the differences in mass numbers for the isotopes—any compound containing either Cl or Br will have molecular ions $2m_u$ apart. The lightest isotopomer of $ClBr_3$ is $^{35}Cl^{79}Br_3$ at $272u$ and the heaviest is $^{37}Cl^{81}Br_3$ at $280u$. Three other molecular masses are possible, giving rise to a total of five peaks in the mass spectrum shown in Figure 8.43. The differences in the relative intensities of these peaks are a consequence of the differences in the percent abundance for each isotope.

S8.11 CHN analysis is used to determine percent composition (mass percentages) of C, H, and N. Because the atomic masses of 5d metals are significantly higher than the atomic masses of 3d metals, the hydrogen percentages will be less accurate as they correspond to smaller fractions of the overall molecular masses of the compounds.

S8.12 The EDAX analysis does not give very accurate quantitative results for the magnesium aluminium silicate because the three elements (Mg, Al, and Si) are next to each other in the periodic table; thus, we can expect some peak overlapping.

S8.13 7.673 mg of tin corresponds to 0.0646 mmol of Sn. The 10.000 mg sample will contain 2.327 mg of oxygen (10.000 mg – 7.673 mg) or 0.145 mmol of O. We could write the initial formula of this oxide as $Sn_{0.0646}O_{0.145}$. The molecular formulas of compounds, however, are generally written using the whole numbers in subscripts (unless the compound is indeed nonstoichiometric) and not fractions or irrational numbers. To convert our subscripts to the whole numbers we divide both with the smaller of the two. We obtain 0.0646/0.0646 = 1 and 0.145/0.0646 = 0.244. The last number is still not a whole number but it becomes obvious that by multiplying both values by 2 we can obtain whole numbers 2 and 5.

S8.14 Os(III) solution at pH 3.1 contains an $Os^{III}OH$ species, whereas Os(IV) solutions at the same pH have an $Os^{IV}O$ species. From Pourbaix diagram we see that $Os^{III}OH$ complex remains protonated in the pH range 3.1 to 13. This means that at very high sweep rates electron transfer is going to be fast in comparison to proton transfer. Therefore, we should see one reversible peak in the cyclic voltamograms in this pH range.

Exercises

E8.1 The three compounds, two starting materials and the spinel product, clearly have different structures and different unit cells. The easiest way to monitor the reaction is powder X-ray diffraction. As long as we can observe the diffraction cones associated with TiO_2 and MgO together with those from Mg_2TiO_4, the reaction is not complete. Once our diffractogram shows only the pattern due to Mg_2TiO_4 the reaction is done!

E8.2 If the laboratory single-crystal diffractometer can study crystals that are 50 μm × 50 μm × 50 μm, with a new synchrotron source that has a millionfold increase in source intensity, one can reduce the crystal volume by $1/10^6$, thus the size would be 0.5 μm × 0.5 μm × 0.5 μm. The opposite happens if the flux is reduced: we need bigger crystal. For the 10^3 times weaker neutron flux we must have a crystal with 10^3 larger volume—the minimum size is then 500 μm × 500 μm × 500 μm.

E8.3 To determine if a hydrogen bond is symmetric or not, we need a precise location of hydrogen atom. The single crystal diffraction techniques provide us with atomic positions within the unit cell. The question now remains which one to use? The neutron diffraction is much better in locating H atoms with high accuracy, but it does need a larger single crystal than the X-ray (see Additional Exercise 8.2 and Section 8.2 *Neutron diffraction*).

In the case of a) BO(OH) we could still get a good accuracy in H atom positions using single crystal X-ray diffraction because B and O are also light elements with few electrons and of low scattering power.

Unfortunately, that is not the case with CrO(OH)–the heavy Cr centre in the structure is going to dominate the electron density obtained from the X-ray scattering. Seeing small almost 'naked' H in this case would be very difficult. Thus, in this case we should hope for a large, good quality single crystal for the neutron diffraction experiment.

E8.4 Unlike X-rays, which are scattered by the electrons, the neutrons are scattered by atomic nuclei in a crystalline sample. The X-ray analysis always underestimates element-hydrogen bond lengths because of very low electron density at H nucleus. H atom, having only one electron, has very low electron density that is further decreased when H bonds to the other atoms because the electron now resides between the two nuclei forming a bond. This is not an issue with neutron diffraction because neutrons will be scattered by hydrogen nucleus providing us with its very accurate location. We could, however, expect less discrepancy with measurement of C–H bonds. This is due to the lower electronegativity of carbon vs. oxygen. In O–H bonds the bonding electron pair (which contains H's electron) is shifted more toward oxygen which makes H atom appear closer in the electron density map. On the other hand, C–H bond is of low polarity and the bonding pair is more equally distributed between the two nuclei. See also Self-test 8.2b and Exercise 8.3.

E8.5 The thiocyanate anion, an ambidentate ligand, has two resonance structures:

When thiocyanate coordinates through sulfur, the resonance structure on the left is favoured because a positively charged metal can stabilize negative charge on sulfur. Note that in this structure, carbon-sulfur bond is single. On the other hand, if the ligand coordinates through nitrogen atom, the resonance structure on the right is stabilized. This structure has a negative charge on N atom and a double carbon-sulfur bond. This structural analysis tells us that S-coordinated thiocyanate has a weaker C-S bond in comparison to N-coordinated SCN^-.

Looking at the compounds given, in $K_2[Co(SCN)_4]$ we can expect κ*N*-thiocyanate because Co^{2+} is relatively hard Lewis acid and would prefer hard Lewis base. In $K_2[Pd(SCN)_4]$ we expect the opposite: Pd^{2+} is a soft Lewis acid and would prefer soft Lewis base–and thiocyanate should be κS.

This hard/soft analysis of bonding matches well with the analysis of SCN^- resonance structures. The stretching frequency of CS bond in Co^{2+} complex is at higher wavenumbers than that observed in Pd^{2+} complex indicating stronger C-S bond. The wavenumber observed for KSCN is in between the two because KSCN is a ionic compound with uncoordinated (free) thiocyanate. The structure of the free SCN^- is a "mix" of the two hybrid structures and hence has intermediate C-S bond strength.

Simple comparison of CS wavenumber found for $RbBi(SCN)_4$ tells us that SCN^- is coordinated through S atom because 722 cm^{-1} observed for Bi complex is very close to 730 cm^{-1} observed for Pd complex.

E8.6 The bond orders for CN^- and CO are the same, but N is lighter than O, hence the reduced mass for CN^- is smaller than for CO. From Equation 8.2a, the smaller effective mass of the oscillator for CN^- causes the molecule to have the higher stretching frequency because they are inversely proportional. The bond order for NO is 2.5, and N is heavier than C, hence CO has a higher stretching frequency than NO. For the carbide anion we should expect the highest frequency because of the triple C-C bond and lightest carbon atoms.

E8.7 Consult the solution for the Example 8.5 for the structure of $^{77}SeF_4$—since Se and S are in the same group of the periodic table the VSEPR theory would predict identical structures, i.e. see-saw.

The fluorine atoms in SeF_4 are in two different magnetic environments: two F atoms form one plane with the lone electron pair on selenium (equatorial F atoms), whereas the other two are perpendicular to this plane (axial F atoms). Thus, we would expect two signals in ^{19}F NMR. However, the F atoms are bonded to the NMR active ^{77}Se with $I = ½$. (Note that the exercise states that the sample contains only ^{77}Se thus the actual abundance of this Se isotope is not relevant in this case.) Thus, the axial F atoms are going to be coupled to ^{77}Se (large one-bond coupling constant) and their signal is going to be split into a doublet. They are further coupled to two equatorial F atoms and the signal is further split into a triplet producing finally a doublet of triplets (see the figure below). The same analysis for the equatorial F atoms will give another doublet of triplets. Thus, the ^{19}F NMR of $^{77}SeF_4$ would consist of two doublet of triplets with relative intensity 1 : 1.

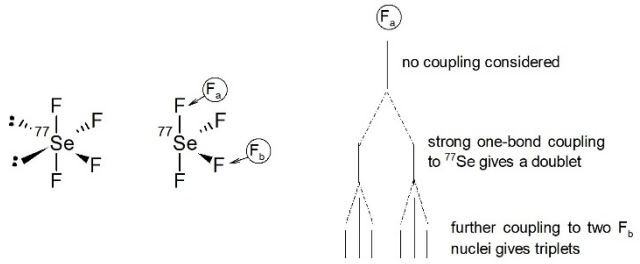

The ^{77}Se NMR would consist of triplet of triplets because ^{77}Se is coupled to two equatorial and two axial ^{19}F nuclei.

E8.8 Using VSEPR theory we can determine that XeF_5^- has a pentagonal planar molecular geometry and all five of the F atoms are magnetically equivalent. Thus, the molecule shows a single ^{19}F resonance. Approximately 25% of the Xe is present as ^{129}Xe, which has $I = 1/2$, and in this case the ^{19}F resonance is split into a doublet. The result is a composite: two lines each of 12.5% intensity from the ^{19}F coupled to the ^{129}Xe, and one line of 75% intensity for the remainder. The ^{129}Xe NMR would show a single resonance split into a binomial sextet by five equivalent F nuclei.

E8.9 The structure of triiron dodecacarbonyl, $[Fe_3(CO)_{12}]$ is shown below:

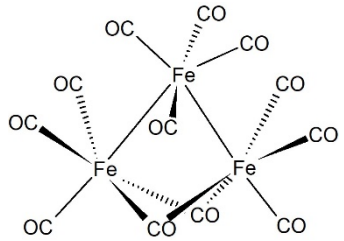

Although this complex has two magnetically distinct carbonyl environments—terminal and bridging carbonyls—the structure is fluxional at room temperature in the solution and the CO ligands are exchanging bridging and terminal position sufficiently fast so that an average signal is seen and only one peak is observed. In the solid state, however, the molecule is locked in the crystal structure and this exchange is either not possible or very slow. Consequently, we can see both terminal and bridging CO ligands in the solid state IR spectrum.

E8.10 The compound has four phosphorus atoms in its structure, and two peaks—a doublet and a quartet—along with their intensities, three and one respectively, tell us that there are two magnetic environments; one has three P atoms (a doublet with intensity 3) and the other has one P atom (a quartet with intensity 1). A possible structure of P_4S_3 is shown below:

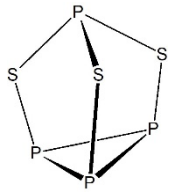

E8.11 Rearranging Equation 8.7 we have $g = \Delta E / \mu_B B_0$. To calculate the g values, we obtain the B_0 values from the EPR spectrum shown in Figure 8.56 (the three lines drawn to the x-axis correspond to 348, 387, and 432 mT) and set the $\Delta E = h\nu$ where ν is equal to the given microwave frequency. The three g values are thus 1.94, 1.74, and 1.56, respectively. See below for an example of the calculation for the first line.

$$g = [(6.626 \times 10^{-34}\ \text{J s})(9.43 \times 10^{9}\ \text{s}^{-1})]/\ (9.27401 \times 10^{-24}\ \text{J/T})(0.348\ \text{T}) = 1.94.$$

E8.12 The structure of tris(2-pyridyl)methane ligand is shown below. Note that the ligand has three Lewis basic nitrogen atoms and hence can be potentially a tridentate ligand.

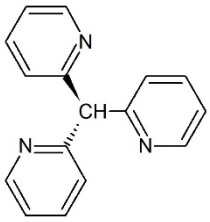

The complex structure is shown below. The counterion, nitrate, is not important because it is not coordinated to the metal and is EPR silent (it has no unpaired electrons). The Cu^{2+} centre has electronic configuration d^9 and its complexes are prone to Jahn-Teller distortions (see Chapter 7). In the structure, two axial Cu–N bonds are marked as "long" to indicate the distortion form the ideal octahedral structure.

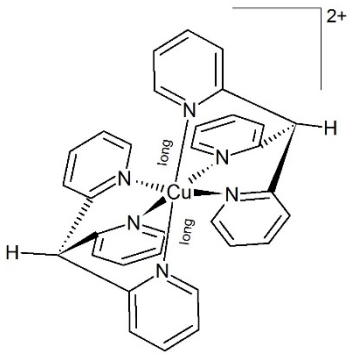

At room temperature, there is a fast exchange between "long" and normal bonds, so fast that EPR instrument observes six bonds of equal, average lengths and consequently an isotropic octahedral geometry. As the temperature is lowered, there is less energy for fluxional movement of the atoms in the molecule and the exchange is slowed down to a point that it becomes slower than EPR measurement. The spectrum becomes axial, as one would expect from the structure.

E8.13 The oxidation state for iron in $Na_3Fe^{(V)}O_4$ results in a $3d^3$ configuration. As the 3d electrons are removed the isomer shift becomes less positive as the 3d electrons partly screen the nucleus from the inner s electrons. Compared to Fe(III) with isomer shift between +0.2 and +0.5 mm s^{-1}, we would expect a smaller positive shift for

Fe(V) below +0.2 mm s^{-1}. The shift for Na_3FeO_4 will be less positive than for Sc_2FeO_4 due to the higher oxidation state of Fe (+5 in Na_3FeO_4 vs. +4 in Sc_2FeO_4).

E8.14 The XANES spectrum could be very useful in deciding on Fe oxidation states found in $CaFeO_3$. The near edge structure can differentiate between different oxidation states and geometries. In this case, the geometry is octahedral at Fe (regardless of the oxidation state) making the interpretation of the spectrum easier.

E8.15 Silver has two isotopes, ^{107}Ag (51.82%) and ^{109}Ag (48.18%). You should look up this information yourself, which can be found in many reference books (e.g., *CRC Handbook of Chemistry and Physics*). Thus the average mass is near 108, but no peak exists at this location because there is no isotope with this mass number. Compounds that contain silver will have two mass peaks flanking this average mass.

E8.16 The molar mass of the dehydrated zeolite, $CaAl_2Si_6O_{16}$, is 518.5 g mol^{-1}. The molar mass of water is 18.0 g mol^{-1}. We can solve for n using the mass percentage of water.

$$\text{Mass \% of } H_2O = \frac{\text{mass of } H_2O \text{ in the sample}}{\text{mass of the sample}} \times 100\% = \frac{18n}{518.5 + 18n} \times 100\% = 20\%$$

$18n = 0.2\ (518.5 + 18n)$

$14.4\ n = 103.7$

$n = 7.2.$

Isolating n as an integer we can estimate that $n = 7$.

E8.17 The complex undergoes a reversible one-electron reduction with a reduction potential of +0.21 V. This can be calculated by taking the mean of E_{pa}(+0.240 V) and E_{pc}(+0.18 V), see Figure 8.57. Above +0.720 V the complex is oxidized to a species that undergoes a further chemical reaction, and thus is not re-reduced. This step is not reversible.

E8.18 The ratio of cobalt to acetylacetone in the complex is 3:1. Converting the given mass percentages of Co and C to moles of Co and C, we find that for every mole of Co in the product we have 15 moles of C: moles of Co = 0.28 mol; moles of C = 4.2 mol. Considering that every $acac^-$ ligand has five carbon atoms, it is obvious that for each mole of Co we have three moles of $acac^-$. This ratio is consistent with the formula $[Co(acac)_3]$. (Consult Section 7.1 for more detail on the acetylacetonate ligand and cobalt coordination complexes.)

E8.19 Microscopy techniques, particularly SEM and TEM, are very useful for determining the nanoparticle size down to 1 μm. The other methods used are based on light scattering. In this case, the particle size must be much smaller than the wavelength of the light used. The light sources are monochromatic (usually lasers) and the wavelength of the light emitted places the limits of the measurement.

Chapter 9 Periodic Trends

Self-Tests

S9.1 **a)** Refer to Figure 9.9 in your textbook. Cd and Pb are classified as chalcophiles and give soft cations. Thus, they will be found as sulfides. Rb and Sr are lithophiles and are hard; they can be found in aluminosilicate minerals. Cr and Pd are siderophiles and give cations of intermediate hardness. As such, they can be found as both oxides and sulphides. Palladium can also be found in elemental form.

b) Thallium is expected to be a chalcophile, and it should occur as a sulphide ore. This can be concluded based on Figure 9.9 or by thallium's position in the periodic table of elements: it is close to lead and bismuth—typical chalcophiles with sulphide ores.

S9.2 **a)** In this case you have to consider two potential reactions: (i) possible oxidation by H^+ and (ii) possible oxidation by O_2. The first case has been covered in the text, but we can look at the two half-reactions, assuming standard conditions:

$$H^+(aq) + e^- \rightarrow \tfrac{1}{2} H_2(g), \qquad E^o = 0.00 \text{ V}$$

$$V^{3+}(aq) + e^- \rightarrow V^{2+}(aq), \qquad E^o = -0.255 \text{ V}.$$

Thus, the overall reaction, $V^{2+}(aq) + H^+(aq) \rightarrow V^{3+}(aq) + \tfrac{1}{2} H_2(g)$, would have a positive potential difference (E = + 0.255 V) and the reaction is spontaneous. (Recall that reactions with a positive potential difference have negative $\Delta_r G$ and are thus spontaneous.) Further oxidation of $V^{3+}(aq)$ by $H^+(aq)$ is not feasible because the potential difference would be negative. For example, consider half-reaction for oxidation of $V^{3+}(aq)$ to $V^{4+}(aq)$ by $H^+(aq)$:

$$H^+(aq) + e^- \rightarrow \tfrac{1}{2} H_2(g), \qquad E^o = 0.00 \text{ V}$$

$$VO^{2+} + e^- + 2H^+ \rightarrow V^{3+}(aq) + H_2O(l), \; E^o = +0.337 \text{ V}.$$

Combining these two reactions we would get a negative potential difference (E = -0.337 V) and a nonspontaneous reaction.

The reduction potential for $O_2(g)$ in acidic medium is +1.23 V (for half-reaction $\tfrac{1}{2}O_2(g) + 2e^- + 2H^+ \rightarrow H_2O(l)$), meaning that O_2 is a better oxidizing agent than H^+. Consequently, $O_2(g)$ will be able to oxidize $V^{2+}(aq)$ to $V^{3+}(aq)$ as well, but we have to check if oxidation of $V^{3+}(aq)$ to VO^{2+} is now possible: E = +1.23 V – (+0.337 V) = + 0.893 V. The potential difference is positive, and $VO^{2+}(aq)$ should be more stable than $V^{3+}(aq)$ and $V^{2+}(aq)$ under these conditions. Similar analysis shows that $VO^{2+}(aq)$ could be further oxidized to $VO_2^+(aq)$ with $O_2(g)$ with potential difference of +0.23 V. Overall, this indicates that $V^{2+}(aq)$ should be oxidized by $O_2(g)$ in the acidic solution all the way to the thermodynamically favoured species $VO_2^+(aq)$. Note that this does not necessarily mean that the process will occur—the kinetics might be slow, and particularly important factor to consider when dealing with $O_2(g)$ oxidation are overpotentials. Consequently, $V^{3+}(aq)$ and/or VO^{2+} might be reasonably long- lived species in acidic medium when exposed to oxygen from air.

b) Mn can have oxidation states from +2 to +7. Looking at the Latimer diagram we can conclude that the most stable oxidation state is +2. Higher oxidation states have positive reduction potential from +7 all the way to +2 indicating that all are good oxidizing agent. The reduction potential for Mn^{2+}/Mn couple is negative telling us that Mn can be easily reduced to +2.

S9.3 **a)** Oxygen forms a double bond that is three times more stable than its single bond. Owing to this tendency to form strong double bonds, it is very unlikely that longer-chain polyoxygen anions would exist. Sulfur is much less likely to form π bonds and therefore more likely to generate catenated polysulfide anions.

b) To answer this self-test, we can extrapolate from the discussion on O and S single and double bonds. A general trend can be stated that the enthalpy of π component of the double bond significantly decreases going down a group in the periodic table. Following this trend, we can expect that Si=Si bond is relatively weak in comparison with C=C and can be easily broken. Another trend worth mentioning here is that large atoms do not form p bonds easily—the separation between p atomic orbitals on two atoms prevents formation of efficient orbital overlap and consequently π bond is weak.

S9.4 **a)** The energy required to convert solid elements into the gaseous atomic form drops going down the group. This is expected because the bond strengths decrease in the same order and it becomes easier to break the molecules in solids. It is evident from the values that as we move down the group from S to Se to Te, the steric crowding of the fluorine atoms is minimized owing to the increasing radius of the central atom. As a result, the enthalpy values become larger and more negative (more exothermic) and the higher steric number compounds (such as TeF_6) are more likely to form.

b) We can consider two reactions to get the best estimate:

$$Te(s) + 2F_2(g) \rightarrow TeF_4$$

and

$$Te(s) + 3F_2 \rightarrow TeF_6.$$

$\Delta_f H$ for two tellurium fluorides and $\Delta H_{sub}(Te)$ are given in the table for part a) and bond dissociation energy for F_2 is provided in the text of Section 9.10(b) *Covalent halides*: 155 kJ mol^{-1}.

For TeF_4:

$$\Delta_f H(TeF_4) = \Delta H_{sub}(Te) + 2\times B(F–F) - 4\times B(Te–F)$$

$$-1036 \text{ kJ mol}^{-1} = +199 \text{ kJ mol}^{-1} + 2\times 155 \text{ kJ mol}^{-1} - 4\times B(Te–F)$$

$$B(Te–F) = (199 \text{ kJ mol}^{-1} + 310 \text{ kJ mol}^{-1} + 1036 \text{ kJ mol}^{-1})/4$$

$$B(Te–F) = 386 \text{ kJ mol}^{-1}.$$

Similar procedure can be applied to TeF_6:

$$\Delta_f H(TeF_6) = \Delta H_{sub}(Te) + 3\times B(F–F) - 6\times B(Te–F)$$

$$-1319 \text{ kJ mol}^{-1} = +199 \text{ kJ mol}^{-1} + 3\times 155 \text{ kJ mol}^{-1} - 6\times B(Te–F)$$

$$B(Te–F) = (199 \text{ kJ mol}^{-1} + 465 \text{ kJ mol}^{-1} + 1319 \text{ kJ mol}^{-1})/6$$

$$B(Te–F) = 330 \text{ kJ mol}^{-1}.$$

Finally, we can find the average of two values:

$$B(Te–F) = (330 \text{ kJ mol}^{-1} + 386 \text{ kJ mol}^{-1})/2 = 358 \text{ kJ mol}^{-1}.$$

S9.5 We would have to know the products formed upon thermal decomposition for P_4O_{10} and thermodynamic data for the product. We could use data for V_2O_5 from the Exercise 9.5.

S9.6 **a)** Xe is the central atom. With 8 valence electrons from Xe and 24 electrons (6 from each O) we have 32 total electrons and 16 electron pairs. We would predict a tetrahedral geometry to minimize electron pair repulsions. Note that to minimize formal charge, the xenon will form double bonds with each oxygen. Because the atomic number of Xe is 54, the Z + 22 is Os (Z = 76). The compound with the same structure is OsO_4.
b) The atomic number of Si is Z = 14 and the Z + 8 element is Ti (Z = 22). Indeed, just like Si, Ti forms a very stable oxide of the formula TiO_2.

Exercises

E9.1 (a) Ba, +2; (b) As, +5; (c) P, +5; (d) Cl, +7; (e) Ti, +4; (f) Cr, +6

E9.2 These elements are Group 15. This group is very diverse. N and P are nonmetals; As and Sb are metalloids, and Bi is metallic. The +5 and +3 oxidation states are common for the group electron configuration of ns^2p^3. Phosphine and arsine are well-known toxic gases.

E9.3 The key steps in the Born–Haber cycle for $NaCl_2$ are:

$Na(s)$	$\rightarrow$	$Na(g)$	sublimation	$\Delta_{sub}H^o(Na)$
$Cl_2(g)$	$\rightarrow$	$2Cl(g)$	dissociation	$\Delta_{dis}H^o(Cl_2)$
$Na(g)$	$\rightarrow$	$Na^+(g) + 1e^-$	first ionization	$I_1(Na)$
$Na^+(g)$	$\rightarrow$	$Na^{2+}(g) + 1e^-$	second ionization	$I_2(Na)$
$2Cl(g) + 2\ e^-$	$\rightarrow$	$2Cl^-(g)$	electron gain	$\Delta_{eg}H^o(Cl)$
$Na^{2+}(g) + 2\ Cl^-(g)$	$\rightarrow$	$NaCl_2(s)$	lattice enthalpy	$-\Delta_L H^o(NaCl_2)$

You can calculate the lattice enthalpy by moving around the cycle and noting that the enthalpy of formation $\Delta_f H^o(NaCl_2) = \Delta_{sub}H^o(Na) + \Delta_{dis}H^o(Cl_2) + I_1(Na) + I_2(Na) - \Delta_{eg}H^o(Cl) - \Delta_L H^o(NaCl_2)$. The second ionization energy of sodium is 4562 kJ mol^{-1} and is responsible for the fact that the compound does not exist as it would result in a large, positive enthalpy of formation.

E9.4 Metallic character and ionic radii decrease across a period and down a group. Ionization energy increases across a period and decreases down a group. Large atoms typically have low ionization energies and are more metallic in character.

E9.5 **a)** Na is the more electronegative one. Recall that electronegativity decreases down a group in the periodic table (see Section 1.7(d) *Electronegativity*).

b) O is the more electronegative one—after fluorine, oxygen is the most electronegative element; also, with respect to Si, it is located closer to the top right corner where the highest electronegativity is found (i.e., that for fluorine).

E9.6 Refer to Sections 9.9(b) *Oxides of the elements* and 4.4 *Anhydrous oxides*:
(a) Na_2O is basic; **(b)** P_2O_5 is acidic; **(c)** ZnO is amphoteric; **(d)** SiO_2 is acidic; **(e)** Al_2O_3 is amphoteric; **(f)** MnO is basic.

E9.7 The covalent character increases with increasing oxidation state of the metal; thus the covalent character is increasing in order $CrF_2 < CrF_3 < CrF_6$. Refer to Section 9.9(c) *Halides of the elements.*

E9.8 The atomic number of P is 15. The Z + 8 element has an atomic number of 23 and is V (vanadium). Both form compounds with varying oxidation states up to a maximum value of +5. Both form stable oxides including ones in +5 oxidation state (V_2O_5 and P_2O_5). Like phosphorus, vanadium forms oxoanions including ortho-, pyro-, and meta-anions. Consult Section 15.15 for analogous phosphorus oxoanions.

E9.9 What we are looking for are Se–F bond dissociation energies in SeF_4 and SeF_6. To determine these values, we have to use the Born-Haber cycle. Looking first at SeF_6, we have:

$$Se(s) + 3F_2(g) \rightarrow SeF_6(g),\ \Delta_f H = -1030\ kJ/mol$$

We can break this reaction into three elementary steps:

1. $Se(s) \rightarrow Se(g);\ \Delta_a H(Se) = +227\ kJ/mol$
2. $3F_2(g) \rightarrow 6F(g);\ \Delta_a H(F) = +159\ kJ/mol \times 3$
3. $Se(g) + 6F(g) \rightarrow SeF_6(g);\ \Delta_r H = X$

Note that $\Delta_a H$ for reaction 2 has to be multiplied by three because we need to atomize (break bonds in) three moles of $F_2(g)$. Also note that in reaction 3 we form six Se–F bonds and no other physical or chemical transformation takes place. If we sum reactions 1–3 we get our first reaction given above. Thus, we can write:

$\Delta_f H = \Delta_a H(Se) + 3\times\Delta_a H(F) + \Delta_r H$. Now substitute given values:

$$-1030\ kJ/mol = 227\ kJ/mol + 3\times159 kJ/mol + X$$

From here:

$$X = -1030\ kJ/mol - 227kJ/mol - 3\times159kJ/mol = -1575\ kJ/mol$$

Since X gives energy released per six Se–F bonds and we need only one Se–F, we have to divide X by 6, and get -262.5 kJ/mol. Further, we have to change the sign to finally obtain B(Se – F) in SeF_6 as 262.5 kJ/mol, because B(Se–F) is bond dissociation energy (energy required to break the bond) not bond formation energy (energy released when a bond is formed).

In a similar way we can determine the B(Se–F) for SeF_4.

$$Se(s) + 2F_2(g) \rightarrow SeF_4(g),\ \Delta_f H = -850\ kJ/mol$$

Elementary steps are:

1. $Se(s) \rightarrow Se(g);\ \Delta_a H(Se) = +227\ kJ/mol$
2. $2F_2(g) \rightarrow 4F(g);\ \Delta_a H(F) = +159\ kJ/mol \times 2$
3. $Se(g) + 4F(g) \rightarrow SeF_4(g);\ \Delta_r H = X$

Note that this time $\Delta_a H$(F) is multiplied by 2 and that in reaction 3 four Se–F bonds are formed. We have:

$$-850\ kJ/mol = 227\ kJ/mol + 2\times159kJ/mol + X$$

And

$$X = -850\ kJ/mol - 227kJ/mol - 2\times159kJ/mol = -1359\ kJ/mol$$

And the bond dissociation energy B(Se–F) in SeF_4 is $(-1359\ kJ/mol \times -1)/4 = 348.7\ kJ/mol$.

Comparing the Se–F bond strength in SeF_4 and S–F bond strength in SF_4 we see that the Se–F bond is slightly stronger (for about 8 kJ/mol) than the S–F bond. However, the Se–F bonds in SeF_6 are significantly weaker in comparison to the S–F bonds in SF_6. This reflects the general periodic trend according to which the E–X bond decreases in strength on going down the group.

Chapter 10 Hydrogen

Self-Tests

S10.1 Table 1.7 lists electronegativity values for the s and p block elements. We have to compare the electronegativity of hydrogen with electronegativity for Group 15 elements keeping in mind that hydridic compounds have hydrogen bound to less electronegative element. Thus, BiH_3 is going to be the most hydridic because of bismuth's low electronegativity (2.02 vs. 2.20 for H, Pauling's electronegativity values both). This is to be expected as well based on the periodic trends: de electronegativity is decreasing going down the group and is generally low for metallic elements. Bismuth is at the bottom of the Group 15 (thus has the lowest electronegativity in the group) and is also metallic element.

S10.2 A good guide as to whether a compound EH_4 will act as a proton donor or hydride donor is provided by the electronegativity difference between H and E (see Self-test 10.1). If E is more electronegative than H, cleavage of an E–H bond releases a proton, H^+. If E is less electronegative than H, cleavage results in transfer of a hydride, H^-. Given the following compounds, CH_4, SiH_4, and GeH_4, carbon is the only E that is more electronegative than H, thus it would be the strongest Brønsted acid. In other words, CH_4 would be more likely to release protons than SiH_4 and GeH_4. Ge has the least electronegative E, thus GeH_4 would be the best hydride donor of the three.

S10.3 **a)** $Ca(s) + H_2(g) \rightarrow CaH_2(s)$. This is the reaction of a reactive s-block metal with hydrogen, which is the way that saline metal hydrides are prepared.

b) $NH_3(g) + BF_3(g) \rightarrow H_3N–BF_3(g)$. This is the reaction of a Lewis base (NH_3) and a Lewis acid (BF_3). The product is a Lewis acid–base complex. (Review Sections 5.6 and 5.7(b)).

c) $LiOH(s) + H_2(g) \rightarrow$ NR. Although dihydrogen can behave as an oxidant (e.g., with Li to form LiH) or as a reductant (e.g., with O_2 to form H_2O), it does not behave as a Brønsted or Lewis acid or base. It does not react with strong bases, like LiOH, or with strong acids.

S10.4 The given reaction,

$$[PdH(PNP)_2]^+ + [Pt(PNP)_2]^{2+} \rightleftharpoons [Pd(PNP)_2]^{2+} + [PtH(PNP)_2]^+ \qquad \Delta rG$$

can be broken into two separate processes:

$$[PdH(PNP)_2]^+ \rightleftharpoons [Pd(PNP)_2]^{2+} + H^- \qquad \Delta_H G(Pd)$$

and

$$[Pt(PNP)_2]^{2+} + H^- \rightleftharpoons [PtH(PNP)_2]^+ \qquad -\Delta_H G(Pt).$$

According to Hess' law:

$$\Delta_r G = \Delta_H G(Pd) + (-\Delta_H G(Pt))$$

where $\Delta_r G$ is the Gibbs energy of the total reaction. $\Delta_r G$ can be calculated from the equilibrium constant that is given and the temperature of 298 K:

$$\Delta_r G = -2.3RT\log K = -2.3 \times 8.314 \text{ K J}^{-1} \text{ mol}^{-1} \times 298 \text{ K} \times \log(450) = -15.1 \text{ kJ mol}^{-1}.$$

From here:

$$\Delta_H G(Pd) = \Delta_r G - (-\Delta_H G(Pt))$$
$$= -15.1 \text{ kJ mol}^{-1} + 232 \text{ kJ mol}^{-1}$$
$$\Delta_H G(Pd) = 227 \text{ kJ mol}^{-1}.$$

(Note: The value for $\Delta_H G(Pt)$ has been taken from Example 10.4.)

S10.4 A possible procedure is as follows:

$$Et_3SnH + 2\,Na \rightarrow 2Na^+\,Et_3Sn^- + H_2$$

$$2Na^+\,Et_3Sn^- + CH_3Br \rightarrow MeEt_3Sn + NaBr.$$

Exercises

E10.1 **a) Hydrogen in Group 1:** Hydrogen has one valence electron like the group 1 metals and is stable as H^+, especially in aqueous media. The other group 1 metals have one valence electron and are stable as M^+ cations in solution and in the solid state as simple ionic salts. In most periodic charts, hydrogen is generally put with this group, given the above information.

b) Hydrogen in Group 17: Hydrogen can fill its 1s orbital and make a hydride H^-. Hydrides are isoelectronic with He, a noble gas configuration, thus are relatively stable. Group 1 and Group 2 metals, as well as transition metals, stabilize hydrides. The halogens form stable X^- anions, obtaining a noble gas configuration, both in solution and in the solid state as simple ionic salts. Some periodic charts put hydrogen both in Group 1 and in Group 17 for the reasons stated above. The halogens are diatomic gases just like hydrogen, so physically hydrogen would fit well in Group 17.

c) Hydrogen in Group 14: All elements in Group 14, however, have four valence electrons and thus are half way to obtaining the octet of a corresponding noble gas (i.e., neon for carbon, Ar for Si etc.). Hydrogen has only one electron and thus is half way toward obtaining a stable electronic configuration of its corresponding noble gas, He. Looking at the physical properties, the addition of hydrogen to Group 14 would add a gaseous non-metal to the group producing a gradual change of the properties to non-metallic (but solid) carbon, then somewhat more metallic solid silicon all the way to purely metallic lead. However, none of these reasons are compelling enough to warrant placing hydrogen in Group 14.

E10.2 As discussed in Section 10.4 *Production of dihydrogen* the three industrial methods of preparing H_2 are: (i) steam (or hydrocarbon) reforming, (ii) coal gasification, and (iii) the water-gas shift reaction. The balanced equations are:

$$\text{(i)} \quad CH_4(g) + H_2O \rightarrow CO(g) + 3H_2(g)\ (1000°C)$$

$$\text{(ii)} \quad C(s) + H_2O \rightarrow CO(g) + H_2(g)\ (1000°C)$$

$$\text{(iii)} \quad CO(g) + H_2O \rightarrow CO_2(g) + H_2(g).$$

Note that in the countries where electricity is cheap, the electrolysis of water may be an important process as well.

These large-scale reactions are not very convenient for the preparation of small quantities of hydrogen in the laboratory. Instead, (iv) treatment of an acid with an active metal (such as zinc) or (v) treatment of a metal hydride with water would be suitable. The balanced equations are:

$$\text{(iv)} \quad Zn(s) + 2HCl(aq) \rightarrow Zn^{2+}(aq) + 2Cl^-(aq) + H_2(g)$$

$$\text{(v)} \quad NaH(s) + H_2O \rightarrow Na^+(aq) + OH^-(aq) + H_2(g).$$

E10.3 If water did not have hydrogen bonds, it most likely would be a gas at room temperature like its heavier homologues H_2S, H_2Se, and H_2Te; see Figure 10.6. Extrapolating the boiling point values, we can estimate a boiling point of about –50°C or below for H_2O without H-bonding. Also, most pure compounds are denser as a solid than as a liquid. Because of hydrogen bonding, water is actually less dense as a solid and has the structure shown in Figure 10.7. Therefore, ice floats. If there were no hydrogen bonds, it would be expected that ice would be denser than water. Consult Section 10.6(a)(iii) *The Influence of Hydrogen bonding* and Figure 10.7 if you need to review this material.

E10.4 **a) BaH_2:** This compound is named barium hydride. It is a saline hydride.

b) SiH_4: This compound is named silane. It is an electron-precise molecular hydride.

c) NH_3: This familiar compound is known by its common name, ammonia, rather than by the systematic names azane or nitrane. Ammonia is an electron-rich molecular hydride.

d) AsH_3: This compound is generally known by its common name, arsine, rather than by its systematic name, arsane. It is also an electron-rich molecular hydride.

e) $PdH_{0.9}$: This compound is named palladium hydride. It is a metallic hydride.

f) HI: This compound is known by its common name, hydrogen iodide, rather than by its systematic name, iodane. It is an electron-rich molecular hydride.

E10.5 Of the compounds listed in Exercise 10.4, BaH_2 and $PdH_{0.9}$ are solids; none is a liquid; and SiH_4, NH_3, AsH_3, and HI are gases (see Figure 10.6). Only $PdH_{0.9}$ is likely to be a good electrical conductor.

E10.6 Reactions (a) and (c) involve the production of both H and D atoms at the surface of a metal. The recombination of these atoms will give a statistical distribution of H_2 (25%), HD (50%), and D_2 (25%). However, reaction (b) involves a source of protons that is 100% $^2H^+$ (i.e., D^+) and a source of hydride ions that is 100% $^1H^-$:

$$D_2O + NaH(s) \rightarrow HD(g) + NaOD(s)$$

$$\text{Net reaction: } D^+ + H^- \rightarrow HD.$$

Thus, reaction (b) will produce 100% HD and no H_2 or D_2.

E10.7 Since Al has the lowest electronegativity of the three elements, B (2.04), Al (1.61), and Ga (1.81, see Table 1.7 and Self-test 10.1 for reference), the Al–H bonds of AlH_4^- are more hydridic than the B–H bonds of BH_4^- or the Ga–H bonds of GaH_4^-. Therefore, since AlH_4^- is more "hydride-like," it is the strongest reducing agent. The reaction of GaH_4^- with aqueous HCl is as follows:

$$GaH_4^- + 4HCl(aq) \rightarrow GaCl_4^-(aq) + 4H_2(g).$$

E10.8 As the data in Table 10.1 illustrate, the thermodynamic stability of hydrides decreases down the group. This fact is reflected in the $\Delta_f H$ values for SbH_3 and BiH_3 provided in the problem. Therefore, it is expected that it would be very difficult to prepare a sample of BiH_3, even more difficult than SbH_3. The direct combination of elements (i.e., $Bi + H_2$) is not a practical approach because the reaction is thermodynamically strongly unfavourable. A good synthetic procedure could be a reaction of Bi_2Mg_3 with water:

$$Bi_2Mg_3(s) + 3H_2O(l) \rightarrow 2BiH_3(g) + 3Mg(OH)_2(aq).$$

However, the current method for the synthesis of bismuthine, BiH_3, is by the redistribution of methylbismuthine, BiH_2Me.

$$3BiH_2Me \rightarrow 2BiH_3 + BiMe_3.$$

The starting material BiH_2Me can be prepared by the reduction of $BiCl_2Me$ with $LiAlH_4$. The precursor, BiH_2Me, is unstable as well. The difficulty in synthesizing BiH_3 is because it involves a multi-step process, all of which deal with extremely reactive and unstable compounds.

BiH_3 is unstable above –45 °C, yielding hydrogen gas and elemental bismuth. The original preparation was reported in 1961, but it was not until 2002 that this procedure was repeated and yielded enough BiH_3 to do spectroscopic characterization!

E10.9 **Potential energy surfaces for hydrogen bonds, see Figure 10.9:** There are two important differences between the potential energy surfaces for the hydrogen bond between H_2O and Cl^- ion and for the hydrogen bond in bifluoride ion, HF_2^-. The first difference is that the surface for the H_2O, Cl^- system has a double minimum (as do most hydrogen bonds, see the potential energy surface for $[ClHCl]^-$ on Figure 10.9) because it is an unsymmetrical H bond, whereas the surface for the bifluoride ion has a single minimum (characteristic of only the symmetrical hydrogen bonds). The second difference is that the surface for the H_2O, Cl^- system is not symmetric because the proton is bonded to two different atoms (oxygen and chlorine), whereas the surface for bifluoride ion is symmetric. The two surfaces are shown below.

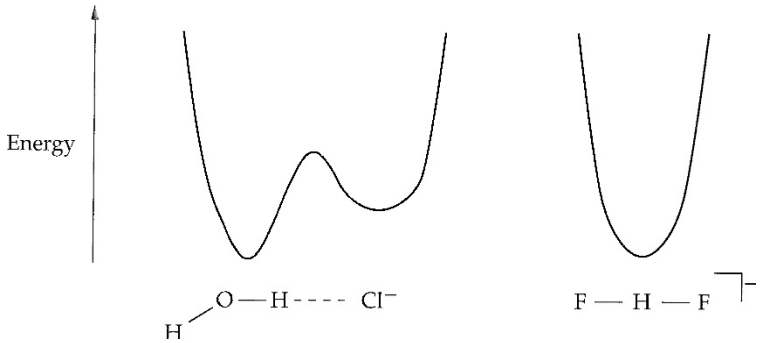

E10.10 The overall reaction is shown below:

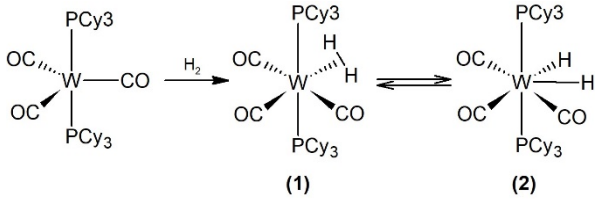

The starting material *trans*-$[W(CO)_3(PCy_3)_2]$ initially adds H_2 molecule to produce a dihydrogen complex *mer*,*trans*-$[W(CO)_3(H_2)(PCy_3)_2]$ **(1)**. In this complex tungsten is still formally in oxidation state 0. Complex **(1)** is in equilibrium with complex **(2)** which is a seven coordinate dihydride W(II) complex. Note the important difference between dihydrogen and dihydride complexes: dihydrogen complexes contain an H_2 molecule bonded to the metal as a ligand with the electron pair coming from the σ_g molecular orbital of H_2 molecule and with H–H bond still present. On the other hand, dihydride complexes contain two hydride, H^-, ligands. Hence, the oxidation state of W in complex **(1)** is 0 whereas in complex **(2)** it is +2. The formation of **(2)** is also an excellent example of *oxidative addition* reactions (a very common type of reaction in organometallic chemistry): the oxidation state of W has increased (i.e., it was oxidised) and the coordination number increased by two (from five in the starting material to seven in **(2)**); that is, two ligands have been added—overall an *oxidative addition*.

E10.11 Recall from Chapter 8 that the energy of a molecular vibration is determined by (Equation 8.4a in your textbook):

$$E_\nu = \left(\nu + \frac{1}{2}\right)\hbar\omega = \hbar\left(\nu + \frac{1}{2}\right)\left(\frac{k}{\mu}\right)^{\frac{1}{2}}, \text{ with } \mu_{^1\text{H}-^{35}\text{Cl}} = \frac{m_{^1\text{H}}m_{^{35}\text{Cl}}}{m_{^1\text{H}} + m_{^{35}\text{Cl}}}, \mu_{^3\text{H}-^{35}\text{Cl}} = \frac{m_{^3\text{H}}m_{^{35}\text{Cl}}}{m_{^3\text{H}} + m_{^{35}\text{Cl}}}.$$

We can make a few reasonable assumptions that will help us to calculate the expected wavenumber for ^{3}H-^{35}Cl stretch from a known ^{1}H-^{35}Cl stretch. First, we can assume that the force constants, *k*, are approximately equal in the two cases. The second approximation is that $m(^1\text{H}) + m(^{35}\text{Cl}) \approx m(^3\text{H}) + m(^{35}\text{Cl}) \approx m(^{35}\text{Cl})$. Thus, keeping in mind these assumptions and all constant values, we can show that, after cancelling, the ratio of vibrational energies is:

$$\frac{E_\nu^{\,^3\text{H}-^{35}\text{Cl}}}{E_\nu^{\,^1\text{H}-^{35}\text{Cl}}} = \frac{\sqrt{\mu_{^1\text{H}-^{35}\text{Cl}}}}{\sqrt{\mu_{^3\text{H}-^{35}\text{Cl}}}} \approx \sqrt{\frac{m_{^1\text{H}}}{m_{^3\text{H}}}}.$$

And from the above ratio:

$$E_\nu^{\,^3\text{H}-^{35}\text{Cl}} = \frac{E_\nu^{\,^3\text{H}-^{35}\text{Cl}}}{\sqrt{m_{^3\text{H}}}} = \frac{E_\nu^{\,^3\text{H}-^{35}\text{Cl}}}{\sqrt{3}}.$$

Considering that the energies and wavenumber are related through $E_\nu = hc\tilde{\nu}$, we finally have:

$$\tilde{\nu}^{\,^3\text{H}-^{35}\text{Cl}} = \frac{\tilde{\nu}^{\,^3\text{H}-^{35}\text{Cl}}}{\sqrt{3}} = \frac{2991 cm^{-1}}{\sqrt{3}} = 2074 cm^{-1}.$$

Chapter 11 The Group 1 Elements

Self-Tests

S11.1 The ionic radius for F^- is 133 pm (Resource Section 1). Considering that the radius ratio values are less than 1, we have to consider the r_-/r_+ ratio:

$$r_-/r_+ = 133 \text{ pm}/196 \text{ pm} = 0.679.$$

This ratio suggests an NaCl-type of structure and 6:6 coordination.

S11.2 Polarizable anions have electronic clouds that can be easily deformed. If the hydride radius suggests a structure with 8:8 coordination but actual structures have a 6:6 coordination then hydride anion must be very polarizable– fitting a large anion into a relatively small octahedral hole (small in comparison to the cubic hole) must be possible only if the anion can be "squished," i.e. deformed.

S11.3 The ionic radii of Fr^+ and I^- are 196 pm and 220 pm respectively. We can use $2(r_+ + r_-)/3^{1/2}$ to calculate the length of the unit cell expected from these radii:

$$d = 2(196 + 220)/3^{1/2} \text{ pm} = 481 \text{ pm}.$$

This value is reasonably close to the observed 490 pm, thus the data are consistent with the prediction.

S11.4 The Kapustinskii equation, given in Section 4.14, is:

$$\Delta H_L^0 = \frac{N_{ion}|z_+ z_-|}{d}\left(1 - \frac{d^*}{d}\right)\kappa \,.$$

We can approximate the interionic distances, d, with the sum of ionic radii for the two compounds in question. Both LiF and CsF have the rock-salt type structure with (6,6) coordination; thus, we have to look for radii in this specific coordination environment.

For LiF we have:

$$\Delta H^\circ{}_L(\text{LiF}) = \frac{2|(+1)\times(-1)|}{(76+133)\text{pm}}\left(1 - \frac{34.5\text{pm}}{(76+133)\text{pm}}\right)\times 1.21\times 10^5 \text{ kJ pm mol}^{-1} =$$

$$= 966.8 \text{ kJ mol}^{-1}.$$

For CsF we have

$$\Delta H^\circ{}_L(\text{CsF}) = \frac{2|(+1)\times(-1)|}{(167+133)\text{pm}}\left(1 - \frac{34.5\text{pm}}{(167+133)\text{pm}}\right)\times 1.21\times 10^5 \text{ kJ pm mol}^{-1} =$$

$$= 713.9 \text{ kJ mol}^{-1}.$$

As expected, the lattice enthalpy for LiF is higher than for CsF. LiF is insoluble, because the hydration enthalpy for Li^+ (956 kJ mol^{-1}) is insufficient to compensate for the lattice enthalpy of LiF. On the other hand, hydration enthalpy for Cs^+ (710 kJ mol^{-1}) is about the lattice enthalpy for CsF, and it is expected that CsF should be more soluble than LiF. Note that both LiF and CsF contain the same anion, F^-, and that the hydration of this anion should also be considered. However, the hydration enthalpy for F^- is insignificant (particularly when compared to the error produced by the Kapustinskii equation) and constant for both compounds, thus it can be ignored for a qualitative analysis like this one.

S11.3 Ozonides decompose to oxygen and superoxides ($MO_3(s) \rightarrow MO_2(s) + ½\ O_2(g)$). All simple ozonides are known except for Li. We can expect a similar trend for ozonides like the one observed for peroxides and superoxides. For example, going down the group the lattice energies for oxides, peroxides, and superoxides decrease; the difference in lattice energies also decreases down the group. Because of this decrease in the difference, the heavy superoxides have less tendency to decompose. By extension, we can expect that the difference between the ozonide and

superoxide lattice energies decreases going down the group; consequently, the stability of ozonides would increase in the same direction. Thus, we would expect that, on warming, NaO_3 would decompose first and CsO_3 last. This indeed is the case: NaO_3 decomposes at 37°C while CsO_3 does so at about 53°C.

S11.6 The answer follows similar reasoning as in Example 11.6 and description of thermal stabilities of Group 1 carbonates in the text. Larger K^+ is going to stabilize SO_3^{2-} anion better than small Li^+. Therefore, K_2SO_3 is going to decompose at higher temperatures.

S11.7 KNO_3 has two different decomposition temperatures, 350°C and 950°C. These correspond to the following changes in the composition:

$$KNO_3(s) \rightarrow KNO_2(s) + {}^1/_2O_2(g)$$

$$2KNO_2(s) \rightarrow K_2O(s) + 2NO_2(g) + {}^1/_2O_2(g).$$

Whereas $LiNO_3$ decomposes in one step at the temperature of 600°C:

$$LiNO_3(s) \rightarrow {}^1/_2\,Li_2O(s) + NO_2(g) + {}^1/_4O_2(g).$$

Both end-products are the binary oxides of lithium and potassium. It is important to remember here that large cations can stabilize large anions whereas small cations can stabilize small anions. Since K^+ is larger than Li^+, the nitrate is more stable in the lattice with K^+ than with Li^+, hence the final decomposition temperature for KNO_3 is higher. Larger size of K^+ is also responsible for the stabilization of the nitrite intermediate (without this added stability, we probably would not be able to observe this intermediate). On the side of the products, Li_2O is more stable, has higher lattice energy, than K_2O. (Recall that the lattice energies dictate the oxidation products: Li with O_2 produces Li_2O, whereas K produces KO_2 with larger superoxide O^{2-} anion). Therefore, $LiNO_3$ goes straight to Li_2O in one step at lower temperature whereas the decomposition of KNO_3 requires higher temperature and includes an intermediate.

S11.8 Li_3N has an unusual crystal structure (Figure 11.11), that consists of two types of layers. The first layer has the composition Li_2N^-, containing six-coordinate Li^+ centres. The second layer consists only of lithium cations. Therefore, the Li^+ ions are in two different chemical and magnetic environments. Therefore, one would expect two peaks in the ^{7}Li NMR spectrum. However, the lithium ion is highly mobile (as discussed in Section 11.12) and, because there are vacant sites in the structure, Li^+ can hop from one site to another. At higher temperatures, all the lithium ions will be fluxional, giving only one averaged resonance in the ^{7}Li NMR. At lower temperatures, the structure would freeze, and two resonances due to the two different environments in the structure would be observed.

Exercises

E11.1 **a)** All Group 1 metals have one valence electron in the ns^1 subshell. They also have relatively low first ionization energies; therefore, loss of one electron to form a closed-shell electronic configuration is favourable.

b) The Group 1 metals are large, electropositive metals and have little tendency to act as Lewis acids. They also lack empty orbitals to which the ligand lone electron pair could be donated. However, they do complex well with hard Lewis bases, such as oxides, hydroxides, and many other oxygen-containing ligands.

E11.2 From the given value for $r(Au^-)$ and ionic radii for Rb^+ (148 pm) and Cs^+ (167 pm):

RbAu: $r(Rb^+)/r(Au^-)$ = (148 pm)/(196 pm) = 0.755; within 0.732 – 1 range with stoichiometry 1 : 1, hence CsCl type structure;

CsAu: $r(Cs^+)/r(Au^-)$ = (167 pm)/(196 pm) = 0.852; within 0.732 – 1 range with stoichiometry 1 : 1, hence CsCl type structure.

E11.3 It would be a good idea to review Section 9.11. Look at the reasons why diagonal relationships between elements occur within the periodic table. Then look for the relevant values of atomic properties for Li and Mg (Chapter 12 or resource sections) and compare them—you will find significant similarities. The similarities in chemistry are related to the similar ionic radii.

E11.4 **a)** $Edta^{4-}$ is expected to give a more stable complex with Cs^+ compared to acetate. In general the Group 1 cations form stable complexes with polydentate ligands like $edta^{4-}$. This ligand has 6 potential donor atoms all of which are hard (four oxygen and two nitrogen donor atoms). On the other hand, acetate has two hard oxygen donor atoms and can act only as a bidentate ligand resulting in a much lower formation constant. The acetate complex is further destabilized due to acetate's small bite angle—the four-member chelating ring formed with relatively large Cs^+ would be rather unstable.

b) K^+ is more likely to form a complex with the cryptate ligand C2.2.2 than Li^+. The difference has to do with the match between the interior size of the cryptate and the ionic radius of the alkali metal ion. According to Figure 11.14, bigger K^+ forms a stronger complex, by about two orders of magnitude, with C2.2.2 than does smaller Li^+.

E11.5 Section 11.8 *Oxides and Related Compounds* briefly describes the synthesis of ozonides. The best method of synthesis uses metal superoxide and dry ozone/oxygen mixture (hydroxides are less desirable starting materials because of potential formation of H_2O which rapidly reacts with the product):

$$CsO_2 + O_3 \rightarrow CsO_3 + O_2.$$

When choosing the solvent for the recrystallization we have to think about the properties of CsO_3: it is a ionic compound that contains a very basic anion. This limits the choice to polar, basic solvents—ideal example of such a solvent is liquid ammonia.

E11.6 It is very likely that FrI would have low solubility in water; similar radii for Fr^+ and I^- (196 pm and 220 pm respectively) would reduce the solubility of this salt (parallel with solubility of Cs salts).
Particularly useful for separation of Fr^+ from Na^+ should be $Na_3[Co(NO_2)_6]$. This yellow sodium salt is soluble in water, but potassium, rubidium and caesium salts with the same anion are not. Thus, it can be expected that $Fr_3[Co(NO_2)_6]$ is not soluble either.

E11.7 Your NaCl structure should look like the one shown in Figure 11.4 and CsCl like the one shown in 11.5. Na^+ is six-coordinate, whereas Cs^+ is eight-coordinate. The compounds have different structures because Na^+ is smaller than Cs^+ resulting in a different r_+/r_- for the same anion. Caesium is so large that it can fill a cubic hole formed in simple cubic packing of Cl^- ions.

E11.8 **(a)** The driving force behind this reaction is the formation of lithium bromide (very large lattice energy and insoluble in organic solvents in which the reaction is performed). The same reasoning applies to reaction **(b)**. For reaction **(c)**, the driving force is the loss of ethane gas and higher acidity of C_6H_6 compared to C_2H_6.

(a) $CH_3Br + Li \rightarrow Li(CH_3) +$ **LiBr**

(b) $MgCl_2 + LiC_2H_5 \rightarrow Mg(C_2H_5)Br +$ **LiCl**

(c) $C_2H_5Li + C_6H_6 \rightarrow LiC_6H_5 +$ $\mathbf{C_2H_6}$

Chapter 12 The Group 2 Elements

Self-Tests

S12.1 Water cannot be used to extinguish a magnesium fire. Hot magnesium reacts with water liberating explosive H_2 gas. Burning magnesium metal can be covered with sand and left to cool down before handling.

S12.2 The oxygen atom in the structure of diethyl ether can behave as Lewis base because it has two lone electron pairs. Thus, diethyl ether can form adducts with Lewis acidic $BeCl_2$. Due to its small size, Be^{2+} likes tetrahedral geometry. Considering that it is already bonded to two Cl^- ions, we can bond two Et_2O molecules to one $BeCl_2$, and the product is expected to be $[BeCl_2(OEt_2)_2]$.

S12.3 The electronegativities of elements are provided in Table 1.7, and consult the Ketelaar triangle (Fig. 2.28). The Pauling electronegativities for Be, Ba, Cl, and F are 1.57, 0.89, 3.16, and 3.98 respectively. The average electronegativity for $BeCl_2$ is (1.57+3.16)/2 = 2.36, and the electronegativity difference is 3.16 – 1.57 = 1.59. These values on the Ketelaar triangle correspond to the covalent bonding. For BaF_2 the average electronegativity is (3.98+0.89)/2 = 2.43 and the difference is (3.98 – 0.89) = 3.09, corresponding to the ionic bond on the Ketelaar triangle.

Considering the bonding type in $BeCl_2$ and Lewis acid character of Be^{2+}, we can predict that $BeCl_2$ will have a polymeric, molecular structure. On the other hand, BeF_2 with its ionic bonding is very likely to adopt CaF_2-type ionic structure.

S12.4 Since Ca is between Mg and Ba in Group 2 we should expect, based on the periodic trends, that the difference in lattice enthalpies for CaO and CaO_2 lies between that of Mg and Ba oxides and peroxides and that the CaO_2 lattice is less stable than the CaO lattice. Using the Kapustinskii equation (Equation 4.4), the ionic radii from Table 12.1, and the appropriate constants—which are $\kappa = 1.21 \times 10^5$ kJ pm mol^{-1}, $N_{ion} = 2$, $z^+_{Ca} = +2$, $z^-_{O} = -2$ — the sum of the thermochemical radii, d_0, 140 pm + 100 pm = 240 pm, and $d^* = 34.5$ pm, find the lattice enthalpy of CaO. For calcium peroxide use $N_{ion} = 2$, $z^+_{Ca} = +2$, $z^-_{O_2} = -2$, and $d_0 = 180$ pm + 100 pm = 280 pm. The lattice enthalpies of calcium oxide and calcium peroxide are 3465 kJ mol^{-1} and 3040 kJ mol^{-1}, respectively. The trend that the thermal stability of peroxides decreases down Group 2 and that peroxides are less thermally stable than the oxides is confirmed.

S12.5 The ionic radius of Be^{2+} is 45 pm (consult Resource Section 1 in your textbook) and the ionic radius of Se^{2-} is 198 pm. The radius ratio is 45 pm/198 pm = 0.23, which according to Table 4.6 should be close to ZnS-like structure.

S12.6 Heating $BeSO_4 \cdot 4H_2O$, the product of reaction (i), would likely result in the formation of anhydrous $BeSO_4$ with loss of all four water molecules. On the other hand, heating $SrBe(OH)_4$, the product of reaction (ii), would produce SrO and BeO with elimination of two equivalents of H_2O:

$$SrBe(OH)_4(s) \xrightarrow{500°C} SrO(s) + BeO(s) + 2H_2O(g).$$

S12.7 Using the Kapustinskii equation (Equation 4.4) and the values of $\kappa = 1.21 \times 10^5$ kJ pm mol^{-1}, $N_{ion} = 3$, $z^+_{Mg} = +2$, $z^-_{F} = -1$, the sum of the thermochemical radii, d_0, 133 pm + 72 pm = 205 pm and $d^* = 34.5$ pm, the calculated lattice enthalpy of MgF_2 is 2945 kJ mol^{-1}. Similarly, for $MgBr_2$, using 196 pm as the ionic radius for Br^-, we can calculate the lattice enthalpy to be 2360 kJ mol^{-1}, whereas for MgI_2 (with 220 pm as I^- radius) we have 2193 kJ mol^{-1} as calculated lattice enthalpy.

Comparing the three calculated values, we see that, as expected, the lattice enthalpies decrease with an increase in the ionic radius of the halide anion; we can expect the increase in solubility in the same direction (i.e., from MgF_2 to MgI_2).

Exercises

E12.1 Be^{2+} has large polarizing power and a high charge density due to its small radius. Also, beryllium has the highest electronegativity among Group 2 elements. Descending Group 2 the atoms of elements increase in size, they are more electropositive (electronegativity drops), and predominantly ionic character of bonds results.

E12.2 All chlorides of Group 2 elements are ionic solids except $BeCl_2$ which is a polymeric covalent solid. Ionic compounds (in general) always have higher melting points than covalent compounds.

E12.3 $Ba + 2H_2O \rightarrow Ba(OH)_2 + H_2$; **A** = $Ba(OH)_2$

$Ba(OH)_2 + CO_2 \rightarrow BaCO_3$; **B** = $BaCO_3$

$2BaCO_3 + 5C \rightarrow 2BaC_2 + 3CO_2$; **C** = BaC_2

$BaC_2 + 2H_2O \rightarrow Ba(OH)_2$ (= compound **A**) + C_2H_2

$Ba(OH)_2 + 2HCl \rightarrow BaCl_2 + 2H_2O$; **D** = $BaCl_2$

E12.4 If you had a problem with this exercise, have a look again at Example 12.2 and Self-test 12.2. Be^{2+} is a strong Lewis acid while NH_3 is a good Lewis base since nitrogen atom has a lone electron pair. Thus, we can expect formation of Lewis acid-base adduct between Be^{2+} and NH_3. This is very similar to the reaction of BeF_2 with H_2O described in Section 12.11. The likely product will be $[Be(NH_3)_4]F_2$ with a tetrahedral geometry at Be^{2+} centre—four NH_3 ligands with fluorides as counterions in the secondary coordination sphere of $[Be(NH_3)_4]^{2+}$.

E12.5 The weight percent of hydrogen in BeH_2 and MgH_2 are:

$$\omega(H)_{BeH_2} = \frac{2 \times M(H)}{M(BeH_2)} \times 100\% = \frac{2 \times 1}{9.01 + 2 \times 1} \times 100\% = 18.2\%$$

$$\omega(H)_{MgH_2} = \frac{2 \times M(H)}{M(MgH_2)} \times 100\% = \frac{2 \times 1}{24.3 + 2 \times 1} \times 100\% = 7.6\% \cdot$$

Although BeH_2 has a higher percentage of H in its composition, it is not investigated as a possible hydrogen storage material because BeH_2 cannot be prepared directly from the elements (unlike MgH_2) but rather from alkyl-beryllium compounds—the fact that complicates its potential use.

E12.6 $Ba(OH)_2$ is a very strong base that gives two equivalents of OH^- per mol of the base. NaOH, although equally strong base provides only one equivalent oh hydroxide ion per mol. Also, $Ba(OH)_2$ is less hygroscopic than NaOH making it easier to obtain more precise weight of the base in moist (humid) environment.

E12.7 Decomposition of $CaCO_3$ produces one mol of CaO and one mole of CO_2. In grams, 56.08 g of CaO is produced for every 44 g of CO_2 released. Multiplying all by "billion tonnes" (note that 1 tonne has 1000 kg) we see that 56.08 billion tonnes of CaO comes with 44 billion tonnes of CO_2. Simple ratio can give us the final answer: 56.08/44 = x/35 or x = 44.6 billion tonnes.

E12.8 Anhydrous Mg and Ca sulphates are preferred as drying agents over the other alkaline earth sulphates. This is because of the higher affinity of Mg and Ca sulphates for water compared to the other alkaline earth sulphates, which are nearly insoluble in water. It may be interesting to note here that $BeSO_4$, although expected to be more hydrophilic, it is not considered as a desiccant because of its higher cost and toxicity. Anhydrous calcium chloride is also a useful drying agent, it is very hygroscopic due to the high hydration energy of Ca^{2+}.

E12.9 The Pauling electronegativity values of Be, Mg, Ba, and Br are 1.57, 1.31, 0.89, and 2.96 respectively.

The average electronegativity of $BeBr_2$ is therefore 2.27 and the difference is 1.39. The values on the Ketelaar triangle indicate that $BeBr_2$ should be covalent.

The average electronegativity of $MgBr_2$ is 2.13 and the difference is 1.65. The values on the Ketelaar triangle indicate that $MgBr_2$ should be ionic.

The average electronegativity of $BaBr_2$ is therefore 1.93 and the difference is 2.07. The values on the Ketelaar triangle indicate that $BaBr_2$ should be ionic.

E12.10 **(a)** The products depend on stoichiometry chosen:

$MgCl_2 + LiC_2H_5 \rightarrow LiCl + (C_2H_5)MgCl$

or

$MgCl_2 + 2LiC_2H_5 \rightarrow 2LiCl + Mg(C_2H_5)_2$

(b) $Mg + (C_2H_5)_2Hg \rightarrow Mg(C_2H_5)_2 + Hg$

(c) $Mg + C_2H_5HgCl \rightarrow C_2H_5MgCl + Hg$

Chapter 13 The Group 13 Elements

Self-Tests

S13.1 Following periodic trends, we could expect nihonium to form Nh_2O. Considering the decrease in formation of trioxides going town the group (i.e. -923 kJ mol^{-1} for In_2O_3 and only -94 kJ mol^{-1} for Tl_2O_3) we should expect Nh_2O_3 to be even less stable (more positive heat of formation). Also, Nh +1 oxidation state should be more stable than +3 (just as observed with Tl) due to the inert pair effect.

S13.2 The structure should be based on face centred lattice of Y^{3+} with all octahedral holes filled with B_{12}^{3-} anions. The cuboctahedron is a polygon with six square faces and eight triangular faces:

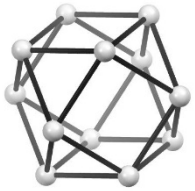

S13.3 VSEPR theory predicts that a species with four bonding pairs of electrons should be tetrahedral.

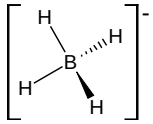

All protons are in equal environment and without coupling to the NMR active ^{11}B nucleus would produce only a singlet. However, coupling to one ^{11}B nucleus splits this singlet in $2nI + 1$ lines or $2\times1\times3/2 + 1 = 4$ lines. Due to this coupling a quartet is produced with four lines of equal intensity (1 : 1 : 1 : 1). (See also Exercise 8.___ and its solution)

S13.4 Look first at the reaction between B_2H_6 and propene ($CH_3CH=CH_2$) in ether. B_2H_6 is a dimer which can easily be cleaved. Since the solvent is ether, the first reaction would involve the cleavage of B_2H_6 with R_2O (ether molecules) to produce symmetric monomers $H_3B - OR_2$:

$$B_2H_6 + 2R_2O \rightarrow 2H_3B{-}OR_2.$$

In the presence of propene, and with heating, the monomer is going to add across C=C bond (hydroboration reaction):

$$H_3B - OR_2 + H_2C{=}CHCH_3 \rightarrow H_2BCH_2{-}CH_2CH_3 + OR_2.$$

In the second reaction, between B_2H_6 and NH_4Cl, THF solvent is also ether. The first step is the same like above with OR_2 replaced with THF:

$$B_2H_6 + 2THF \rightarrow 2H_3B{-}THF.$$

NH_4Cl contains a protic (acidic) cation (NH_4^+), whereas H_3B–THF is a hydridic hydride. Thus, the reaction between NH_4^+ and H_3B–THF is going to produce hydrogen gas and:

$$H_3B{-}THF + NH_4Cl \rightarrow H_2 + H_2B{-}NH_2 + HCl + THF.$$

S13.5 **a) BCl_3 and ethanol:** As mentioned in the example, boron trichloride is vigorously hydrolyzed by water. Therefore, a good assumption is that it will also react with protic solvents such as alcohols, forming HCl and B–O bonds:

$$BCl_3(g) + 3\ EtOH(l) \rightarrow B(OEt)_3(l) + 3\ HCl(g).$$

b) BCl_3 and pyridine in hydrocarbon solution: Neither pyridine nor hydrocarbons can cause the protolysis of the B–Cl bonds of boron trichloride, so the only reaction that will occur is a complex formation reaction, such as the one shown below. Note that pyridine, C_5H_5N, with a lone electron pair on N atom is a good Lewis base, whereas hydrocarbons with no lone electron pairs are very weak Lewis bases. Thus, pyridine, and not hydrocarbon, is going to react with BCl_3 as Lewis acid:

$$BCl_3(g) + C_5H_5N(l) \rightarrow Cl_3B{-}NC_5H_5(s).$$

c) BBr_3 and $F_3BN(CH_3)_3$: Since boron tribromide is a stronger Lewis acid than boron trifluoride, it will displace BF_3 from its complex with $N(CH_3)_3$:

$$BBr_3(l) + F_3BN(CH_3)_3(s) \rightarrow BF_3(g) + Br_3BN(CH_3)_3(s).$$

S13.6 *N*,*N*′,*N*″-trimethyl-*B*,*B*′,*B*″-trimethylborazine is hexamethylborazine. The reaction of ammonium chloride with boron trichloride yields *B*,*B*′,*B*″-trichloroborazine, whereas the reaction of a primary ammonium chloride with boron trichloride yields *N*-alkyl substituted *B*,*B*′,*B*″-trichloroborazine, as shown below:

$$3[CH_3NH_3]Cl + 3BCl_3 \xrightarrow{\text{Heat}} 9HCl + Cl_3BNCH_3.$$

Therefore, if you use methylammonium chloride you will produce $Cl_3BN(CH_3)_3$ (i.e., R = CH_3). This product can be converted to the desired one by treating it with an organometallic methyl compound of a metal that is more electropositive than boron. Either methyllithium or methylmagnesium bromide could be used, as shown below:

$$Cl_3BNCH_3 + 3CH_3MgBr \rightarrow (CH_3)_3B_3N_3(CH_3)_3 + 3Mg(Br, Cl)_2.$$

The structure of *N*,*N*′,*N*″-trimethyl-*B*,*B*′,*B*″-trimethylborazine:

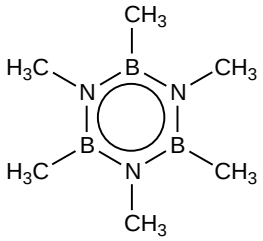

S13.7 **a)** The formula B_4H_{10} belongs to a class of borohydrides having the formula B_nH_{n+6}, which is characteristic of a *arachno* species. Assume one B–H bond per B atom, there are 4 BH units, which contribute 4×2 = 8 electrons, and the six additional H atoms, which contribute a further 6 electrons, giving 14 electrons, or seven electron pairs per cluster structure, which is n+3 with n = 4; this is characteristic of *arachno* clusters. The resulting seven pairs are distributed—two are used for the additional terminal B–H bonds, four are used for the four BHB bridges, and one is used for the central B–B bond.
The structure of B_4H_{10}:

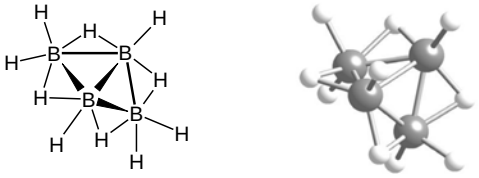

b) $[B_5H_8]^-$ has 5 B–H units contributing 5×2 = 10 electrons to the skeleton. There are three additional H atoms; each contributes one electron, for a total of three electrons. Finally, there is one negative charge on the cluster providing an additional electron. In total there are 10 + 3 + 1 = 14 skeletal electrons or seven skeletal electron pairs. This gives *n* + 2 (for *n* = 5) and a *nido* structure type. The structure is based on octahedron with one missing vertex:

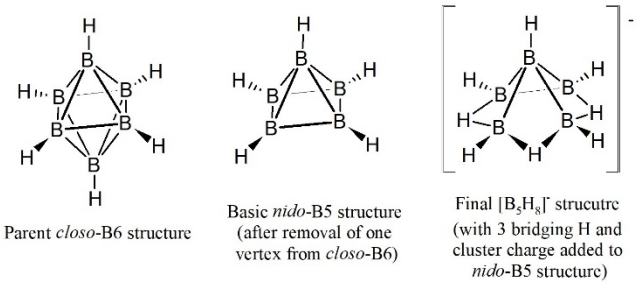

Parent *closo*-B6 structure

Basic *nido*-B5 structure (after removal of one vertex from *closo*-B6)

Final $[B_5H_8]^-$ strucutre (with 3 bridging H and cluster charge added to *nido*-B5 structure)

S13.8 General equation for hydrolysis of borohydrides is:

$$B_nH_m + 3nH_2O \rightarrow nB(OH)_3 + (3n+m)/2\ H_2$$

In our case, five moles of $B(OH)_3$ have been produced, meaning that n in above equation is 5. From this value and the fact that 12 moles of H_2 have been liberated, we can find m:

$$(3n+m)/2 = 12, \text{ hence } 3\times5 + m = 12\times2, \text{ and } m = 9$$

thus, the formula is B_5H_9.

This borohydride has 14 skeletal electrons (10 from five BH units, and four from additional four H atoms) or seven electron pairs. This means the cluster is *nido* and is based on *closo*-B6 octahedral cage:

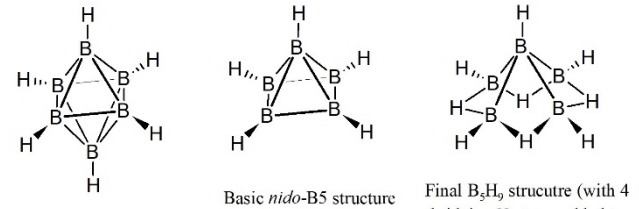

Parent *closo*-B6 structure

Basic *nido*-B5 structure (after removal of one vertex from *closo*-B6)

Final B_5H_9 strucutre (with 4 bridging H atoms added to *nido*-B5 structure)

S13.9 $C_2B_4H_6$ has $(6 \times 2) + 2 = 14$ skeletal electrons or seven skeletal electron pairs. This corresponds to $n + 1$, or a *closo* structure (octahedral).

S13.10 **a) $(CH_3)_2SAlCl_3$ and $GaBr_3$:** $GaBr_3$ is the softer Lewis acid, so the reaction is $(Me)_2SAlCl_3 + GaBr_3 \rightarrow Me_2SGaBr_3 + AlCl_3$ (Soft Lewis acid migrates from a hard Lewis acid to a soft one).

b) $TlCl_3$ and formaldehyde (HCHO) in acidic aqueous solution: Thallium trihalides are very unstable and are easily reduced, as shown below:

$$2\ TlCl_3 + H_2CO + H_2O \rightarrow 2TlCl + CO_2 + 4\ H^+ + 4\ Cl^-.$$

Exercises

E13.1 Boron is recovered from the mineral borax, $Na_2B_4O_5(OH)_4{\cdot}8H_2O$. Borax is hydrolized in the presence of a strong acid to boric acid, $B(OH)_3$:

$$Na_2B_4O_5(OH)_4(aq) + 2H_3O^+(aq) + H_2O(l) \rightarrow 2Na^+(aq) + 4B(OH)_3(s).$$

Boric acid precipitates from cold solution. This acid is then converted to B_2O_3 under heat:

$$2B(OH)_3(s) \xrightarrow{heat} B_2O_3(s) + 3H_2O(g).$$

Finally, the oxide is reacted with magnesium to liberate elemental boron:

$$B_2O_3 + 3Mg \rightarrow 2B + 3MgO.$$

E13.2 Generally, when aluminium surface gets in contact with air, a thin layer of Al_2O_3 is formed that actually protects the metal form further reaction with oxygen from air. When a droplet of Hg is added to a clean aluminium surface, however, aluminium amalgam is formed, an alloy of mercury and aluminium. The Al atoms in the amalgam react with O_2 producing Al_2O_3 which is insoluble in mercury. This leads to further dissolution of Al in Hg and the reaction proceeds until there is Al to react.

E13.3 For a given halogen, the order of acidity for Group 13 halides toward hard Lewis bases (such as dimethylether or trimethylamine) is $BX_3 > AlX_3 > GaX_3$, whereas the order toward soft Lewis bases (such as dimethylsulfide or trimethylphosphine) is $BX_3 < AlX_3 < GaX_3$. For boron halides, the order of acidity is $BF_3 < BCl_3 < BBr_3$, exactly opposite to the order expected from electronegativity trends. This fact establishes the order of Lewis acidity as $BCl_3 > BF_3 > AlCl_3$ toward hard Lewis bases:

(a) $BF_3N(CH_3)_3 + BCl_3 \rightarrow BCl_3N(CH_3)_3 + BF_3$ ($BCl_3 > BF_3$)

(b) $BH_3CO + BBr_3 \rightarrow NR$ (BH_3 is softer than BBr_3, and CO is a soft base)

E13.4

$4BF_3 + 3LiAlH_4 \rightarrow 2B_2H_6 + 3LiBF_4$; **A** = B_2H_6

$B_2H_6 + 6H_2O \rightarrow 2B(OH)_3 + 6H_2$; **B** = $B(OH)_3$

$2B(OH)_3 + \text{heat} \rightarrow B_2O_3 + 3H_2O$; **C** = B_2O_3

$B_2O_3 + 3CaF_2 \rightarrow 2BF_3 + 3CaO$

E13.5 **a)** The structure of B_5H_{11}:

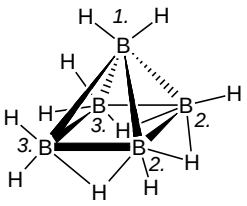

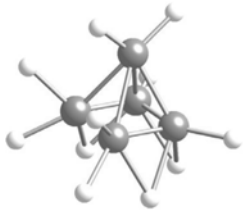

This cluster would have three different environments in the proton-decoupled ^{11}B-NMR: the apical B atom (marked as *1.*), two basal B atoms bonded to two bridging and one terminal hydrides each (B atoms *2.*), and two B atoms bonded to one bridging and two terminal H each (B atoms *3.*).

b) The structure of B_4H_{10}:

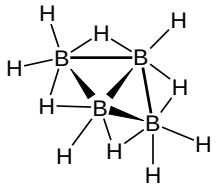

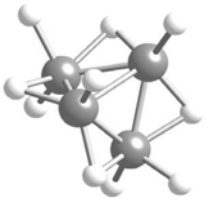

Two different boron environments are present in the proton-decoupled ^{11}B-NMR of this compound: there are two equivalent B atoms in the middle of the structure (bonded to only one terminal H atom) and two B atoms on each side (bonded to two terminal H atoms).

E13.6 Give combustion reaction as:

$$B_2H_6(g) + 3O_2(g) \rightarrow B_2O_3(s) + 3H_2O(g).$$

In the first step, we will calculate the $\Delta_r H$ using the relationship:

$$\Delta_r H = \Sigma\Delta_f H_{\text{products}} - \Sigma\Delta_f H_{\text{reactants}}.$$

The enthalpies of formation of B_2H_6, H_2O, and B_2O_3 are given and the enthalpy of formation for O_2 is zero as per the definition. Thus:

$$\Delta_r H = [\,3(-242\ \text{kJ mol}^{-1}) + (-1264\ \text{kJ mol}^{-1})] - [31\ \text{kJ mol}^{-1}]$$
$$= -2021\ \text{kJ mol}^{-1}.$$

To calculate the heat released, when 1 kg (1000 g) of B_2H_6 is used, we use the following procedure (using 27.62 g/mol as molecular weight of B_2H_6):

$$\frac{1000\,\text{g}}{27.62\,\text{g mol}^{-1}} \times \left(-2021\frac{\text{kJ}}{\text{mol}}\right) = -73{,}172\,\text{kJ}.$$

Diborane is extremely toxic. It is an extremely reactive gas and hence should be handled in a special apparatus. Moreover, a serious drawback to using diborane is that the boron-containing product of combustion is a solid, B_2O_3. If an internal combustion engine is used, the solid will eventually coat the internal surfaces, increasing friction, and will clog the exhaust valves.

E13.7 The chelating agent, $F_2B–C_2H_4–BF_2$, can be prepared by adding B_2F_4 to ethene. Starting with BCl_3, the first step is to prepare B_2Cl_4 and then convert it to B_2F_4 with a double replacement reagent such as AgF or HgF_2, as follows:

$$2BCl_3 + 2Hg \xrightarrow{\text{electron impact}} B_2Cl_4 + 2HgCl_2$$
$$B_2Cl_4 + 4AgF \rightarrow B_2F_4 + 4AgCl$$
$$B_2F_4 + C_2H_4 \rightarrow F_2BH_2CH_2BF_2$$

E13.8 **a)** IUPAC name for boron hydrides is boranes. B_2H_6 is simply called diborane. In the name of neutral boranes, the number of B atoms is indicated by a Greek prefix while the number of H atoms in the cluster is given at the end in brackets. The name should be preceded by *closo*, *nido* or arachno as appropriate.
Thus, $B_{10}H_{14}$ is called *nido*-decaborane(14)

b) The BH anions are named by providing the number of hydrogen atoms and number of boron atoms in Greek. The name has *-ate* ending to indicate negative charge with the actual charge given at the end in brackets: *closo*-dodecahydrododecaborate(2-). Note that hydrogen becomes "hydro" in the name and that the Greek numbers are added before "hydro" for hydrogen and before "borate" for boron. The prefix *closo* can also be placed before "borate" part: dodecahydro-*closo*-dodecaborate(2-).

c) *Arachno*-tetradecahydrododecaborate(2-) or tetradecahydro-*arachno*-dodecaborate(2-)

E13.9 **a)** $NaBH_4$ can be converted to BCl_3 using a solution of HCl in ether (with hydrogen gas and solid NaCl as by-products):

$$NaBH_4 + 4HCl(\text{ether sol.}) \rightarrow BCl_3 + NaCl(s) + 4H_2(g).$$

After NaCl is removed by filtration, the remaining filtrate (which is solution of BCl_3 in ether) is reacted with ethyl Grignard reagent:

$$BCl_3 + 3C_2H_5MgBr \rightarrow B(C_2H_5)_3 + 3MgBrCl.$$

b) Starting from $NaBH_4$ and $[HN(C_2H_5)_3]Cl$**,** we should expect NaCl, with its high lattice enthalpy, to be a likely product. If this is the case we shall be left with BH_4^- and $[HN(C_2H_5)_3]^+$. The interaction of the hydridic BH_4^- ion with the protic $[HN(C_2H_3)_5]^+$ ion will evolve dihydrogen gas to produce triethylamine and BH_3. In the absence of other Lewis bases, the BH_3 molecule would coordinate to THF; however, the stronger Lewis base triethylamine is produced in the initial reactions, so the overall reaction will be :

$$[HN(C_2H_5)_3]Cl + NaBH_4 \rightarrow H_2 + H_3BN(C_2H_5)_3 + NaCl.$$

E13.10 In general, boron hydrides with more hydrogen atoms are thermally unstable. The compounds B_6H_{10} and B_6H_{12} belong to two different classes of boranes, B_nH_{n+4} and B_nH_{n+6}, respectively, with the first class having less H atoms per boron. In this case, *n* is six for both compounds.; hence we expect B_6H_{10} to be stable relative to B_6H_{12}.

E13.11 **a)** The formula $B_{10}H_{14}$ belongs to a class of borohydrides with the general formula B_nH_{n+4}, characteristic of a *nido* species.

b) There are 10 BH units, which contribute 10×2 = 20 electrons (assuming one B–H bond per B atom), and the four additional H atoms, which contribute four additional electrons, giving a total of 24 electrons, or 12 electron pairs, which is n+2 for n = 10. This is characteristic of *nido* clusters.

c) The total number of valence electrons for $B_{10}H_{14}$ is (10×3)+(14×1) = 44. Since there are ten 2*c*-2*e* B–H bonds, which account for 20 of the total number of valence electrons, the number of cluster electrons is the remainder of 44-20=24.

E13.12 General equation for hydrolysis of borohydrides is:

$$B_nH_m + 3nH_2O \rightarrow nB(OH)_3 + (3n+m)/2\ H_2.$$

In our case, six moles of $B(OH)_3$ have been produced, meaning that n in above equation is 6. From this value and the fact that 15 moles of H_2 have been liberated, we can find m:

$$(3n+m)/2 = 15, \text{ hence } 3\times6 + m = 15\times2, \text{ and } m = 12;$$

thus, the formula is B_6H_{12}.

This borohydride has 18 skeletal electrons (12 from six BH units, and six from additional six H atoms) or nine electron pairs. This means the cluster is *arachno* and is based on *closo*-B8 structure cage.

E13.13 **a)** The ^{11}B NMR spectrum of BH_3CO would show one quartet resonance due to ^{11}B being coupled to three equivalent H nuclei.

b) $[B_{12}H_{12}]^{2-}$ has two distinct ^{11}B environments in its structure: two apical B atoms and 10 equivalent B atoms in two five-membered rings. Thus the ^{11}B NMR should show two signals in relative intensity 1 : 5 both of which should be, if we assume no B-B coupling, doublets because each B atom in $[B_{12}H_{12}]^{2-}$ is bonded to only one H atom.

E13.14 **a)** The products are $B(OH)_3$ and HCl. See Section 13.7 *Boron Trihalides.*

b) BCl_3 is a Lewis acid while $S(CH_3)_3$ is a Lewis base, thus the product is a Lewis acid-base adduct, $BCl_3S(CH_3)_2$

E13.15 **a) The structures.** Both substances have layered structures. The planar sheets in boron nitride and in graphite consist of edge-shared hexagons such that each B or N atom in BN has three nearest neighbors that are the other type of atom, and each C atom in graphite has three nearest neighbor C atoms. The structure of graphite is shown in Figure 14.2. The B–N and C–C distances within the sheets, 1.45 Å and 1.42 Å, respectively, are much shorter than the perpendicular interplanar spacing, 3.33 Å and 3.35 Å, respectively. In BN, the B_3N_3 hexagonal rings are stacked directly over one another so that B and N atoms from alternating planes are 3.33 Å apart, whereas in graphite the C_6 hexagons are staggered (see Section 13.9) so that C atoms from alternating planes are either 3.35 Å or 3.64 Å apart (you should determine this yourself using trigonometry).

b) Their reactivity with Na and Br_2? Graphite reacts with alkali metals and with halogens. In contrast, boron nitride is quite unreactive.

c) Explain the differences? The large HOMO–LUMO gap in BN, which causes it to be an insulator, suggests an explanation for the lack of reactivity: since the HOMO of BN is a relatively low-energy orbital, it is more difficult to remove an electron from it than from the HOMO of graphite, and since the LUMO of BN is a relatively high energy orbital, it is more difficult to add an electron to it than to the LUMO of graphite.

E13.16 A plausible structure can be determined when we note that the nitrogen atom in the structure provides two more skeletal electrons than the B atom would on its place. Thus, if the compound had only B atoms, we would have 24 skeletal electrons (from 12 B–H units) or 12 skeletal electron pairs. To this we have to add two more electrons (or one more electron pair) to account for two extra valence electrons on the nitrogen atom. This gives 26 skeletal electrons or 13 pairs. This is n+1 (for n = 12), and the structure is *closo* and it corresponds to the icosahedral structure with one BH unit replaced with an NH unit.

a) $Ph_3N_3B_3Cl_3$. The reaction of a primary ammonium salt with boron trichloride yields *N*-substituted *B*-trichloroborazines:

$$3\ [PhNH_3]Cl + 3\ BCl_3 \rightarrow Ph_3N_3B_3Cl_3 + 9\ HCl.$$

b) $Me_3N_3B_3H_3$. First prepare $Me_3N_3B_3Cl_3$ using $[MeNH_3]Cl$ and the method described above, and then perform a Cl^-/H^- metathesis reaction using LiH (or $LiBH_4$) as the hydride source:

$$3\ MeNH_3^+Cl^- + 3\ BCl_3 \rightarrow Me_3N_3B_3Cl_3 + 9\ HCl$$

$$Me_3N_3B_3Cl_3 + 3\ LiH \rightarrow Me_3N_3B_3H_3 + 3\ LiCl.$$

The structures of $Ph_3N_3B_3Cl_3$ and $Me_3N_3B_3H_3$ are shown below:

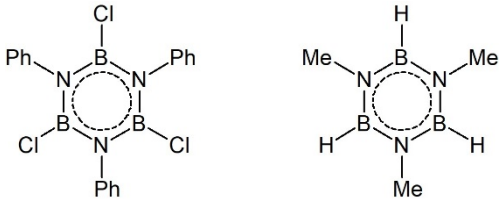

E13.17 The common oxidation states of indium are +1 and +3. The oxidation states of In in In_5Cl_9 must sum to +9 to maintain the electroneutrality of the compound. We can suggest having two of them in +3 oxidation state (giving +6) and the other three in +1 (for a total of +9). The formula is then rewritten as $In_3^{(I)}[In_2^{(III)}Cl_9]$. Because they have a similar chemical composition, the structures of $In_2Cl_9^{3-}$ and $Tl_2Cl_9^{3-}$ are the same and consists of two MCl_6 octahedra sharing a face (M = In or Tl):

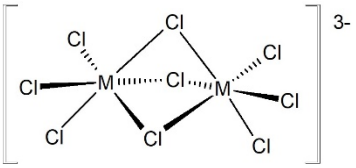

This structure can be proposed by a bit of "trial-and-error" with number of bridges and stoichiometry, the driving force behind the bridge formation is the Lewis acidity of Group 13 trihalides.

E13.18 Table 13.5 provides the band gap energies for GaN, GaAs and GaSb. Since P lies between N and As in the periodic table and the band gap energies decrease going down the Group 15, we can estimate the band gap for GaP as an average band gap energy of that for GaN and for GaAs:

$$(3.40\ eV + 1.35\ eV)/2 = 2.37\ eV.$$

This corresponds to 3.79×10^{-19} J ($1\ eV = 1.60 \times 10^{-19}$ J).

The energy is related to the wavelength:

$$E = \frac{hc}{\lambda} \Rightarrow \lambda = \frac{hc}{E}.$$

From here we have:

$$\lambda = \frac{6.626\times10^{-34}\,\text{Js}\times3\times10^{8}\,\text{m/s}}{3.79\times10^{-19}\,\text{J}} = 5.24\times10^{-7}\,\text{m} = 524\text{nm}.$$

The green light has a wavelength of about 550 nm. Thus, our estimate is consistent with the observation of green light emitted by GeP LEDs.

Chapter 14 The Group 14 Elements

Self-Tests

S14.1 Increase in pressure favours always a denser structure. In this case, that is the cubic structure. Thus, at higher pressures, the phase change can occur at even lower temperatures.

S14.2 It has to be noted that given formulas lack the required charges. This is easy to observe: in the first formula, we have germanium in oxidation state +2 boned to three fluorine atoms in oxidation state -1, thus $[Ge(II)F_3]$ should have overall negative one charge. Thus, we have four valence electrons from Ge, 21 valence electrons from three fluorine atoms plus one extra for the negative charge, in total 26 valence electrons to account for. We can suggest a tetrahedral electron geometry with trigonal pyramidal molecular geometry:

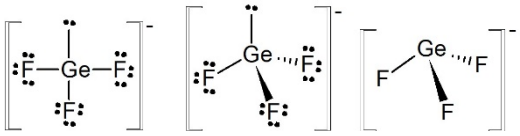

Similar analysis shows that $[Ge(IV)F_6]$ has a 2- charge with a total valence electron count of 48 electrons. This composition and number of electrons result in an octahedral electron and molecular geometry:

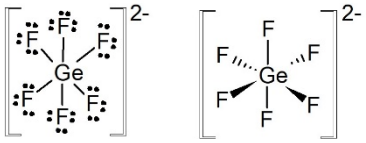

What might be somewhat confusing at the end are the charges: the sum of charges on the structural units is 3- and there are no additional cations, while the compound in question is neutral Ge_3F_8. The reason for this apparent discrepancy is that our focus in this self-test was on the geometries of the structural units *not* how the units interact in the structure. In the Ge_3F_8 structure the octahedra and trigonal pyramids are connected through bridging fluorides. This is also apparent when we look at the stoichiometry: the formula Ge_3F_8 is not the sum of its structural units $2\times[Ge(II)F_3] + [Ge(IV)F_6]$—the sum has four more F atoms than the formula.

S14.3 **a)** The extended π system for each of the planes of graphite results in a band of π orbitals. The band is half filled in pure graphite; that is, all bonding MOs are filled and all antibonding MOs are empty. The HOMO–LUMO gap is ~0 eV, giving rise to the observed electrical conductivity of graphite. Chemical reductants, like potassium, can donate their electrons to the LUMOs (graphite π* MOs), resulting in a material with a higher conductivity.

b) Chemical oxidants, like bromine, can remove electrons from the HOMOs (π MOs) of graphite. This also results in a material with a higher conductivity.

S14.4 The enthalpy of formation is calculated as the difference between the bonds broken and the bonds formed in the reaction.

Four C–H bonds are formed in the formation of methane from graphite and hydrogen gas:

$$C(\text{graphite}) + 2\ H_2(g) \rightarrow CH_4(g).$$

$\Delta_f H\ (CH_4,g)$ = (bonds broken) – (bonds formed) = $[715+2(436)]\text{kJ mol}^{-1} - [4(412)]\ \text{kJ mol}^{-1}$

$\Delta_f H = -61\text{kJ mol}^{-1}$

Four Si–H bonds are formed in the synthesis of silane from silicon with hydrogen gas:

$$Si(s) + 2\ H_2(g) \rightarrow SiH_4\,(g).$$

$\Delta_f H\ (SiH_4,g)$ = (bonds broken) – (bonds formed) = $[439+2(436)]\text{kJ mol}^{-1} - [4(318)]\ \text{kJ mol}^{-1}$

$\Delta_f H = +39\ \text{kJ mol}^{-1}$

S14.5 The first step of synthesis would be the oxidation of ^{13}CO to $^{13}CO_2$. Carbon dioxide is Lewis acidic and can react with strong Lewis bases. Thus, we can treat $^{13}CO_2$ with a source of deuteride ion, D^-, a good Lewis base. A convenient source would be LiD (or NaD). The entire synthesis would be:

$$^{13}CO(g) + 2\ MnO_2(s) \rightarrow {}^{13}CO_2(g) + Mn_2O_3(s)$$

$$2\ Li(s) + D_2 \rightarrow 2\ LiD(s)$$

$$^{13}CO_2(g) + LiD(ether) \rightarrow Li^+D^{13}CO_2^-(ether)$$

S14.6 Oxidation of C_2^{2-} to C_2^- would result in removal of one of the electrons found in $2\sigma_g$ molecular orbital. This molecular orbital is bonding in character, and removal of one of the electrons from this orbital would give the $1\sigma_g^2\ 1\sigma_u^2\ 1\pi_u^4\ 2\sigma_g^1$ electronic configuration resulting in a decrease in bond order—from 3 to 2.5: $b = ½\ (2 - 2 + 4 + 1) = 2.5$. Therefore, C–C bond length in C_2^- would be longer than in C_2^{2-}.

Exercises

E14.1 Statement **(a)** is incorrect—tin and lead are metallic elements.

Statement **(b)** is correct.

Statement **(c)** is partially correct—whereas it is true that both CO_2 and CS_2 are weak Lewis acids, CS_2 is softer (not harder) than CO_2.

Statement **(d)** is incorrect—zeolites are framework aluminosilicates (not layered like mica) and they do contain metal cations in their composition to balance the negative charge of the aluminosilicate framework.

Statement **(e)** is correct—hydrolysis of CaC_2, a ionic compound, produces $HC{\equiv}CH$ and $Ca(OH)_2$.

E14.2 $SiCl_3F$, $SiCl_2F_2$, and $SiClF_3$ have tetrahedral structures as shown below. Each Si has an octet and each molecule conforms with VSEPR theory:

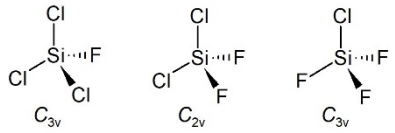

The point groups for each molecule are given below the structure. At this point in the course you should be very familiar in using the decision tree (Chapter 4, Figure 4.9) for identification of point groups.

E14.3 The bond enthalpy of a C–F bond is higher than the bond enthalpy of a C–H bond, making C–F bond more difficult to break. Further, the combustion of CH_4 produces not only CO_2 but H_2O as well, a very stable compound. Formation of both CO_2 and H_2O thermodynamically drive the combustion of CH_4. There is no equivalent to the formation of H_2O in the combustion of CF_4.

E14.4 The chemical equation for reaction of SiF_4 with $[(CH_3)_4N]F$:

$$SiF_4 + [(CH_3)_4N]F \rightarrow [(CH_3)_4N]^+[SiF_5]^-.$$

a) The cation is $[(CH_3)_4N]^+$. (At this point in the material, you should be very familiar with VSEPR theory so only a brief outline is given here!) The number of valence electrons present on central N atom is eight and the number of valence electron pairs is four. Therefore, VSEPR theory predicts that a species with four bonding pairs of electrons should be tetrahedral.

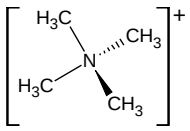

The anion is SiF_5^-. The number of valence electrons present on central Si atom is 10 and the number of valence electron pairs is five. Therefore, VSEPR theory predicts that a species with five pairs of electrons should be trigonal bipyramidal.

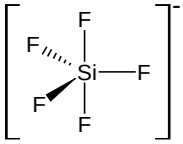

b) The ^{19}F NMR shows two fluorine environments because in the structure of the anion there are two different fluorine environments: axial and equatorial.

E14.5 Trimethylstannylphosphine is $(CH_3)_3SnPH_2$. The relevant NMR data can be found in Table 8.4: ^{119}Sn, abundance 8.58% with $I = ½$ and ^{31}P abundance 100% with $I = ½$.

a) For the ^{119}Sn NMR spectrum, we can ignore relatively weak, two bond $^2J(^{119}Sn\text{-}^1H)$ couplings. In this case, the spectrum would show one doubled due to one bond coupling between ^{119}Sn and ^{31}P.

b) For the ^{31}P spectrum, we cannot ignore one bond couplings to two hydrogen nuclei directly bonded to P. This strong coupling would produce a triplet. This spectrum would also show satellites due to the one-bond coupling between ^{119}Sn and ^{31}P nuclei: a doublet of triplets lines would flank the central triplet.

E14.6

$Si + 2\ Cl_2 \rightarrow SiCl_4$	**A** = $SiCl_4$
$SiCl_4 + RLi \rightarrow SiRCl_3 + LiCl$	**B** = $SiRCl_3$
$SiRCl_3 + 3\ H_2O \rightarrow RSi(OH)_3 + 3\ HCl$	**C** = $RSi(OH)_3$
$2\ RSi(OH)_3 \rightarrow RSiOSiR + H_2O$	**D** = RSiOSiR
$SiCl_4 + 4\ RMgBr \rightarrow SiR_4 + 4\ MgBrCl$	**E** = SiR_4
$SiCl_4 + 2\ H_2O \rightarrow SiO_2 + 4\ HCl$	**F** = SiO_2

Note that in the reaction with RLi the products can be $RSiCl_3$, R_2SiCl_2, R_3SiCl, and R_4Si depending on the stoichiometry used; thus, product **B** has more than one possibility considering that the stoichiometry is not clearly given. For the reaction with water, however, your product must contain Si–Cl bonds; this excludes R_4Si as a possible product. Considering that product **B** has more than one possibility, products **C** and **D** vary. For example, if **B** is R_2SiCl_2, then reaction with water would give $R_2Si(OH)_2$ as **C** that would further condense to cyclic $(R_2SiO)_3$ product **D**. Consult Section 14.16 for further details.

E14.7 The most stable oxidation state of Pb is +2. Combining Pb^{4+}, an oxidizing agent, with a good reducing agent, I^-, will lead to a redox reaction and PbI_4 breaks down into PbI_2 and I_2. On the other hand, since F_2 is one of the strongest oxidizing agents, F^- has virtually no reducing ability. As such we can prepare PbF_4 as a stable compound. As a matter of fact, F_2 is such a strong oxidizing reagent that it can oxidize Pb straight to otherwise unstable Pb^{4+}.

E14.8 Silicon is recovered from silica (SiO_2) by reduction with carbon:

$$SiO_2(s) + C(s) \rightarrow Si(s) + CO_2(g) \qquad \Delta_r H < 0.$$

The reaction takes place in an electric arc furnace because it has high activation energy due to the strong Si–O bonds.

Germanium is recovered from its oxide by reduction with hydrogen:

$$GeO_2(s) + 2\ H_2(g) \rightarrow Ge(s) + 2\ H_2O(g) \qquad \Delta_r H < 0.$$

GeO_2 can also be reduced by CO:

$$GeO_2(s) + 2CO(g) \rightarrow Ge(s) + 2CO_2(g).$$

E14.9 Consult Figure 14.13 and Section 14.13.

	Ionic carbides	Metallic carbides	Metalloid carbides
Group I elements	Li, Na, K, Rb, Cs		
Group II elements	Be, Mg, Ca, Sr, Ba		
Group 13 elements	Al		B
Group 14 elements			Si
3d elements		Sc, Ti, V, Cr, Mn, Fe, Co, Ni	
4d elements		Zr, Nb, Mo, Tc, Ru	
5d elements		La, Hf, Ta, W, Re, Os	
6d elements		Ac	
Lanthanides		Ce, Pr, Nd, Pm, Sm, Eu, Gd, Tb, Dy, Ho, Er, Tm, Yb, Lu	

E14.10 Both compounds react with acid to produce the oxide, which for carbon is CO_2 and for silicon is SiO_2. The balanced equations are:

$$K_2CO_3(aq) + 2HCl(aq) \rightarrow 2KCl(aq) + CO_2(g) + H_2O(l)$$

$$Na_4SiO_4(aq) + 4HCl(aq) \rightarrow 4NaCl(aq) + SiO_2(s) + 2H_2O(l)$$

The second equation represents one of the ways that silica gel is produced. Note that in the second reaction the first product is silicic acid, H_4SiO_4. However, this acid rapidly polymerizes and loses H_2O, forming a network of very strong Si–O bonds.

E14.11 In contrast with the extended three-dimensional structure of SiO_2, the structures of jadeite and kaolinite consist of extended one- and two-dimensional structures, respectively. The $[SiO_3^{2-}]_n$ ions in jadeite are a linear polymer of SiO_4 tetrahedra, each one sharing a bridging oxygen atom with the tetrahedron before it and the tetrahedron after it in the chain (see Structure **17** in the chapter). Each silicon atom has two bridging oxygen atoms and two terminal oxygen atoms. The two-dimensional aluminosilicate layers in kaolinite represent another way of connecting SiO_4 tetrahedra (see Figure 14.18). Each silicon atom has three oxygen atoms that bridge to other silicon atoms in the plane, and one oxygen atom that bridges to an aluminium atom.

E14.12 Both pyrophyllite, $Al_2Si_4O_{10}(OH)_2$, and muscovite, $KAl_2(Si_3Al)O_{10}(OH)_2$, belong to the phyllosilicate subclass of silicate class. The phyllosilicates are characterised with two-dimensional sheets composed of vertex-sharing SiO_4-tetrahedra; each SiO_4-tetrahedron is connected to three neighbouring SiO_4-tetrahedra via bridging O atoms. These sheets are negatively charged and held together via electrostatic interactions with cations sandwiched between the sheets. Because of this layered structure and relatively weak electrostatic interactions keeping them together, both pyrophyllite and muscovite have excellent cleavage parallel to the layers (just like graphite). The hardness of two minerals is, however, somewhat different—muscovite is harder than pyrophyllite (although both are very soft and can be scratched with a nail). The reason for this is in the chemical composition. Pyrophyllite layers are composed of exclusively SiO_4 tetrahedra held together with sandwiched Al^{3+} cations located in octahedral holes. In muscovite structure, however, every fourth Si^{4+} in the layer is replaced with Al^{3+} (see the formula—Si_3Al). The replacement of one +4 charge with +3 decreases the overall charge of layers and an additional cation is required to balance the charge. Strictly speaking one Si^{4+} is replaced with the Al^{3+}/K^+ pair. Lower charge on layers and more cations in between layers hold the muscovite structure tighter than pyrophyllite, and the result is higher hardness in muscovite.

E14.13 The silicate sheets are represented on Figures 14.17 and 14.18. An edge view of these sheets is sketched below where every tetrahedron represents one SiO_4 unit. There is a rather extensive substitution of Si^{4+} with Al^{3+} (every second Si^{4+} has been substituted with Al^{3+}, as can be seen from the mineral formula) in these sheets. Note that two tetrahedral AlSi sheets are oriented with respect to each other, in such a way that unshared oxygen atoms on each

sheet are facing each other. It is within this space between the sheets that octahedral holes are formed—they are defined by six unshared oxygen atoms, three from the top and three from the bottom SiAl-sheet. The rest of Al^{3+} cations (those that are not substituted for Si^{4+}) occupy these holes. Ca^{2+} cations are, however, too large for the octahedral holes, and it is more likely that they will be found in larger holes with coordination number 12.

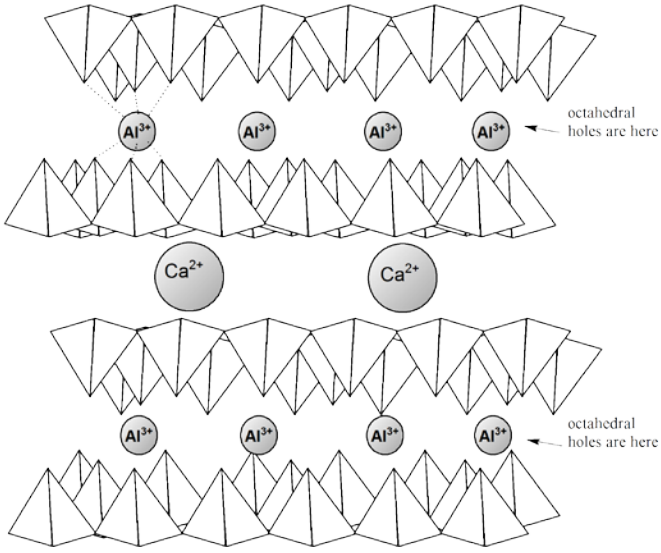

Chapter 15 The Group 15 Elements

Self-Tests

S15.1 The combustion reaction is:

$$P_4 + 5O_2 \rightarrow P_4O_{10}.$$

P_4 molecule is tetrahedral (structure **1** in your textbook) with four P–P single bonds. Structure **6** in the textbook shows one molecule of P_4O_{10}: this molecule has four P=O double bonds and 10 P–O single bonds. This gives us the summary of bonds broken and bonds formed: four P–P single bonds and five O=O double bonds have to be broken and four P=O double bonds and 10 P–O single bonds have to be formed:

$\Delta_f H = 4\times B(\text{P–P}) + 5\times B(\text{O=O}) - 4\times B(\text{P=O}) - 10\times B(\text{P–O})$

$= 4\times 201 \text{ kJ mol}^{-1} + 5\times 497 \text{ kJ mol}^{-1} - 4\times 560 \text{ kJ mol}^{-1} - 10\times 407 \text{ kJ mol}^{-1}$

$= -3021 \text{ kJ mol}^{-1}$.

This very negative value shows how stable P_4O_{10} is and why P_4 spontaneously bursts in flames when exposed to air. The actual value for $\Delta_f H(P_4O_{10})$ is -2986 kJ mol^{-1}, very close to our calculated one. The discrepancy lies in the sublimation enthalpies of P_4 and P_4O_{10}—under standard conditions both are solids. P_4 has to be converted into gas phase before P–P bonds can be broken, and this process requires energy. The product is converted from the gas phase into solid and the sublimation enthalpy is released.

S15.2 **a)** N_2O is linear molecule because it is resonance stabilized:

b) NO_2^- anion has a bent geometry (with trigonal planar electron geometry):

S15.3 **a)** Yes, the structure is consistent with the VSEPR model. Considering the three nearest neighbours only, the structure around each Bi atom is trigonal pyramidal, like NH_3. VSEPR theory predicts this geometry for an atom that has a Lewis structure with three bonding pairs and a lone pair. A side view of the structure of bismuth is shown below.

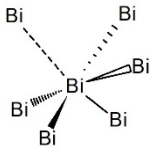

b) Two nitrogen atoms in N_2 molecule have 10 valence electrons (each contributing five electrons). If we make only one bond between N atoms, then we have a sextet around each N atom (as shown in Figure S15.3(A)). Making the double bond gives each N atom an additional electron pair and a septed at each N (Figure S15.3(B)). Only if we make a triple bond between two N atoms (Figure S15.3(C)) each nitrogen can achieve octet giving also a final Lewis structure for N_2.

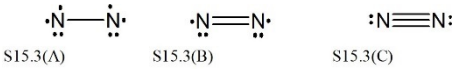

S15.3(A) S15.3(B) S15.3(C)

Nitrogen is a gas under standard contitions as can be expected from the final structure: non-polar, low-molocular weight molecule. It is also diamagnetic as can be expected from the fact that all electrons are paired with an octet. N_2 could also react as a Lewis base: each N atom still has a lone electron pair, but it is likely to be a weak one due to the fact that N atoms have high electronegativity and the electrons have low energy. N_2 is also a very unreactive gas as can be expected from a triple bond between its atoms.

S15.4 **a)** As we descend the Group 15, the element–hydrogen bonds become weaker. This is also the trend in basicity decrease: weak element–hydrogen bonds make the formation of fourth unlikely particularly if proton has to be transferred from a weak acid. For example, H_2O can protonate ammonia but stronger acids (such as HCl are required to protonate PH_3 and AsH_3. Formation of the fourth As–H bond (to make AsH_4^-) is not sufficient driving force to allow for heterolytical cleavage of H–O bond in H_2O.

b) We have to estimate the enthalpies of formation for NF3 and NCl3 based on the following equations:

$$N_2(g) + 3F_2(g) \rightarrow 2NF_3$$

$$N_2(g) + 3Cl_2(g) \rightarrow 2NCl_3.$$

The estimate can be made following our established route: looking at the change in bond enthalpies before and after the reaction (if you need more details, see Self-test 15.1). From Table 2.8 the relevant bond enthalpies are:

$B(N{\equiv}N) = 946 \text{ kJ mol}^{-1}$,

$B(F–F) = 155 \text{ kJ mol}^{-1}$,

$B(Cl–Cl) = 242 \text{ kJ mol}^{-1}$,

$B(N–F) = 270 \text{ kJ mol}^{-1}$ and

$B(N–Cl) = 200 \text{ kJ mol}^{-1}$.

First, we consider the formation of NF_3 and its $\Delta_f H$:

$$\Delta_f H(NF_3) = B(N{\equiv}N) + 3{\times}B(F–F) - 6{\times}B(N–F)$$

$$\Delta_f H(NF_3) = 946 \text{ kJ mol}^{-1} + 3{\times}155 \text{ kJ mol}^{-1} - 6{\times}270 \text{ kJ mol}^{-1}$$

$$\Delta_f H(NF_3) = -209 \text{ kJ mol}^{-1}.$$

Now we consider the formation of NCl_3 and its $\Delta_f H$:

$$\Delta_f H(NCl_3) = B(N{\equiv}N) + 3{\times}B(Cl–Cl) - 6{\times}B(N–Cl)$$

$$\Delta_f H(NCl_3) = 946 \text{ kJ mol}^{-1} + 3{\times}242 \text{ kJ mol}^{-1} - 6{\times}200 \text{ kJ mol}^{-1}$$

$$\Delta_f H(NCl_3) = 472 \text{ kJ mol}^{-1}.$$

We can see that the synthesis of NF_3 from elements is a thermodynamically favourable process and this fluoride is stable, but that the synthesis of NCl_3 from elements is not thermodynamically favourable process and NCl_3 is unstable. The reasons for the instability (and reactivity) of NCl_3 is strong Cl–Cl bond (in comparison to F–F bond) and weak N–Cl bond (in comparison to N–F).

S15.5 Dimehylhydrazine ignites spontaneously; unlike H_2 and low hydrocarbons, it is not a gas and does not need to be liquified making its handling easier and more energy efficient. In comparison to hydrocarbons, it produces less CO_2.

S15.6 Sulfur is on the right-hand side of phosphorus in the same period (period 3) in the periodic table. Two trends are important for this pair: 1) moving from left to right the non-metallic character of the elements is increasing, and 2) the electronegativity values are increasing. High electronegativity and strong non-metallic character are typical of good oxidizing agents. Thus, because sulfur is on the right side, it is more non-metallic than phosphorus and has higher electronegativity, making it a better oxidizing agent than phosphorus. This becomes more qualitative if we look at the reduction potentials for phosphorus and sulfur. From the table of standard reduction potentials in Resource Section 3 you can obtain the following information:

$$P(s) + 3e^- + 3\,H^+(aq) \rightarrow PH_3(aq) \quad E^o = -0.063 \text{ V}$$

$$S(s) + 2e^- + 2\,H^+(aq) \rightarrow H_2S(aq) \quad E^o = 0.144 \text{ V}$$

Since $\Delta G = -\nu F E°$, sulphur is more readily reduced and is therefore the better oxidizing agent. This is in harmony with the higher electronegativity of sulphur ($\chi = 2.58$) than phosphorus ($\chi = 2.19$).

S15.7 **a)** Brown, gaseous NO_2 is not easily oxidized. Since it contains N in an intermediate oxidation state (+4), it is prone to disproportionation in aqueous solutions. Unlike NO_2, the colourless NO is rapidly oxidized by O_2 in air producing NO_2. N_2O is unreactive for purely kinetic reasons.
b) The reactions that are employed to synthesize hydrazine are as follows:

$$NH_3 + ClO^- + H^+ \rightarrow [H_3N{—}Cl\text{-}O]^- + H^+ \rightarrow H_2NCl + H_2O$$

$$H_2NCl + NH_3 \rightarrow H_2NNH_2 + HCl.$$

Both can be thought of as redox reactions because the formal oxidation state of the N atoms changes (from –3 to –1 in the first reaction and from –1 and –3 to –2 and –2 in the second reaction). Mechanistically, both reactions appear to involve nucleophilic attack by NH_3 (a Lewis base) on either ClO^- or NH_2Cl (acting as Lewis acids).

The reaction employed to synthesize hydroxylamine, which produces the intermediate $N(OH)(SO_3)_2$, probably involves the attack of HSO_3^- (acting as a Lewis base) on NO_2^- (acting as a Lewis acid), although, because the formal oxidation state of the N atom changes from +3 in NO_2^- to +1 in $N(OH)(SO_3)_2$, this can also be seen as a redox reaction. Whether one considers reactions such as these to be redox reactions or nucleophilic substitutions may depend on the context in which the reactions are being discussed. It is easy to see that these reactions do not involve simple electron transfer, such as in $2\ Cu^+(aq) \rightarrow Cu^0(s) + Cu^{2+}(aq)$.

S15.8 The strongly acidic OH groups are titrated by the first 30.4 cm^3 and the two terminal –OH groups are titrated by the remaining 45.6 cm^3 – 30.4 cm^3 = 15.2 cm^3. The concentrations of analyte and titrant are such that each OH group requires 15.2 cm^3 /2 =7.6 cm^3 of NaOH. There are therefore (30.4 cm^3)/(7.6 cm^3) = 4 strongly acidic OH groups per molecule. A molecule with two terminal –OH groups and four central –OH groups is a tetrapolyphosphate.

Exercises

E15.1 The answers are summarized in the table below:

	Type of element	Diatomic gas?	Achieves maximum oxidation state?	Displays inert pair effect?
N	nonmetal	yes	yes	no
P	nonmetal	no	yes	no
As	nonmetal	no	yes	no
Sb	metalloid	no	yes	no
Bi	metalloid	no	yes	yes

E15.2 The bond enthalpy of N≡N bond is very large (946 kJ mol^{-1}, Table 2.8) making N_2 molecule a preferred form for nitrogen. Any other allotrope would be based on N–N and N=N bonds, which are significantly weaker (163 kJ mol^{-1} and 946 kJ mol^{-1} respectively). This difference in bond enthalpies would make any nitrogen allotrope unstable (even explosively so).
P–P single bond is stable enough (bond enthalpy 201 kJ mol^{-1}) to allow for many different combinations and phosphorus exists in several allotropes.

E15.3 **a) High-purity phosphoric acid.** The starting point is hydroxyapatite, $Ca_5(PO_4)_3OH$, which is converted to crude $Ca_3(PO_4)_2$. This compound is treated with carbon to reduce phosphorus from P(V) in PO_4^{3-} to P(0) in P_4 and with silica, SiO_2, to keep the calcium-containing products molten for easy removal from the furnace. The impure P_4 is purified by sublimation and then oxidized with O_2 to form P_4O_{10}, which is hydrated to form pure H_3PO_4.

$$2Ca_3(PO_4)_2 + 10C + 6SiO_2 \rightarrow P_4 + 10CO + 6CaSiO_3$$

$$P_4\ (pure) + 5O_2 \rightarrow P_4O_{10}$$

$$P_4O_{10} + 6H_2O \rightarrow 4H_3PO_4\ (pure)$$

b) Fertilizer-grade H_3PO_4. In this case, hydroxyapatite is treated with sulfuric acid, producing phosphoric acid that contains small amounts of impurities.

$$Ca_5(PO_4)_3OH + 5H_2SO_4 \rightarrow 3H_3PO_4(impure) + 5CaSO_4 + H_2O$$

c) Account for the difference in cost. The synthesis of fertilizer-grade (i.e., impure) phosphoric acid involves a single step and gives a product that requires little or no purification for further use. In contrast, the synthesis of pure phosphoric acid involves several synthetic steps and a time-consuming and expensive purification step, the sublimation of white phosphorus, P_4.

E15.4 NH_4NO_3 in water dissociates to give ammonium cation and nitrate anion:

$$NH_4NO_3(s) + H_2O(l) \rightarrow NH_4^+(aq) + NO_3^-(aq).$$

The ammonium ion is the conjugate acid of the weak base, ammonia, and hence expected to be moderately acidic (relative to water). Accordingly, the equation below explains the observed acidity of ammonium ions.

$$NH_4^+(aq) + H_2O(l) \rightarrow NH_3(aq) + H_3O^+(aq)$$

Note that NO_3^- is the conjugate base of the strong acid HNO_3 and therefore itself is an extremely weak base.

E15.5 Inductive effects of very electronegative fluorine atoms make the lone pair on nitrogen atom unavailable for bonding: partial positive charge on N atom, $N^{\delta+}$–$F^{\delta-}$, stabilizes the lone pair. PF_3 has also stabilized lone pair on P atom but larger size of phosphorus atom is better at reducing charge density and making this lone pair somewhat more available. However, more important for the formation of the metal complexes is PF_3's ability to behave as a π acceptor. Its empty antibonding MOs are a good match for the d orbitals on metal centres in complexes. Thus, while PF_3 is a weak σ donor, it is a very good π acceptor and can form a strong bond by accepting electronic density form the metals. Similar MOs exist in NF_3 but their energy is too low for an overlap with d orbitals on the metal. Consequently, NF_3 cannot act as a ligand.

Since NF_5 does not exist, the existence of NOF_3 (another N(V)species) might be surprising. However, oxygen is very good at stabilizing high oxidation states—if you do not recall this fact from before, just look at the N(V) species covered in this chapter: they all contain NO bonds. Each bonded O atom "neutralises" two positive charges, in comparison to one for each fluorine. Thus, while it is difficult to make five F–N(V) covalent bonds (there is no enough room around N(V) for them) and have a trigonal pyramidal geometry, it is feasible to have coordination four and tetrahedral arrangement around N(V).

E15.6 The Lewis structures and molecular geometries are summarized in the table below.

a) PCl_4^+: Four bonding pairs of electrons around the central phosphorus atom, and no lone electron pairs, suggest tetrahedral molecular geometry.

b) PCl_4^-: Four bonding pairs of electrons and one lone pair of electrons around the central phosphorus atom, the molecular structure is a see-saw (trigonal bipyramidal electron pair geometry with the lone pair in the equatorial plane).

c) $AsCl_5$: Five bonding pairs of electrons around the central arsenic atom, the structure is a trigonal bipyramid (both the electron pair and molecular geometries).

d) SbF_5^{2-}: Five bonding and one lone electron pair around Sb give a tetragonal pyramidal geometry.

e) SbF_6^-: Six bonding pairs around Sb result in an octahedral geometry.

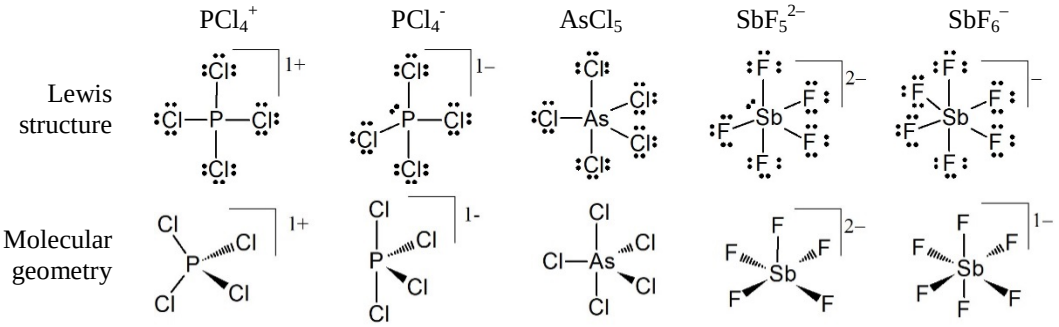

E15.7 **a) Oxidation of P_4 with excess O_2.** The balanced equation is:

$$P_4 + 5O_2 \rightarrow P_4O_{10}.$$

b) Reaction of the product from part (a) with excess H_2O. The balanced equation is:

$$P_4O_{10} + 6H_2O \rightarrow 4H_3PO_4.$$

c) Reaction of the product from part (b) with solution of $CaCl_2$. The products of this reaction would be calcium phosphate and a solution of hydrochloric acid. The balanced equation is:

$$2H_3PO_4(l) + 3CaCl_2(aq) \rightarrow Ca_3(PO_4)_2(s) + 6HCl(aq).$$

E15.8 Phosphorus(V) oxide, P_4O_{10}, is formed by the complete combustion of white phosphorus:

$$P_4(s) + 5O_2(g) \rightarrow P_4O_{10}(s).$$

where P_4 is white phosphorus. As discussed in Section 15.1, white phosphorus (P_4) is adopted as the reference phase for thermodynamic calculations although it is not the most stable phase of elemental phosphorus – in this sense using P_4 as a reference state differs from the usual practice.

E15.9 The rates of reactions in which nitrite ion is reduced (i.e., in which it acts as an oxidizing agent) are increased as the pH is lowered. That is, acid enhances the rate of oxidations by NO_2^-. The reason is that NO_2^- is converted to the nitrosonium ion, NO^+, in strong acid:

$$HNO_2(aq) + H^+(aq) \rightarrow NO^+(aq) + H_2O(l).$$

This cationic Lewis acid can form complexes with the Lewis bases undergoing oxidation (species that can be oxidized are frequently electron rich and hence are Lewis bases). Therefore, at low pH the oxidant (NO^+) is a different chemical species than at higher pH (NO_2^-) (see Section 15.13(b) *Nitrogen(IV) and nitrogen(III) oxides and oxoanions*).

E15.10 The problem provides us with $\Delta_r G = -26.5$ kJ mol^{-1} for the following reaction:

$$\tfrac{1}{2}\, N_2(g) + 3/2H_2(g) \rightarrow NH_3(aq).$$

This is a redox reaction, which can be broken into two half-reactions:

Reduction half-reaction: $\tfrac{1}{2}\, N_2(g) + 3e^- + 3H^+ \rightarrow NH_3(aq)$ $E_{red} = ?$

Oxidation half-reaction: $3/2\ H_2 \rightarrow H^+(aq) + 3e^-$ $E_{ox} = -0.059\text{V}\times\text{pH}$

We are looking for the standard reduction potential in basic aqueous solution, so the potential of standard hydrogen electrode has to be modified for the pH of the solution (pH = 14).

From the thermodynamic data, we can calculate the potential of the overall reaction from $\Delta_r G = \nu F E°$:

$$E^o = -\frac{\Delta_f G}{\nu F} = -\frac{-26.5\,\text{kJ mol}^{-1}}{3\times 96.48\,\text{kC mol}^{-1}} = +0.09\,\text{V}.$$

At pH = 14 the potential of H^+/H_2 electrode is:

$$E_{ox} = -0.059\text{V} \times 14 = -0.826\ \text{V}.$$

Finally, the unknown potential is:

$$E = +0.09\text{V} = E_{red} - (-0.826\text{V})$$

$$E_{red} = -0.736\text{V}.$$

E15.11 In both PF_3 and POF_3 there is only one P environment and we can expect only one signal in ^{31}P NMR. For both compounds this signal is going to appear as a quartet because in each case P atom is bonded to three F atoms with $I = \tfrac{1}{2}$. Thus, splitting pattern will not be helpful. In POF_3, however, P atom is in higher oxidation state (+5) and is bonded to one more electronegative atom (oxygen) in comparison to PF_3 (P oxidation state +3). Therefore, P atom in POF_3 is more deshielded and its resonance will appear downfield in comparison to the P resonance in PF_3.

E15.12 In P_4 structure, each P atom contributes three valence electrons to the skeletal valence electron count. Since there are four P atoms, there are 12 valence skeletal electrons or six skeletal electron pairs. So P_4 would be n + 2 cluster (n = 4) making the structure *nido* type. Formally, its structure then should be derived from a trigonal bipyramid. This is indeed a reasonable solution because removal of one vertex from a trigonal bipyramid leaves a tetrahedral structure.

E15.13 The two possible isomers of $[AsF_4Cl_2]^-$ are shown below. The chlorines are adjacent in the *cis* form and are opposite in the *trans* form, leading to two fluorine environments in the *cis* form and one in the *trans*. The *cis* isomer gives two ^{19}F signals (both will appear as doublets) and the *trans* isomer gives one signal (a singlet).

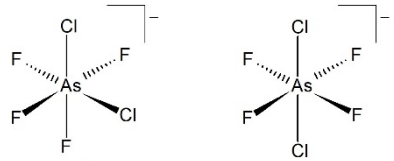

cis-$[AsF_4Cl_2]^-$ *trans*-$[AsF_4Cl_2]^-$

E15.14 Recall that if the potential to the right is more positive than the potential to the left, the species is thermodynamically unstable and likely to disproportionate. However, no kinetic information (i.e., how fast a species would disproportionate) can be deduced. The species of N and P that disproportionate are N_2O_4, NO, N_2O, NH_3OH^+, $H_4P_2O_6$, and P.

Chapter 16 The Group 16 Elements

Self-Tests

S16.1 The principles of molecular orbital theory are described in *Molecular Orbital Theory* part of Chapter 2, in sections 2.8 *Homonuclear diatomic molecules* and 2.10 *Bond Properties*.

Considering that oxygen and sulfur are in the same group of the periodic table of the elements, it might be tempting to take the molecular orbitals for dioxygen (O_2) and apply it to S_2. Since S is below oxygen, the energy difference between 3s and 3p orbitals is much smaller than the energy difference between 2s and 2p orbitals in O. Consequently, the order of molecular orbitals in S_2 would be closer to that in C_2 (see Figure 2.17). Another difference is the number of shells in S atom vs. in O atom: three and two respectively. This means we have to have one more set of σ and π molecular orbitals in S_2 molecule (and by extension S_2^{2-} anion. Summing this up, we have the following molecular orbitals for S_2 molecule/S_2^{2-} dianion:

$$1\sigma_g 1\sigma_u 2\sigma_g 2\sigma_u\ 1\pi_u 3\sigma_g 1\pi_g 3\sigma_u 4\sigma_g 4\sigma_u 2\pi_u 5\sigma_g 2\pi_u 5\sigma_g.$$

We have to ill these orbitals with 34 electrons (16 from each S atom and two additional for minus two charge) keeping in mind that s molecular orbitals are singly degenerate and take two electrons while p molecular orbitals are doubly degenerate and can accommodate up to four electrons:

$$1\sigma_g^{\ 2} 1\sigma_u^{\ 2} 2\sigma_g^{\ 2} 2\sigma_u^{\ 2} 1\pi_u^{\ 4} 3\sigma_g^{\ 2} 1\pi_g^{\ 4} 3\sigma_u^{\ 2} 4\sigma_g^{\ 2} 4\sigma_u^{\ 2} 2\pi_u^{\ 4} 5\sigma_g^{\ 2} 2\pi_g^{\ 4} 5\sigma_g^{\ 0}.$$

The bond order can be calculated as half of the difference between the number of electrons in bonding and electrons in antibonding molecular orbitals. Also recall that s_g and p_u are bonding while s_u and p_g are antibonding orbitals:

$$b = 1/2\ (2\text{-}2\text{+}2\text{-}2\text{+}4\text{+}2\text{-}4\text{-}2\text{+}2\text{-}2\text{+}4\text{+}2\text{-}4) = 1.$$

The bond order between two sulfur atoms in S_2^{2-} is one.

S16.2 In order to behave as a catalyst, Br^- must react with H_2O_2 (reaction 1, below) and then be regenerated (reaction 2):

1) $2Br^-(aq) + H_2O_2(aq) + 2H^+(aq) \rightarrow Br_2 + 2H_2O(l)$;

2) $Br_2(aq) + H_2O_2(aq) \rightarrow 2Br^-(aq) + O_2\ (g) + 2H^+(aq)$.

The net reaction is simply the decomposition of H_2O_2:

3) $2H_2O_2 \rightarrow O_2(g) + 2H_2O(l)$.

The first reaction is the difference between the half-reactions:

$H_2O_2(aq) + 2H^+(aq) + 2e^- \rightarrow 2H_2O(l)$ $\qquad E^o = +1.77$ V

$Br_2 + 2\ e^- \rightarrow 2\ Br^-$ $\qquad E^o = +1.06$ V.

And therefore $E^o_{cell} = +\ 0.71$ V. This reaction is spontaneous because $E_{cell} > 0$.

The second reaction is the difference between the half-reactions:

$Br_2 + 2e^- \rightarrow 2Br^-$ $\qquad E^o = +1.06$ V

$O_2(g) + 2\ H^+ + 2e^- \rightarrow H_2O_2$ $\qquad E^o = +0.70$ V.

And therefore $E^o_{cell} = +0.36$ V. This reaction is also spontaneous.

Because both reactions are spontaneous, the decomposition of H_2O_2 is thermodynamically favoured in the presence of Br^-.

Similar analysis applies to Cl^-. Starting from the analogous reactions 1) and 2) we have:

1) $2Cl^-(aq) + H_2O_2(aq) + 2H^+(aq) \rightarrow Cl_2 + 2H_2O(l)$;

2) $Cl_2\ (aq) + H_2O_2\ (aq) \rightarrow 2Cl^-(aq) + O_2(g) + 2H^+(aq)$.

The net reaction is again simply the decomposition of H_2O_2:

3) $2H_2O_2 \rightarrow O_2(g) + 2H_2O\ (l)$

The first reaction is the difference between the half-reactions

$H_2O_2\ (aq) + 2H^+(aq) + 2e^- \rightarrow 2\ H_2O\ (l)$ $\quad E^o = +1.77$ V

$Cl_2 + 2e^- \rightarrow 2Cl^-$ $\quad E^o = +1.36$ V.

And therefore $E^o_{cell} = +\ 0.41$ V. This reaction is spontaneous.

The second reaction is the difference between the half-reactions

$Cl_2 + 2e^- \rightarrow 2Cl^-$ $\quad E^o = +1.36$ V

$O_2\,(g) + 2H^+ + 2e^- \rightarrow H_2O_2$ $\quad E^o = +0.70$ V.

And therefore $E^o_{cell} = +\ 0.66$ V. This reaction is spontaneous.

Because both reactions are spontaneous, the decomposition of H_2O_2 is thermodynamically favoured in presence of Cl^-.

S16.3 The Lewis structure of gaseous SO_3 is shown below. Note that SO_3 is a hybrid structure of three resonance structures. The SO_3 molecule is planar and belongs to the D_{3h} point group.

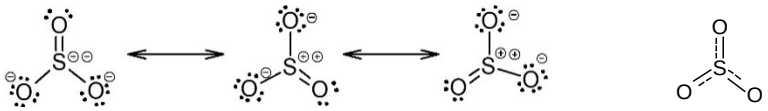

The Lewis structure of SO_3F^- anion is shown below. The molecular geometry is tetrahedral, but the point group is C_{3v}.

S16.4 It is reasonable to make the same assumption as in the Example: each S and N have a lone electron pair and form two bonds in the cyclic S_4N_4 molecule. That leaves four S atoms each still carrying an electron pair available for π bonding. This gives eight electrons from S atoms that could contribute to the π bonding. Four N atoms have one electron each, thus N atoms combined contribute four electrons. In total, there are 8 + 4 = 12 electrons in the system that could be used for π bonding. Consequently, S_4N_4 is aromatic because the $2n + 2$ rule is satisfied for $n = 5$: $2\times5 + 2 = 12$.

Exercises

E16.1 Remember that in general (with some exceptions) the oxides of non-metals are acidic and of metals are basic. Thus, CO_2, SO_3, and P_2O_5, are acidic, Al_2O_3 can react with either acids or bases, so it is considered amphoteric (an exception). CO is neutral (again an exception); and MgO and K_2O are basic. Review Section 5.4 if you had problems with this exercise.

E16.2 **a) The disproportionation of H_2O_2.** To calculate the standard potential for a disproportionation reaction, you must sum the potentials for the oxidation and reduction of the species in question. For hydrogen peroxide in acid solution, the oxidation and reduction are:

$H_2O_2(aq) \rightarrow O_2(g) + 2e^- + 2H^+(aq)$ $\quad E° = -0.695$ V

$H_2O_2(aq) + 2\ e^- + 2H^+(aq) \rightarrow 2H_2O(l)$ $\quad E° = +1.763$ V.

Therefore, the standard potential for the net reaction 2 $H_2O_2(aq) \rightarrow O_2(g) + 2H_2O(1)$ is (–0.695 V) + (+1.763 V) = +1.068 V.

b) Catalysis by Cr^{2+}. Cr^{2+} can act as a catalyst for the decomposition of hydrogen peroxide if the Cr^{3+}/Cr^{2+} reduction potential falls between the values for the reduction of O_2 to H_2O_2 (+0.695 V) and the reduction of H_2O_2 to H_2O (+1.76 V). Reference to Resource Section 3 reveals that the Cr^{3+}/Cr^{2+} reduction potential is –0.424 V, so Cr^{2+} is *not* capable of decomposing H_2O_2. See also Example and Self-Test 16.1.

c) The disproportionation of HO_2. The oxidation and reduction of superoxide ion (O_2^-) in acid solution are:

$$HO_2(aq) \rightarrow O_2(g) + e^- + H^+(aq) \qquad E° = +0.125 \text{ V}$$

$$HO_2(aq) + e^- + H^+(aq) \rightarrow H_2O_2(aq) \qquad E° = +1.51 \text{ V}$$

Therefore, the standard potential for the net reaction 2 $HO_2(aq) \rightarrow O_2(g) + H_2O_2(aq)$ is (+0.125 V) + (+1.51 V) = +1.63 V. $\Delta_r G° = -\nu F E_{cell} = -1 \times 96500 \text{ C mol}^{-1} \times 1.63\text{V} = 157 \text{ kJ mol}^{-1}$. Similarly, we can obtain the Gibbs energy for the disproportionation of H_2O_2 (part **(a)**), $\Delta_r G° = 103 \text{ kJ mol}^{-1}$.

E16.3 Hydrogen bonds are stronger in molecules where hydrogen is bonded directly to a highly electronegative atom such as O, N, or F. Since S has smaller electronegativity compared to oxygen, we expect O–H···S hydrogen bonds to be stronger.

E16.4 Anionic species such as S_4^{2-} and Te_3^{2-} are intrinsically basic species that cannot be studied in solvents that are Lewis acids because complex formation (the Lewis acid–base pair) will destroy the independent identity of the anion. Since the basic solvent ethylenediamine will not react with Na_2S_4 or with K_2Te_3, it is a better solvent choice than sulfur dioxide.

E16.5 The reduction potential of sulfite ions in basic solution = –0.576 V. Using the data in Resource Section 2 in your textbook for Mn we can construct the following table:

Oxidation states of Mn	Standard reduction potential of Mn couples	$E^o_{cell} = E^o_{red} - E^o_{ox}$
7	+7 to +6 = +0.56 V	+ 1.136 V
6	+6 to +5 = +0.27 V	+ 0.847 V
5	+5 to +4 = +0.93 V	+ 1.506 V
4	+4 to +3 = +0.15 V	+ 0.726 V
3	+3 to +2 = –0.25 V	+ 0.326 V
2	+2 to 0 = –1.56 V	–0.984 V

From the table we can see that except the +2 oxidation state of Mn, all other oxidation states of Mn will be reduced by sulfite ions in basic solution because in each case we can obtain $E_{cell} > 0$, indicating spontaneous reaction.

E16.6 If the potential to the right is more positive than the potential to the left, the species is unstable and likely to disproportionate. $S_2O_6^{2-}$and $S_2O_3^{2-}$are unstable with respect to disproportionation.

E16.7 The half-potentials for the reduction of VO^{2+}, Fe^{3+}, and Co^{3+} are +1.00V, +0.771V, and +1.92 V, respectively. All will be reduced as their potentials are greater than the potential of thiosulfate.

E16.8 SF_3^+ has a trigonal pyramidal molecular geometry with tetrahedral electron pair geometry, BF_4^- tetrahedral (both molecular and electron pair geometry).

E16.9 The Frost diagram reveals that the stability of the lowest oxidation state is decreasing descending the group. Oxygen is very stable in oxidation state 2- and species containing oxygen in this state will be prevalent. Looking at

the diagram overall, the same can be said for the other Group 16 elements: negative two oxidation state is the lowest on the diagram (besides the elemental form for all) and sulphides, selenides and tellurides should be the most stable compounds of these elements. Descending the group (starting with S already) positive oxidation states are accessible. All have good oxidizing properties. In the case of tellurium +4 and -2 have about the same stability. This is a consequence of the increased stability of higher oxidation states as we descend a group.

E16.10

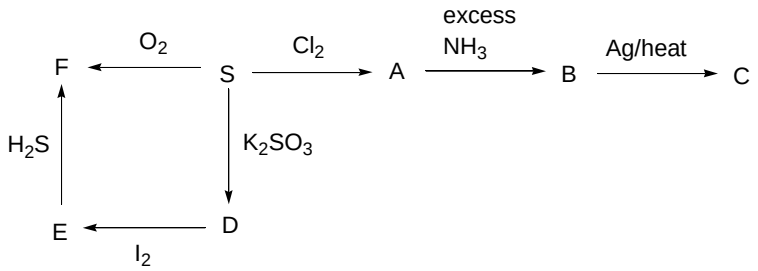

A = S_2Cl_2, **B** = S_4N_4, **C** = S_2N_2, **D** = $K_2S_2O_3$, **E** = $S_2O_6^{2-}$, **F** = SO_2

Note: Sulfur reacts with Cl_2 to produce both S_2Cl_2 and SCl_2. However, of the two possible chlorides, only S_2Cl_2 can be taken in further reactions with NH_3 (to give S_4N_4) and Ag (to produce S_2N_2 from S_4N_4). Thus, the acceptable product **A** is S_2Cl_2.

E16.11 Sulfuric and selenic acids are rather similar. When pure, both are hygroscopic, very viscous liquids. Both form crystalline hydrates. Sulfuric and selenic acids react with their anhydrides, SO_3 and SeO_3, to produce trisulfuric and triselenic acids respectively. Much like sulfuric acid, selenic acid is a strong acid in the first dissociation step, and the acids have the same order of magnitude for Ka_2 ($\sim 10^{-2}$). Both produce two types of salts: hydrogensulfates/sulfates and hydrogenselentates/selenates. The salts also have similar solubilities. The most important difference between the two acids is their oxidizing power: H_2SeO_4 is a very strong oxidizing agent capable even of oxidizing gold and palladium.

Telluric acid is remarkably different from sulfuric and selenic acid. When pure, it is a solid composed of discrete $Te(OH)_6$ octahedra. This structure is retained in the solution as well. As it can be expected, it forms more than two types of salts: $H_5TeO_6^-$, $H_4TeO_6^{2-}$, $H_2TeO_4^{4-}$, and TeO_6^{6-}. It is a weak acid even in the first dissociation step. At elevated temperatures it loses water molecules to produce various polytelluric acids. What is similar to sulfuric and selenic acid is that $Te(OH)_6$ can produce well-defined, crystalline hydrates. Telluric acid is a weaker oxidizing agent than selenic acid in both acidic and alkaline medium, but is a stronger oxidant than sulfuric acid in either medium.

Chapter 17 The Group 17 Elements

Self-Tests

S17.1 A quick glance at the Latimer diagram for chlorine in acidic solution (Resource Section 3) shows that $HClO_2$ can disproportionate to ClO_3^- and HClO:

$$2HClO_2(aq) \rightarrow ClO_3^-(aq) + HClO(aq).$$

S17.2 The anion Cl_3^- has 2 valence electrons to account for: 3×7 = 21 for Cl atoms and one more for the negative charge. This anion, thus, as a trigonal bipyramidal electron geometry but the shape is linear:

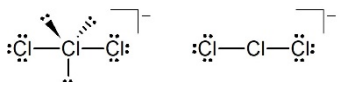

S17.3 Since the IO_3^-/I_2 standard reduction potential is +1.19 V (see Resource Section 3), many species can be used as reducing agents, including $SO_2(aq)$ and $Sn^{2+}(aq)$: the HSO_4^-/H_2SO_3 and Sn^{4+}/Sn^{2+} reduction potentials are +0.158 V and +0.15 V, respectively. The balanced equations would be as follows:

$$2IO_3^- + 5H_2SO_3 \rightarrow I_2 + 5HSO_4^- + H_2O + 3H^+$$

$$2IO_3^- + 5Sn^{2+} + 12H^+ \rightarrow I_2 + 5Sn^{4+} + 6H_2O.$$

The reduction of iodate with aqueous sulfur dioxide would be far cheaper than reduction with Sn^{2+} because sulfur dioxide costs less than tin. One reason this is so is because sulfuric acid, for which SO_2 is an intermediate, is prepared worldwide on an enormous scale.

S17.4 The ordering of molecular orbitals in F_2 is the same as in Cl_2. The difluorine molecule has 14 valence electrons and the following electronic configuration:

$$1\sigma_g^{\,2}1\sigma_u^{\,2}2\sigma_g^{\,2}1\pi_u^{\,4}1\pi_g^{\,4}.$$

The bond order is:

$$b = ½\,(8\text{-}6) = 1.$$

And just like in Cl_2 molecule from the Example 17.4, F–F is a single bond.

The anion F_2^- has one more valence electron—15 in total—and the electronic configuration would be:

$$1\sigma_g^{\,2}1\sigma_u^{\,2}2\sigma_g^{\,2}1\pi_u^{\,4}1\pi_g^{\,4}2\sigma_u^{\,1}.$$

The bond order is:

$$b = ½\,(8\text{-}7) = 0.5.$$

Since F_2^- has a lower bond order than F_2, the F–F bond is longer in the anion, F_2^-.

S17.5 Iodine is the central atom in the molecule. Seven valence electrons form bonds with seven fluorine atoms, giving a total of seven bonding electron pairs, and structure is pentagonal bipyramid.

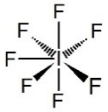

The ^{19}F-NMR spectrum of IF_7 contains two resonances. One is sextet for two axial F atoms (coupled to five equatorial F atoms), and another one is a triplet due to the five equatorial F atoms (coupled to two axial F atoms). The intensity ratios of the two resonances is 1:5.

S17.6 The reaction is:

$$ClF_3 + SbF_5 \rightarrow [ClF_2][SbF_6].$$

The shape of the reactants:

ClF_3: This is an XY_3 interhalogen. The central Cl atom is surrounded by five electron pairs: two are lone electron pairs and three are boding pairs resulting in a trigonal bipyramidal electron geometry and a distorted T-shaped molecular geometry.

SbF_5: There are five electron pairs around the central atom, Sb, all of which are bonding pairs resulting in a trigonal bipyramidal geometry.

The shape of the products:

$[ClF_2]^+$: After the removal of one F^- during the reaction, the central Cl atom is now surrounded by four electron pairs: two bonding and two lone electron pairs. This results in a tetrahedral electron group geometry and a bent molecular shape.

$[SbF_6]^-$: After bonding to one F^- the central Sb now has six electron pairs around it, all of which are bonding. This results in an octahedral molecular shape.

The structures of all four are shown below:

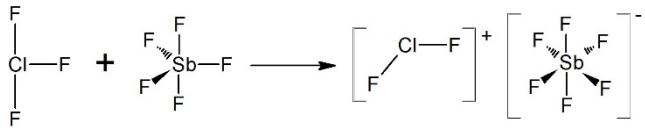

S17.7 Examples include I_3^-, IBr_2^-, ICl_2^-, and IF_2^-. One way of describing the bonding in these species is based on Lewis acids and bases. In all cases, consider that the central I^+ species has a vacant orbital (and is a Lewis acid) that interacts with two electron pair donors (Lewis bases): pyridine (C_5H_5N) in the case of $[py–I–py]^+$ or I^- in the case of I_3^-.

In terms of VSEPR and molecular orbital theories, the same analysis applies as in Exercise 17.7 The listed species have 10 valence electrons at central I+. This results in trigonal bipyramidal electron geometry with linear shapes for the complexes. The four electrons in two bonds are also placed in two molecular orbitals, one bonding, and one nonbonding. The antibonding orbital remains empty.

S17.8 **a)** Bromine species that will disproportionate in a basic solution are Br_2 and BrO^-:

$$Br_2 + 2OH^- \rightarrow Br^- + BrO^- + H_2O$$

$$BrO^- + 2OH^- \rightarrow Br^- + BrO_3^- + H_2O$$

Note that the disproportionation of Br_2 is likely going to produce Br^- and BrO_3^- because BrO^-, the initial product, is also prone to disproportionation.

b) Iodine species that will disproportionate in a basic solution are: I_2 and IO^-:

$$I_2 + 2OH^- \rightarrow I^- + IO^- + H_2O$$

$$IO^- + 2OH^- \rightarrow I^- + IO_3^- + H_2O$$

with the similar note pertaining to the I_2 disproportionation product as in **(a)** for bromine above.

Exercises

E17.1 The table summarizes the facts:

		Physical state	Electronegativity	Hardness of halide ion	Colour
Fluorine	F_2	gas	highest (4.0)	hardest	light yellow
Chlorine	Cl_2	gas	lower	softer	yellow-green
Bromine	Br_2	liquid	lower	softer	dark red-brown
Iodine	I_2	solid	lowest	softest	dark violet

E17.2 Follow the procedure described in Exercise 17.4 and its accompanying Self-Test. The Br_2 molecule has 14 valence electrons (just like Cl_2 and F_2) and the following simplified electronic configuration:

$$1\sigma_g^{\,2}1\sigma_u^{\,2}2\sigma_g^{\,2}1\pi_u^{\,4}1\pi_g^{\,4}.$$

This gives bond order 1 and a single Br–Br bond.

Br_2^+ has one valence electron less (13 in total) and the following simplified electronic configuration:

$$1\sigma_g^{\,2}1\sigma_u^{\,2}2\sigma_g^{\,2}1\pi_u^{\,4}1\pi_g^{\,3}.$$

This electronic configuration results in bond order 1.5. Since the cation has a higher bond order, Br–Br bond in Br_2^+ is shorter than in Br_2.

E17.3 According to Figure 17.5, the vacant anti-bonding orbital of a halogen molecule is $2\sigma_u^*$ and is composed primarily of halogen atomic p orbitals; recall that the *n*s–*n*p gap is larger toward the right-hand side of the periodic table, and the larger the gap, the smaller the amount of s–p mixing. A sketch of the empty $2\sigma_u^*$ anti-bonding orbital is shown below:

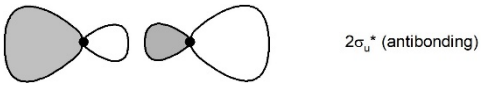

Since the $2\sigma_u^*$ anti-bonding orbital is empty (hence it is LUMO for an X_2 molecule), it is the orbital that accepts the pair of electrons from a Lewis base B when a dative $B:\rightarrow X_2$ bond is formed. From the shape of the LUMO, we can conclude that the B–X–X unit should be linear.

E17.4 **a) The difference in volatility.** Ammonia is one of many substances that exhibit very strong hydrogen bonding. The very strong $N–H^{\delta+}\cdots N^{\delta-}$ intermolecular interactions lead to a relatively large enthalpy of vaporization and a relatively high boiling point for NH_3 (–33°C). In contrast, the intermolecular forces in liquid NF_3 are relatively weak dipole–dipole forces. In comparison to hydrogen bonding, dipole-dipole forces require less energy to be broken, resulting in a smaller enthalpy of vaporization and a low boiling point (–129°C) for NF_3.

b) Explain the difference in basicity. The strong electron-withdrawing effect of the three fluorine atoms in NF_3 lowers the energy of the nitrogen atom lone pair. This lowering of energy has the effect of reducing the electron-donating ability of the nitrogen atom in NF_3, reducing the basicity.

E17.5 **a)**

$$\underset{(1.84\text{ g, }10\text{ mmol})}{IF_3} + \underset{(0.93\text{ g, }10\text{ mmol})}{[(CH_3)_4N]F} \longrightarrow {}_{[}N(CH_3)_4][IF_4] \quad (10\text{ mmol})$$

Note that IF_3 and $[(CH_3)_4N]F$ react in 1 : 1 ratio and that only one product X is formed; therefore the product X is $[N(CH_3)_4][IF_4]$.

b) A reliable way to predict the structure of IF_3 is to draw its Lewis structure and then apply VSEPR theory. In the Lewis structure for IF_3, iodine is the central atom. Three bonding pairs and two lone pairs on the iodine yield trigonal bipyramidal electron geometry and T-shaped molecular geometry, as shown below.

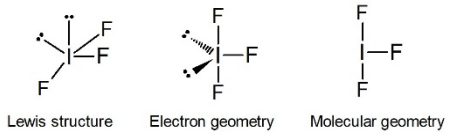

The shape of anion IF_4^- is square planar (see the structure below). The iodine atom is at the centre of the ion. Four electron pairs form bonds to F atoms, and two electron pairs do not take part in bonding.

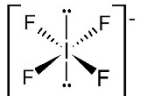

The shape of cation $(CH_3)_4N^+$ is tetrahedral. The nitrogen atom is at the centre of the cation. Nitrogen has five valence electrons. Three electrons form bonds to CH_3, plus one lone pair forms coordinate covalent bond with CH_3^+.

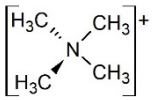

c) The ^{19}F-NMR spectrum of IF_3 contains two resonances: one doublet is for axial F atoms and another triplet is for an equatorial F atom.

The ^{19}F-NMR spectrum of IF_4^- contains one resonance, a singlet.

E17.6 $SbCl_5$ is trigonal bipyramidal, and $FClO_3$ is tetrahedral.

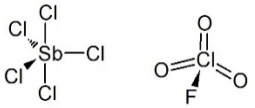

E17.7 The complex MCl_4F_2 can have two isomers: *cis* and *trans* (see below). Both isomers have one resonance in ^{19}F-NMR. MCl_3F_3 also has two isomers: *fac* and *mer*. The *fac* isomer has one resonance and the *mer* isomer has two resonances—one will appear as a doublet for two mutually *trans* F atoms coupled to the *cis* F atom, and one triplet for the *cis* F atom coupled to two mutually *trans* F atoms.

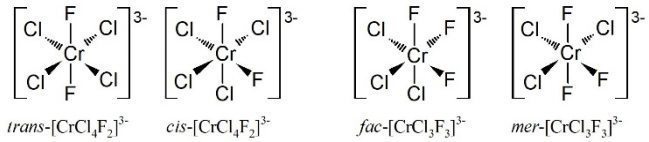

17.8 I_2Cl_6 is the dimer of ICl_3 with two Cl atoms acting as bridges. Therefore, each iodine atom contains 12 valence electrons, or four bonding pairs and two non-bonding pairs. VSEPR theory predicts that the electron geometry around each iodine atom with six pairs of electrons should be octahedral, and with four bonding and two non-bonding electron pairs, the molecular geometry should be square planar for each iodine atom. In this structure four Cl atoms occupy the corners of square plane. In the solid state, the compound is a planar dimer (I_2Cl_6) with bridging Cl atoms.

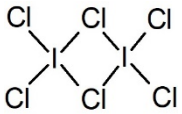

The point group of I_2Cl_6 is D_{2h}.

E17.9 The acid/base properties of liquid BrF_3 result from the following autoionization reaction:

$$2\ BrF_3 \rightarrow BrF_2^+ + BrF_4^-$$

The acidic species is the cation BrF_2^+ and the basic species is the anion BrF_4^-.

a) SbF_5? Adding the powerful Lewis acid SbF_5 will increase the concentration of BrF_2^+, thus increasing the acidity of BrF_3 by the following reaction:

$$BrF_3 + SbF_5 \rightarrow BrF_2^+ + SbF_6^-$$

b) SF_6? Adding SF_6 will have no effect on the acidity or basicity of BrF_3 because SF_6 is neither Lewis acidic nor Lewis basic.

c) CsF? Adding CsF, which contains the strong Lewis base F^-, will increase the concentration of BrF_4^-, thus increasing the basicity of BrF_3, by the following reaction:

$$BrF_3 + F^- \rightarrow BrF_4^-$$

E17.10 Iodine is the central atom in IF_5. Five unpaired electrons form bonds with five fluorine atoms, plus one lone electron, giving a total of six electron pairs. Therefore, the electronic geometry is octahedral with one position occupied by a lone pair giving a square pyramidal arrangement of atoms.

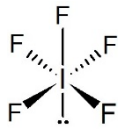

The structure of the cation IF_5^+ is similar—removal of one electron from IF_5 converts a lone electron pair into an unpaired electron. There will be less repulsion between a lone electron and bonding electron pairs in I–F bonds but the arrangement of atoms would remain square pyramidal. Thus, the ^{19}F-NMR spectrum of IF_5^+ contains two resonances—one is doublet for four basal F atoms coupled to the axial F, and another one is quintet for the axial F atom coupled to the four basal F atoms.

E17.11 Since Br_3^- is only moderately stable it is likely going to produce Br_2 and Br^- in solution. IBr is, however, fairly stable. Hence, the probable reaction will be:

$$Br_3^- + I_2 \rightarrow 2IBr + Br^-.$$

The IBr may associate to some extent with Br^- to produce IBr_2^-.

E17.12 **a) ClO_2.** The Lewis structure and the predicted shape of ClO_2 are shown below. The bent shape is a consequence of repulsions between the bonding and non-bonding electrons. With three non-bonding electrons, the O–Cl–O angle in ClO_2 is 118°. With four non-bonding electrons, as in ClO_2^-, the repulsions are greater and the O–Cl–O angle is only 111°. The point group is C_{2v}.

b) I_2O_6. The easiest way to determine this structure is to bond one more oxygen atom to any iodine atoms in the structure of I_2O_5 (structure 15 in this chapter). This derived Lewis structure and the predicted molecular geometry of I_2O_6 are shown below. The central O atom has two bonding pairs of electrons and two lone pairs, like H_2O, so it should be no surprise that the I–O–I bond angle is less than 180º. One iodine atom is trigonal pyramidal because it has three bonding pairs and one lone pair; while the other iodine atom, with four bonding pairs, is tetrahedral. The point group is C_s for the geometry shown.

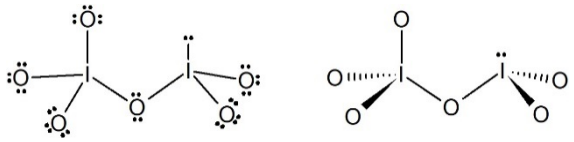

E17.13 **a) The expected trend.** Looking at Figure 17.14, we observe that *E* decreases as the pH increases.

b) *E* at pH 0 and pH 7 for ClO_4^-. The balanced equation for the reduction of ClO_4^- is:

$$ClO_4^-(aq) + 2H^+(aq) + 2e^- \rightarrow ClO_3^-(aq) + H_2O(l).$$

The value of $E°$ for this reaction at pH = 0 is +1.201 V. The potential at any $[H^+]$, given by the Nernst equation, is

$$E = E° - (0.059\ V/2)(\log([ClO_3^-]/[ClO_4^-][H^+]^2)).$$

At pH 7, $[H^+] = 10^{-7}$ M and if both perchlorate and chlorate ions are present at unit activity, the reduction potential is

$$E = +1.201\ V - (0.0295\ V)(\log 10^{14}) = +1.201\ V - 0.413\ V = 0.788\ V.$$

Thus, the potential at pH = 7 is less positive than at pH = 0 resulting in lower oxidizing power of ClO_4^- as we would predict from part (a).

E17.14 Recall from Chapter 5 that the reduction potential of a non-adjacent couple in the Latimer diagram can be calculated using the formula:

$$E^o = \frac{\nu_a \times E_a^o + \nu_b E_b^o + \ldots}{\nu_a + \nu_b \ldots}.$$

From the Frost diagram, the potential can be calculated as a slope of the line connecting the points of the two species in question. Since the reduction potential from the Latimer diagrams are easily accessible (i.e., do not require geometrical constructions), they are a better choice for calculations such as the ones in this exercise.

a) ClO_4^-/ClO^- potential. The relevant part of the Latimer diagram for chlorine is shown below. The numbers above the arrows connecting two species are the standard reduction potential (as is written per convention) for that redox couple. The numbers in the brackets represent the number of electrons received (ν in the equation above).

$$ClO_4^- \xrightarrow{+0.374V\,(\nu=2)} ClO_3^- \xrightarrow{+0.295V\,(\nu=2)} ClO_2^- \xrightarrow{+0.681V\,(\nu=2)} ClO^-$$

Substituting the values from the diagram into the equation we have:

$$E^o_{ClO_4^-/ClO^-} = \frac{2\times(+0.374V) + 2\times(+0.295V) + 2\times(+0.681V)}{2+2+2} = +0.45V.$$

The same procedure is used to calculate the potentials in (b) and (c).

b) BrO_4^-/BrO^- potential.

$$E^o_{BrO_4^-/BrO^-} = \frac{2\times(+1.025V) + 4\times(+0.492V)}{2+4} = +0.67V.$$

c) IO_4^-/IO^- potential.

$$E^o_{IO_4^-/IO^-} = \frac{2\times(+0.65V) + 4\times(+0.15V)}{2+4} = +0.317V.$$

E17.15 The key to answering this question is to decide if the perchlorate ion, which is a very strong oxidant, is present along a species that can be oxidized. If so, the compound *does* represent an explosion hazard.

a) NH_4ClO_4. Ammonium perchlorate is a dangerous compound because the N atom of the NH_4^+ ion is in its lowest oxidation state (–3) and can be oxidized.

b) $Mg(ClO_4)_2$. Since Mg^{2+} cannot be oxidized to a higher oxidation state, magnesium perchlorate is a stable compound and is not an explosion hazard.

c) $NaClO_4$. The same answer applies here as above for magnesium perchlorate. Sodium has only one common oxidation state. Even the strongest oxidants, such as F_2, FOOF, and ClF_3, cannot oxidize Na^+ to Na^{2+}.

d) $[Fe(H_2O)_6][ClO_4]_2$. Although the H_2O ligands cannot be oxidized, the metal ion can. This compound presents an explosion hazard because Fe(II) can be oxidized to Fe(III) by a strong oxidant such as perchlorate ion.

E17.16 **A** = ClF $F_2(g) + Cl_2(g) \rightarrow 2ClF(g)$

E = $CsClF_2$ $ClF + CsF \rightarrow CsClF_2$

B = OF_2 $2\ F_2(g) + 2\ OH^-(aq) \rightarrow OF_2(g) + H_2O(l) + 2\ F^-(aq)$

C = HF $F_2(g) + H_2O\ (l) \rightarrow 2\ HF(aq) + ½\ O_2(g)$

D = SiF_4 $SiO_2(s) + 2\ F_2(g) \rightarrow SiF_4(g) + O_2(g)$

G = CaF_2 $CaF_2(s) + H_2SO_4 \rightarrow 2\ HF(g) + CaSO_4(s)$

E17.17 Statement **(a)** is correct.

Statement **(b)** is incorrect—the two anions do not have identical structures.

Statement **(c)** is incorrect—it is the nucleophilicity of the Cl atom in ClO^- that is crucial for the oxidation mechanism.

Statement **(d)** is correct.

Chapter 18 The Group 18 Elements

Self-Tests

S18.1 The XeF^+ cation has 14 electrons: eight from Xe plus seven from F and minus one electron to account for a positive charge. The electronic configuration is:

$$1\sigma_g^{\,2}1\sigma_u^{\,2}2\sigma_g^{\,2}1\pi_u^{\,4}1\pi_g^{\,4}2\sigma_u^{\,0}.$$

Bond order is:

$$b = (8\text{-}6) = 1.$$

S18.2 The reaction we are looking at:

$$Xe(g) + 3F_2(g) \rightarrow XeF_6(s).$$

From the reaction, three F–F bonds have to be broken while 6 Xe–F bonds are formed:

$$\Delta_f H \approx 3\times B(\text{F–F}) - 6\times B(\text{Xe–F}) =$$
$$= 3\times 155 \text{ kJ mol}^{-1} - 6\times 144 \text{ kJ mol}^{-1} =$$
$$= -408 \text{ kJ mol}^{-1}.$$

This is only an estimate because our $\Delta_f H$ does not consider the sublimation (or lattice) enthalpy of XeF_6: $XeF_6(g) \rightarrow XeF_6(s)$.

S18.3 As the self-test states, xenate ($HXeO_4^-$) decomposes to perxenate (XeO_6^{4-}), xenon, and oxygen, so the equation that must be balanced is:

$$HXeO_4^- \rightarrow XeO_6^{4-} + Xe + O_2 \quad \text{(not balanced)}.$$

Since the reaction occurs in a basic solution, we can use OH^- and H_2O to balance the equation, if necessary. You notice immediately that there is no species containing hydrogen on the right-hand side of the equation, so H_2O should go on the right and OH^- should go on the left. The balanced equation is

$$2HXeO_4^-(aq) + 2OH^-(aq) \rightarrow XeO_6^{4-}(aq) + Xe(g) + O_2(g) + 2H_2O(l).$$

Since the products are perxenate (an Xe(VIII) species) and elemental xenon, this reaction is a disproportionation of the Xe(VI) species $HXeO_4^-$. Oxygen is produced from a thermodynamically unstable intermediate with Xe(IV), possibly as follows:

$$HXeO_3(aq) \rightarrow Xe(g) + O_2(g) + OH^-(aq)$$

Exercises

E18.1 All the original He and H_2 present in the Earth's atmosphere when our planet originally formed has been lost. Earth's gravitational field is not strong enough to hold these light gases, and they eventually diffuse away into space. The small amount of helium that is present in today's atmosphere is the product of ongoing radioactive decay.

E18.2 **a) Synthesis of XeF_2.** XeF_2 can be prepared in two different ways. First, a mixture of Xe and F_2 that contains an excess of Xe is heated to 400°C. The excess Xe prevents the formation of XeF_4 and XeF_6. The second way is to photolyze a mixture of Xe and F_2 at room temperature. For either method of synthesis, the balanced equation is:

$$Xe(g) + F_2(g) \rightarrow XeF_2(s).$$

At 400°C the product is a gas, but at room temperature it is a solid.

b) Synthesis of XeF_6. For the synthesis of this compound you would want also to use a high temperature, but unlike the synthesis of XeF_2, you want to have a *large* excess of F_2:

$$Xe(g) + 3F_2(g) \rightarrow XeF_6(s).$$

As with XeF_2, xenon hexafluoride is a solid at room temperature.

c) Synthesis of XeO_3. This compound is endergonic, so it cannot be prepared directly from the elements. However, a sample of XeF_6 can be carefully hydrolysed to form the desired product:

$$XeF_6(s) + 3H_2O(l) \rightarrow XeO_3(s) + 6HF(g).$$

If a large excess of water is used, an aqueous solution of XeO_3 is formed instead.

E18.3 The Lewis structures of $XeOF_4$, XeO_2F_2, and XeO_6^{4-} are shown below.

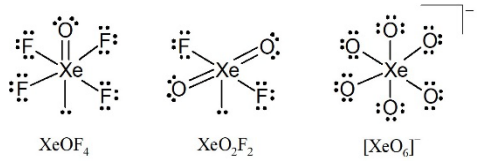

E18.4 **a)** The Lewis structure for XeF_7^- is shown below.

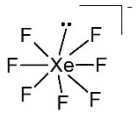

b) The structure of XeF_5^-, with seven pairs of electrons, is based on a pentagonal bipyramidal array of electron pairs with two stereochemically active lone pairs (see Structure **9**) resulting in overall pentagonal planar molecular geometry. The ion XeF_8^{2-}, on the other hand, has nine pairs of electrons, but only eight are stereochemically active (see Structure **10**) giving a square-antiprism molecular geometry. It is possible that the structure of XeF_7^-, with eight pairs, would be a pentagonal bipyramid, with one stereochemically inactive lone pair.

The real structure of this anion is capped octahedral with a very long "capping" Xe–F bond, as shown below, confirming that the lone pair is indeed stereochemically inert.

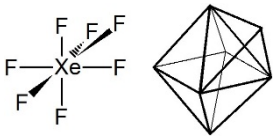

E18.5 According to molecular orbital theory, the electronic configuration of He_2^+ is $1\sigma_g^2\,1\sigma_u^1$. There are two electrons in bonding σ ($1\sigma_g$) orbital and one electron in an antibonding σ^* orbital ($1\sigma_u$), therefore the bond order is $\frac{1}{2}(2 - 1) = 0.5$.

The electronic configuration of Ne_2^+ is $1\sigma_g^2 1\sigma_u^2 2\sigma_g^2 1\pi_u^4 1\pi_g^4 2\sigma_u^1$. Recall that the bonding orbitals are $1\sigma_g$, $2\sigma_g$, $1\pi_u$, and $2\pi_u$. The bond order is therefore $\frac{1}{2}(8 - 7) = 0.5$.

E18.6

A = $XeF_2(g)$	$Xe + F_2 \rightarrow XeF_2$
B = $[XeF]^+[MeBF_3]^-$	$XeF_2(g) + MeBF_2 \rightarrow [XeF]^+[MeBF_3]^-$
C = XeF_6	$Xe + F_2$ (excess) $\rightarrow XeF_6$
D = XeO_3	$XeF_6 + H_2O \rightarrow XeO_3$
E = $XeF_4(g)$	$Xe + 2F_2 \rightarrow XeF_4(g)$

E18.7 The structure of $XeOF_3^+$ is shown below. The ^{129}Xe-NMR would consist of one resonance split into a 1:3:3:1 quartet due to the coupling to three equivalent ^{19}F nuclei.

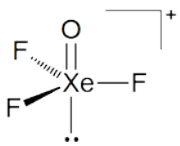

Chapter 19 The d-block Elements

Self-Tests

S19.1 The Latimer diagram for vanadium in basic solution is provided in Resource Section 3. The reduction potential for O_2/H_2O couple in alkaline solution is:

$$E = +1.229\ \text{V} - 0.059\text{V} \times \text{pH} = +\ 1.229\text{V} - 0.059\text{V} \times 14 = +0.403\text{V}$$

The reduction potential for VO/V_2O_3 couple in the basic solution is –0.486V. The potential difference for oxidation of VO to V_2O_3 with oxygen is

$$E_{\text{cell}} = +0.403\text{V} - (-0.486\text{V}) = +0.889\text{V}$$

Thus, VO will be oxidized to V_2O_3 by oxygen in air. The next oxidation step is oxidation from V_2O_3 to $HV_2O_5^-$ with reduction potential +0.542V. This reaction has the following potential difference:

$$E_{\text{cell}} = +0.403\text{V} - (+0.542\text{V}) = -0.139\text{V}$$

This step has a negative potential and is not a thermodynamically spontaneous process. This means that a basic solution oxidation of VO to V_2O_3 is a thermodynamically favourable process, and V_2O_3 is more stable than VO in presence of oxygen.

S19.2 Re_3Cl_9 is a trimer (see Structure 19). When ligands are added, such as PPh_3, discrete molecular species such as $Re_3Cl_9(PPh_3)_3$ are formed (see below). Sterically, the most favourable place for each bulky triphenylphosphine ligand to go is in the terminal position in the Re_3 plane.

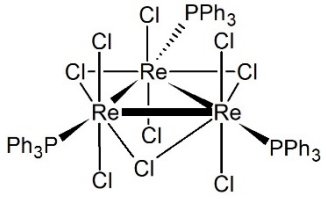

Exercises

E19.1 The table below summarizes the highest oxidation states of the first-row transition metals, gives examples of oxo species containing metals in the highest oxidation state, and contrasts them with the second- and third-row elements.

Group	**3**	**4**	**5**	**6**	**7**	**8**	**9**	**10**	**11**	**12**
1st row	Sc	Ti	V	Cr	Mn	Fe	Co	Ni	Cu	Zn
Max. OS	3	4	5	6	7	6	4	4	2	2
Max. group OS?	*Yes*	*Yes*	*Yes*	*Yes*	*Yes*	*No*	*No*	*No*	*No*	*No*
Example*	Sc_2O_3	TiO_4	VO_2^+	CrO_3	MnO_4^-	FeO_4^{2-}	Co_2O_3	NiO	CuO	ZnO
2nd/3rd row	Y/La	Zr/Hf	Nb/Ta	Mo/W	Tc/Re	Ru/Os	Rh/Ir	Pd/Pt	Ag/Au	Cd/Hg
Max. OS	3	4	5	6	7	8	6	4/6	3/5	2
Example	Y_2O_3 La_2O_3	ZrO_2 HfO_2	Nb_2O_5 Ta_2O_5	MoO_3 WO_3	Tc_2O_7 ReO_4^{3-}	RuO_4 OsO_4	RhO_2 IrO_2	PdO_2 PtO_2	AgO Au_2O_3	CdO HgO

*Note that the highest oxidation state oxo species do not exist for all elements, particularly late transition metals. For example, the highest well-defined oxidation state for Rh and Ir is +6, with representative compound being hexafluoride of two metals. However, the maximum oxidation state in which oxo species occur is +4 in RhO_2 and IrO_2.

It is clear from the table that the maximum oxidation state of the group increases from left to right, peaks at Group 7 for the first row and at Group 8 for the second- and third-row transition metals, and then steadily decreases toward the end of the transition metal series. Within a group, the heavier elements can achieve higher oxidation states than first-row members (see, for example, Group 8).

E19.2 **(a)** $\mathbf{Cr_2O_7^{2-}}$

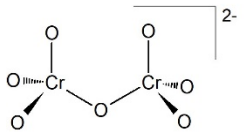

(b) $\mathbf{VO^{2+}}$

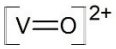

(c) $\mathbf{VO_4^{3-}}$

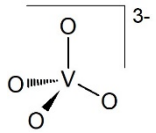

(d) $\mathbf{MnO_4^{2-}}$

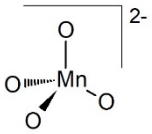

Note: In structures (a), (b), and (d) the terminal metal-oxygen bond order is higher than 1 but lower than 2 due to the resonance effects; these given structures depict the geometry rather than exact bond orders.

E19.3 Statement **(a)** is correct.

Statement **(b)** is also correct.

Statement **(c)** is incorrect: the atomic volumes of the transition metals decrease steadily from left to right; the lanthanide contraction also affects the atomic volumes of third-row transition elements so that their atomic volumes are almost identical to those found for the second-row transition metals directly above. Consequently, transition metals are very dense. For example, osmium with density of 22.6 g/cm^3 is one of the densest materials known.

Statement **(d**) is correct.

E19.4 HfO_2 and ZrO_2 are isostructural and, because ionic radii of Hf^{4+} and Zr^{4+} are almost identical, they likely have very similar unit cell parameters and consequently unit cell volume. Thus, the difference in density can be explained by difference in atomic mass for Hf and Zr. Since, the atomic mass of Hf (and consequently molecular mass of HfO_2) is higher than Zr (and ZrO_2 has lower molecular weight than HfO_2) more mass is "packed" in about the same volume. Consider also that the ratio of molecular masses is very similar to the ratio of the densities: $Mr(HfO_2)/Mr(ZrO_2) = 210.49/123.22 = 1.72$ vs. $\rho(HfO_2)/\rho(ZrO_2) = 9.68/5.73 = 1.69$.

E19.5 Pigments should be permanent and stable. They should be as inert as possible to the atmosphere—they should be stable toward oxidation with O_2, should not react with moisture, and should not be light-sensitive. Considering the increased atmospheric pollution, they should be as resistant as possible to the effects of gases such as H_2S, CO_2, SO_2, etc. They should also be non-toxic and have low vapour pressure. A good pigment would have very good coverage ability; that is, small amount of pigment should cover a large surface area. If the material is natural in origin, then its extraction and storage should be easy. If the pigment is synthetic, then the manufacturing process should be cheap.

Chapter 20 d-Metal Complexes: Electronic Structure and Properties

Self-Tests

S20.1 A high-spin d^7 configuration is $t_{2g}^5e_g^2$. To calculate the ligand field stabilization energy LFSE we should note that each electron in the t_{2g} stabilizes the CFSE for –0.4 units and destabilizes by 0.6 units when placed in the e_g level. Accordingly, for the high spin d^7 configuration, we should expect $5\times(-0.4\Delta_o) + 2 \times 0.6\Delta_o$ or $-0.8\Delta_o$. The LFSE of a low-spin d^7 with a configuration of $t_{2g}^6e_g^1$, is expected to have $-1.8\Delta_o + P$ [$6 \times(-0.4\ \Delta_o) + 0.6\ \Delta_o = -1.8\Delta_o$] where P is electron-pairing energy. Note that although high-spin d^7 configuration has two electron pairs in t_{2g} level, they do not contribute to LFSE because they would be paired in a spherical field as well. The low-spin configuration adds one more electron pair (a pair that did not exist in a spherical field before the orbital splitting), and this pair has to be accounted for.

S20.2 Since each isothiocyanate ligand has a single negative charge, the oxidation state of the manganese ion is +2. Mn(II) is d^5, and there are two possibilities for an octahedral complex, a low-spin (t_{2g}^5), with one unpaired electron, or a high-spin ($t_{2g}^3e_g^2$), with five unpaired electrons. The observed magnetic moment of 6.06 μ_B is close to the spin-only value for five unpaired electrons, $(5 \times 7)^{1/2} = 5.92\ \mu_B$ (see Table 20.3). Therefore, this complex is high spin and has a $t_{2g}^3e_g^2$ configuration.

S20.3 If it were not for LFSE, MF_2 lattice enthalpies would increase from Mn(II) to Zn(II). This is because the decreasing ionic radius, which is due to the increasing Z_{eff} as you cross through the d-block from left to right, leads to decreasing M–F separations (straight line on diagram below). Therefore, you expect that ΔH_{latt} for MnF_2 (2 780 kJ mol^{-1}) would be smaller than ΔH_{latt} for ZnF_2 (2985 kJ mol^{-1}). In addition, as discussed for aqua ions and oxides, we expect additional LFSE for these compounds. From Table 20.2, you see that LFSE = 0 for Mn(II), $-0.4\Delta_o$ for Fe(II), $-0.8\Delta_o$ for Co(II), $-1.2\Delta_o$ for Ni(II), and 0 for Zn(II). The deviations of the observed values from the straight line connecting Mn(II) and Zn(II) are not quite in the ratio 0.4:0.8:1.2, but note that the deviation for Fe(II) is smaller than that for Ni(II).

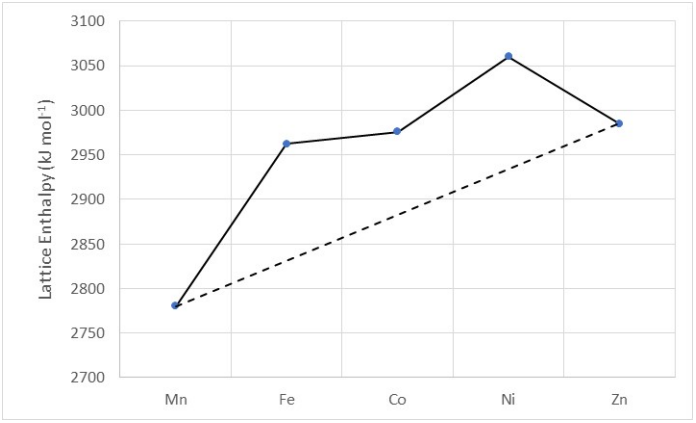

S20.4 In the spectrum of $[Mo(CO)_6]$ (Fig. 20.17), the ionization energy around 8 eV was attributed to the t_{2g} electrons that are largely metal-based (see Example 20.4). The biggest difference between the photoelectron spectra of ferrocene and magnesocene is in the 6–8 eV region. Fe(II) has six d electrons (like Mo(0)), while Mg(II) has no d electrons. Therefore, the differences in the 6–8 eV region can be attributed to the lack of d electrons in Mg(II) omplex. The group of energies around 14 eV and 18 eV in both compounds can be attributed to M–Cp orbitals and ionization of Cp itself, respectively.

S20.5 A p^1d^1 configuration will have $L = 1 + 2 = 3$ (an electron in a p orbital has $l = 1$, whereas an electron in a d orbital has $l = 2$). This value of L corresponds to an F term. Since the electrons may have antiparallel ($S = -½ + ½ = 0$, multiplicity $2S + 1 = 2 \times 0 + 1 = 1$) or parallel spins ($S = + ½ + ½ = 1$, multiplicity $2S + 1 = 2 \times 1 + 1 = 3$), both ^1F and ^3F terms are possible.

S20.6 **a) $2p^2$ ground term**. Two electrons in a p subshell can occupy separate p orbitals and have parallel spins (S = + ½ + ½ = 1), so the maximum multiplicity $2S + 1 = 2 \times 1 + 1 = 3$. The maximum value of M_L is 1 + 0 = 1, which corresponds to a P term (according to the Pauli principle, m_l cannot be +1 for both electrons if the spins are parallel, thus one electron has m_l = +1 and the other m_l = 0). Thus, the ground term is ^{3}P (called a "triplet P" term).

b) $3d^9$ ground term. The largest value of M_S for nine electrons in a d subshell is 1/2 (eight electrons are paired in four of the five orbitals, while the ninth electron has $m_s = \pm 1/2$). Thus S = 1/2 and the multiplicity $2S + 1 = 2$. Notice that the largest value of M_S is the same for one electron in a d subshell. Similarly, the largest value of M_L is 2, which results from the following nine values of m_l: +2, +2, +1, +1, 0, 0, –1, –1, –2. Notice also that M_L = 2 corresponds to one electron in a d subshell. Thus, the ground term for a d^9 or a d^1 configuration is ^{2}D (called a "doublet D" term).

S20.7 An F term arising from a d^n configuration correlates with $T_{1g} + T_{2g} + A_{2g}$ terms in an O_h complex. The multiplicity is unchanged by the correlation, so the terms in O_h symmetry are $^3T_{1g}$, $^3T_{2g}$, and $^3A_{2g}$. Similarly, a D term arising from a d^n configuration correlates with $T_{2g} + E_g$ terms in an O_h complex. The O_h terms retain the singlet character of the ^{1}D free ion term, and so are $^1T_{2g}$ and ^1E_g.

S20.8 The two transitions in question are $^4T_2 \leftarrow {}^4A_2$ and $^4T_1 \leftarrow {}^4A_2$ (the first one has a lower energy and hence a lower wave number). Since Δ_0 = 17 600 cm^{-1} and B = 700 cm^{-1}, you must find the point 17 600/700 = 25.1 on the x axis of the Tanabe-Sugano diagram. Then, the ratios E/B for the two bands are the y values of the points on the $^4T_2$ and $^4T_1$ lines, 25 and 32, respectively, as shown below on a partial Tanabe Sugano diagram for the d^3 configuration. Therefore, the two lowest-energy spin-allowed bands in the spectrum of $[Cr(H_2O)_6]^{3+}$ will be found at (700 cm^{-1})(25) = 17 500 cm^{-1} and (700 cm^{-1})(32) = 22 400 cm^{-1}.

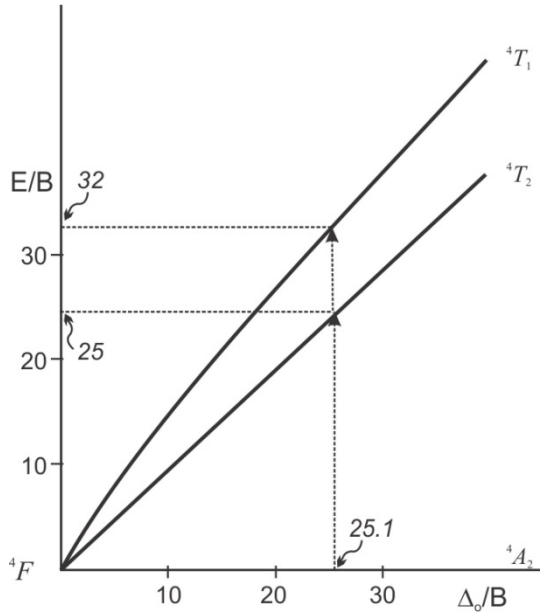

S20.9 This six-coordinate d^3 complex undoubtedly has an O_h symmetry, so the general features of its spectrum will resemble the spectrum of $[Cr(NH_3)_6]^{3+}$, shown in Figure 20.23. The very low intensity of the band at 16 000 cm^{-1} is a clue that it is a spin-forbidden transition, probably $^2E_g \leftarrow {}^4A_{2g}$. The spin-allowed but Laporte-forbidden bands typically have $\varepsilon \sim 100$ M^{-1} cm^{-1}, so it is likely that the bands at 17 700 cm^{-1} and 23 800 cm^{-1} are of this type (they correspond to the $^4T_{2g} \leftarrow {}^4A_{2g}$ and $^4T_{1g} \leftarrow {}^4A_{2g}$ transitions, respectively). The band at 32 400 cm^{-1} is probably a charge transfer band because its intensity is too high to be a ligand field (d–d) band. Since you are provided with the hint that the NCS^- ligands have low-lying π^* orbitals, it is reasonable to conclude that this band corresponds to a MLCT transition. Notice that the two spin-allowed ligand field transitions of $[Cr(NCS)_6]^{3-}$ are at lower energy than those of $[Cr(NH_3)_6]^{3+}$, showing that NCS^- induces a smaller Δ_o on Cr^{3+} than does NH_3. Also notice that $[Cr(NH_3)_6]^{3+}$ lacks an intense MLCT band at ~30 000–40 000 cm^{-1}, showing that NH_3 does not have low-lying empty molecular orbitals.

Exercises

E20.1 **a) $[Co(NH_3)_6]^{3+}$.** Since the NH_3 ligands are neutral, the cobalt ion in this octahedral complex is Co^{3+}, which is a d^6 metal ion. Ammonia is in the middle of the spectrochemical series but because the cobalt ion has a 3+ charge, this is a strong field complex and hence is a low spin complex, with $S = 0$ and has no unpaired electrons (the configuration is t_{2g}^6). The LFSE is $6(-0.4\Delta_o) = -2.4\Delta_o + 2P$.

b) $[Fe(OH_2)_6]^{2+}$. The iron ion in this octahedral complex, which contains only neutral water molecules as ligands, is Fe^{2+}, a d^6-metal ion. Since water is lower in the spectrochemical series than NH_3 (i.e., it is a weaker field ligand than NH_3) *and* since the charge on the metal ion is only 2+, this is a weak field complex and hence is high spin, with $S = 2$ and four unpaired d electrons (the configuration is $t_{2g}^4e_g^2$). The LFSE is $4(-0.4\Delta_o) + 2(0.6\Delta_o) = -0.4\Delta_o$. Compare this small value to the large value for the low spin d^6 complex in part **(a)** above.

c) $[Fe(CN)_6]^{3-}$. The iron ion in this octahedral complex, which contains six negatively charged CN^- ligands, is Fe^{3+}, which is a d^5 metal ion. Cyanide ion is a very strong field ligand, so this is a strong-field complex and hence is a low spin complex, with $S = 1/2$ and one unpaired electron. The configuration is t_{2g}^5 and the LFSE is $-2.0\Delta_o + 2P$.

d) $[Cr(NH_3)_6]^{3+}$. The complex contains six neutral NH_3 ligands, so chromium is Cr^{3+}, a d^3 metal ion. The configuration is t_{2g}^3, and so there are three unpaired electrons and $S = 3/2$. Note that, for octahedral complexes, only d^4–d^7 metal ions have the possibility of being either high spin or low spin. For $[Cr(NH_3)_6]^{3+}$, the LFSE = $3(-0.4\Delta_o) = -1.2\Delta_o$. (For d^1–d^3, d^8, and d^9 metal ions in octahedral complexes, only one spin state is possible.)

e) $[W(CO)_6]$. Carbon monoxide (i.e., the carbonyl ligand) is neutral, so this is a complex of W(0). The W atom in this octahedral complex is d^6. Since CO is such a strong field ligand (it is even higher in the spectrochemical series than CN^-), $W(CO)_6$ is a strong-field complex and hence is low spin, with no unpaired electrons (the configuration is t_{2g}^6). The LFSE = $6(-0.4\Delta_o) + 2P = -2.4\Delta_o + 2P$.

f) Tetrahedral $[FeCl_4]^{2-}$. The iron ion in this complex, which contains four negatively charged Cl^- ion ligands, is Fe^{2+}, which is a d^6 metal ion. All tetrahedral complexes are high spin because Δ_T is much smaller than Δ_o ($\Delta_T = (4/9)\Delta_o$ if the metal ion, the ligands, and the metal-ligand distances are kept constant), so for this complex $S = 2$ and there are four unpaired electrons. The configuration is $e^3t_2^3$. The LFSE is $3(-0.6\Delta_T) + 3(0.4\Delta_T) = -0.6\ \Delta_T$.

g) Tetrahedral $[Ni(CO)_4]$? The neutral CO ligands require that the metal centre in this complex is Ni^0, which is a d^{10}-metal atom. Regardless of geometry, complexes of d^{10}-metal atoms or ions will never have any unpaired electrons and will always have LFSE = 0, and this complex is no exception.

E20.2 The formula for the spin-only moment is $\mu/\mu_B = [(N)(N + 2)]^{1/2}$ where N is the number of unpaired electrons. Therefore, the spin-only contributions are:

Complex	N	$\mu/\mu_B = [(N)(N + 2)]^{1/2}$
$[Co(NH_3)_6]^{3+}$	0	0
$[Fe(OH_2)_6]^{2+}$	4	4.9
$[Fe(CN)_6]^{3-}$	1	1.7
$[Cr(NH_3)_6]^{3+}$	3	3.9
$[W(CO)_6]$	0	0
$[FeCl_4]^{2-}$	4	4.9
$[Ni(CO)_4]$	0	0

E20.3 The colours of metal complexes are frequently caused by ligand-field transitions involving electron promotion from one subset of d orbitals to another (e.g., from t_{2g} to e_g for octahedral complexes or from e to t_2 for tetrahedral complexes). Of the three complexes given, the lowest energy transition probably occurs for $[CoCl_4]^{2-}$ because it is tetrahedral ($\Delta_T = (4/9)(\Delta_o)$) and because Cl^- is a weak-field ligand. This complex is blue because a solution of it will absorb low-energy red light and reflect blue—that is, the complement of red. Of the two complexes that are left, $[Co(NH_3)_6]^{2+}$ probably has a higher energy transition than $[Co(OH_2)_6]^{2+}$ because NH_3 is a stronger field ligand

than H_2O (see Table 20.1). The complex $[Co(NH_3)_6]^{2+}$ is yellow because only a small amount of visible light, at the blue end of the spectrum, is absorbed by a solution of this complex. By default, you should conclude that $[Co(OH_2)_6]^{2+}$ is pink.

E20.4 As in the answer to Self-test 20.3, there are two factors that lead to the values given in this question and plotted below: decreasing ionic radius from left to right across the d block, leading to a general increase in ΔH_{latt} from CaO to NiO, and LFSE, which varies in a more complicated way for high-spin metal ions in an octahedral environment, increasing from d^0 to d^3, then decreasing from d^3 to d^5, then increasing from d^5 to d^8, then decreasing again from d^8 to d^{10}. The straight line through the black squares is the trend expected for the first factor, the decrease in ionic radius (the last black square is not a data point, but simply the extrapolation of the line between ΔH_{latt} values for CaO and MnO, both of which have LFSE = 0). The deviations of ΔH_{latt} values for TiO, VO, FeO, CoO, and NiO from the straight line are a manifestation of the second factor, the non-zero values of LFSE for Ti^{2+}, V^{2+}, Fe^{2+}, Co^{2+}, and Ni^{2+}. TiO and VO have considerable metal–metal bonding, and this factor also contributes to their stability.

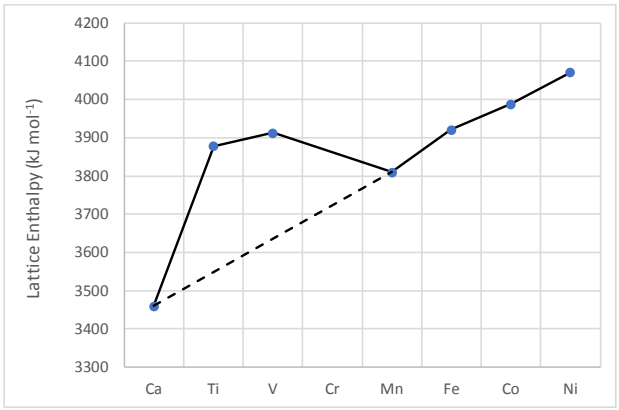

E20.5 Perchlorate, ClO_4^-, is a very weak basic anion (consider that $HClO_4$ is a very strong Brønsted acid). Therefore, in the compound containing Ni(II), the neutral macrocyclic ligand, and two ClO_4^- anions, there are probably a four-coordinate square-planar Ni(II) (d^8) complex and two non-coordinated perchlorate anions. Square-planar d^8 complexes are diamagnetic because they have a configuration $(xz, yz)^4 (z^2)^2(xy)^2$ with all electrons paired. When SCN^- ligands are added, they coordinate to the nickel ion, producing an essentially octahedral complex that has two unpaired electrons (configuration $t_{2g}^6 e_g^2$).

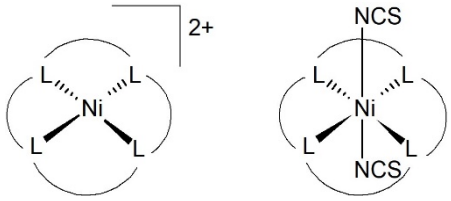

E20.6 The ground state of $[Ti(OH_2)_6]^{3+}$, which is a d^1 complex, is not one of the configurations that usually leads to an observable Jahn-Teller distortion (the three main cases are listed in the answer E20.8, above). However, the electronic excited state of $[Ti(OH_2)_6]^{3+}$ has the configuration $t_{2g}^0 e_g^1$, and so the excited state of this complex possesses an e_g degeneracy. Therefore, the "single" electronic transition is really the superposition of two transitions, one from an O_h ground-state ion to an O_h excited-state ion, and a lower energy transition from an O_h ground-state ion to a lower energy distorted excited-state ion (probably D_{4h}). Since these two transitions have slightly different energies, the unresolved superimposed bands result in an asymmetric absorption peak.

E20.7 **a) ^3F, ^3P, ^1P, ^1G?** Recall Hund's rules: (1) the term with the greatest multiplicity lies lowest in energy; (2) for a given multiplicity, the greater the value of L of a term, the lower the energy. Therefore, the ground term in this

case will be a triplet, not a singlet (rule 1). Of the two triplet terms, ^{3}F lies lower in energy than ^{3}P: $L = 3$ for ^{3}F, $L = 1$ for ^{3}P (rule 2). Therefore, the ground term is ^{3}F.

b) ^{5}D, ^{3}H, ^{3}P, ^{1}G, ^{1}I? The ground term is ^{5}D because this term has the highest multiplicity.

c) ^{6}S, ^{4}G, ^{4}P, ^{2}I? The ground term is ^{6}S because this term has the highest multiplicity.

E20.8 The diagram below outlines the relative energies of the ^{3}F, ^{1}D, and ^{3}P terms. It can be seen that the 10 642 cm^{-1} energy gap between the ^{3}F and ^{1}D terms is $5B + 2C$, while the 12 920 cm^{-1} energy gap between the ^{3}F and ^{3}P terms is $15B$. From the two equations

$$5B + 2C = 10\,642\ \text{cm}^{-1} \quad \text{and} \quad 15B = 12\,920\ \text{cm}^{-1}$$

you can determine that $B = (12\,920\ \text{cm}^{-1})/(15) = 861.33\ \text{cm}^{-1}$ and $C = 3\,167.7\ \text{cm}^{-1}$.

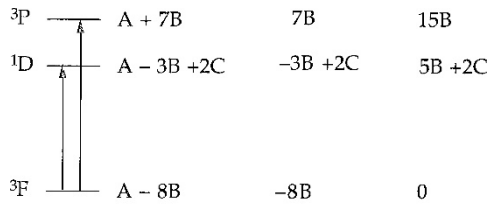

Relative Energies

E20.9 a) $[Ni(H_2O)_6]^{2+}$ (absorptions at 8 500, 15 400, and 26 000 cm^{-1}). According to the d^8 Tanabe-Sugano diagram (Resource Section 6), the absorptions at 8 500 cm^{-1}, 15 400 cm^{-1}, and 26 000 cm^{-1} correspond to the following spin-allowed transitions, respectively: $^3T_{2g} \leftarrow {}^3A_{2g}$, $^3T_{1g} \leftarrow {}^3A_{2g}$, and $^3T_{1g} \leftarrow {}^3A_{2g}$. The ratios 15 400/8 500 = 1.8 and 26 000/8 500 = 3.0 can be used to estimate $\Delta_o/B \approx 11$. Using this value of Δ_o/B and the fact that $E/B = \Delta_o/B$ for the lowest-energy transition, $\Delta_o = 8\,500\ \text{cm}^{-1}$ and $B \approx 770\ \text{cm}^{-1}$. Note that B for a gas-phase Ni^{2+} ion is 1 080 cm^{-1}. The fact that B for the complex is only ~70% of the free ion value is an example of the nephalauxetic effect.

b) $[Ni(NH_3)_6]^{2+}$ (absorptions at 10 750, 17 500, and 28 200 cm^{-1}). The absorptions for this complex are at 10 750 cm^{-1}, 17 500 cm^{-1}, and 28 200 cm^{-1}. The ratios in this case are 17 500/10 750 = 1.6 and 28 200/10 750 = 2.6, and lead to $\Delta_o/B \approx 15$. Thus, $\Delta_o = 10\,750\ \text{cm}^{-1}$ and $B \approx 720\ \text{cm}^{-1}$. It is sensible that B for $[Ni(NH_3)_6]^{2+}$ is smaller than B for $[Ni(H_2O)_6]^{2+}$ because NH_3 is higher in the nephalauxetic series than is H_2O.

E20.10 If $[Co(NH_3)_6]^{3+}$, a d^6 complex, were high spin, the only spin-allowed transition possible would be $^5E_g \leftarrow {}^5T_{2g}$ (refer to the d^6 Tanabe-Sugano diagram). On the other hand, if it were low spin, several spin-allowed transitions are possible, including $^1T_{1g} \leftarrow {}^1A_{1g}$, $^1T_{2g} \leftarrow {}^1A_{1g}$, $^1E_g \leftarrow A_{1g}$, etc. The presence of *two* moderate-intensity bands in the visible/near-UV spectrum of $[Co(NH_3)_6]^{3+}$ suggests that it is low spin. The first two transitions listed above correspond to these two bands. The very weak band in the red corresponds to a spin-forbidden transition such as $^3T_{2g} \leftarrow {}^1A_{1g}$.

E20.11 NH_3 and CN^- ligands are quite different with respect to the types of bonds they form with metal ions. Ammonia and cyanide ion are both σ-bases, but cyanide is also a π-acid. This difference means that NH_3 can form molecular orbitals only with the metal e_g orbitals, while CN^- can form molecular orbitals with the metal e_g and t_{2g} orbitals. The formation of molecular orbitals is the way that ligands "expand the clouds" of the metal d orbitals—the bonding between Co^{3+} and the ligand has more covalent character in $[Co(CN)_6]^{3-}$ than in $[Co(NH_3)_6]^{3+}$.

E20.12 The Fe^{3+} ions in question are d^5 metal ions. If they were low spin, several spin-allowed ligand field transitions would give the glass a colour even when viewed through the wall of the bottle (see the Tanabe-Sugano diagram for d^5 metal ions). Therefore, the Fe^{3+} ions are high spin, and as such have no spin-allowed transitions (the ground state of an octahedral high-spin d^5 metal ion is $^6A_{1g}$, and there are no sextet excited states). The faint green colour, which is only observed when looking through a *long* pathlength of bottle glass, is caused by spin-forbidden ligand field transitions (recall the Lambert-Beer's law, $A = \varepsilon l c$, where l is the optical pathlength).

E20.13 The d_{z2} orbital in $[CrCl(NH_3)_5]^{2+}$ complex is left unchanged by each of the symmetry operations of the C_{4v} point group. It therefore has A_1 symmetry. The Cl^- lone electron pairs can form π molecular orbitals with d_{xz} and d_{yz}. These metal atomic orbitals are π-antibonding MOs in $[CoCl(NH_3)_5]^{2+}$ (they are nonbonding in $[Co(NH_3)_6]^{3+}$), and so they will be raised in energy relative to their position in $[Co(NH_3)_6]^{3+}$, in which they were degenerate with d_{xy}. Since Cl^- ion is not as strong a σ-base as NH_3 is, the d_z^2 orbital in $[CoCl(NH_3)_5]^{2+}$ will be at lower energy than in $[Co(NH_3)_6]^{3+}$, in which it was degenerate with d_{x2-y2}. A qualitative d-orbital splitting diagram for both complexes is shown below (L = NH_3).

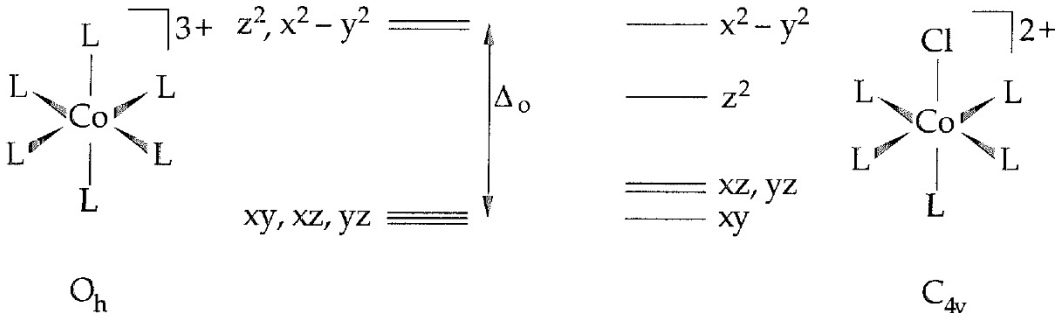

Chapter 21 Coordination Chemistry: Reactions of Complexes

Self-Tests

S21.1 We can use Equation 21.6 to calculate the rate constant:

$$\log k_2(NO_2^-) = Sn_{Pt}(NO_2^-) + C$$

where S is the nucleophilic discrimination factor for this complex, $n_{Pt}(NO_2^-)$ is the nucleophilicity parameter of nitrite ion, and C is the logarithm of the second order rate constant for the substitution for Cl^- in this complex by MeOH. S was determined to be 0.41 in the example, and $n_{Pt}(NO_2^-)$ is given as 3.22. C is a constant for a given complex and is –0.61 in this case, as determined in the example also. Therefore, $k_2(NO_2^-)$ can be calculated as follows:

$$\log k_2(NO_2^-) = (0.41)\times(3.22) - 0.61 = 0.71$$

$$k_2(NO_2^-) = 10^{0.71} = 5.1\ dm^3mol^{-1}s^{-1}.$$

S21.2 For the three ligands in question, Cl^-, NH_3, and PPh_3, the *trans* effect series is $NH_3 < Cl^- < PPh_3$. This means that a ligand *trans* to Cl^- will be substituted at a faster rate than a ligand *trans* to NH_3, and a ligand *trans* to PPh_3 will be substituted at a faster rate than a ligand *trans* to Cl^-. Since our starting material is $[PtCl_4]^{2-}$, two steps involving substitution of Cl^- by NH_3 or PPh_3 must be used.

If you first add NH_3 to $[PtCl_4]^{2-}$, you will produce $[PtCl_3(NH_3)]^-$. Now if you add PPh_3, one of the mutually *trans* Cl^- ligands will be substituted faster than the Cl^- ligand *trans* to NH_3, and the *cis* isomer will be the result. If you first add PPh_3 to $[PtCl_4]^{2-}$, you will produce $[PtCl_3(PPh_3)]^-$. Now if you add NH_3, the Cl^- ligand *trans* to PPh_3 will be substituted faster than one of the mutually *trans* Cl^- ligands, and the *trans* isomer will be the result.

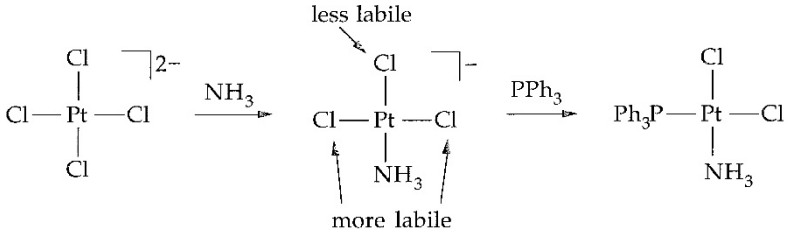

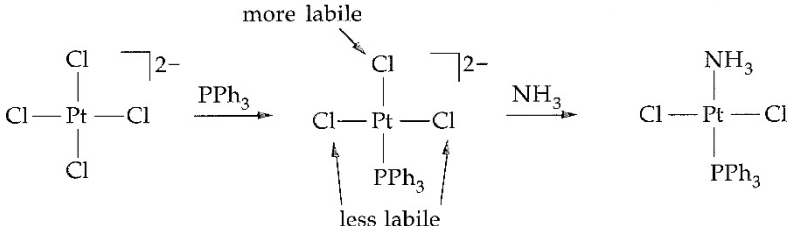

S21.3 As discussed in Section 21.6, the Eigen-Wilkins mechanism for substitution in octahedral complexes suggests the formation of an encounter complex $\{[V(H_2O)_6]^{2+}, Cl^-\}$, in the first, fast step:

$$[V(H_2O)_6]^{2+} + Cl^- \rightarrow \{[V(H_2O)_6]^{2+}, Cl^-\}.$$

The second, slow step of the mechanism is producing the product:

$$\{[V(H_2O)_6]^{2+}, Cl^-\} \rightarrow [VCl(H_2O)_5]^+ + H_2O.$$

The observed rate constant, k_{obs}, is given by:

$$k_{obs} = kK_E$$

and in the case of the substitution of H_2O by Cl^- in $[V(H_2O)_6]^{2+}$ $k_{obs} = 1.2 \times 10^2$ $dm^3mol^{-1}s^{-1}$. You will be able to calculate k if you can estimate a proper value for K_E. Inspection of Table 21.6 shows that $K_E = 1$ dm^3mol^{-1} for the encounter complex formed by F^- or SCN^- and $[Ni(H_2O)_6]^{2+}$. This value can be used for the reaction in question because (i) the charge and size of Cl^- are similar to those of F^- and SCN^-, and (ii) the charge and size of $[Ni(H_2O)_6]^{2+}$ are similar to those of $[V(H_2O)_6]^{2+}$. Therefore, $k = k_{obs}/K_E = (1.2 \times 10^2\ dm^3mol^{-1}\ s^{-1})/(1\ dm^3mol^{-1}) = 1.2 \times 10^2\ s^{-1}$.

Exercises

E21.1 If the mechanism of substitution were to be associative, the nature of incoming ligand should affect the rate of the reaction. This is because the rate-limiting step would require the formation of M–X bonds (X = incoming ligand). In the present case, however, the rate of the reaction does not vary much with the nature or the size of the incoming ligand. Therefore, the more likely mechanism would be *dissociative.*

E21.2 Since the rate of substitution is the same for a variety of different entering ligands L (i.e., phosphines and or phosphites), the activated complex in each case must not include any significant bond making to the entering ligand. Thus, the reaction must be *d*. If the rate-determining step included any Ni–L bond making, the rate of substitution would change as the electronic and steric properties of L were changed.

E21.3 If ligand substitution takes place by a *d* mechanism, the strength of the metal-leaving group bond is directly related to the substitution rate. Metal centres with high oxidation numbers will have stronger bonds to ligands than metal centres with low oxidation numbers. Furthermore, period 5 and 6 d-block metals have stronger metal ligand bonds (see Section 21.1). Therefore, for reactions that are dissociatively activated, complexes of period 5 and 6 metals are less labile than complexes of period 3 metals, and complexes of metals in high oxidation states are less labile than complexes of metals in low oxidation states (all other factors remaining equal).

E21.4 Since the rate of loss of chlorobenzene, PhCl, from the tungsten complex becomes faster as the cone angle of L increases, this is a case of dissociative activation (i.e., steric crowding in the transition state accelerates the rate).

E21.5 The fact that the five-coordinate complex $[Ni(CN)_5]^{3-}$ can be detected does indeed explain why substitution reactions of the four-coordinate complex $[Ni(CN)_4]^{2-}$ are fast. The reason is that, for a detectable amount of $[Ni(CN)_5]^{3-}$ to build up in solution, the forward rate constant k_f must be numerically close to or greater than the reverse rate constant k_r:

$$[Ni(CN)_4]^{2-} + CN^- \underset{k_r}{\overset{k_f}{\rightleftharpoons}} [Ni(CN)_5]^{3-}$$

If k_f were much smaller than k_r, the equilibrium constant $K = k_f/k_r$ would be small and the concentration of $[Ni(CN)_5]^{3-}$ would be too small to detect. Therefore, because k_f is relatively large, you can infer that rate constants for the association of other nucleophiles are also large, with the result that substitution reactions of $[Ni(CN)_4]^{2-}$ are very fast.

E21.6 Starting with $[PtCl_4]^{2-}$, you need to perform two separate ligand substitution reactions. In one, NH_3 will replace Cl^- ion. In the other, NO_2^- ion will replace Cl^- ion. The question is which substitution to perform first. According to the *trans* effect series shown in Section 21.4, the strength of the *trans* effect for the three ligands in question is $NH_3 < Cl^- < NO_2^-$. This means that a Cl^- ion *trans* to another Cl^- will be substituted faster than a Cl^- ion *trans* to NH_3, while a Cl^- ion *trans* to NO_2^- will be substituted faster than a Cl^- ion *trans* to another Cl^- ion.

If you first add NH_3 to $[PtCl_4]^{2-}$, you will produce $[PtCl_3(NH_3)]^-$. Now if you add NO_2^-, one of the mutually *trans* Cl^- ligands will be substituted faster than the Cl^- ligand *trans* to NH_3, and the *cis* isomer will be the result.
If you first add NO_2^- to $[PtCl_4]^{2-}$, you will produce $[PtCl_3(NO_2)]^{2-}$. Now if you add NH_3, the Cl^- ligand *trans* to NO_2^- will be substituted faster than one of the mutually *trans* Cl^- ligands, and the *trans* isomer will be the result. These two-step syntheses are shown below:

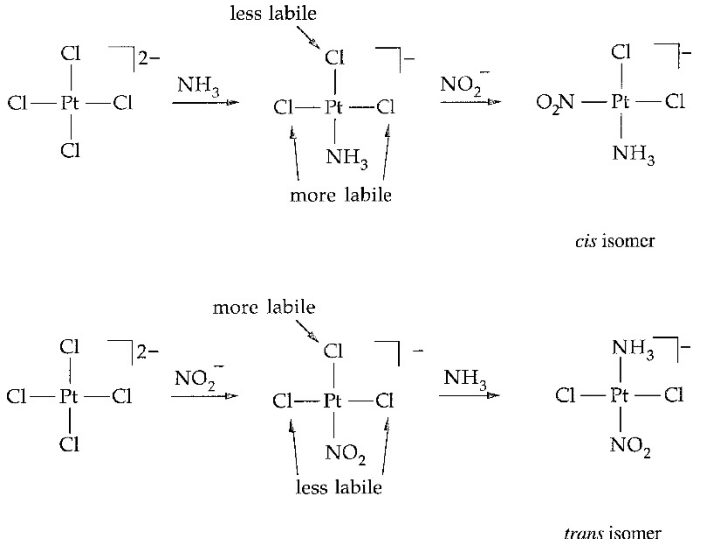

E21.7 The general trend is easy to explain: the octahedral $[Co(H_2O)_6]^{3+}$ complex undergoes dissociatively activated ligand substitution. The rate of substitution depends on the nature of the bond between the metal and the leaving group because this bond is partially broken in the activated complex. The rate is independent of the nature of the bond to the entering group because this bond is formed in a step after the rate-determining step. The anomalously high rate of substitution by OH^- signals an alternate path, that of base hydrolysis, as shown below (see Section 21.7):

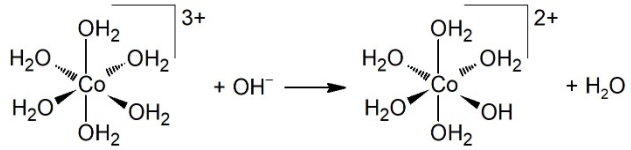

The deprotonated complex $[Co(H_2O)_5(OH)]^{2+}$ will undergo loss of H_2O faster than the starting complex $[Co(H_2O)_6]^{3+}$, because the anionic OH^- ligand is both better σ and π donor than H_2O. Therefore, the bond *trans* to Co–OH bond is going to be weaker, and substitution is going to proceed faster. The implication is that a complex without protic ligands will not undergo anomalously fast substitution reaction in the presence of OH^-.

E21.8 The three amine complexes will undergo substitution more slowly than the two aqua complexes. This is because of the higher overall complex charge and their low-spin d^6 configurations. You should refer to Table 21.8, which lists ligand field activation energies (LFAE) for various d^n configurations. While low-spin d^6 is not included, note the similarity between d^3 (t_{2g}^3) and low-spin d^6 (t_{2g}^6). A low-spin octahedral d^6 complex has LFAE = $0.4\Delta_{oct}$, and consequently is inert to substitution. Of the three amine complexes listed above, the iridium complex is the most inert, followed by the rhodium complex, which is more inert than the cobalt complex. This is because Δ_{oct} increases on descending a group in the d-block. Of the two aqua complexes, the Ni complex, with LFAE = $0.2\Delta_{oct}$, undergoes substitution more slowly than the Mn complex, with LFAE = 0. Thus, the order of increasing rate is $[Ir(NH_3)_6]^{3+} < [Rh(NH_3)_6]^{3+} < [Co(NH_3)_6]^{3+} < [Ni(OH_2)_6]^{2+} < [Mn(OH_2)_6]^{2+}$.

E21.9 The inner-sphere pathway is shown below (solvent = H_2O):

$$[Co(N_3)(NH_3)_5]^{2+} + [V(OH_2)_6]^{2+} \rightarrow \{[Co(N_3)(NH_3)_5]^{2+}, [V(OH_2)_6]^{2+}\}$$

$$\{[Co(N_3)(NH_3)_5]^{2+}, [V(OH_2)_6]^{2+}\} \rightarrow \{[Co(N_3)(NH_3)_5]^{2+}, [V(OH_2)_5]^{2+}, H_2O\}$$

$$\{[Co(N_3)(NH_3)_5]^{2+}, [V(OH_2)_5]^{2+}, H_2O\} \rightarrow \underset{\text{Co(III)}}{[(NH_3)_5Co}\text{–N=N=N–}\underset{\text{V(II)}}{V(OH_2)_5]^{4+}} + H_2O$$

$$\underset{\text{Co(III)}}{[(NH_3)_5Co}\text{–N=N=N–}\underset{\text{V(II)}}{V(OH_2)_5]^{4+}} \rightarrow \underset{\text{Co(II)}}{[(NH_3)_5Co}\text{–N=N=N–}\underset{\text{V(III)}}{V(OH_2)_5]^{4+}}$$

$$H_2O + [(NH_3)_5Co\text{–}N{=}N{=}N\text{–}V(OH_2)_5]^{4+} \rightarrow [Co(NH_3)_5(OH_2)]^{2+} + [V(N_3)(OH_2)_5]^{2+}$$
$$\text{Co(II)} \qquad\qquad \text{V(III)}$$

The pathway for outer-sphere electron transfer is shown below:

$$[Co(N_3)(NH_3)_5]^{2+} + [V(OH_2)_6]^{2+} \rightarrow \{[Co(N_3)(NH_3)_5]^{2+}, [V(OH_2)_6]^{2+}\}$$
$$\{[Co(N_3)(NH_3)_5]^{2+}, [V(OH_2)_6]^{2+}\} \rightarrow \{[Co(N_3)(NH_3)_5]^{+}, [V(OH_2)_6]^{3+}\}$$
$$\{[Co(N_3)(NH_3)_5]^{+}, [V(OH_2)_6]^{3+}\} + H_2O \rightarrow [Co(NH_3)_5(OH_2)]^{2+} + [V(OH_2)_6]^{3+} + N_3^-$$

In both cases, the cobalt-containing product is the aqua complex because H_2O is present in abundance, and high-spin d^7 complexes of Co(II) are substitution labile. However, something that distinguishes the two pathways is the composition of the vanadium-containing product. If $[V(N_3)(OH_2)_5]^{2+}$ is the product, then the reaction has proceeded via an inner-sphere pathway. If $[V(OH_2)_6]^{3+}$ is the product, then the electron-transfer reaction is outer-sphere. The complex $[V(N_3)(OH_2)_5]^{2+}$ is inert enough to be experimentally observed before the water molecule displaces the azide anion to give $[V(OH_2)_6]^{3+}$.

E21.10 In the case of reactions with Co(II), the difference in the rate of reduction can be explained by different mechanisms for the two reactions. The reduction of $[Co(NH_3)_5(OH)]^{2+}$ proceeds via inner-sphere mechanism: Co(II) complexes are labile (see Fig. 21.1) whereas $[Co(NH_3)_5(OH)]^{2+}$ has OH^- ligand that can serve as a bridging ligand. The $[Co(NH_3)_5(H_2O)]^{3+}$ has no bridging ligands and the only mechanistic pathway for the electron-transfer is outer sphere.

On the other hand, both reactions with $[Ru(NH_3)_6]^{2+}$ as a reducing agent likely proceed via the same mechanism, the outer-sphere mechanism because Ru(II) complex, being a complex of the second row transition element with high LFSE, is more inert than Co(II) complex.

E21.11 Using the Marcus cross-relation (Equation 21.16), we can calculate the rate constants. In this equation $[k_{12} = [k_{11}\cdot k_{22}\cdot K_{12}\cdot f_{12}]^{1/2}$, the values of k_{11} and k_{22} can be obtained from Table 21.13. We can assume f_{12} to be unity. The redox potential data allows us to calculate K_{12} because $E° = [RT/\nu F]\ln K$. The value of $E°$ can be calculated by subtracting the anodic reduction potential (the Cr^{3+}/Cr^{2+} couple serves as the anode) from the cathodic one.

a) k_{11} (Cr^{3+}/Cr^{2+}) = 1×10^{-5} $dm^3\,mol^{-1}\,s^{-1}$; k_{22} (Ru^{3+}/Ru^{2+} for the hexamine complex) = 6.6×10^3 $dm^3\,mol^{-1}\,s^{-1}$; f_{12} = 1; $K_{12} = e^{[nF\,\varepsilon^o/RT]}$ where ε^o = 0.07 V – (–0.41V) = 0.48 V; n = 1; F = 96485 C; R = 8.31 J $mol^{-1}K^{-1}$ and T = 298 K. Using these values, we get $K_{12} = 1.32 \times 10^8$. Substitution of these values in the Marcus-Cross relationship gives $k_{12} = 2.95 \times 10^3$ $dm^3mol^{-1}s^{-1}$.

b) $k_{11}(Cr^{3+}/Cr^{2+}) = 1\times10^{-5}$ $dm^3mol^{-1}s^{-1}$; $k_{22}(Fe^{3+}/Fe^{2+}$, aqua complex) = 1.1 $dm^3mol^{-1}s^{-1}$; f_{12} = 1; $K_{12} = e^{[\nu F\,E\circ/RT]}$ where $E°$ = 0.77 V – (–0.41V) = +1.18 V; ν = 1; F = 96485 C mol^{-1}; R = 8.31 $Jmol^{-1}K^{-1}$ and T = 298 K. Using these values, we get $K_{12} = 9.26 \times 10^{19}$. Substitution of these values in the Marcus cross-relation gives $k_{12} = 3.19 \times 10^7$ $dm^3mol^{-1}s^{-1}$.

c) k_{11} (Cr^{3+}/Cr^{2+}) = 1×10^{-5} $dm^3mol^{-1}s^{-1}$; k_{22} (Ru^{3+}/Ru^{2+} for the bpy complex) = 4×10^8 $dm^3mol^{-1}s^{-1}$; f_{12} = 1; $K_{12} = e^{[\nu F\,E\circ/RT]}$ where $E°$ = 1.26 V – (–0.41V) = 1.67 V; ν = 1; F = 96485 C mol^{-1}; R = 8.31 $Jmol^{-1}K^{-1}$ and T = 298 K. Using these values, we get $K_{12} = 1.81 \times 10^{28}$. Substitution of these values in the Marcus cross-relation gives $k_{12} = 8.51 \times 10^{15}$ $dm^3mol^{-1}s^{-1}$.

Note: The assumption that f_{12} = 1 is used in all cases; however, a more precise value would be needed for cases (b) and (c) because of higher values of the equilibrium constant.

To compare the obtained value, we first note that k_{11} is the same for all three reactions because the reducing agent is the same and that we approximated f_{12} to be 1. Thus, the differences lie in the reduction potential differences (essentially K_{12} with all reactions being one electron processes) and k_{22} values. Although the iron aqua complexes have a slower self-exchange rate than Ru hexamine ones, the $E_{red} - E_{ox}$ difference (and hence larger K_{12} value) for the reduction of $[Fe(H_2O)_6]^{3+}$ is large enough (and hence K_{12}) to significantly influence the reaction rate with Fe complex. In the case of Ru bpy complexes both the reduction potential difference and the self-exchange rate are large and this reaction has the highest k_{12}.

E21.12 The intense band at ~250 nm is an LMCT transition (specifically a Cl^--to-Cr^{3+} charge transfer). Irradiation at this wavelength should produce a population of $[CrCl(NH_3)_5]^{2+}$ ions that contain Cr^{2+} ions and Cl atoms instead of Cr^{3+} ions and Cl^- ions. Irradiation of the complex at wavelengths between 350 and 600 nm will not lead to photoreduction. The bands that are observed between these two wavelengths are ligand field transitions: the electrons on the metal are rearranged, and the electrons on the Cl^- ion are not involved.

Chapter 22 d-Metal Organometallic Chemistry

Self-Tests

S22.1 A Mo atom (group 6) has six valence electrons, and each CO ligand is a two-electron donor. Therefore, the total number of valence electrons on the Mo atom in this compound would be 6 + 7(2) = 20. Since organometallic compounds with more than 18 valence electrons on the central metal are unstable, $[Mo(CO)_7]$ is *not* likely to exist. On the other hand, the compound $[Mo(CO)_6]$, with exactly 18 valence electrons, is very stable.

S22.2 For the donor-pair method, treat Cl as a chloride anion, Cl^-, and $CH_2{=}CH_2$ as a neutral, two-electron donor as stated in the exercise (and Table 22.2). Considering that the anion of Zeise's salt has –1overall charge, the charge on Pt centre must be +2. Since Pt has 10 valence electrons, Pt(II) must have eight and electronic configuration d^8. Then, the electron count is 8 (from Pt(II)) + 3×2e (from 3 Cl^-) + 1×2e (from $CH_2{=}CH_2$) = 16 electrons. This is a common electron count for d^8 square planar complexes like this one.

S22.3 The formal name of $[Ir(Br)_2(CH_3)(CO)(PPh_3)_2]$ is dibromidocarbonylmethylbis(triphenylphosphine)iridium(III).

S22.4 $Fe(CO)_5$ will have the higher CO stretching frequency and the longer bond. As noted in Example 22.4, PEt_3 is a good σ donor and causes increased M→CO backbonding, a lower CO stretching frequency, and a shorter Fe-C bond.

S22.5 **a) $[(\eta^6\text{-}C_7H_8)Mo(CO)_3]$ (54).** The η^6-C_7H_8 provides six electrons, as does a formally neutral Mo atom. Each carbonyl provides another two electrons, giving a total of 18.

b) $[(\eta^7\text{-}C_7H_7)Mo(CO)_3]^+$(56)? The η^7-$C_7H_7^+$ group provides six electrons, leaving a formally neutral Mo atom and the three carbonyl groups each providing a further six, giving a total of 18.

S22.6 Consider the reactions of carbonyl complexes discussed in Section 22.18. The Mn–Mn bond in the starting material, $[Mn_2(CO)_{10}]$, can be reductively cleaved with sodium, forming $Na[Mn(CO)_5]$:

$$Mn_2(CO)_{10} + 2Na \rightarrow 2Na[Mn(CO)_5].$$

The anionic carbonyl complex, $[Mn(CO)_5]^-$, is a relatively good nucleophile. When treated with CH_3I, it displaces I^- to form $[Mn(CH_3)(CO)_5]$:

$$Na[Mn(CO)_5] + CH_3I \rightarrow [Mn(CH_3)(CO)_5] + NaI.$$

Many alkyl-substituted metal carbonyls undergo a migratory insertion reaction when treated with basic ligands. The alkyl group (methyl in this case) migrates from the Mn atom to an adjacent C atom of a CO ligand, leaving an open coordination site for the entering group (PPh_3 in this case) to attack:

$$[Mn(CH_3)(CO)_5] + PPh_3 \rightarrow [Mn(COCH_3)(CO)_4(PPh_3)].$$

S22.7 The CO stretching bands at 1857 cm^{-1} and 1897 cm^{-1} are both lower in frequency than typical terminal CO ligands (recall that for terminal CO ligands, ν(CO) > 1900 cm^{-1}). Therefore, it seems likely that $[Ni_2(\eta^5\text{–}Cp)_2(CO)_2]$ only contains bridging CO ligands. The presence of two bands suggests that the bridging CO ligands are probably *not* colinear because only one band would be observed if they were.

S22.8 The neutral ferrocene contains 18 valence electrons (six from Fe^{2+} and 12 from the two Cp^- ligands). The MO diagram for ferrocene is shown in Figure 22.13. The 18 electrons will fill the available molecular orbitals up to the second a_1' orbital. Since this orbital is the highest occupied molecular orbital (HOMO), oxidation of ferrocene will result in removal of an electron from it, leaving the 17-electron ferricinium cation, $[Fe(\eta^5\text{–}Cp)_2]^+$. If this orbital were strongly bonding, removal of an electron would result in weaker Fe–C bonds. If this orbital were strongly antibonding, removal of an electron would result in stronger Fe–C bonds. However, this orbital is essentially nonbonding (see Figure 22.13). Therefore, oxidation of $[Fe(\eta^5\text{–}Cp)_2]$ to $[Fe(\eta^5\text{–}Cp)_2]^+$ will not produce a substantial change in the Fe–C bond order or the Fe–C bond length.

S22.9 There are four relevant pieces of information provided. First, the fact that $[Fe_4(Cp)_4(CO)_4]$ is a highly coloured compound suggests that it contains metal–metal bonds. Second, the composition can be used to determine the cluster valence electron count, which can be used to predict which polyhedral structure is the likely one:

$(Fe^+)_4$	$4(7e^-)$	= 28 valence e^-
$(Cp^-)_4$	$4(6e^-)$	= 24 valence e^-
$(CO)_4$	$4(2e^-)$	= 8 valence e^-
Total		= 60 valence e^- (a tetrahedral cluster)

Third, the presence of only one line in the ^1H NMR spectrum suggests that the Cp ligands are all equivalent and are η^5. Finally, the single CO stretch at 1640 cm^{-1} suggests that the CO ligands are triply bridging. Also, the facts that there is only one line in ^1H-NMR and only one CO stretch suggest a structure of high symmetry (otherwise both NMR and IR spectra would show more lines). A likely structure for $[Fe_4Cp_4(CO)_4]$ is shown below.

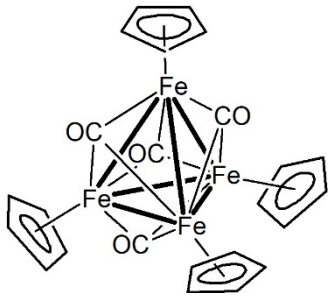

The tetrahedral Fe_4 core of this cluster exhibits six equivalent Fe–Fe bond distances and corresponds to the CVE count from above. Each Fe atom has a Cp ligand with η^5 bonding mode, each able to freely rotate around Fe–Cp bond even at low temperatures (hence one line in ^1H NMR), and each of the four triangular faces of the Fe_4 tetrahedron are capped by a triply bridging CO ligand—the CO ligands are all symmetrical and give one IR stretch.

S22.10 Since $[Mo(CO)_3L_3]$ is a highly substituted complex, the effects of steric crowding must be considered. The steric crowding is particularly important in this case because six-coordinate tricarbonyl complexes adopt a *fac* geometry —all three L ligands would be "squeezed" forming one side of the coordination octahedron. In this case, the two ligands should be very similar electronically but very different sterically. The cone angle for $P(CH_3)_3$, given in Table 22.11, is 118°. The cone angle for $P(t\text{-}Bu)_3$, also given in the table, is 182°. Therefore, because of its smaller size, PMe_3 would be preferred.

S22.11 Fluorenyl compounds are more reactive than indenyl because fluorenyl compounds have two aromatic resonance forms when they bond in the η^3 mode.

S22.12 The starting, six-coordinate palladium compound is an 18-electron Pd(IV) species. The four-coordinate product is a 16-electron Pd(II) species. The decrease in both coordination number and oxidation number by 2 identifies the reaction as a reductive elimination.

S22.13 The ethyl group in $[Pt(PEt_3)_2(Et)(Cl)]$ is prone to β-hydride elimination giving a hydride complex with the loss of ethene, whereas the methyl group in $[Pt(PEt_3)_2(Me)(Cl)]$ is not.

S22.14 In the case of cyclohexene, only one hydroformylation product is possible: cyclohexanecarboxaldehyde. Unlike the unsaturated compounds mentioned in the text and in Example 25.1, cyclohexene, due to its cyclic structure, cannot produce linear and branched isomers.

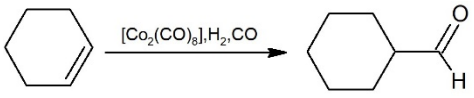

S22.15 The complex $[RhH(CO)(PPh_3)_3]$ is an 18-electron species that must lose a phosphine ligand before it can enter the catalytic cycle:

$$\underset{(18\ e^-)}{RhH(CO)(PPh_3)_3} \rightleftharpoons \underset{(16\ e^-)}{RhH(CO)(PPh_3)_2} + PPh_3$$

The coordinatively and electronically unsaturated complex $[RhH(CO)(PPh_3)_2]$ can add the alkene that is to be hydroformylated. Added phosphine will shift the above equilibrium to the left, resulting in a lower concentration of the catalytically active 16-electron complex. Thus, you can predict that the rate of hydroformylation will be decreased by added phosphine.

S22.16 The polymerization of mono-substituted alkenes introduces sterogenic centres along the carbon chain at every other position. Without R groups attached to the Zr centre there is no preference for specific binding of new alkenes during polymerization and thus the repeat is random or atactic (shown below).

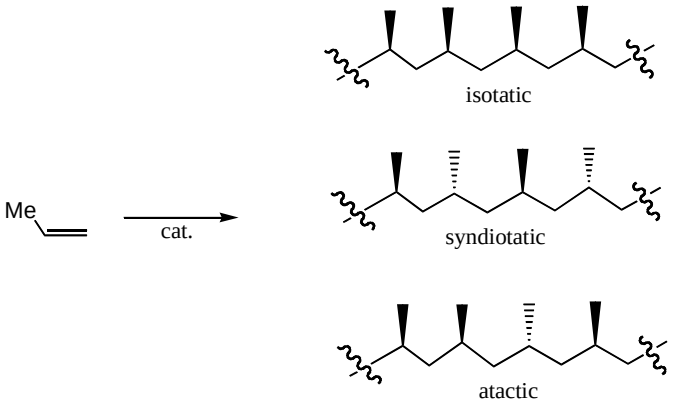

As you can see, the atactic is the most random polymer, meaning that nothing is driving the stereochemistry of the polymer. $[Cp_2ZrCl_2]$ has simple cyclopentadienes as ancillary ligands, which generally do not have enough steric bulk to drive the formation of a specific isomer; therefore, primarily atactic polypropene is produced. Placing bulking alkyl groups on the Cp^- rings offers one way to obtain a specific geometry and thus mediate the properties of polypropene.

Exercises

E22.1 **a)** [**$Fe(CO)_5$**]. Pentacarbonyliron(0), $18e^-$.

b) **[$Mn_2(CO)_{10}$].** Decacarbonyldimanganese(0), $18e^-$.

c) [**$V(CO)_6$**]. Hexcarbonylvanadium(0), $17e^-$; can be easily reduced to $[V(CO_6)]^-$.

d) **[$Fe(CO)_4]^{2-}$.** Tetracarbonylferrate(II), $18e^-$.

e) [**$La(\eta^5\text{-}Cp^*)_3$**]. Tris(pentamethylcyclopentadienyl)lanthanum(III), $18e^-$.

f) [**$Fe(\eta^3\text{-allyl})(CO)_3Cl$**]. η^3-allyltricarbonylchloridoiron(II), $18e^-$.

g) **[$Fe(CO)_4(PEt_3)$].** Tetracarbonyltriethylphosphineiron(0) $18e^-$.

h) [**$Rh(CO)_2(Me)(PPh_3)$**]. Dicarbonylmethyltriphenylphosphinerhodium(I),$16e^-$; a square planar complex, undergoes oxidative addition easily.

i) [**$Pd(Cl)(Me)(PPh_3)_2$**]. Chloridomethylbis(triphenylphosphine)palladium(II), $16e^-$; a square planar complex, undergoes oxidative addition easily.

j) [**$Co(\eta^5\text{-}C_5H_5)(\eta^4\text{-}C_4Ph_4)$**]. η^5-cyclopentadienyl-η^4-tetraphenylcyclobutadienecobalt(I), $18e^-$.

k) $[Fe(\eta^5\text{-}C_5H_5)(CO_2)]^-$. η^5-cyclopentadienyldicarbonylferrate(0), $18e^-$.

l) $[Cr(\eta^6\text{-}C_6H_6)(\eta^6\text{-}C_7H_8)]$. η^6-benzene-η^6-cycloheptatrienechromium(0), $18e^-$.

m) $[Ta(\eta^5\text{-}C_5H_5)_2Cl_3]$. Trichloridobis($\eta^5$-cyclopentadineyl)tanatalum(V), $18e^-$.

n) $[Ni(\eta^5\text{-}C_5H_5)NO]$. η^5-cyclopentadineylnitrosylnickel(II),$16e^-$; a rather reactive complex.

E22.2

a) C_2H_4? Ethylene coordinates to d-block metals in only one way, using its π-electrons to form a metal–ethylene σ-bond (there may also be a significant amount of back donation if ethylene is substituted with electron-withdrawing groups; see Section 22.9). Therefore, C_2H_4 is always η^2.

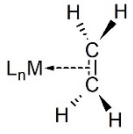

b) Cyclopentadienyl? This is a very versatile ligand that can be η^5 (a six-electron donor in the donor-pair method for electron counting), η^3 (a four-electron donor similar to simple allyl ligands), or η^1 (a two-electron donor similar to simple alkyl and aryl ligands). These three bonding modes are shown below.

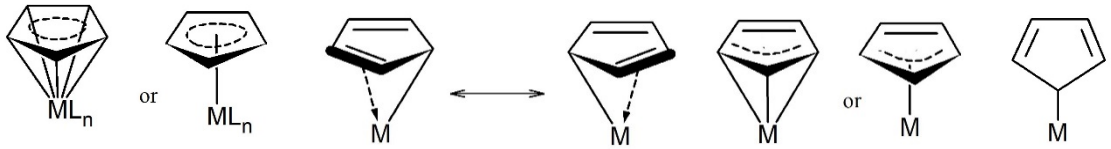

η^5–C_5H_5 η^3–C_5H_5 η^1-C_5H_5

c) C_6H_6? This is also a versatile ligand, which can form η^6, η^4, and η^2 complexes. In such complexes, the ligands are, respectively, six-, four-, and two-electron donors. The structures are very similar as the cyclopentadienyl ones above–there is one extra CH group in the ring.

d) Cyclooctadiene? This ligand can form η^2 (two-electron donor) and η^4 (four-electron donor, shown below) complexes.

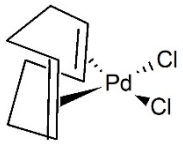

e) Cyclooctatetraene? This ligand contains four C=C double bonds, any combination of which can coordinate to a d-block (or f-block) metal. Thus *cyclo*-C_8H_8 can be η^8 (an eight-electron donor), η^6 (a six-electron donor), η^4 (a four-electron donor, very similar to the one above for cyclooctadiene), and η^2 (a two-electron donor, in which it would resemble an η^2-ethylene complex, except that three of the four C=C double bonds would remain uncoordinated).

E22.3 As discussed in Section 22.18, the two principal methods for the preparation of simple metal carbonyls are (1) direct combination of CO with a finely divided metal and (2) reduction of a metal salt under CO pressure with a presence of a reducing agent. Two examples are shown below, the preparation of hexacarbonylmolybdenum(0) and octacarbonyldicobalt(0). Other examples are given in the text.

(1) $Mo(s) + 6CO(g) \rightarrow [Mo(CO)_6](s)$ (high temperature and pressure required; the product sublimes easily)

(2) $2CoCO_3(s) + 2H_2(g) + 8CO(g) \rightarrow [Co_2(CO)_8](s) + 2CO_2 + 2H_2O$

The reason that the second method is preferred is kinetic, not thermodynamic. The atomization energy (i.e., sublimation energy) of most metals is simply too high for the first method to proceed at a practical rate.

E22.4 **a) $[Mo(PF_3)_3(CO)_3]$ 2040, 1991 cm^{-1} versus $[Mo(PMe_3)_3(CO)_3]$ 1945, 1851 cm^{-1}.** The two CO bands of the trimethylphosphine complex are 100 cm^{-1} or more lower in frequency than the corresponding bands of the

trifluorophosphine complex because PMe_3 is a σ-donor ligand, whereas PF_3 is a strong π-acid ligand (PF_3 is the ligand that most resembles CO in π acidity). The CO ligands in $[Mo(PF_3)_3(CO)_3]$ have to compete with the PF_3 ligands for electron density from the Mo atom for back donation. Therefore, less electron density is transferred from the Mo atom to the CO ligands in $[Mo(PF_3)_3(CO)_3]$ than in $[Mo(PMe_3)_3(CO)_3]$. This makes the Mo–C bonds in $[Mo(PF_3)_3(CO)_3]$ weaker than those in $[Mo(PMe_3)_3(CO)_3]$, but it also makes the C–O bonds in $[Mo(PF_3)_3(CO)_3]$ stronger than those in $[Mo(PMe_3)_3(CO)_3]$, and stronger C–O bonds will have higher CO stretching frequencies.

b) $[MnCp(CO)_3]$ 2023, 1939 cm^{-1} vs. $[MnCp^*(CO)_3]$ 2017, 1928 cm^{-1}? The two CO bands of the Cp* complex are slightly lower in frequency than the corresponding bands of the Cp complex. Recall that the Cp* ligand is η^5-C_5Me_5 (pentamethylcyclopentadienyl). Due to the presence of five electron donating CH_3 groups, this ligand is a stronger electron donor than unsubstituted Cp (the inductive effect of the five methyl groups). Therefore, the Mn atom in the Cp* complex has a greater electron density than in the Cp complex, and hence there is more back-donation to the CO ligands in the Cp* complex than in the Cp complex. As explained in part **(a)** above, more back-donation leads to lower stretching frequencies.

E22.5 The 18-electron $[W(CO)_6]$ complex undergoes ligand substitution by a dissociative mechanism. The rate-determining step involves cleavage of a relatively strong W–CO bond. In contrast, the 16-electron $[Ir(CO)Cl(PPh_3)_2]$ complex undergoes ligand substitution by an associative mechanism, which does not involve Ir–CO bond cleavage in the activated complex. Accordingly, $[IrCl(CO)(PPh_3)_2]$ undergoes faster exchange with ^{13}CO than does $[W(CO)_6]$.

E22.6 **a)** In $[W(\eta^6\text{–}C_6H_6)(CO)_n]$ $n = 3$ (W contributes six electrons and the benzene ring gives six electrons; three carbonyls at two electrons each gives us 18 electrons for the complex);

b) In $[Rh(\eta^5\text{–}C_5H_5)(CO)_n]$ $n = 2$ (Rh^+ contributes eight electrons and the Cp^- ring gives six electrons; two COs at two electrons each yield an 18-electron complex;

c) In $[Ru_3(CO)_n]$ $n = 12$ (This is a cluster compound with three Ru atoms in the centre. Table 22.9 predicts a CVE count of 48 electrons. Each Ru contributes eight electrons, giving 24 electrons; to reach 48 we need 12 COs that each contribute two electrons.)

E22.7 The product of the first reaction contains a –C(=O)Ph ligand formed by the nucleophilic attack of Ph^- on one of the carbonyl C atoms:

$$[Mo(CO)_6] + PhLi \rightarrow Li[Mo(CO)_5(C(O)Ph)].$$

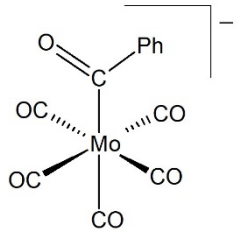

The most basic site on this anion is the acyl oxygen atom, and it is the site of attack by the methylating agent $CH_3OSO_2CF_3$:

$$Li[Mo(CO)_5(COPh)] + CH_3OSO_2CF_3 \rightarrow [Mo(CO)_5(C(OCH_3)Ph)] + LiSO_3CF_3.$$

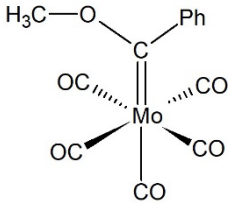

The final product is a carbene (alkylidene) complex. Since the carbene C atom has an oxygen-containing substituent, it is an example of a Fischer carbene (see Section 22.15). The structures of two reaction products are shown above.

E22.8 Suggest syntheses of (a) and (b)?

a) $[Mo(\eta^7\text{-}C_7H_7)(CO)_3]BF_4$ from $[Mo(CO)_6]$. Reflux $[Mo(CO)_6]$ with cycloheptatriene to give $[Mo(\eta^6\text{-}C_7H_8)(CO)_3]$; treat this product with the trityl tetrafluoroborate to abstract a hydride from coordinated cycloheptatriene and give the final $[Mo(\eta^7\text{-}C_7H_7)(CO)_3]BF_4$.

$$[Mo(CO)_6] + C_7H_8 \rightarrow [Mo(\eta^6\text{-}C_7H_8)(CO)_3] + 3CO$$

$$[Mo(\eta^6\text{-}C_7H_8)(CO)_3] + [CPh_3][BF_4] \rightarrow [Mo(\eta^7\text{-}C_7H_7)(CO)_3][BF_4] + HCPh_3.$$

b) $[IrCl_2(COMe)(CO)(PPh_3)_2]$ from $[IrCl(CO)(PPh_3)_2]$. React $[IrCl(CO)(PPh_3)_2]$ with MeCl to give $[IrMeCl_2(CO)(PPh_3)_2]$ (oxidative addition) and then expose to CO atmosphere to induce the $–CH_3$ group migration and produce $[IrCl_2(COMe)(CO)(PPh_3)_2]$:

$$[IrCl(CO)(PPh_3)_2] + MeCl \rightarrow [IrMeCl_2(CO)(PPh_3)_2]$$

$$[IrMeCl_2(CO)(PPh_3)_2] + CO \rightarrow [IrCl_2(COMe)(CO)(PPh_3)_2].$$

E22.9 In either case compounds formed are tetraalkyl titanium(IV) complexes, TiR_4. Notice that neither the methyl or trimethylsilyl groups have β hydrogens. Thus, unlike $[TiEt_4]$, $[TiMe_4]$ and $[Ti(CH_2SiMe_3)_4]$, cannot undergo a low energy β-hydride elimination decomposition reaction.

E22.10 Give the equation for a workable reaction for the conversion of

a) $[Fe(\eta^5\text{-}C_5H_5)_2]$ to $[Fe(\eta^5\text{-}C_5H_5)(\eta^5\text{-}C_5H_4COCH_3)]$. The Cp^- rings in cyclopentadienyl complexes behave like simple aromatic compounds such as benzene, and so are subject to typical reactions of aromatic compounds such as Freidel-Crafts alkylation and acylation. If you treat ferrocene with acetyl chloride and some aluminum(III) chloride as a catalyst, you will obtain the desired compound:

$$[Fe(\eta^5\text{-}C_5H_5)_2] + CH_3COCl \xrightarrow{AlCl_3} [Fe(\eta^5\text{-}C_5H_5)(\eta^5\text{-}C_5H_4COCH_3)] + HCl$$

b) $[Fe(\eta^5\text{-}C_5H_5)_2]$ to $[Fe(\eta^5\text{-}C_5H_5)(\eta^5\text{-}C_5H_4CO_2H)]$. The following sequence of reaction is the best route:

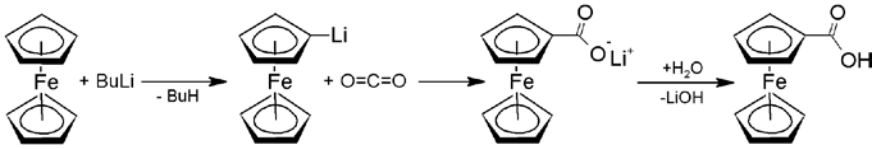

E22.11 Protonation of $[FeCp_2]$ at iron does not change its number of valence electrons: both $[FeCp_2]$ and $[FeCp_2H]^+$ are 18-electron species:

$[FeCp_2]$		**$[FeCp_2H]^+$**	
Fe^{2+}	6 electrons	Fe^{3+}	5 electrons
2 Cp^- (6 electrons each)	12 electrons	2 Cp^- (6 electrons each)	12 electrons
		H^-	2 electrons
		Positive charge	–1 electron
Total	**18 electrons**	**Total**	**18 electrons**

Since $[NiCp_2]$ is a 20-electron complex, the hypothetical metal-protonated species $[NiCp_2H]^+$ would also be a 20-electron complex. On the other hand, protonation of $[NiCp_2]$ at a Cp carbon atom produces the 18-electron

complex $[NiCp(\eta^4\text{-}C_5H_6)]^+$. Therefore, the reason that the Ni complex is protonated at a carbon atom is that a more stable (i.e., 18-electron) product is formed.

E22.12 One of the possible routes involves initial slip of Cp^- ring from η^5 to η^3 bonding mode creating a 16-electron complex that can coordinate a phosphine ligand producing new 18-electron $[Mo(\eta^3\text{-}C_5H_5)(CO)_3Me(PR_3)]$ complex. This complex loses one CO ligand giving a new 16-electron intermediate $[Mo(\eta^3\text{-}C_5H_5)(CO)_2Me(PR_3)]$ that converts to the stable 18-electron complex $[Mo(\eta^5\text{-}C_5H_5)(CO)_2Me(PR_3)]$. The steps of this route are shown below:

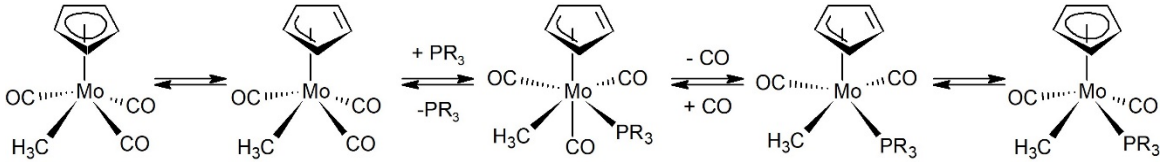

The second route starts with CO insertion (or methyl group migration) to produce a 16-electron acyl complex. This complex can coordinate one PR_3 ligand to give an 18-electron species, which if heated can lose one CO ligand and undergo reverse alkyl group migration. The steps for this route are outlined below:

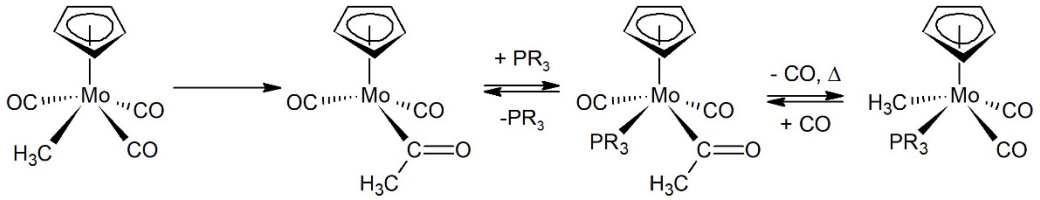

E22.13 **a) [$Co_3(CO)_9CH$] → OCH_3, $N(CH_3)_2$, or $SiCH_3$.** Isolobal groups have the same number and shape of valence orbitals *and* the same number of electrons in those orbitals. The CH group has three sp^3 hybrid orbitals that contain a single electron each. The $SiCH_3$ group has three similar orbitals, similarly occupied, so it is isolobal with CH and would probably replace CH in $[Co_3(CO)_9CH]$ to form $[Co_3(CO)_9SiCH_3]$. In contrast, the OCH_3 and $N(CH_3)_2$ groups are not isolobal with CH. Instead, they have, respectively, three sp^3 orbitals that contain a pair of electrons each and two sp^3 orbitals that contain a pair of electrons each.

b) [$(OC)_5Mn$$\mathbf{Mn(CO)_5}$] → I, CH_2, or CCH_3? The $Mn(CO)_5$ group has a single σ-type orbital that contains a single electron. An iodine atom is isolobal with it because I atom also has a singly occupied s orbital. Therefore, you can expect the compound $[Mn(CO)_5I]$ to be reasonably stable. In contrast, the CH_2 and CCH_3 are not isolobal with $Mn(CO)_5$. The CH_2 group has either a doubly occupied σ orbital and an empty p orbital or a singly occupied σ orbital and a singly occupied p orbital. The CCH_3 group has three singly occupied σ orbitals (note that it is isolobal with $SiCH_3$).

E22.14 The catalytic cycle for homogeneous hydrogenation of alkenes by Wilkinson's catalyst, $[RhCl(PPh_3)_3]$, is shown in Figure 22.18. For the olefin substrate to coordinate to the Rh centre in complex **C** (a 16- electron species), complex **B** (an 18-electron species) must first lose one PPh_3 ligand. Although this is not usually shown when depicting catalytic cycles, we have to keep in mind that all steps are (generally) reversible, and complex **C** and free PPh_3 are in equilibrium with complex **B**. Increasing the concentration of PPh_3 shifts the equilibrium toward complex **B,** which is not able to bind the olefin and the hydrogenation rate will drop.

E22.15 The catalytic cycle for the formation of both *n* (linear) and *iso* (branched) products is shown below. The starting point of the cycle is the active catalyst $[HCo(CO)_4]$ formed from hydrogenolysis of $[Co_2(CO)_8]$. The linear product (*n* isomer) is butanal, whereas the branched product (*iso* isomer) is 2-methylpropanal. The selectivity step is the hydride migration onto the coordinated prop-1-en in $[HCo(CO)_4(H_2C{=}CHCH_3)]$ complex. Note that migration can produce either primary (outer path) or secondary (inner path) alkyl coordinated to the Co centre.

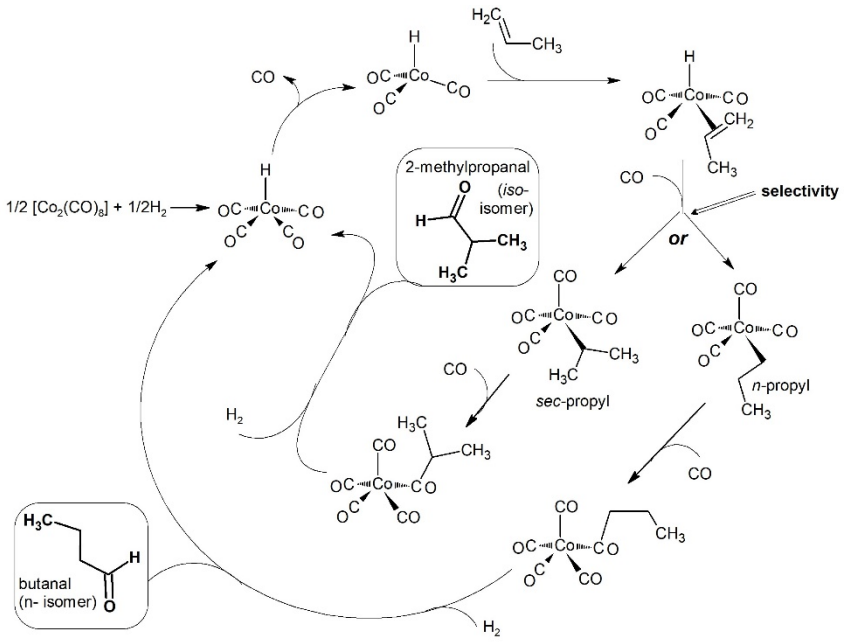

E22.16 **a)** Attack by dissolved hydroxide**.**

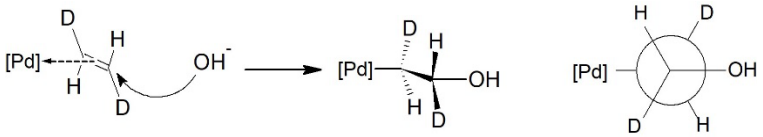

b) Attack by coordinated hydroxide.

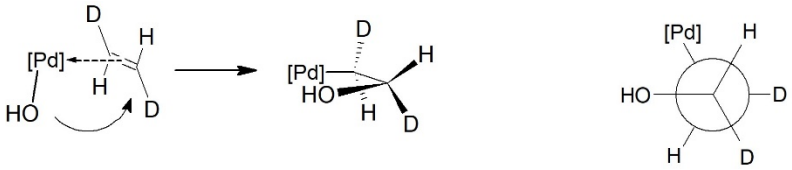

c) Differentiate of the stereochemistry. Yes. Detailed stereochemical studies indicate that the hydration of the alkene-Pd(II) complexes occurs by attack of water from the solution on the coordinated ethene rather than the insertion of coordinated OH.

Chapter 23 The f-Block Metals

Self-Tests

S23.1 Consult Table 23.3 to make sure you are starting with correct electronic configurations of the elements listed. The table below lists the spectroscopic terms for Ln^{2+} and Ln^{3+}. The procedure is outlined for Pr^{2+} and Pr^{3+} only since the other term symbols are derived the same. The table also lists the change in L going from Ln^{2+} to Ln^{3+}.
Pr has an electronic configuration [Xe]$4f^36s^2$; thus Pr^{2+} and Pr^{3+} have electronic configurations [Xe]$4f^3$ and [Xe]$4f^2$ respectively. The three f electrons in Pr^{2+} would share the same $\ell = 3$ quantum number. Their individual m_l and m_s numbers are: $m_\ell = +3$ and $m_s = +½$, $m_\ell = +2$ and $m_s = +½$; $m_\ell = +1$ and $m_s = + ½$. The maximum M_L value is (+3) + (+2) + (+1) = +6 that must come from a state with $L = 6$, an I term. The S value is 3/2 (= + ½ + ½ + ½) with multiplicity $2S+1 = 4$. The term is ^4I. The total angular momentum of a term with $L = 6$ and $S = 3/2$ will be J = 15/2, 6, or 9/2. Finally, the ground state term for Pr^{2+} is $^4I_{9/2}$.

The electronic configuration of Pr^{3+} is $4f^2$ and the maximum M_L value is (+3) + (+2) = 5 giving us $L = 5$ and an H term with $S = 1$, a triplet: ^3H. The total angular momentum can take J values 6, 5 or 4. The term is hence $^3H_4$.

Ln	**Pr**	**Nd**	**Pm**	**Dy**	**Ho**	**Er**
El. Config./[Xe]	$4f^36s^2$	$4f^46s^2$	$4f^56s^2$	$4f^{10}6s^2$	$4f^{11}6s^2$	$4f^{12}6s^2$
Ln^{2+}	**Pr^{2+}**	**Nd^{2+}**	**Pm^{2+}**	**Dy^{2+}**	**Ho^{2+}**	**Er^{2+}**
El. Config./[Xe]	$4f^3$	$4f^4$	$4f^5$	$4f^{10}$	$4f^{11}$	$4f^{12}$
Term	$^4I_{9/2}$	$^5I_4$	$^6H_{5/2}$	$^5I_8$	$^4I_{15/2}$	$^3H_6$
Ln^{3+}	**Pr^3**	**Nd^{3+}**	**Pm^{3+}**	**Dy^{3+}**	**Ho^{3+}**	**Er^{3+}**
El. Config./[Xe]	$4f^2$	$4f^3$	$4f^4$	$4f^9$	$4f^{10}$	$4f^{11}$
Term	$^3H_4$	$^4I_{9/2}$	$^5I_4$	$^6H_{15/2}$	$^5I_8$	$^4I_{15/2}$
Change in L	Decrease	The same	Increase	Decrease	The same	Increase

From the table, we see that the L does not change for ionizations $Nd^{2+}(g) \rightarrow Nd^{3+}(g) + e^-(g)$ and $Ho^{2+}(g) \rightarrow Ho^{3+}(g) + e^-(g)$, a quarter- and three quarter-shell effects—positions where we find small irregularities in I_3.

S23.2 GdO should be a slat-like compound—looking at Figure 23.8 we can see that Gd^{2+} 4f orbitals are significantly lower in energy than its 5d orbital. This means that the occupancy of higher energy 5d orbitals is not favourable making this oxide an insulating one. Considering that gadolinium's second and third ionization energies are close, this oxide should be considered relatively unstable.

S23.3 A bridge is going to be formed if there is a ligand capable of bridging and if metal centres do not have complete coordination. Lanthanoid cations have high coordination numbers and hydride ligands can make bridges, so the fact that the product is a hydride-bridged dimer is not surprising. To prevent bridge formation, and keep hydride ligands we have to find a way to increase the coordination number around Ln^{3+} cation. Considering that these cations are hard cations, a choice of a hard-donor ligand is the best. For example, THF—with oxygen donor atom—could be a good choice. Many Ln^{3+} complexes with coordinated THF are known.

S23.4 From the Frost diagram in Figure 23.17, the most stable oxidation state of uranium in aqueous acid is U^{4+} (i.e., it has the most negative free energy of formation, the quantity plotted on the y axis). However, the reduction potentials for the UO_2^{2+}/UO_2^{+} and UO_2^{+}/U^{4+} couples are quite small, +0.170 and +0.38 V, respectively (hence, the UO_2^{+}/U^{4+} potential is +0.275 V). Therefore, because the O_2/H_2O reduction potential is 1.229 V, the most stable uranium ion is UO_2^{2+} if sufficient oxygen is present:

$$2U^{4+} + O_2 + 2H_2O \rightarrow 2UO_2^{2+} + 4H^+ \qquad E^\circ = +1.229\text{ V} - (+0.275\text{ V}) = +0.0954\text{ V}.$$

S23.4 The e_{2g} interactions are sketched below. Note that this overlap involves a 6d atomic orbital on the actionoid atom and that the overlap is δ type.

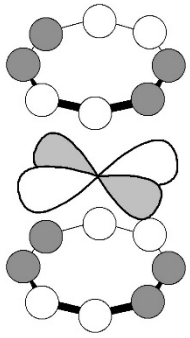

Exercises

E23.1 **a) Balanced equation.** All lanthanoids are very electropositive and reduce water (or protons) to H_2 while being oxidized to the trivalent state. If Ln is used as the symbol for a generic lanthanoid element, the balanced equation is:

$$2Ln(s) + 6H_3O^+(aq) \rightarrow 2Ln^{3+}(aq) + 3H_2(g) + 6H_2O(l).$$

b) Reduction potentials. The reduction potentials for the Ln^{3+}/Ln^0 couples in acid solution range from –1.99 V for europium to –2.38 V for lanthanum, a remarkably self-consistent set of values spanning 15 elements. Since the potential for the H_3O^+/H_2 reduction is 0 V, the $E°$ values for the equation shown in part **(a)** for all lanthanides range from 1.99 to 2.38 V, a very large driving force.

c) Two unusual lanthanides. The usual oxidation state for the lanthanide elements in aqueous acid is +3. There are two lanthanides that deviate slightly from this trend. The first is Ce^{4+}, which, while being a strong oxidizing agent, is kinetically stable in aqueous acid. Since Ce^{3+} is $4f^1$ and Ce^{4+} is $4f^0$, you can see that the special stability of tetravalent cerium is because of its stable $4f^0$ electron configuration. The second deviation is Eu^{2+}, which is a strong reducing agent but exists in a growing number of compounds. Since Eu^{2+} is $4f^7$ and Eu^{3+} is $4f^6$, you can see that the special stability of divalent europium is because of its stable $4f^7$ electron configuration (half-filled f subshell).

E23.2 The unusual oxidation states displayed by two of the lanthanoids, +4 for Ce and +2 for Eu (see Exercise 23.1) were exploited in separation procedures because their charge/radius ratios are very different than those of the typical Ln^{3+} ions. Tetravalent cerium can be precipitated as $Ce(IO_3)_4$, leaving all other Ln^{3+} ions in solution because their iodates are soluble. Divalent europium, which resembles Ca^{2+}, can be precipitated as $EuSO_4$ leaving all other Ln^{3+} ions in solution because their sulfates are soluble.

E23.3 The chemistry of the transition metals is dominated by their ability to access several oxidation states. For example, recall that Mn can have oxidation states from +2 to +7 and that osmium can reach +8. Another characteristic feature of their chemistry is extensive use of d orbitals in bonding. This is similar to the actinoid chemistry—early actinoids also have several oxidation states accessible (consider for example U) and their 6d orbitals are more diffuse than lanthanoid's 5d. Lanthanoids have limited range of oxidation states, mostly 3+, and 5d orbitals are core-like.

E23.4 The reduction potentials for Pu^{4+}/Pu, Pu^{3+}/Pu are –1.25 V and –2.00 V respectively, indicating that Pu metal is going to readily (at least from the thermodynamic point of view) dissolve in HCl. However, the composition of the solution can be complicated and could contain Pu(III), Pu(IV), Pu(V), and even Pu(VI) species because the potentials for the couples Pu(VI)/Pu(V), Pu(V)/Pu(IV), and Pu(IV)/Pu(III) are very similar (ca. +1 V). Addition of F^- to the solution is likely going to precipitate PuF_3, which is insoluble in water, like UF_3.

E23.5 Refer to Resource Section 2 in the online resources for the electronic configuration of neutral atoms.

Tb^{3+} is a $4f^8$ system. Therefore $M_L = +3$ and $S = 3$. The term will be ^7F. The expected term symbol is $^7F_6$.

Nd^{3+} is a $4f^3$ system. Therefore $M_L = +6$ and $S = 3/2$. The term will be ^4I. The term symbol is $^4I_{9/2}$

Ho^{3+} is a $4f^{10}$ system. Therefore $M_L = +6$ and $S = 2$. The term will be ^5I. The term symbol is $^5I_8$.

Er^{3+} is a $4f^{11}$ system. Therefore $M_L = +6$ and $S = 3/2$. The term will be ^4I. The term symbol is $^4I_{15/2}$

Lu^{3+} is a $4f^{14}$ system. Therefore $M_L = 0$ and $S = 0$. The term will be ^1S. The term symbol is $^1S_0$.

Compare your answer with Table 23.5. See also Self-Test 23.1.

E23.6 Apart from the fact that the discovery of a Ln(V) species would open a whole new avenue of chemistry, it would also shake the theoretical foundation of the claim that the lanthanide 4f subshell is rather inert. A good candidate could be Pr. This element is early in the lanthanoid series, meaning that its 4f orbitals are still comparatively high in energy. Also, removal of an electron from Pr(IV), a somewhat stable species, would produce a $4f^0$ electronic configuration for Pr(V), the same $4f^0$ configuration that stabilizes Ce(IV).

E23.7 Stable carbonyl compounds need backbonding from metal orbitals of the appropriate symmetry into the antibonding π MO on CO. Thus, a metal centre has to be electron rich to stabilize M–CO bond. With the lanthanoids, the 5d orbitals are empty, and the 4f orbitals are deeply buried in the inert [Xe] core and cannot participate in bonding.

E23.8 There is a considerable difference between the interactions of the 4f orbitals of the lanthanide ions with ligand orbitals and the 5f orbitals of the actinide ions with ligand orbitals. In the case of the 4f orbitals, interactions with ligand orbitals are negligible. Therefore, splitting of the 4f subshell by the ligands is also negligible and does not vary as the ligands vary. Since the colours of lanthanide ions arise due to 4f–4f electronic transitions, the colours of Eu^{3+} complexes are invariant as a function of ligand. In contrast, the 5f orbitals of the actinide ions interact more strongly with ligand orbitals, and the splitting of the 5f subshell, as well as the colour of the complex, varies as a function of ligand.

E23.9 Similarity in bond lengths between U–O and Os–O bonds implies that U–O bond is of higher order than Os–O bond—if they were of the same order, then U–O should be longer due to the larger U(IV) radius. In Exercise 23.8 we concluded, using MO diagram in Figure 23.18, that U–O bond is 3. Thus, we would expect the Os–O bond order to be lower, about 2. The bond order is lowered because Os(VI) has still two valence electrons (electronic configuration $5d^2$) which would occupy anti-bonding MOs of OsO_2^{2+} fragment and thus lower the bond order.

Chapter 24 Materials Chemistry and Nanochemistry

Self-Tests

S24.1 **a)** $SrTiO_3$ can be prepared from $SrCO_3$ and TiO_2 in 1 : 1 ratio. The two are grinded together and the well-mixed material is heated to the temperature above the temperature of $SrCO_3$ thermal decomposition.

b) $Sr_3Ti_2O_7$ can be prepared in similar manner to $SrTiO_3$ but starting from 3 : 2 stoichiometry ($SrCO_3$: TiO_2); alternatively, it can be prepared from $SrTiO_3$ and SrO in 2 : 1 stoichiometry.

c) $AlPO_4$ is aluminium salt of phosphoric acid (H_3PO_4). Thus, reasonable starting reagents could be $Al(OH)_3$ and H_3PO_4. Considering that aluminium hydroxide is a very weak base and cannot completely deprotonate the acid, just mixing the reagents would not produce the desired product—hydrothermal synthesis should do the trick. To ensure the product is porous, we should add a structure-directing agent, such as tetraalkylammonium hydroxide, to the reaction mixture.

S24.2 Increasing the pressure on a crystal compresses it, reducing the spacing between ions (e.g., subjecting NaCl to a pressure of 24,000 atm reduces the Na–Cl distance from 2.82 Å to 2.75 Å). In a rigid lattice such as β-alumina, larger ions migrate more slowly than smaller ions with the same charge (as discussed in the example). At higher pressures, with smaller conduction plane spacings, *all* ions will migrate more slowly than they do at atmospheric pressure. However, larger ions will be impeded to a greater extent by smaller spacings than will smaller ions. This is because the ratio (radius of migrating ion)/(conduction plane spacing) changes more, per unit change in conduction plane spacing, for a large ion than for a small ion. Therefore, increased pressure reduces the conductivity of K^+ more than that of Na^+ because K^+ is larger than Na^+.

S24.3 In the normal AB_2O_4 spinel structure, the A^{2+} ions (Fe^{2+} in this example) occupy tetrahedral sites and the B^{3+} ions (Cr^{3+} in this example) occupy octahedral sites. The fact that $FeCr_2O_4$ exhibits the normal spinel structure can be understood by comparing the ligand-field stabilization energy of high-spin octahedral Fe^{2+} and octahedral Cr^{3+}. With six d electrons, LFSE = $-0.4\Delta_o$ for high-spin Fe^{2+}. With only three d electrons, LFSE = $-1.2\Delta_o$ for Cr^{3+}. Since the Cr^{3+} ions experience more stabilization in octahedral sites than do the Fe^{2+} ions, the normal spinel structure is more stable than the inverse spinel structure, which would exchange the positions of the Fe^{2+} ions with half of the Cr^{3+} ions.

S24.4 A pure silica analogue of ZSM-5 would contain only weakly Brønsted acidic Si–OH groups and no strongly acidic Al–OH_2 groups found in aluminosilicates. Only strong Brønsted acids can protonate an alkene to form the carbocations that are necessary intermediates in benzene alkylation. Therefore, a pure silica analog of ZSM-5 would not be an active catalyst for benzene alkylation.

S24.5 MCM-41 is a better choice as it has a range of pore sizes from 2 to 10 nm. These can better accommodate QDs with diameters ranging from 2 to 8 nm than typical ZSM-5 with pore sizes of less than 1 nm.

Exercises

E24.1 **a)** $MgCr_2O_4$ can be prepared by heating a 1:1 mixture of $MgCO_3$ (or $Mg(NO_3)_2$) and $(NH_4)_2Cr_2O_7$ at high temperature. Note that thermal decomposition of $(NH_4)_2Cr_2O_7$ produces Cr_2O_3 in a finely divided and reactive form:

$$(NH_4)_2Cr_2O_7(s) \rightarrow N_2(g) + 4H_2O(g) + Cr_2O_3(s).$$

Then

$$Cr_2O_3(s) + MgCO_3(s) \xrightarrow{1400^\circ C} MgCr_2O_4(s).$$

b) $LaFeO_3$ can be prepared by coprecipitating La^{3+} and Fe^{3+} hydroxides and then, after filtration, heat the precipitate and eliminate water:

$$La^{3+}(aq) + Fe^{3+}(aq) + 6OH^{-}(aq) \rightarrow La(OH)_3 \cdot Fe(OH)_3(s) \xrightarrow{450^\circ C} LaFeO_3(s) + 3H_2O(g).$$

Note the low final thermal decomposition temperature as a result of the fine atomic mixing achieved by the initial solution stage.

c) Ta_3N_5 can be prepared heating Ta_2O_5 under a flow of NH_3 at high temperature:

$$3\ Ta_2O_5(s) + 10\ NH_3(g) \xrightarrow{600^\circ C} 2\ Ta_3N_5(s) + 15\ H_2O(g).$$

Note that the equilibrium is pushed to the right by the removal of steam in the gas stream.

d) $LiMgH_3$ can be prepared by heating a molar mixture of LiH and MgH_2 (under hydrogen or an inert gas) in a direct reaction, or by heating a mixture of the elements under hydrogen.

e) This complex fluoride can be prepared from solution of $CuBr_2$ and KF as a precipitate:

$$CuBr_2(aq) + 3\ KF(aq) \rightarrow KCuF_3(s) + 2\ KBr(aq).$$

f) The gallium analogue of zeolite A can be prepared starting from sodium gallate, $NaGaO_2$ (instead of sodium aluminate) and sodium silicate. The reaction would be undertaken hydrothermally in a sealed reaction vessel:

$$12NaGaO_2(s) + 12Na_2SiO_3(aq) \xrightarrow{150^\circ C} \rightarrow Na_{12}[Si_{12}Ga_{12}O_{48}] \cdot nH_2O(s) + 24NaOH(aq).$$

E24.2 The electronic conductivity of the solid increases owing to formation of $(Ni_{1-x}Li_x)O$ containing Ni(III) and a free electron that can hop through the structure from Ni(II) to Ni(III), thus promoting increased conductivity in the structure.

E24.3 A solid solution would contain a random collection of defects, whereas a series of crystallographic shear plane structures would contain ordered arrays of crystallographic shear planes. Because of the lack of long-range order, the solid solution would give rise to an electron micrograph showing a random distribution of shear planes. In addition, the solid solution would not give rise to new X-ray diffraction peaks. In contrast, the ordered phases of the solid on the right would be detectable by electron microscopy and by the presence of a series of new peaks in the X-ray diffraction pattern, arising from the evenly spaced shear planes.

E24.4 The unit cell for ReO_3, which is shown in Figure 24.16(a), is reproduced in the figure on the left below (the O^{2-} ions are the open spheres). As you can see, the structure is very open, with a very large hole in the centre of the cell, and it does appear to be sufficiently open to undergo Na^+ ion intercalation. We can calculate if this is indeed possible if we note that the length of the ReO_3 unit cell, a, can be calculated as $a = 2r(O^{2-}) + 2r(Re^{6+})$. Re^{6+} is six coordinate and, form Resource Section 1, its radius is 55 pm. There is no O^{2-} radius for the coordination two, but we can approximate it with about 140 pm. Then $a = 2\times55$ pm $+ 2\times140$ pm $= 390$ pm. The face diagonal of the cube, d, can be calculated as $d = 2^{1/2}a$ (we are looking at the face diagonal because any cation that would fill the hole would be in contact with larger O^{2-} anions; see figure on the right). Hence d = 1.414×390 pm = 551.5 pm. To really calculate the maximum radius of a metal that can fit in the central hole, we must subtract $2r(O^{2-})$ from d (because that is the part of the diagonal "occupied" by neighbouring O^{2-} ions) and then divide the difference by 2: $r(M^+) = (551.5 \text{ pm} - 2\times140 \text{ pm})/2 = 135.7$ pm. Since the radius of Na^+ (eight coordinate, the maximum provided in Resource Section 1) is 132 pm, we can say that Na^+ can indeed fit inside the hole. An ReO_3 unit cell containing an Na^+ ion (large, heavily shaded sphere) at its centre is shown on the right below. For the 1 : 1 Na:Re ratio the structure type can be described as that of perovskite ($CaTiO_3$).

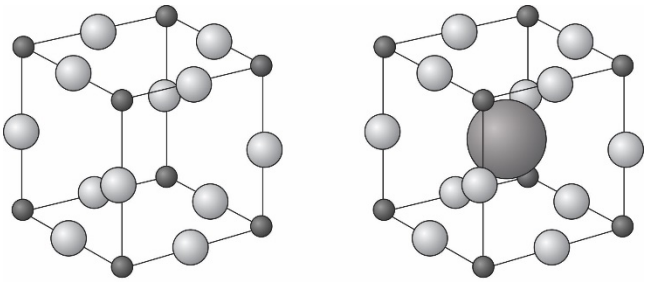

E24.5 Sn^{2+} is smaller than Pb^{2+} so the $ASnI_3$ unit cell is expected to be smaller than $APbI_3$ unit cell. Thus, possible candidates for A^+ cation are Li^+ and Na^+—the smallest unipositive cations.

E24.6 A sulfide with the spinel structure could be $ZnCr_2S_4$ and a fluoride $NiLi_2F_4$.

E24.7 White Ta_2O_5 reacts with ammonia at high temperature to produce red Ta_3N_5:

$$3Ta_2O_5(s) + 10NH_3(g) \rightarrow 2Ta_3N_5\,(s) + 15H_2O\,(g).$$

E24.8 BeO, B_2O_3, and to some extent GeO_2 because they involve metalloid and non-metal oxides. Transition metal and rare earth oxides are typically non–glass-forming oxides, many of which have crystalline phases.

E24.9 The two methods for the preparation of the intercalation compound Li_xTiS_2 ($0 \leq x \leq 1$) are:

(a) direct combination of lithium and TiS_2 at elevated temperatures:

$$Li(g) + TiS_2(s) \rightarrow Li_xTiS_2(s).$$

(b) electrointercalation, with the following process occurring on electrodes:

anodic process: $Li(s) \rightarrow Li^+(aq) + e^-$

cathodic porcess: $TiS_2(s) + x\,Li^+(aq) + x\,e^- \rightarrow Li_xTiS_2$.

E24.10 The structure of Mo_6S_8 unit can be described as a cube of S atoms with an octahedron of Mo atoms inside so that each cube face has an Mo atom in the centre. The Mo_6S_8 units are further bonded via Mo – S bridges. The S atoms in one cube donate an electron pair from a filled p orbital to the empty $4d_{z2}$ orbital on Mo located on a neighbouring cube.

E24.11 The following zeotypes are possible: $(AlP)O_4$, $(BP)O_4$, $(ZnP_2)O_6$.

E24.12 Zeolites are porous alumosilicates. The Al/Si framework defines channels and pores—the dimensions of these pores and channels dictate the molecular selectivity: only molecules of certain shape and size can enter the zeolite framework. This is the basis of their use as molecular sieves. The exchange of Sin^{4+} for Al^{3+} also requires additional cations to be brought inside the framework to balance the charges. If the cation is H^+ (or better H_3O^+) the resulting zeolite behaves as a very strong acid (even more acidic than H_2SO_4). The acidity can be fine-tuned by replacement of some H^+ with other cations (for example lanthanoids). The Brønsted acidity can be converted into Lewis acidity by dehydration. Al^{3+} sites are responsible for this type of acidity. Thus, zeolites are heterogeneous catalysts in which the size selectivity and type of acidity can be designed.

The zeolite structure controls both reactant and product selectivity. Only the reactants of appropriate size and shape can enter the zeolite structure. Similarly, only products of certain shape and size can *exit* the structure. Another way in which zeolite structure can control the outcome of the reaction is through transition-state selectivity: specific orientation (dictated by the pore/channel shape and size) of reactive intermediates determines the products of reaction.

These points have been illustrated in the text (Section 24.13) using zeolite-catalysed isomerization of xylenes.

E24.13 The mass percent of hydrogen in $NaBH_4$ is 10.6%. This is above the range for technical targets (6–9%) and $NaBH_4$ could be a good candidate to consider. The problem, however, is that elevated temperatures for decomposition are required to liberate the hydrogen gas (typically above 500°C).

E24.14 With 18.1% per weight of hydrogen, BeH_2 would be an excellent candidate for hydrogen storage. Unfortunately, this compound is thermodynamically unstable ($\Delta_f H \sim 0$ kJ mol^{-1}) and very easily decomposes to give Be(s) and H_2(g). Consequently, the synthesis of BeH_2 is not straightforward like the synthesis of, for example, MgH_2.

E24.15 The blue colour of the solution is due to the presence of anionic radical S_3^-, identical to that found as S_3^- in lapis lazuli described in Section 24.16. The cause of colour is the excitation of the unpaired electron in the electronic structure. In polysulfide solution, radical anions are very sensitive to O_2 from the atmosphere and upon oxidation the colour is lost.

E24.16 BN > C(diamond) > AlP > InSb. See Sections 3.19, 3.20 and 24.19 for more details.

E24.17 **a) Surface areas.** 1.256×10^3 nm^2 versus 1.256×10^7 nm^2 (a factor of 10^4).

b) Nanoparticles based on size. Recall that nanoparticles are particles or layers with at least one dimension in the 1–100 nm range. Thus, the 10 nm particle can be considered a nanoparticle, whereas the 1000 nm particle cannot.

c) Nanoparticles based on properties. A true nanoparticle should have a localized surface plasmon without characteristic momentum and of high intensity.

E24.18 **a) Steps in solutions synthesis of nanoparticles.** All reacting species and additives must first be solvated; then stable nuclei of nanometer dimensions must be formed from solution and finally growth of particles to the final desired size will occur.

b) Why should the last two steps occur independently? The last two steps should be independent so that nucleation fixes the total number of particles and growth leads to a controlled size and a narrow size distribution.

c) Role of stabilizer molecules. Stabilizers prevent unwanted Ostwald ripening, a process in which smaller particles present in the solution dissolve and the re-solvated material from these particles precipitate again but on the surface of larger particles. The Ostwald ripening decreases the number of particles in the solution and increases size distribution and thus is unwanted process during nanoparticle synthesis.

E24.19 **a) Core-shell nanoparticle diagram.** A schematic of the core and shell of the nanoparticle is shown below.

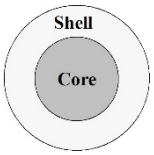

b) Production. i) *Solution based method*: first grow the core in solution and then add the additive and material for the growth of shell. ii) *Vapor-deposition method*: first deposit the material for the core and then the material for the shell.

c) Use. In biosensing, the dielectric property of the shell can control the surface plasmon of the core, while the shell can be affected by the environment. In drug delivery, the shell could react with a specific location and the core could be used as a treatment (drug).

E24.20 Special measures are required in heterogeneous catalysis to ensure that the reactants achieve contact with catalytic sites. For a given amount of catalyst, as the surface area increases, the number of catalytically active sites increases. A thin foil of platinum-rhodium will not have as much surface area as an equal amount of small particles finely dispersed on the surface of a ceramic support. The diagram below shows this for a "foil" of catalyst that is 1000 times larger in two dimensions than in the third dimension (i.e., the thickness is 1; note that the diagram is not to scale). If the same a mount of catalyst is broken into cubes that are 1 unit on a side, the surface area of the catalyst is increased by nearly a factor of three.

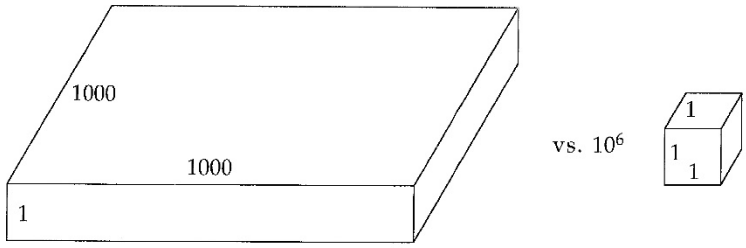

E24.21 The reduction of hydrogen ions to H_2 on Pt surface probably involves the formation of the surface hydride species. Dissociation of H_2 by reductive elimination would complete the catalytic cycle. However, platinum not only has a strong tendency to chemisorb H_2, but it also has a strong tendency to chemisorb CO. If the surface of platinum is covered with CO, the number of catalytic sites available for H^+ reduction will be greatly diminished and the rate of H_2 production will decrease.

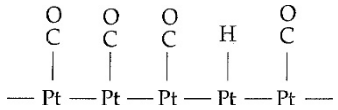

Chapter 25 Biological Inorganic Chemistry

Self-Tests

S25.1 Uncomplexed Fe^{2+} is present at very low concentrations (approximately 10^{-7} M). By contrast, Fe^{3+} is strongly complexed (relative to Fe^{2+}) by highly specific ligands such as ferritin and by smaller polyanionic ligands, particularly citrate. Free Fe^{2+} is therefore easily oxidized.

S25.2 The protein's tertiary structure can place any atom or group in a suitable position for axial coordination. Thus, the protein folding is responsible for bringing the unusual methionine sulfur atoms (recall that sulfur is a soft donor) in axial sites. This prevents water molecules (which would be the natural choice for Mg^{2+}, a hard cation) from occupying the axial sites.

S25.3 Blood plasma contains 0.1 M Na^+ but very little K^+; the opposite is true inside cells (see Table 25.1). This differential results in an electrical potential that is used to drive reactions. If a patient was given an intravenous fluid containing KCl instead of NaCl, the potential across the cell membrane would collapse, with severe consequences.

S25.4 Calmodulin does not bind to the pump unless Ca^{2+} is coordinated to it. As the Ca^{2+} concentration increases in the cell, the Ca-calmodulin complex is formed. The binding of this Ca-calmodulin complex to the pump is thus a signal informing the pump that the cytoplasmic Ca^{2+} level has risen above a certain level and to start pumping Ca^{2+} out.

S25.5 A possible reaction sequence is shown below. Starting from a Fe(II) porphyrin complex (L is a neutral axial ligand throughout the sequence) we first obtain a peroxo bridged Fe(III) porphyrin dimer. Peroxo bridge can oxidatively cleave producing two equivalents of oxido Fe(IV) porphyrin monomers. This rather reactive species (recall that +4 is not a stable oxidation state for Fe and that Fe compounds with oxidations states above +3 are strong oxidizing agents) can react with another equivalent of the starting Fe(II) porphyrin complex producing an oxido-bridged Fe(III) porphyrin dimer. Note that all complexes are neutral species.

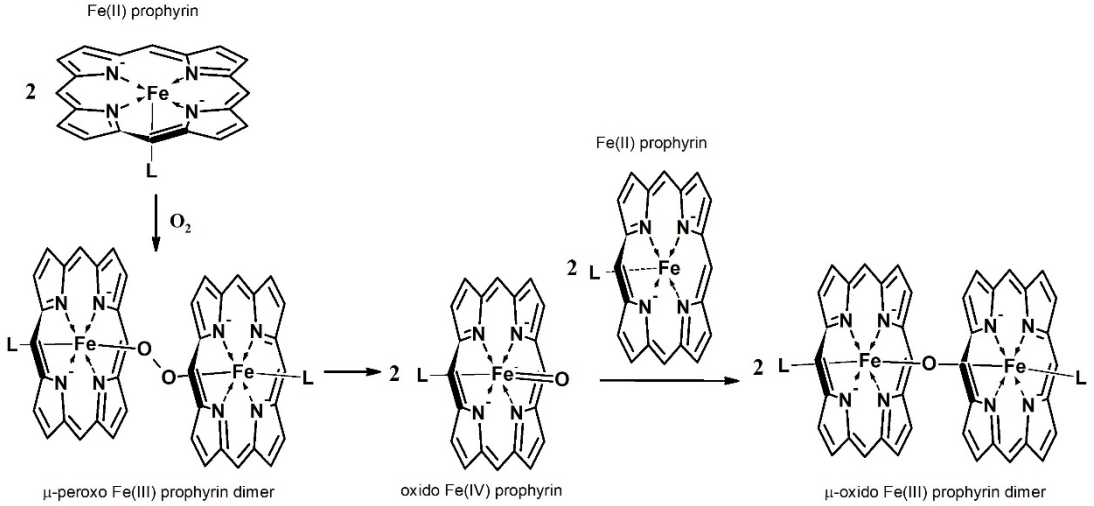

S25.6 Hydrogen bonding and replacement of one cysteine with a histidine should lead to an increase in the reduction potential of an Fe-S cluster. Hydrogen bonding should stabilize the more reduced, electron-rich oxidation level of an Fe-S cluster. Two His-for-Cys substitutions raise the reduction potential in the Rieske centres because imidazole is a better ligand to Fe(II) than Fe(III) sites. Surrounding a cluster with negatively charged protein residues would likely decrease the cluster's reduction potential because it will be more difficult to add an electron to a site that is already negatively charged in a low dielectric medium.

S25.7 There is greater covalence in blue Cu centres than in simple Cu(II) compounds. The unpaired electron is delocalized onto the cysteine sulphur and spends more time away from the Cu nucleus, decreasing the coupling. In most of the Cu blue centres, the reduced form is Cu(I), which is a soft acid, so it makes sense that it bonds well with sulfur-containing ligands such as a cysteine residue.

S25.8 Cu(III) is a d^8 metal centre. It is likely to be highly oxidizing, and probably diamagnetic with a preference for square-planar geometry, a favoured geometry for the d^8 electronic configuration.

S25.9 If we want to obtain a better model for Fe(IV) oxo centres is to force the octahedral geometry at Fe(IV). This would produce a complex molecular orbital diagram as shown in the Example 25.9. For non-haem Fe proteins the ligands should contain N and O donor atoms (hard donors).

S25.10 Species such as CH_3Hg^+ and $(CH_3)_2Hg$ are hydrophobic and can penetrate cell membranes. Cobalamins are very active methyl-transfer reagents that can methylate anything in the cell, which is bad news for the human body. Unlike many other mercury compounds, methylmercury is soluble in water. Methylation of Hg^{2+} thus increases concentration of this cation in body fluids.

S25.11 Spectroscopic measurements that are metal specific, such as EPR, which detects the number of unpaired electrons, could be used on both enzyme and isolated cofactor. Attempts could be made to grow single crystals from the solution and perform single-crystal X-ray diffraction and EXAFS to reveal molecular geometry, bond distances, and angles between Fe or Mo and the sulphur ligands. Both these techniques can be carried out on the enzyme and cofactor dissolved in DMF. Of these, single-crystal X-ray diffraction is our most powerful technique for determining structure. Mössbauer spectroscopy could also be useful in determining (average) oxidation states and geometries at Fe centres.

S25.12 Cu(I) has an ability to undergo linear coordination by sulphur-containing ligands. The only other metals with this property are Ag(I), Au(I), and Hg(II), but these are not common in biology. Cu(I) can also be found in trigonal planar and tetrahedral coordination environments. Binding as Cu(II) would be less specific because it shows a strong preference for square planar or tetragonal geometries. Also, importantly, Cu(II) is able to oxidise thiolates ($R\text{-}S^-$) to RS-SR.

Exercises

E25.1 We should compare the ions in question with what we know about K^+ and the potassium channel. In comparison to K^+, Na^+ is smaller and consequently has a higher charge density. Thus, for a channel or ionophore to be Na^+ specific it must have smaller cavity than K-channel. The preferred donor atoms for Na^+ binding are the same as for K^+ binding—both atoms form more stable complexes with electronegative oxygen donor atoms. Since both are s-block elements, and lack LFSE (no d orbitals), neither has a clear geometry preference. Consequently, the geometry of an Na^+ binding site is dictated by the size—if the K-channel provides eight O donors in cubic arrangement, an equivalent for Na^+ should provide (for example) 6 or 7 O donors in octahedral or pentagonal bipyriamidal geometry. Ca^{2+} is the smallest of the three cations, and having also a 2+ charge, it has the highest charge density. Consequently, Ca^{2+} is going to bind more tightly than either Na^+ or K^+ to the residues that have negative charge—for example deprotonated –OH groups. It is also a cation of a s-block element and has no LFSE that could dictate a preferred geometry. Cl^- is obviously different from the other three by being an anion (and significantly larger than all others). Thus, to move Cl^- we would need to have a large cavity and rely on hydrogen bonds formed with –NH and –OH functional groups.

E25.2 Co(II) commonly adopts distorted tetrahedral and five-coordinate geometries typical of Zn(II) in enzymes. When substituted for Zn(II) in the parent enzyme, the enzyme generally retains catalytic activity. Zn(II) is d^{10} and therefore colourless; however, Co(II) is d^7, and its peaks in the UV-Vis spectrum are quite intense (see Chapter 20) and report on the structure and ligand-binding properties of the native Zn sites. Furthermore, it is almost impossible to use ^1H NMR to study the active site of zinc enzymes because of all the interferences and overlaps one gets with the amino acids themselves. Fortunately, Co(II) is paramagnetic, enabling Zn enzymes to be studied by EPR after substitution.

E25.3 Since iron(V) would have the electron configuration of $[Ar]3d^3$, the ion would have three unpaired electrons. The logical choice would be either EPR (electron paramagnetic resonance) or Mössbauer spectroscopy. See Chapter 8, Physical Techniques in Inorganic Chemistry, for more discussion on both instruments.

E25.4 The structural changes accompanying oxidation of the P-cluster raise the possibility that the P-cluster may be involved in coupling of electron and proton transfer in nitrogenase. Among the important changes in the structures is the change in coordination of the cluster. The oxidized form of the P-cluster has a serine and the amide nitrogen of a cystine residue coordinated to Fe atoms which dissociate in the reduced form. Since both ligands might be protonated in their free states and may be deprotonated in their bond states, this raises the possibility that two-electron oxidation of the P-cluster simultaneously releases two protons. Transfer of electrons and protons to the FeMo-cofactor active site of nitrogenase needs to be synchronized; the change in structure suggests that the coupling of proton and electron transfer can also occur at the P-cluster by controlling protonation of the exchangeable ligands.

E25.5 The discovery of substantial amounts of O_2 would indicate the presence of photosynthesis and consequently some life-form that is capable of photosynthesis. On Earth, the plants are organisms capable of photosynthesis, but this does not preclude a possibility of some other photosynthetic life form.

E25.6 One possible mechanism is shown on the figure below. The first step is formation of halogen bond between electron rich Co(I) (a Lewis base) and X-R (a σ* orbital of RX acts as a Lewis acid). This Co(I)–X–R fragment is linear (see Section 5.7f *Group 17 Lewis Acids*). Next, Co(I) is oxidized to Co(III) and Co–X bond is formed. Note that this step is not a oxidative addition, although it might appear as such, because the coordination number at Co is increased only by one, not two. The conserved tyrosine residue protonates R^- and forms R–H product. This removes very nucleophilic reagent that is also capable of bonding to Co. The Co(III) is next reduced twice with electrons supplied through two 4Fe–4S clusters present in the structure of this protein. This regenerates Co(I) active site and releases chloride as the second product of the reaction.

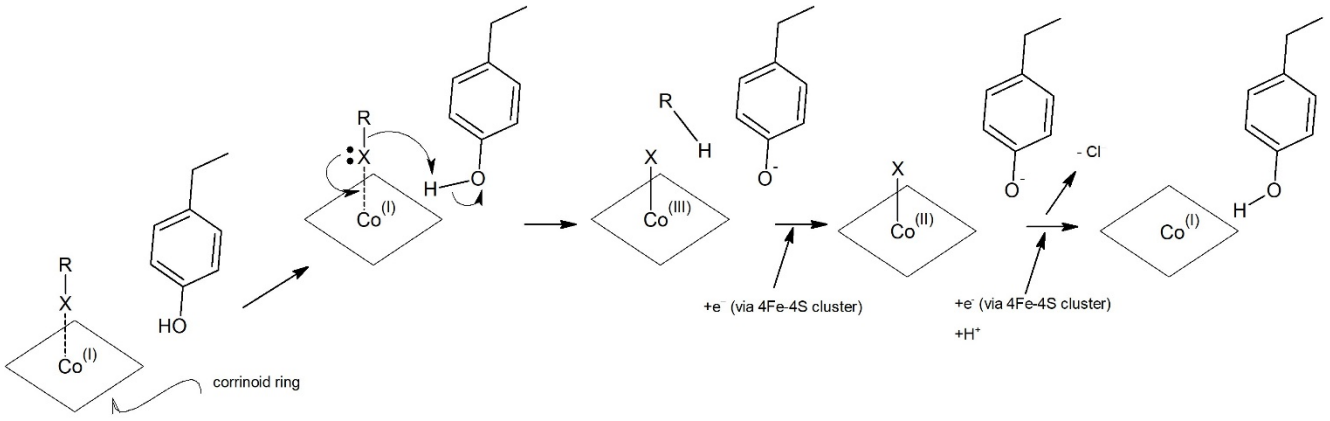

Chapter 26 Inorganic Chemistry in Medicine

Self-Tests

S26.1 A general structure of semithiocarbazide ligand is shown below. The easiest and most straightforward way to fine-tune the reduction potentials of Cu(II) complexes is by modifying R substituents (R^1–R^5) on the ligand backbone. The Cu semithocarbazide complexes used in medicine usually contain tetradentate versions of the general structure shown.

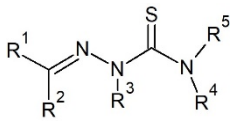

Exercises

E26.1 Au(III) is in many ways similar to Pt(II), with similarities mostly arising because the two are isoelectronic species with d^8 electronic configuration. Thus, both prefer square planar geometry that seems to be necessary for the activity of Pt(II) anticancer drugs. Au(III) is also a soft Lewis acid, meaning that it has low preference for Cl^- and O-donor ligands. The major difference between Pt(II) and Au(III) is that Au(III) is easily reduced under hypoxic conditions to Au(I), which prefers linear geometry as in $[AuCl_2]^-$. Au(I) can also disproportionate to Au(0) and Au(III).

E26.2 Likely products of the $[H_3BCO_2]^{2-}$ decomposition are $B(OH)_3$, H_2, CO, and OH^-.

By analogy to carbonate, you can expect boranocarbonate to be a rather good base. Consequently it can be stable in a basic medium (just like carbonate), but in neutral or mildly acidic medium it would be protonated to produce hydrogenboranocarbonate:

$$[H_3BCO_2]^{2-} + H_2O \rightarrow [H_3BCOO_2H]^- + OH^-$$

Hydrogenboranocarbonate can eliminate OH^- to produce $[H_3BCO]$ adduct (boranocarbonyl):

$$[H_3BCO_2H]^- \rightarrow [H_3BCO] + OH^-$$

$[H_3BCO]$ is unstable when not under CO atmosphere and CO can be easily displaced by water molecules. The intermediate aquo adduct $[H_3B(OH_2)]$ rapidly decomposes to give H_2BOH and H_2. H_2BOH reacts rapidly with another two water molecules to produce the final products $B(OH)_3$ and two more equivalents of H_2. The overall reaction is:

$$[H_3BCO] + 3\ H_2O \rightarrow B(OH)_3 + CO + 3\ H_2$$

E26.3 Gallium(III) can bind to transferrin and lactoferrin, and can even be incorporated into ferritin (a biological “iron storage”). These enzymes use nitrogen and oxygen donors to bind iron. Since Ga(III) also has a good affinity for the same donors, it can compete with Fe(III) for the binding sites. One major difference between Fe(III) and Ga(III) is their redox chemistry. While Fe(III) can be reduced to Fe(II), Ga(III) cannot. This is an important difference because the reduction is used to liberate Fe from ferritin—Fe(II) is more labile and hence can easily be released from the complex. Ga(III) cannot be reduced and would remain bound in ferritin.